

Mechanical, Thermal and Physical Properties of Hybrid Banana-Jute Fibers Reinforced Epoxy and Polyester Composites: Modeling and Experiments

Siva Bhaskara Rao Devireddy



Department of Mechanical Engineering
National Institute of Technology Rourkela

Mechanical, Thermal and Physical Properties of Hybrid Banana-Jute Fibers Reinforced Epoxy and Polyester Composites: Modeling and Experiments

*Dissertation submitted to the
National Institute of Technology Rourkela
in partial fulfillment of the requirements
of the degree of
Doctor of Philosophy*

in

Mechanical Engineering

by

Siva Bhaskara Rao Devireddy

(Roll Number: 512ME103)

under the supervision of

Prof. Sandhyarani Biswas



August, 2016

Department of Mechanical Engineering
National Institute of Technology Rourkela



Department of Mechanical Engineering
National Institute of Technology Rourkela

Prof. Sandhyarani Biswas

Assistant Professor

August 23, 2016

Supervisor's Certificate

This is to certify that the work presented in this dissertation entitled “*Mechanical, Thermal and Physical Properties of Hybrid Banana-Jute Fibers Reinforced Epoxy and Polyester Composites: Modeling and Experiments*” by “*Siva Bhaskara Rao Devireddy*”, Roll Number 512ME103, is a record of original research carried out by him under my supervision and guidance in partial fulfillment of the requirements of the degree of *Doctor of Philosophy in Mechanical Engineering*. Neither this dissertation nor any part of it has been submitted for any degree or diploma to any institute or university in India or abroad.

Sandhyarani Biswas

Dedicated to

My Friend Anand Babu

Declaration of Originality

I, Siva Bhaskara Rao Devireddy, Roll Number 512ME103 hereby declare that this dissertation entitled “*Mechanical, Thermal and Physical Properties of Hybrid Banana-Jute Fibers Reinforced Epoxy and Polyester Composites: Modeling and Experiments*” represents my original work carried out as a doctoral student of NIT Rourkela and, to the best of my knowledge, it contains no material previously published or written by another person, nor any material presented for the award of any other degree or diploma of NIT Rourkela or any other institution. Any contribution made to this research by others, with whom I have worked at NIT Rourkela or elsewhere, is explicitly acknowledged in the dissertation. Works of other authors cited in this dissertation have been duly acknowledged under the section "Bibliography". I have also submitted my original research records to the scrutiny committee for evaluation of my dissertation.

I am fully aware that in case of any non-compliance detected in future, the Senate of NIT Rourkela may withdraw the degree awarded to me on the basis of the present dissertation.

August 23, 2016
NIT Rourkela

Siva Bhaskara Rao Devireddy

Acknowledgment

It gives me immense pleasure to express my deep sense of gratitude to my supervisor **Prof. Sandhyarani Biswas** for her invaluable guidance, motivation, keen encouragement and above all for her ever co-operating attitude that enabled me in bringing up this thesis in the present form.

I would like to express my sincere thanks to **Prof. Ranjit Kumar Sahoo**, honorable Director, National Institute of Technology, Rourkela for being a constant source of inspiration for me. I am equally grateful to **Prof. Siba Sankar Mahapatra**, Head of the Department of Mechanical Engineering for his timely help during the entire course of my research work.

I would like to record my sincere thanks to **Prof. S. S. Mahapatra, Prof. J. Srinivas, Prof. S. Sen** and **Prof. K. K. Paul**, learned members of my Doctoral Scrutiny Committee (DSC) for the guidance, review and critical suggestions during the entire course of this work.

I greatly appreciate and convey my heartfelt thanks to **Prabina Kumar Patnaik, Priyadarshi Tapas Ranjan Swain, Vivek Mishra** and **Prity Aniva Xess** for helping me out with their abilities for developing the research work and for making past couple of years more delightful.

I would also take this opportunity to thank my friend **Anand Babu Kotta** who played a major role in this inning of my life right from the beginning. I am also thankful to my friends, offering me advice and supporting me through this entire process. Special thanks to **Gangadharudu Talla, Vinay Sagar Kommukuri and Hari Sankar Bendu**.

My very special thanks go to all my family members, for all their love and marvelous support in the most difficult times of my life. Without their unwavering support, love, and understanding, I would have never been able to complete this journey.

Finally, but most importantly, I thank **Almighty God**, the Creator and the Guardian, to whom I owe my very existence. I am grateful to God for giving me strength that keeps me standing and for the hope that keeps me believe that this study would be possible. I thank God for reasons too numerous to mention.

August 23, 2016
NIT Rourkela

Siva Bhaskara Rao Devireddy
Roll Number: 512ME103

Abstract

During the last few years, natural fiber reinforced polymer composites are widely used due to their advantages such as ease of fabrication, low density, biodegradability, low thermal conductivity, renewability, nontoxicity, combustibility and low cost of production. Prediction of mechanical and thermal properties of fiber reinforced polymer hybrid composites is a challenging task for current simulation techniques, so does the need to understand the numerical simulation of such materials. The present work reports the analytical, numerical and experimental study on mechanical and thermal behaviour of fiber reinforced polymer hybrid composites. Banana and jute fibers in unidirectional and short form are considered as reinforcement with different fiber loading (0-40 wt.%) and with different weight ratio (1:1, 1:3, and 3:1). Two theoretical models were developed based on one dimensional heat conduction model for calculating the thermal conductivity of unidirectional and short fiber reinforced hybrid composites. The three-dimensional micromechanical models based on finite element method with representative volume element are employed to predict the elastic and thermal conductivity of unidirectional and short banana-jute fiber reinforced polymer hybrid composites. The experimental work presents the test results in regard to the physical, mechanical and thermal behaviour of the epoxy and polyester based composites reinforced with unidirectional and short fibers. Finally, this work includes the comparison of the micromechanical models with experimental and existing analytical formulations like rule of hybrid mixture, geometric mean, Halpin-Tsai, and Lewis and Nielsen models that are used extensively in material modeling. For unidirectional fiber based composites, with addition of 7.5 wt.% banana and 22.5 wt.% jute fiber as reinforcement, the longitudinal tensile strength of epoxy increases from 32.28 MPa to 84.48 MPa and that of polyester increases from 20.72 MPa to 66.89 MPa and the ILSS of epoxy increases from 6.92 MPa to 20.53 MPa and that of polyester increases from 4.05 MPa to 16.16 MPa with same fiber loading. For short fiber based composites, with the addition of 7.5 wt.% banana and 22.5 wt.% jute as reinforcement, the tensile strength of epoxy increased by 103% and reaches 65.84 MPa, flexural strength of epoxy increased by 146% and reaches to 114.31 MPa and its flexural modulus increased by 120% and reaches to 7.33 GPa. Whereas, in polyester based hybrid composites with similar fiber loading, the tensile strength of polyester increased by 171% and reaches to 56.25 MPa, flexural strength of polyester increased by 98.9% and reaches to 81.93 MPa and its flexural modulus increased by 91.39% and reaches to 3.09 GPa. For unidirectional fiber based composites, with the incorporation of 10 wt.% banana and 30 wt.% jute fiber, the longitudinal thermal conductivity of neat epoxy reduced by 32.23% and reaches to 0.246

W/m-K and that of neat polyester reduced by 28.50% and reaches to 0.143 W/m-K. For short fiber based composites at the same fiber loading, the effective thermal conductivity of epoxy reduces from 0.363 W/m-K to 0.239 W/m-K and that of polyester reduces from 0.20 W/m-K to 0.14 W/m-K. The study reveals that the performance of hybrid composites with the weight ratio of banana and jute fiber as 1:3 shows better than the weight ratio of 1:1 and 3:1. With low thermal conductivity and improved mechanical properties, the banana-jute fiber reinforced polymer hybrid composites can be considered in thermal insulation and structural applications in order to reduce the dependence on non-renewable material sources and energy consumption.

Keywords: Natural fibers; Hybrid composites; Micromechanics; Physical properties; Mechanical properties; Thermal properties

Contents

Supervisor’s Certificate	iii
Dedication	iv
Declaration of Originality	v
Acknowledgment	vi
Abstract	vii
List of Tables	xii
1 Introduction	1
1.1 Background and Motivation	1
1.2 Thesis Outline.	7
2 Literature Review	9
2.1 On Natural Fiber and Natural Fiber Reinforced Composites	9
2.2 On Mechanical and Physical Behaviour of Natural Fiber Reinforced Polymer Composites	16
2.3 On Thermal Behaviour of Natural Fiber Reinforced Polymer Composites . .	21
2.4 On Banana and Jute Fiber Reinforced Polymer Composites	24
2.4.1 On Mechanical Properties	24
2.4.2 On Thermal Properties.	26
2.5 On Micromechanical Analysis of Fiber Composites	27
2.5.1 Existing Analytical Homogenization Models.	28
2.5.2 On Elastic Properties of Composites.	31
2.5.3 On Thermal Properties of Composites.	32
2.6 The Knowledge Gap in Earlier Investigations.	34
2.7 Objectives of the Present Work.	34
3 Development of Theoretical Models for Thermal Conductivity of Fiber Reinforced Hybrid Composites	36
3.1 Basic Principles.	36
3.1.1 Background.	36

3.1.2	Law of Minimal Thermal Resistance and Equal Law of Specific Equivalent Thermal Conductivity.	36
3.2	Development of Theoretical Model for Unidirectional Fiber Reinforced Hybrid Composites	37
3.2.1	Nomenclature.	37
3.2.2	Generation of the Unit Cell.	38
3.2.3	Heat Transfer Modeling.	39
3.3	Development of Theoretical Model for Short Fiber Reinforced Hybrid Composites.	45
3.3.1	Generation of the Unit Cell.	45
3.3.2	Heat Transfer Modeling.	46
4	Materials and Methods	52
4.1	Materials.	52
4.1.1	Matrix Material.	52
4.1.2	Fiber Material	53
4.2	Composite Fabrication.	55
4.3	Testing of Physical Properties	58
4.3.1	Density and Void Content.	58
4.3.2	Water Absorption	59
4.3.3	Kinetics of Water Absorption.	59
4.4	Testing of Mechanical Properties.	61
4.4.1	Single Fiber Tensile Test.	61
4.4.2	Tensile Properties.	61
4.4.3	Flexural Properties.	62
4.4.4	ILSS.	63
4.4.5	Impact Test.	64
4.4.6	Micro-Hardness.	64
4.4.7	Scanning Electron Microscopy.	65
4.5	Testing of Thermal Properties.	65
4.5.1	Thermal Conductivity.	65
4.5.2	Differential Scanning Calorimeter and Thermogravimetry Analysis.	68
4.6	Micromechanical Methods for Hybrid Composites.	69
4.6.1	Analytical Methods.	69
4.6.2	Numerical Methods.	71

5	Results and Discussion – I: Unidirectional Fiber Reinforced Composites	73
5.1	Elastic and Thermal Conductivity of Unidirectional Fiber Reinforced Composites.	73
5.1.1	Development of Micromechanical Model in ANSYS.	73
5.1.2	Elastic Properties of Unidirectional Fiber Reinforced Hybrid Composites	86
5.1.3	Thermal Conductivity of Unidirectional Fiber Reinforced Hybrid Composites.	102
5.2	Physical, Mechanical and Thermal Behaviour of Unidirectional Fiber Reinforced Composites.	118
5.2.1	Physical Properties.	118
5.2.2	Mechanical Properties.	125
5.2.3	Thermal Properties.	142
6	Results and Discussion – II: Short Fiber Reinforced Composites	145
6.1	Elastic and Thermal Conductivity of Short Fiber Reinforced Composites. . .	145
6.1.1	Development of Micromechanical Model in ANSYS.	145
6.1.2	Elastic Properties of Short Fiber Reinforced Hybrid Composites. . .	152
6.1.3	Thermal Conductivity of Short Fiber Reinforced Hybrid Composites.	161
6.2	Physical, Mechanical and Thermal Behaviour of Short Fiber Reinforced Composites.	170
6.2.1	Physical Properties.	170
6.2.2	Mechanical Properties.	176
6.2.3	Thermal Properties.	182
7	Conclusions and Scope for Future Work	187
7.1	Conclusions.	187
7.2	Recommendation for Potential Application.	189
7.3	Scope for Future Work.	190
	Bibliography	191
	Dissemination	219
	Brief Bio-Data of the Author	221

List of Tables

2.1	Annual production of natural fibers and their producers	11
2.2	Physical and mechanical properties of natural fibers.	12
2.3	Chemical properties of natural fibers.	14
2.4	Thermosetting and thermoplastic matrix based natural fiber composites.	15
2.5	Value of ξ for various systems.	30
2.6	Value of φ_m for various systems.	30
4.1	Some important properties of matrix materials under investigation.	53
4.2	Detailed designation and composition of epoxy based composites reinforced with unidirectional and short fibers.	56
4.3	Detailed designation and composition of polyester based composites reinforced with unidirectional and short fibers.	57
4.4	Traditional Halpin-Tsai parameters for fiber reinforced hybrid composites.	71
5.1	Volume fraction of banana and jute fiber at different fiber loadings.	75
5.2	Periodic boundary conditions for square and hexagonal RVE.	80
5.3	Percentage errors associated with the transverse thermal conductivity values of epoxy based composites obtained from different models.	116
5.4	Percentage errors associated with the transverse thermal conductivity values of polyester based composites obtained from different models.	117
5.5	Theoretical and measured densities of the epoxy based composites.	119
5.6	Theoretical and measured densities of the polyester based composites.	119
5.7	The dependence of moisture sorption constant n and k for all formulations.	123
5.8	Values of maximum water uptake, diffusion coefficient, sorption coefficient, and permeability coefficient for unidirectional fiber reinforced	123

	epoxy composites.	
5.9	Values of maximum water uptake, diffusion coefficient, sorption coefficient, and permeability coefficient for unidirectional fiber reinforced polyester composites.	124
5.10	Specific heat and thermal diffusivity of the unidirectional fiber reinforced composites.	143
6.1	Percentage errors associated with the effective thermal conductivity values of epoxy based composites obtained from different models.	168
6.2	Percentage errors associated with the effective thermal conductivity values of polyester based composites obtained from different models.	169
6.3	Theoretical and measured densities of the epoxy based composites.	171
6.4	Theoretical and measured densities of the polyester based composites.	171
6.5	The dependence of moisture sorption constant n and k for all formulations. .	174
6.6	Values of maximum water uptake, diffusion coefficient, sorption coefficient, and permeability coefficient for short fiber reinforced epoxy composites.	174
6.7	Values of maximum water uptake, diffusion coefficient, sorption coefficient, and permeability coefficient for short fiber reinforced polyester composites.	175
6.8	Specific heat and thermal diffusivity of the short fiber reinforced composites.	183
6.9	Thermal degradation of the short fiber reinforced composites.	185

Chapter 1

Introduction

1.1 Background and Motivation

Engineering materials create the foundation of technology, whether the technology relates to structural, thermal, electronic, environmental, electrochemical, biomedical or other applications. The desired properties of these materials are high stiffness, light weight, good mechanical and thermal durability, high yield strength under static or dynamic loading and good surface hardness. Generally, homogeneous materials satisfy only some of the desired properties. That is why during the last few decades have experienced a surge in the advancement of science and technology for heterogeneous materials. Examples of these materials are alloys that contain multiple phases such as grains, precipitates and pores, and composite materials with a dispersion of fibers, whiskers or particulates in various matrix materials [1]. The development of composite materials and their related design and manufacturing technologies is one of the most important advances in the history of materials. The word ‘composites’ derived from the Latin word *compositus*, which means ‘put together’ signifying something made by putting together different parts or materials [2]. Composite materials are combinations of two or more chemically distinct materials to form a new material with enhanced material properties non-attainable by any of the individual materials alone. Strictly speaking, the composite materials are not new to the mankind. Nature is full of examples wherein the idea of composites is used. Typical examples of natural composites are stone, timber, human bone, and so on. In ancient Egypt, people used to build walls from the bricks made of mud with straw as reinforcing component [3]. Composite materials possess applications in aerospace, automobile, buildings and public works, electrical and electronics, general mechanical components, rail transports, marine transports, space transport, sports and recreation, cable transports etc. [4]. The main constituents of composite materials are the reinforcement phase, the matrix phase and the interphase. In composite materials, the discontinuous phase is usually stronger and harder than the continuous phase and is called the reinforcement. Generally, the reinforcing phase is embedded in the matrix phase. The matrix material is a continuous phase and present in greater quantity in composite material. The matrix phase is acts as to transfer stresses between the reinforcing materials and to protect them from mechanical and/or environmental damage. In composite materials, phase between the surface of the reinforcement and surface of the matrix are collectively referred as

interphase. The interphase property of the composite varies between the fiber and matrix properties and has great influence on the various properties of composites.

Composite materials are commonly classified at two distinct levels. The first level of classification is generally made with respect to the matrix phase. The major composite classes include metal matrix composites (MMCs), ceramic matrix composites (CMCs) and polymer matrix composites (PMCs). PMCs consist of a polymer resin as the matrix material which filled with a variety of reinforcements. Polymer matrices are most commonly used because of cost efficiency, ease of fabricating complex parts with less tooling cost and they also have excellent room temperature properties when compared to metal and ceramic matrices. Over the past few decades, it is found that polymers have replaced many of the conventional metals/materials in various applications. This kind of composite is used in the greatest diversity of composite applications due to its advantages such as low density, good thermal and electrical insulator. In most of these applications, the properties of polymers are modified by using fibers to suit the high strength/high modulus requirements. Based on their behaviour and structure, polymer matrices can be classified as thermoplastic and thermoset. The most common matrix materials used in thermosetting and thermoplastic composites is shown in Figure 1.1.

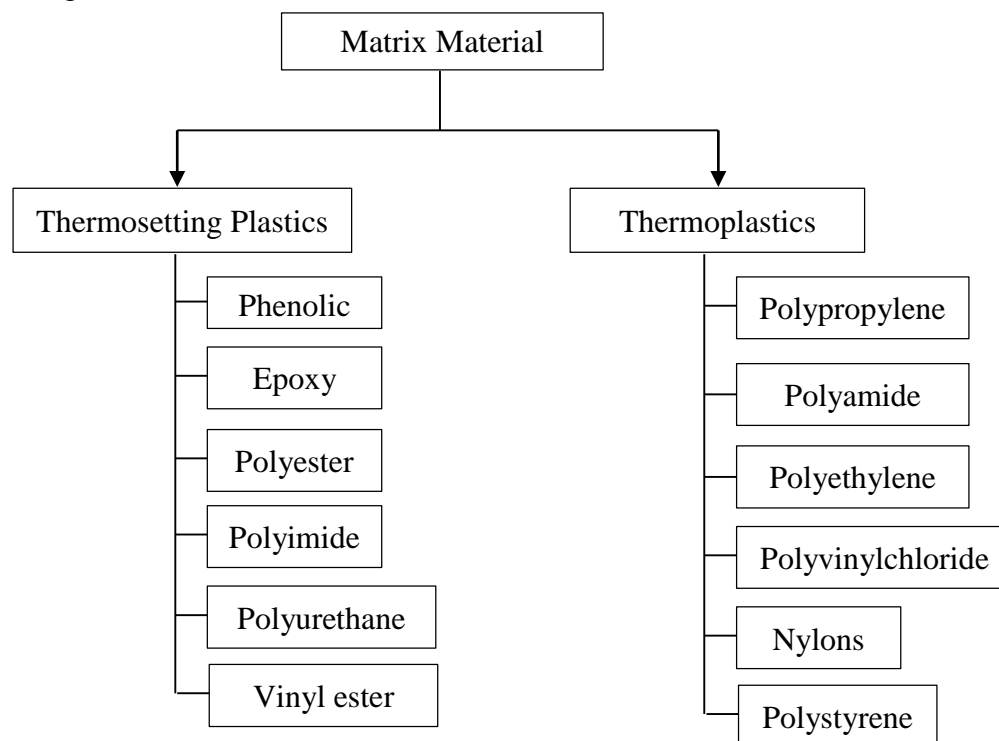


Figure 1.1: Classification of thermosetting and thermoplastic matrix materials

Thermoplastics consist of branched or linear-chain molecules having weak intermolecular bonds and strong intramolecular bonds. Solidification and melting of these polymers are reversible and can be reshaped by application of heat and pressure. Thermoset matrix materials have cross-linked or network structures with covalent bonds between all molecules. Once solidified by cross-linking process, these materials cannot be re-melted or reshaped. In thermoset matrix composites, the fibers are impregnated with thermosetting resins and then exposed to high temperatures for curing. These materials possess distinct advantages over the thermoplastics such as creep resistance, higher operating temperature and good affinity to heterogeneous materials [5]. Based on the reinforcement phase, the classification of composites is shown in Figure 1.2.

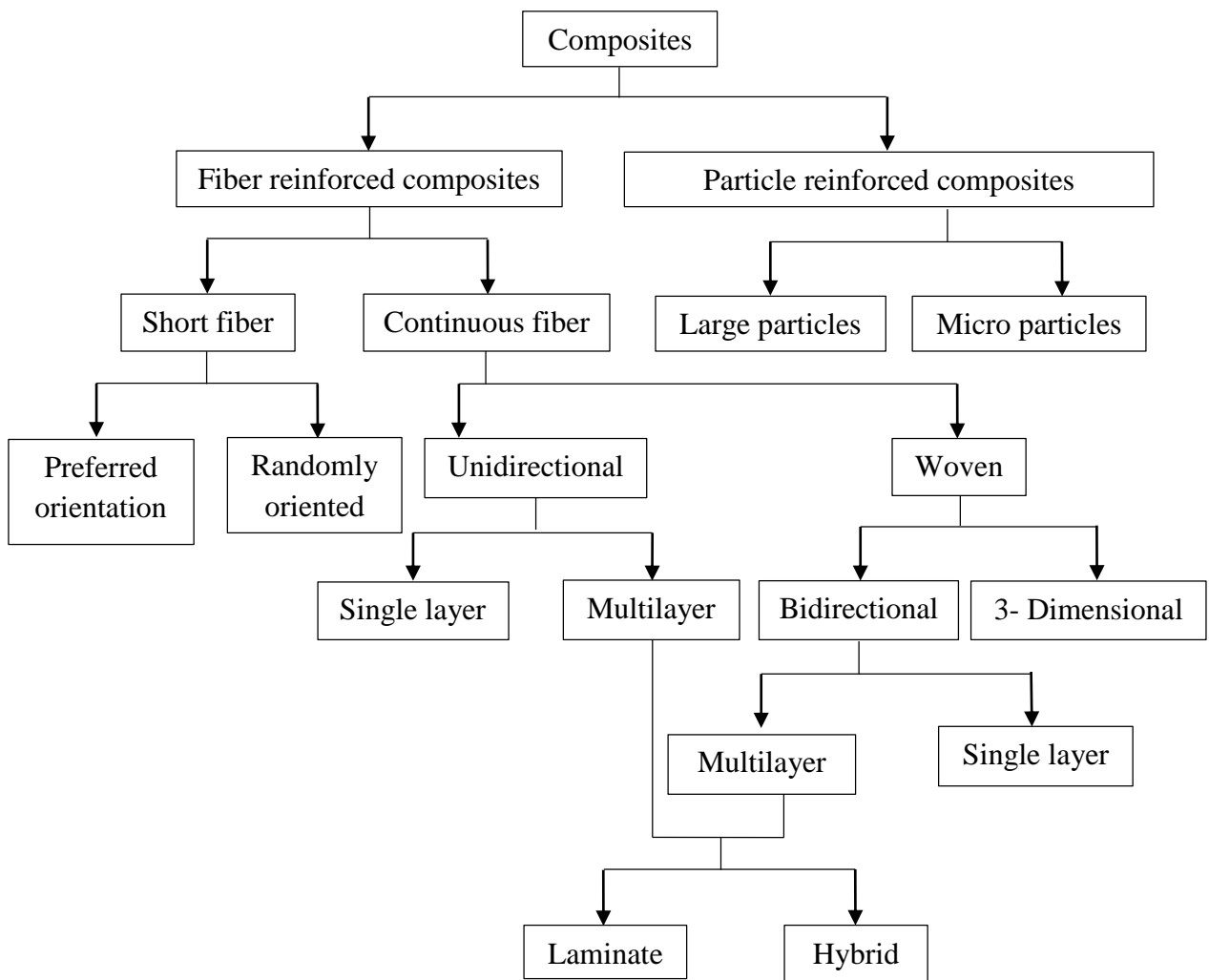


Figure 1.2: Classification of composites based on reinforcement

The major classes in this level include fiber reinforced composites and particulate reinforced composites. The particulate reinforced composites mainly consisting of reinforcing material that is in the form particles. Fiber reinforced composites are composed of fibers and a matrix. Fibers are the reinforcement materials which dispersed throughout the matrix material to increase its rigidity and strength. For the past few decades, fiber reinforced polymer composites acquired an important space in the field of composite materials. Fiber reinforced polymer composites have been widely used in various applications, i.e. aerospace, automotive, defence, marine, and sports goods because of their high specific modulus and strength [6]. These materials provide high durability, design flexibility, lightweight and excellent corrosion resistance which make them attractive material in these applications [7]. The fiber reinforcing agent may be either synthetic or natural. Various types of synthetic fibers have been developed such as carbon, aramid, glass, nylon, rayon, acrylic, olefin etc. On the other hand, some of the known natural fibers are jute, banana, cotton, silk, wool, hemp, ramie, linen, coir, pineapple, pinewood, mohair, kapok, angora, sisal, angora, flax, kenaf, bamboo etc. [8]. Composites made of the same reinforcing material system may not give better results as it undergoes different loading conditions during the service life. Nowadays, it is observed that a range of properties can be obtained by combining two or more different types of fibers in a common matrix. A hybrid composite is a combination of two or more different types of fiber in which one type of fiber balance the deficiency of another fiber. The concept of hybridization gives flexibility to the design engineer to tailor the material properties according to the requirements, which is one of the major advantages of composites. By careful selection of reinforcing fibers, the material costs can be substantially reduced.

As a result of growing social, ecological and economic awareness, high rate of depletion of petroleum resources, industrial ecology, principles of sustainability, eco-efficiency and new environmental regulations have stimulated the development of the next generation of composite materials compatible with the environment to reduce greenhouse gas emissions worldwide. The effective use of eco-friendly materials in a variety of applications, with a particular focus on cost effective materials, energy efficient, is one of the daunting challenges of the twenty-first century [3]. The meaning of eco-material includes ‘safe’ material systems for human and other life forms at all times. The bio based materials including wood, grasses, agricultural waste and plant fibers are growing rapidly both in terms of their industrial applications and fundamental research. Their renewability, availability, low density, and price as well as satisfactory mechanical properties make them an attractive ecological substitute to glass, carbon and other man-made fibers used for the manufacturing

of composite materials. Natural fibers are playing very important part in the present natural conditions to determine current biological and ecological issues [9]. The mechanical properties of natural fibers, particularly hemp, sisal, flax, and jute are relatively good, and may compete with glass fiber in terms of specific strength and modulus [10]. Due to its hollow and cellular nature, natural fibers possess excellent acoustic and thermal insulators, and also exhibit reduced bulk density [11]. Interestingly, numerous types of natural fibers which are abundantly available have proved to be effective and good reinforcement in the thermoplastic and thermoset matrices. Among all the natural fibers, jute is more promising as it is relatively inexpensive and commercially available in various forms [12]. Over hundreds of years jute has been used in the applications of ropes, beds, bags etc. Jute is an important agro-fiber which has gained world-wide attention as a potential material for polymer reinforcement due to its natural properties such as high tensile modulus, low density and low elongation at break, low cost, no health risk, high specific strength and modulus, renewability, easy availability and much lower energy requirement for processing. Jute fiber is multicelled in structure [13] and is derived from the stem of a jute plant. This fiber is an annual plant that grows to 2.5-4.5 m [14] and are separated from the woody stalk centers by retting. Jute is a lingo-cellulosic fiber because its major chemical constituents are lignin and cellulose. About 95% of the global production of jute fibers is produced by India, China, Bangladesh, Thailand and Nepal [15]. Similarly, among different natural fibers, banana fiber also has the potential to be used as reinforcement in polymer composites. It is a well-known fact that banana fiber is a waste product of banana cultivation. Hence, without any additional cost these fibers can be obtained in bulk quantity and used for industrial purposes. Around 70 million metric tons of banana are produced every year by the tropical and subtropical regions of the world [16], [17]. It is a lingo-cellulosic fiber, which can be extracted from the pseudo-stem of banana plant with better mechanical properties [18], [19]. The fiber separation process involves cutting pieces of banana from the stem and passing them through a mangle to remove excess moisture, and then dried at ambient temperatures. Banana fibers are generally used for making paper, cloths, ropes etc. Akubueze et al. [20] reported the process technology for the production of biodegradable agro-sack from banana fibers for packaging a wide range of industrial and agricultural based produce such as cotton lintens, cocoa, onions, potatoes, grains, oil seeds. Yusuf et al. [21] fabricated an effective and environmentally friendly mulching thin film of waste banana peel as agricultural applications. The various forms of banana and jute fibers are continuous, short and woven. The continuous fibers can be processed to different forms like yarn or mats. Short fibers are used in composites manufacturing to attain complex geometry in automobile and aerospace industry [22], [23].

Now-a-days, the demand for the light weight, thermal insulation, cost effective and structurally stable materials is increasing rapidly. Many parts of the world experience large changes in temperature from season to season. So, there is a great need for building materials with insulating properties. With the development of new technologies, the scenario in the field of industries, entertainment, transportation, and medical services is much the same. Generally, the thermal insulation is to retard the heat flow and is important in some cases, for the survival of humans and animals. Insulation also lowers the cooling and heating costs, and prevents damage to various components by high temperatures or freezing. The conventional materials are unable to meet the requirement of these special properties like low thermal conductivity, high strength and low density. Air is a poor conductor of heat, and when surrounded in a hollow area is an excellent insulator. Other insulating materials, some of which depend on air pockets for much of their insulating effect, include mineral wool, wood, glass fiber, asbestos, concrete and plant fiber. These materials retard the conduction and convection of heat. At present, glass fibers and synthetic fibers derived from the petroleum based resources are the widely used insulating materials in various industries. Unfortunately, petroleum based materials are nonrenewable and glass fiber based materials are known to have carcinogenic effects [24]. This opens up another option for composite materials based on natural fibers.

The mechanical and thermal response of composite materials is a challenging problem requiring expertise in a wide range of fields ranging from quantum mechanics to continuum mechanics depending on the length scale that is being studied. Generally, the analysis of composite materials can be examined from two distinct levels: macromechanical approach and micromechanical approach. In macromechanical approach, each layer of the composites is considered as a homogeneous, orthotropic, and elastic continuum [25]. Based on the known properties of the individual layers, the macromechanical analysis involves investigation of the interaction of the individual layers of the laminate and their effect on the overall response of the laminate. Although, the macromechanical analysis has the advantage of simplicity, it is not possible to identify the stress/strain states in the fiber and matrix level. In contrast, in the micromechanical approach, the fiber and matrix materials are distinctively considered to predict the overall response of the composite as well as the damage propagation and damage mechanisms in the composite [26]. The micromechanical analysis can predict the effective properties of composite material from the knowledge of the individual constituents. The recent dramatic growth in computational capability for mathematical modelling and simulation increases the possibilities that the micromechanical methods can play an important role in the analysis of composite materials. The representative

volume element (RVE) or representative unit cell can be used in the micromechanics to calculate the effective properties of composites materials [27].

The novelty of the current research work is to study the potential utilization of banana-jute fiber reinforced hybrid composites to develop low cost and thermal insulation materials. In order to evaluate the thermal conductivity, a theoretical heat transfer model for fiber reinforced hybrid composites based on the law of minimal thermal resistance and equal law of specific equivalent thermal conductivity is considered. Two theoretical models for estimation of thermal conductivity of unidirectional and short fiber reinforced polymer composites with different fiber loadings were proposed. The validation of proposed theoretical models and finite element results has been made by comparing the experimental results and results obtained using existing analytical methods. A numerical homogenization technique based on the finite element method (FEM) with RVE is used to predict the elastic and thermal conductivity properties of banana-jute fiber reinforced hybrid composites. An attempt has been made in this research work to develop a cost-effective and user-friendly composite material with better mechanical and thermal properties by hybridizing jute and banana fiber. The specific objectives of this work are clearly outlined in the next chapter.

1.2 Thesis Outline

The rest of the thesis is organized as follows:

Chapter 2

This chapter includes a literature review designed to provide a summary of the base of knowledge already available involving the issues of interest. It presents research work on natural fiber reinforced polymer composites as well as micromechanical analysis of fiber composites with emphasis on physical, mechanical and thermal behaviour reported by previous investigators.

Chapter 3

This chapter presents the development of theoretical models for estimation of thermal conductivity of the unidirectional and short fiber reinforced hybrid composites.

Chapter 4

This chapter includes a description of the raw materials used and the test procedures followed. It presents the details of fabrication and characterization of the fiber reinforced hybrid composites under investigation.

Chapter 5

This chapter presents the test results in regard to the physical, mechanical and thermal characteristics of the epoxy and polyester based unidirectional fiber reinforced composites under study.

Chapter 6

This chapter presents the test results in regard to the physical, mechanical and thermal characteristics of the epoxy and polyester based short fiber reinforced composites under study.

Chapter 7

This chapter provides the summary of the findings of the research work, outlines specific conclusions drawn from the experimental, analytical and numerical efforts, recommended applications and directions for future research.

Chapter 2

Literature Review

The purpose of this literature review is to provide background information on the issues to be considered in this thesis and to highlight the importance of the present study. The literature review is focused on the various aspects of the fiber reinforced polymer composites with a special reference to their physical, mechanical and thermal characteristics. This chapter contains review of existing research reports:

- On natural fiber and natural fiber reinforced composites
- On mechanical and physical behaviour of natural fiber reinforced polymer composites
- On thermal behaviour of natural fiber reinforced polymer composites
- On banana and jute fiber reinforced polymer composites
- On micromechanical analysis of fiber reinforced composites

Based on the literature review, the knowledge gap in the earlier investigations is presented at the end of this chapter. Subsequently, the objectives of the present research work are also outlined.

2.1 On Natural Fiber and Natural Fiber Reinforced Composites

Generally, the fibers that are derived from natural resources like plants or some other living species are called natural fibers. Natural fibers have many advantages compared to the traditional fibers like low cost, easily availability, light weight, low density, biodegradability, renewability, nontoxicity, combustibility and high specific mechanical properties [28]. It is also known that natural fibers are non-uniform with irregular cross sections, which make their structures quite unique and much different from conventional or man-made fibers such as carbon fibers, glass fibers etc. These fibers can be divided into three groups based on their origin, i.e. vegetable/plant fibers, animal/protein fibers and mineral fibers. Figure 2.1 shows the classification of natural fibers [29]. Animal fibers contain protein as their major component, whereas mineral fibers exist within the asbestos group of minerals. Now-a-days, these fibers are avoided due to associated health problems and are banned in many countries [30]. Plant fibers obtain higher stiffness and strengths than the readily available animal fibers. In India, natural fibers such as jute, banana, bamboo, cotton, coir, pineapple, sisal, and ramie are available abundantly for the development of natural fiber based composites primarily to explore the value added application avenues.

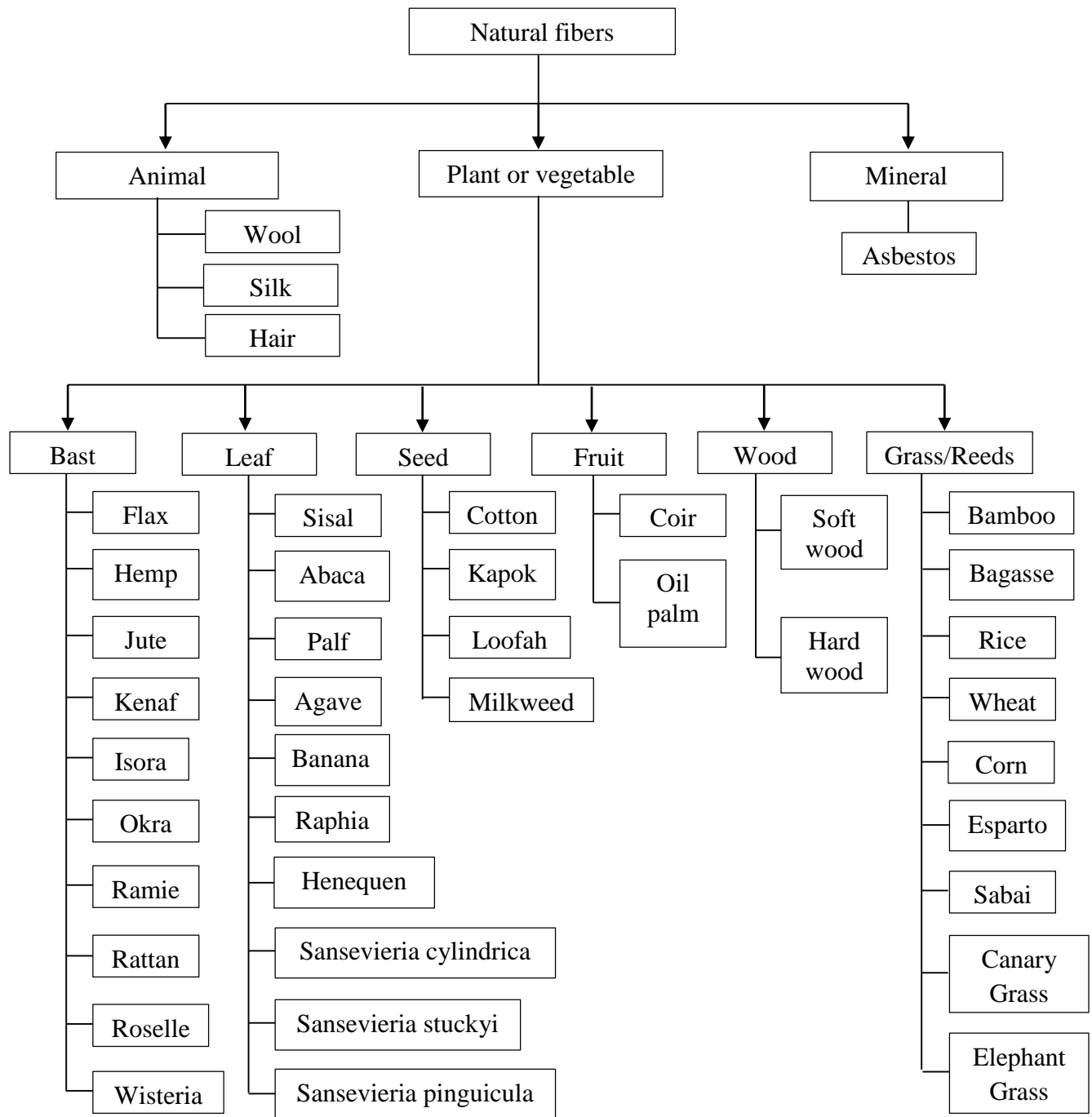


Figure 2.1: Classification of natural fibers [29]

The annual production of few natural fibers and their geographical distribution is presented in Table 2.1 [31]–[33]. The properties of natural fibers mainly depend on the nature of the plant, age of the plant, locality in which it is grown, and the extraction method

used. Table 2.2 presents the physical and mechanical properties of some natural fibers [34], [35]. Physical properties such as crystalline packing order, morphology, amorphous content regularity or irregularity along and across the fiber main axis, and chemical composition of the fibers have an influence on the strength of the fiber [36]. Natural fibers are generally lignocelluloses in nature, consisting of helically wound cellulose micro fibrils in a matrix of lignin and hemicellulose [37]. The microstructure of natural fiber is shown in Figure 2.2 [38]. The main constituents of natural fiber or plant fiber are cellulose, hemicellulose, lignin, pectin, waxes and some water-soluble compounds [39]. The property of each constituent contributes to the overall properties of the fiber. Characterization of natural fiber can be done based on its cellular structure. Each cell of fiber comprises of crystalline cellulose regions (microfibrils) which are interconnected via hemicellulose and lignin fragments.

Table 2.1: Annual production of natural fibers and their producers [31]–[33]

Fiber source	Botanical name	World production (10 ³ tonnes)	Largest Producers
Bamboo	<i>Gigantochloa scortechinii</i>	30,000	India, China, Indonesia
Jute	<i>Corchorus capsularis</i>	2300	India, China, Bangladesh
Kenaf	<i>Hibiscus cannabinus</i>	970	India, Bangladesh, USA
Flax	<i>Linum usitatissimum</i>	830	Canada, France, Belgium
Sisal	<i>Agave sisilana</i>	378	Tanzania, Brazil
Roselle	<i>Hibiscus sabdariffa</i>	250	China, Thailand
Hemp	<i>Cannabis sativa</i> L	214	China, France, Philippines
Banana	<i>Musa sapientum</i>	200	India, Sri Lanka
Coir	<i>Cocos nucifera</i> L	100	India, Sri Lanka
Ramie	<i>Boehmeria nivea</i> Gaud	100	China, Brazil, Philippines, India
Abaca	<i>Musa textilis</i>	70	Philippines, Ecuador, Costa Rica
Bagasse	<i>Saccharum officinarum</i> L	75,000	Brazil, India, China
Cotton Lint	<i>Gossypium</i> spp	18,500	China, India, USA
Wood	>10,000 species	1, 750,000	-

Table 2.2: Physical and mechanical properties of natural fibers [34], [35]

Fiber	Density (g/cm ³)	Elongation (%)	Tensile strength (MPa)	Young's modulus (GPa)
Abaca	1.5	3-10	400	12
Alfa	0.89	5.8	350	22
Bagasse	1.25	-	290	17
Bamboo	0.6-1.1	-	140-230	11-17
Banana	1.35	5.9	500	12
Coir	1.2	30	175	4-6
Cotton	1.5-1.6	7-8	287-597	5.5-12.6
Curaua	1.4	3.7-4.3	500-1,150	11.8
Date palm	1-1.2	2-4.5	97-196	2.5-5.4
Flax	1.5	2.7-3.2	345-1,035	27.6
Hemp	1.48	1.6	690	70
Henequen	1.2	4.8 ± 1.1	500 ± 70	13.2 ± 3.1
Isora	1.2-1.3	5-6	500-600	-
Jute	1.3	1.5-1.8	393-773	26.5
Kapok	1.47	2-4	45-64	1.73-2.55
Kenaf	1.31	1.6	930	53
Nettle	-	1.7	650	38
Oil palm	0.7-1.55	25	248	3.2
Okra	-	4-8	184-557.3	8.9-11.8
Petiole bark	-	2.1	185.52	15.09
Piassava	1.4	21.9-7.8	134-143	1.07-4.59
Pineapple	0.8-1.6	14.5	400-627	1.44
Rachilla	0.65	8.1	61.36	2.34
Rachis	0.61	13.5	74.26	2.31
Ramie	1.5	2.5	560	24.5
Roselle	-	5-8	147-184	2.76
Sisal	1.5	2.0-2.5	511-635	9.4-22
Spatha	0.69	6	75.66	3.14

The natural fiber cell walls are divided into two sections, the primary wall and the secondary wall. The primary wall is the first layer deposited during cell growth surrounding a secondary wall. The secondary wall consists of three distant layers i.e. S1 (outer layer), S2

(middle layer) and S3 (inner layer). Middle layer is the thickest and the most important to determine the mechanical properties of the fiber [34]. The middle layer contains a series of helically wound cellular microfibrils formed from long chain cellulose molecules: the angle between the fiber axis and the microfibrils is called the microfibrillar angle. It is observed that the higher fiber strength takes place when the microfibrils are arranged more parallel to the fiber axis [29].

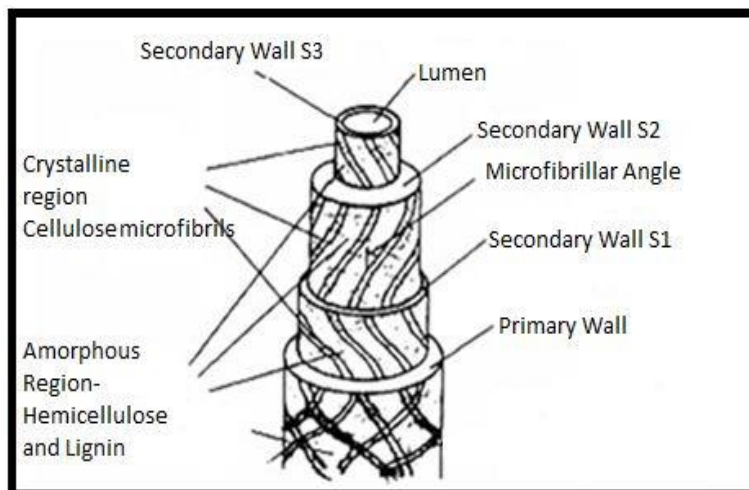


Figure 2.2: Structure of natural fiber [38]

Cellulose is the major framework constituent of the fiber and provides the stiffness strength, and structural stability of the fiber [40]. Hemicellulose comprises of short, highly branched chains of sugars. Hemicellulose is hydrophilic in nature, soluble in alkali and easily hydrolyzed in acids [34]. It occurs mainly in the primary cell wall and have branched polymers carbon sugars with varied chemical structure [40]. Lignin is a complex hydrocarbon polymer with aliphatic and aromatic constituents. Its molecules are three-dimensional and are heavily cross-linked polymer network. The distinct cells of hard plant fibers are bonded together by lignin, acting like a cementing material. Lignin is less polar than cellulose and acts as a chemical adhesive within and between fibers [41]. Lignin and hemicellulose contributes to the characteristic properties of fiber. Toughness depends on the hemicellulose and lignin content of the plant fiber. It decreases with the decrease in the amount of lignin and/or hemicellulose, while at the same time the stiffness and strength of the fiber increases up to a limit [33]. Pectins form a collective of highly heterogeneous and branched polysaccharides those are rich in D-galacturonic acid residues. It provides flexibility to plant fibers. Waxes make up the last part of fibers and they consist of different types of alcohols. The physical properties of natural fibers are mainly influenced by their

chemical and physical composition, such as cellulose content, structure of fibers, angle of fibrils, degree of polymerization, crystallinity and orientation of fibers [42]. Table 2.3 shows the chemical composition of some natural fibers. Fibers with higher degree of polymerization, higher cellulose content, small fiber diameter, high aspect ratio and a lower microfibrillar angle exhibit higher tensile strength and modulus [36], [43].

Table 2.3: Chemical properties of natural fibers [34], [35]

Fiber	Cellulose (wt.%)	Hemicellulose (wt.%)	Lignin (wt.%)	Waxes (wt.%)
Abaca	56–63	20–25	7–9	3
Agave	68.42	4.85	4.85	0.26
Alfa	45.4	38.5	14.9	2
Bagasse	55.2	16.8	25.3	-
Bamboo	26–43	30	21–31	-
Banana	63–64	19	5	-
Coir	32–43	0.15–0.25	40–45	-
Coniferous	40–45	-	26–34	-
Cotton	85–90	5.7	-	0.6
Curaua	73.6	9.9	7.5	-
Deciduous	38–49	-	23–30	-
Flax	71	18.6–20.6	2.2	1.5
Hemp	68	15	10	0.8
Henequen	60	28	8	0.5
Isora	74	-	23	1.09
Jute	61–71	14–20	12–13	0.5
Kenaf	72	20.3	9	-
Kudzu	33	11.6	14	-
Nettle	86	10	-	4
Oat	31–48	-	16–19	-
Piassava	28.6	25.8	45	-
Pineapple	81	-	12.7	-
Ramie	68.6–76.2	13–16	0.6–0.7	0.3
Rice husk	38–45	12–20	-	-
Sisal	65	12	9.9	2
Sponge gourd	63	19.4	11.2	3

Recently, the rapidly increasing environmental awareness, increasing crude oil prices, growing global waste problem and high processing cost trigger the development concepts of sustainability and reconsideration of renewable resources. The use of natural fibers, derived from annually renewable resources, as reinforcing materials in both thermoplastic and thermoset matrix composites provides positive environmental benefits with respect to ultimate disposability and raw material utilization [44]. The advantages associated with the use of natural fibers as reinforcement in polymers are their availability, non-abrasive nature, low energy consumption, biodegradability and low cost. In addition, natural fibers have low density and high specific properties. The specific mechanical properties of these fibers are comparable to those of traditional reinforcements. The natural fiber reinforced polymer composites are more environmentally friendly, and are used frequently in transportation (railway coaches, automobiles, aerospace), military applications, building and construction industries (ceiling paneling, partition boards), packaging etc. A number of investigations have been carried out to assess the potential of natural fibers as reinforcement in both thermosetting and thermoplastic matrices as reported in Table 2.4.

Table 2.4: Thermosetting and thermoplastic matrix based natural fiber composites

Fiber	Thermosetting matrix	Thermoplastic matrix	References
Bagasse	Phenolic	Polypropylene	[45], [46]
Bamboo	Epoxy, Polyester	Polypropylene	[47]–[49]
Banana	Polyester, Phenolic		[50], [51]
Cellulose	Epoxy	Polypropylene, Polyethylene	[52]–[54]
Coir	Polyester		[55]
Cotton	Polyester		[56]
Flax	Epoxy	Polypropylene, Polyethylene	[57]–[59]
Hemp	Epoxy, Polyester, Vinylester		[60]–[62]
Jute	Epoxy, Polyester, Vinylester	Polypropylene	[63]–[66]
Kenaf	Epoxy, Phenolic	Polypropylene	[44], [67], [68]
Oil palm	Polyester, Phenolic		[69], [70]
Pineapple	Polyester, Phenolic	Polyethylene	[71]–[73]
Ramie		Polypropylene	[74]
Sisal	Epoxy, Polyester	Polypropylene, Polyethylene	[75]–[78]
Wood flour	Polyester	Polypropylene, Polyethylene	[79]–[81]

2.2 On Mechanical and Physical Behaviour of Natural Fiber Reinforced Polymer Composites

Many of the composite materials during its service life are exposed to different types of forces or loads. Thus, it is very important to understand the mechanical behaviour of composite materials so that the product made from it will not result in any failure during its life cycle. An adequate knowledge of mechanical properties of material helps in selection of its suitable applications. Tensile modulus and strength, flexural modulus and strength, inter-laminar shear strength, impact strength and hardness are the important mechanical properties of the fiber reinforced polymer composites. Most of the studies reveal that the mechanical properties of natural fiber reinforced composites are affected by a number of parameters such as fiber loading, fiber orientation, fiber aspect ratio, fiber dispersion, fiber-matrix adhesion, fiber geometry and stress transfer at the interface [82]. Therefore, both the matrix and fiber properties are important in improving mechanical properties of the composites. A great deal of work has already been done on the effect of various factors on mechanical behavior of natural fiber reinforced polymer composites [72], [83]–[88]. Many researchers in the past have studied the performance of hybrid composites using synthetic-natural fibers such as banana/glass [89], jute/glass [90], sisal/glass [91], oil palm/glass [92], pineapple/glass [93], kenaf/glass [94] and sugar palm/glass [95]. Bhagat et al. [96] studied the physical and mechanical behavior of coir/glass fiber reinforced epoxy based hybrid composites. The effect of fiber loading and length on the mechanical properties like flexural strength, tensile strength, and hardness of composites were studied. Karina et al. [97] investigated the mechanical properties of oil palm empty fruit bunch/glass fiber reinforced polyester composites at 15 vol% of fiber loading and found that the addition of 40% of oil palm empty fruit bunch fiber in 60% of glass fiber resulted in same mechanical properties with glass fiber reinforced polyester composites. Research on various aspects of banana fiber reinforced polymer composites using polyester as the matrix material has been reported by few investigators [87], [98], [99]. The mechanical behaviour of natural fibers like sisal, jowar, bamboo and PALF (pineapple leaf fiber) in various matrices has been studied by Prasad et al. [100] and Arib et al. [101].

In structural applications, tensile modulus and strength are considered as most important material properties. The tensile modulus and strength of composite is more sensitive to fiber and matrix properties [102]. The tensile properties of composites mainly depend on the modulus and strength of fibers, the chemical stability and strength of the resin and the bonding between the fibers and matrix in transferring stress across the interface [12].

The tensile properties such as tensile modulus and tensile strength of napier grass fiber reinforced polyester based composites has been reported by previous reserchers [103], [104]. Khanam et al. [105] evaluated the effect of fiber length on the tensile strength of short sisal/silk fiber reinforced hybrid composites and observed that the tensile strength is slightly higher for the 20 mm fiber length based composites as compared to the 10 mm and 30 mm fiber length based composites. Sreekumar et al. [106] studied the tensile properties of sisal leaf fiber reinforced composites fabricated by compression and resin transfer moulding techniques and concluded that the composites prepared by resin transfer moulding obtain the maximum tensile modulus and strength at 43 vol.% of fiber loading and 30 mm fiber length. Kiran et al. [107] evaluated the tensile strength of natural fibers like sun hemp, sisal and banana fiber reinforced polyester composites and found that the tensile strength of 30 mm fiber length based composites increased gradually from 0 wt. % to 55 wt. % of fiber and then there is a drop in tensile strength. Thakur and Singha [108] investigated the mechanical and wear properties of pine needles reinforced phenol-formaldehyde composite and observed that the properties of the composite is better than the parent polymeric phenol-formaldehyde matrix. Athijayamani et al. [109] investigated the tensile strength of roselle/sisal fiber reinforced polyester hybrid composites at different fiber lengths and weight ratio and concluded that the tensile strength increased with the fiber loading and fiber length. Kumar et al. [110] prepared tri layer hybrid fiber reinforced polyester composites based on sisal and coconut sheath fibers with six different stacking sequences and observed that the tensile strength of hybrid composite having coconut sheath as skin and sisal as core material is slightly higher than the other stacking sequences. Hepworth et al. [111] fabricated the unidirectional hemp fiber reinforced epoxy composites by pinning-decortications and hand combing with a fiber volume fraction of 0.2 and found the maximum tensile modulus of 8 GPa and tensile strength of 90 MPa. The longitudinal and transverse tensile properties of short sisal fiber reinforced starch-based composites has been investigated by Alvarez et al. [112] and observed that the tensile properties for longitudinally oriented samples displayed much higher values than transversally oriented samples.

Flexural properties are also another important mechanical property for any material. In flexural testing, different mechanisms such as compression, tension, and shearing takes place instantaneously [113]. Several investigations have also been done on the flexural behaviour of natural fiber reinforced polymer composites. Khanam et al. [105] studied the effect of the fiber length on the flexural strength of short sisal/silk fiber reinforced hybrid composites and found that 20 mm fiber length based composites exhibit higher flexural strength than 10 mm and 30 mm based composites. Gowda et al. [12] evaluated the flexural

properties of jute fiber reinforced polyester composites. Sana et al. [114] investigated the effect fiber weight ratio on the flexural behaviour of Typha fiber reinforced polyester composites and found the maximum flexural modulus and strength of 6.16 GPa and 69.8 MPa, respectively at 12.6 % fiber weight ratio. Van de Weyenberg et al. [115] evaluated the flexural behaviour of unidirectional flax fiber reinforced composites in both longitudinal and transverse direction and observed that the flexural modulus and strength of composites attained in longitudinal direction is better than the transverse direction and epoxy resin. Athijayamani et al. [109] investigated the flexural strength of roselle/sisal fiber reinforced composites and found the maximum flexural strength of 76.3 MPa at 30 wt. % of fiber content and 150 mm fiber length. Shibata et al. [116] studied the flexural modulus of the unidirectional composites made from bamboo and kenaf fibers and found that the flexural modulus of the composite increased with increasing fiber volume fraction up to 60% for kenaf fiber and 72% for bamboo fiber. Osorio et al. [117] evaluated the flexural properties of unidirectional long bamboo fiber reinforced epoxy composites along the longitudinal and transverse direction and concluded that the flexural properties in the longitudinal direction is higher than in the transverse direction. Tao et al. [118] studied the flexural strength of short jute/PLA composites and reported an increase in flexural strength at fiber content up to 30 %. Mohanty et al. [119] investigated the flexural strength of jute-polyester amide composites and reported an increase in flexural strength for fiber loading from 20 to 32 wt. %.

Inter-laminar shear strength (ILSS) may be defined as the resistance of a laminated composite to internal forces that tend to induce relative motion parallel to, and between the laminae [120]. ILSS of composites is mainly depends on matrix properties rather than the fiber properties [121]. ILSS is often used as a key measure in judging the soundness of fiber matrix interface [122]. Hamdan et al. [123] investigated the ILSS of treated and untreated kenaf fiber reinforced epoxy composites and reported that the ILSS of the composites with untreated fiber is higher than the composite with treated fibers. Romanzini et al. [124] studied the ILSS of glass-ramie fiber reinforced polyester composites at different volume ratio of glass and ramie (0:100, 25:75, 50:50, and 75:25) and concluded that the maximum ILSS value of 18 MPa occurred for 75:25 composite at fiber loading of 31 vol. %. Gowda et al. [12] studied the ILSS of the jute fiber reinforced polyester composites and found that the average ILSS of the composites is 10 MPa. Arun et al. [125] studied the ILSS of glass/ silk fabric reinforced polymer hybrid composites under normal condition and sea water environments and reported that the equal percentage of glass and silk fabric reinforced composites shows higher ILSS. Reddy et al. [126] investigated the influence of fiber loading, hybridization, and surface modification on the ILSS of the kapok/glass fiber reinforced

hybrid composites and concluded that hybridization is the most significant factor in influencing the ILSS composites. Zhang et al. [127] studied the ILSS of unidirectional flax and glass reinforced hybrid composites and reported that the ILSS of the hybrid composites improved compared to glass fiber reinforced composites. Das and Bhowmick [128] investigated the ILSS of raw jute and jute sliver fiber reinforced composites with three different fiber loading (25, 35, and 44 (w/w) %) and found that the ILSS properties of composites with 25 (w/w) % fiber loading made from raw jute is found to be higher than composites made from jute sliver.

Impact strength shows the ability of the material to absorb impact energy. The fiber reinforcement plays an important role in the impact resistance of the composite materials as they interact with the crack formation in the matrix and act as stress transferring medium [129]. A great deal of work has been done by researchers on impact strength of natural fiber reinforced polymer composites. Romanzini et al. [124] evaluated the impact strength of glass-ramie fiber reinforced polyester composites at 10, 21 and 31 vol. % of fiber content and found that the hybrid composites showed higher impact strength than the pure polyester resin. Gowda et al. [12] studied the impact properties of jute fiber reinforced polyester composites and observed the maximum impact energy of 1.76 Kj/m² and 29 Kj/m² for neat polyester resin and jute fiber reinforced polyester composites, respectively. An attempt has been made by Kumar et al. [110] to examine the impact strength of coconut sheath (CS) and sisal (S) fiber reinforced hybrid composites and found that the impact strength of hybrid composites is higher than the pure coconut sheath and sisal fiber based composites. Also, reported that the hybrid composite with CS/S/CS sequence shows better impact strength than composites with other sequences. Öztürk et al. [130] studied the impact behaviour of jute/rockwool reinforced phenol formaldehyde (PF) composites by varying fiber loadings (16, 25, 34, 42, 50, and 60 vol.%) and found that the impact strength of jute/PF composite increased with jute fiber loading up to 50 vol.%. Dhakal et al. [131] investigated the impact energy of non-woven hemp fiber reinforced unsaturated polyester composites at different volume fractions of hemp fiber (0, 0.06, 0.10, 0.15, 0.21 and 0.26). They reported that at higher fiber volume fractions, the failure mode of the composites is more ductile with correspondingly higher energy absorption characteristics and at lower fiber volume fractions the composite exhibit brittle fracture behaviour. Mylsamy and Rajendran [132] evaluated the influence of fiber length (3 mm, 7 mm and 10 mm) on impact strength of short agave fiber reinforced epoxy composites and reported that the impact strength increased linearly with decreasing fiber length from 10 mm to 3 mm.

Hardness is defined as the resistance of material to permanent deformation such as scratch or indentation. A number of studies have been done on the hardness test of natural fiber reinforced composites. Kumar et al. [91] evaluated the effect of fiber length on the hardness of sisal-glass fiber reinforced epoxy based hybrid composites using Rockwell hardness tester and found that the 20 mm fiber length based composites had a higher hardness than 10 and 30 mm fiber length based composites. Rezaei et al. [133] evaluated the effect of fiber length and fiber content on hardness of short carbon fiber reinforced polypropylene composite and reported that the hardness of composite increases with carbon fiber and it is relative to fiber loading and modulus of the composite. Srinivasa and Bharath [134] studied the hardness of areca fiber reinforced epoxy composites and found that the incorporation of areca fibers inside epoxy increases the hardness of composites. Reddy et al. [135] determined the hardness of the short uniaxially oriented kapok/glass polyester hybrid composites by keeping the volume ratios of kapok to glass at 3:1, 1:1, and 1:3 at constant fiber volume percentage of 9 vol% and found that the maximum hardness of kapok/glass composites is observed at 1:3 volume ratio of kapok and glass fiber. The micro-hardness of the bagasse/sugarcane fiber reinforced unsaturated polyester composites is studied by Oladele [136]. The investigation revealed that the micro-hardness of composite increases due to adequate wetting and bonding between the sugarcane fiber and the polyester.

A number of studies have also been devoted to the physical properties of natural fiber reinforced polymer composites. Aseer et al. [137] studied the water absorption behavior of municipal solid waste/banana fiber reinforced urea formaldehyde composites and found that by addition banana fiber in to the municipal solid waste increased the water absorption properties of composites. Similarly, an investigation on bamboo fiber reinforced epoxy composite exhibited that by the addition of cenosphere particulate filler decreases the water absorption capacity [138]. The effect of fiber loading on moisture absorption behaviour a of Lantana camara fiber reinforced epoxy composites is studied by Deo and Acharya [139]. The study revealed that moisture absorption increases with fiber loading due to increased voids and cellulose content and the fabricated composites followed the kinetics of Fickian diffusion. Alamri et al. [140] carried out a study on water absorption characteristics of recycled cellulose fiber reinforced epoxy composites and the study revealed that the values of maximum water absorption and diffusion coefficient were increase with an increase in fiber loading. Tajvidi et al. [141] compared the water absorption of different natural fiber (wood flour, rice hulls, newsprint fibers, and kenaf fibers) reinforced polypropylene composites at room temperature for 5 weeks and found that the water diffusion coefficients of the composites were about 3 orders of magnitude higher than that of pure polypropylene. The

effect of fiber surface modification on the water absorption characteristics of sisal fiber reinforced polyester composites has been investigated by Sreekumar et al. [142] and concluded that the water absorption, diffusion, sorption and permeability coefficients were decreased after the surface treatment as compared to the untreated composites. Panthapulakkal et al. [143] studied the effect of hybridization on the water absorption and the kinetics of water absorption of the hemp-glass fiber reinforced polypropylene composites and reported that the incorporation of glass fiber in hemp fiber reinforced composites improve the moisture resistance significantly at 40 wt.% of fiber loading.

2.3 On Thermal Behaviour of Natural Fiber Reinforced Polymer Composites

An understanding of the thermal characteristics of the natural fiber reinforced polymer composites is extremely important in the structure-property relationship and industrial production. Generally, the fiber reinforced polymer composite processing techniques are based on heating and understanding the processing temperature is very important to find the thermal properties for optimizing and controlling the manufacturing process. The temperature dependent properties (thermal conductivity, specific heat capacity, thermal diffusivity, and some other parameters) of the composite materials are based on the solution of the coefficient inverse heat transfer problems. A great deal of work has already been done on the thermal behaviour of natural fiber reinforced polymer composites. Takagi et al. [144] evaluated the theoretical and experimental thermal conductivity of the bamboo and abaca fibers and found that the thermal conductivity of the bamboo fiber reinforced composites increases with the increase in fiber loading. On the other hand that of abaca fiber reinforced composites decreases due to the air filled in the lumens in the abaca fibers. Melo et al.[145] determined the transverse thermal conductivity of the sisal fiber reinforced polyester composites. In another study, Takagi et al. [146] fabricated the green composites with bamboo fibers and poly lactic acid (PLA) by using conventional hot pressing method to calculate the thermal conductivity and found that the thermal conductivity of the bamboo fiber reinforced composites is lower than the glass fiber and carbon fiber reinforced plastics. Ramanaiah et al. [147], [148] studied the thermal properties of biodegradable natural fiber reinforced polyester composites by experimentally and analytically and found that the values of thermal conductivities obtained from empirical models were in good agreement with the experimentally measured values. Also, reported that these biodegradable natural fibers exhibited good thermal insulating properties. Kim et al. [149] carried out a systematic study on thermal conductivity of several natural fiber (kenaf/hemp/flax/sisal) reinforced

polypropylene composites and found that the thermal conductivity is in the range of 0.05-0.07W/m-K at 48.5 wt. % of natural fiber. Luo and Netravali [150] studied the thermal behaviour of unidirectional pineapple leaf fiber (PALF) reinforced poly hydrobutyrate-co-valerate (PHBV) composites using differential scanning calorimetry (DSC) and thermogravimetric analysis (TGA) and reported that there is no effect of the fiber content on the thermal properties of the resin because of the poor interaction between the hydrophobic PHBV resin and hydrophilic PALF. In another study, Chollakup et al. [151] investigated the effect of fiber length (long and short fibers) and fiber content on the thermal characteristics of PALF reinforced Polypropylene (PP) and lowdensity polyethylene (LDPE) composites and confirmed from the DSC results that the decrease of crystallinity in the PALF reinforced thermoplastic composites is due to the interruption of fiber migration and diffusion of polymer chains in the crystal formation.

Kuranska and Prociak [152] evaluated the effect of fiber length and fiber content of flax and hemp fibers on thermal conductivity of rigid polyurethane composites and observed that the composite with 0.5 mm fiber length of flax fiber shows the good thermal insulation. Yusriah et al. [153] studied the thermal conductivity, thermal diffusivity and thermal degradation properties of betel nut husk (BNH) fiber reinforced vinyl ester (VE) composites and reported that the thermal conductivity, thermal diffusivity and thermal stability of the composites decreases with the increase in ripe BNH fiber content. Ramanaiah et al. [154] investigated on the thermo-physical properties of Vakka natural fiber reinforced polyester composites. The study revealed that the thermal conductivity of the composites decreased from 6.53% to 26.94% over pure matrix against increase of volume fraction from 0.164 to 0.352, respectively. Mangal et al. [73] evaluated the effective thermal conductivity and thermal diffusivity of pineapple leaf fiber (PALF) reinforced phenolformaldehyde (PF) composites by using transient plane source technique. The effect of different weight percentage (15, 20, 30, 40 and 50%) on these properties has been investigated. The experimental investigation revealed that with increase in the weight percentage of PALF, the thermal conductivity of the composite decreases due to the lower thermal conductivity of the PALF (0.21 W/m-K) than the thermal conductivity of the PF matrix (0.34 W/m-K). On the other hand, the thermal diffusivity of the composite is also show the similar trend because it is directly proportional to the conductivity. Majumdar et al. [155] investigated the thermal properties of three different knitted fabric structures made from cotton, regenerated bamboo and cotton-bamboo blended yarns and found that with addition of bamboo fiber, the thermal conductivity of knitted fabrics decreased. Among the three knitted structures, the thermal conductivity and thermal resistance values of plain knitted fabrics show the minimum

followed by the rib and interlock fabrics. Kawabata and Rengasamy [156] and Rengasamy et al. [157] studied the thermal conductivity of fiber reinforced composites made from different fiber yarns and found that the thermal conductivity values along the longitudinal direction are higher than the values in the transverse direction for all types of fibers. Aji et al. [158] studied the thermogravimetric and derivative thermogravimetric analysis of kenaf/PALF fiber reinforced HDPE hybrid composites and reported the improvement of thermal stability of hybrid composites at lower fiber loading. Chikhi et al. [159] developed a new biocomposite material made of gypsum and date palm fiber for thermal insulation purpose and investigated the effect of fiber loading on thermal conductivity, water absorption and mechanical properties.

Li et al. [160] evaluated the thermal diffusivity, thermal conductivity, and specific heat properties of flax fiber reinforced high density polyethylene biocomposites by varying the weight fraction of the flax fiber and found that the properties are decreased with increasing fiber loading and there is no significant effect with temperature range of 170-200°C. Kalaprasad et al. [161] studied the thermal conductivity and thermal diffusivity of sisal, glass, and sisal/glass hybrid fiber reinforced polyethylene composites and observed that the variation of thermal diffusivity with temperature is just opposite to that of thermal conductivity. Few researchers [162], [163] have also studied the thermal conductivity of bamboo fiber reinforced composites and observed that these composites shows low thermal conductivities. Also, reported that these composites can be used in automotive industry and low-energy building design to save energy by reducing rate of heat transfer. Azwa and Yousif [164] studied the thermal degradation of treated and untreated kenaf fiber reinforced epoxy composites by thermo gravimetric analysis. From their study, the addition of fibers into the epoxy matrix improves the charring capability of the specimens as well as its thermal stability. Manfredi et al. [165] investigated the thermal degradation of jute, sisal, and flax fiber reinforced composites and concluded that the flax fiber composite exhibit the good thermal resistance due to their low lignin content among the other natural fibers. Trigui et al. [166] studied the thermal conductivity and diffusivity of the maize fiber reinforced high density polyethylene composites with fiber loading in the range 10–40 wt.%. The study revealed that the properties of the composites decrease with fiber content. Sweeting et al. [167] developed a new experimental method to determine thermal conductivities of polymer matrix composites along the in-plane and through-thickness directions. The validation of the method is conducted using aluminium alloy composites with known thermal properties, and excellent correlation is found between the known and experimentally determined thermal conductivities. Agrawal et al. [168] evaluated the thermal conductivity and thermal

diffusivity properties of untreated and treated oil palm fiber reinforced phenolformaldehyde composites using transient plane source technique. They have concluded that the thermal properties of the composites increased after silane and alkali treatments of fibers as compared to the untreated composites.

2.4 On Banana and Jute Fiber Reinforced Polymer Composites

Among various natural fibers, jute (*Corchorus capsularis*) and banana (*Musa Sapientum*) fibers have the potential to be used as reinforcement in polymer composites which is abundantly available in countries like India, Sri Lanka, and some of the African countries but are not optimally utilized [11]. The inborn properties of jute fiber such as low density, low elongation at break and its specific stiffness and strength comparable to those of glass fiber draws the attention of the world. It is a well-known fact that banana is one of the oldest cultivated plants in the world. Banana fiber can be easily obtained from the pseudo stem after the fruits and leafs are utilized. It is also considered as a potential reinforcement for polymer composites due to its many advantages. Furthermore, banana grows to its mature size in only 10 months, whereas wood takes a minimum of 10 years [169]. Thus, considerable research and development efforts need to be undertaken in finding useful utilization of the banana fiber. This will also surely help in solving the environmental problems related to the disposal of banana fibrous wastes. Although a great deal of work has been done on the various properties of jute and banana fiber reinforced polymer composites, the work done on the mechanical and thermal behaviour of these fibers as reinforcement in polymer composites is reported below:

2.4.1 On Mechanical Properties

The effect of the fiber loading and fiber length on mechanical properties of short banana fiber reinforced epoxy composites has been investigated by several researchers [170], [171]. Sreekumar et al. [172] studied the fiber length and fiber loading on mechanical behaviour of short banana fiber reinforced polyester composites fabricated by resin transfer molding technique and reported that the impact strength is maximum for composite having fiber length of 30 mm and fiber loading of 40 vol %. Idicula et al. [42] evaluated the mechanical properties of hybrid composites by adding the short banana/sisal fiber as a reinforcement material and observed that the composite fabricated at 0.40 volume fraction showed better performance with relative volume fraction of banana and sisal fiber as 3:1. This study also reported that the banana as the skin material and sisal as the core material gives slightly

higher tensile properties as compared to other composites. Venkateshwaran et al. [173] studied the tensile and water absorption behavior of randomly oriented banana/sisal reinforced hybrid composites and the results are compared with analytical methods. Haneefa et al. [89] evaluated the influence of volume fraction of fiber and hybrid effect on the tensile and flexural properties of banana/glass fiber reinforced hybrid composites. They reported that the modification of the banana fiber improves the tensile and flexural properties. Herrera-Estrada et al. [174] studied the flexural strength of short banana fiber reinforced eco-polyester composites and compared them with the banana fiber/epoxy composites and observed that the flexural strength of polyester based composite is 14.78% higher than the epoxy based composite. Jawaid et al. [175] investigated the effect of layering sequence on the flexural properties of woven jute (Jw) and oil palm empty fruit bunch (EFB) reinforced epoxy based hybrid composites and observed that the flexural modulus and strength of Jw/EFB/Jw hybrid composite shows higher values than EFB/Jw/EFB, Jute/EFB/Jute and EFB/Jute/EFB. Samal et al. [176] evaluated the mechanical properties of banana-glass fiber reinforced polypropylene hybrid composites and the results are compared with the banana fiber reinforced polypropylene composites. Pothan et al. [177] studied the static and dynamic mechanical properties of banana/glass woven fabric reinforced polyester composites and reported that banana fiber reinforced polyester composites shows better fiber/matrix bonding at 40% fiber loading as compared to 10 and 20% fiber loading. The effect of glass fiber hybridization with the randomly oriented banana and sisal fiber has been studied by Arthanarieswaran et al. [178]. This study concluded that the tensile, flexural and impact properties are affected by the factors such as formation of micro cracks, presence of voids, poor adhesion between fiber and matrix, and fiber pullout. Ramesh et al. [179] investigated the mechanical properties such as tensile, flexural and impact strength of sisal-jute-glass fiber reinforced polyester composites and observed that the incorporation of sisal-jute fiber with glass fiber in polymer composites can improve the properties. Saw et al. [180] studied the physical and mechanical properties of jute-coir fiber reinforced epoxy based hybrid composites and found that the hybridization of coir fibers with jute fibers can improve the density, dimensional stability and extensibility of pure coir fiber based composites.

The effect of the stacking sequence on mechanical properties of jute and glass fiber reinforced hybrid composites has been studied by Gujjala et al. [90] and Ahmed and Vijayarangan [181]. Their study reported that the tensile, flexural and interlaminar shear properties of hybrid composites with glass fibers as extreme layers on both sides shows good improvement in properties. Sapuan et al. [182] carried out the tensile and flexural tests on woven banana fiber reinforced epoxy composites and found that the maximum Young's

modulus value along longitudinal and transverse direction is 0.976 GPa and 0.863 GPa and stress in longitudinal and transverse direction is 14.14 MPa and 3.398 MPa, respectively. Satapathy et al. [183] studied the effect of fiber loading on mechanical properties of jute fiber reinforced epoxy composites and found that the tensile strength, flexural strength and ILSS of jute fiber reinforced epoxy composites increases with the fiber loading. Mariatti et al. [184] investigated the flexural and impact strength of banana and pandanus woven fiber reinforced unsaturated polyester composites and concluded that the banana fiber composites exhibit higher flexural and impact strength compared to that of pandanus fiber composites. Srinivasan et al. [185] studied the mechanical characteristics of hybrid composites consisting of flax, banana and glass fiber and found that the hybrid composite has better tensile, impact, and flexural properties compared to the single glass fiber reinforced composites. Ratna Prasad et al. [169] investigated the flexural properties of banana empty fruit bunch fiber reinforced polyester composites and found that the flexural strength is decreased and the flexural modulus is increased by 33% at a volume fraction of fiber as 0.10. Shanmugam and Thiruchitrabalam [186] studied the tensile strength of alkali treated unidirectional palmyra palm leaf stalk (P) and jute (J) fiber reinforced polyester composites and concluded that the tensile strength of P75J25, P50J50 and P25J75 composites increased by 6%, 12% and 46% respectively compared to the P100 composites. Gowda et al. [12] examined the tensile properties of jute fabric reinforced polyester composites and found that the average values of ultimate tensile modulus, strength and Poisson's ratio of the composites is 7 GPa, 60 MPa and 0.257 respectively, and the corresponding values for polyester resin is 1.4 GPa, 12.1 MPa and 0.38, respectively. Sathishkumar et al. [187] studied the mechanical behaviour of randomly oriented snake grass (SG) fiber with banana (B) and coir (C) fiber reinforced polyester composites and found that the maximum tensile modulus and strength is obtained for the SG/B composites as compared to the SG/C and SG composites. Vijaya Ramnath et al. [188] investigated the tensile, flexural, impact and double shear properties of banana and jute fiber reinforced hybrid composite and concluded that the hybrid composite shows better overall mechanical properties when compared to single fiber based composites.

2.4.2 On Thermal Properties

Idicula et al. [189] evaluated the thermophysical properties of short randomly oriented banana/sisal hybrid fiber reinforced polyester composites at constant fiber loading of 0.40 and concluded that the chemical treatments of the fibers improved the thermal conductivity of the composites in comparison with the untreated fiber composites. Srinivasan et al. [185] evaluated the thermal stability of banana-flax natural fiber reinforced epoxy composite and

found that the hybrid composites of flax and banana with glass fiber have improved the thermal stability with stage decomposition at 365°C and 654°C as compared to the individual composites. Boopalan et al. [190] studied the thermal behaviour of woven jute and banana fiber reinforced epoxy hybrid composites and concluded that the addition of banana fiber in jute/epoxy composites of up to 50% by weight results in increasing the thermal stability of the hybrid composite. Zainudin et al. [191] investigated the effect of resin modification and fiber loading on the thermal stability of banana pseudo-stem reinforced unplasticized polyvinyl chloride composite by means of thermogravimetric analysis. It is found that the thermal stability of composite decreases by incorporation of banana fiber for the case of non-acrylic. Jawaid et al. [192] studied the thermal stability of oil palm/jute bilayer hybrid composites and reported that the thermal stability of oil palm composites increased with incorporation of jute fiber due to higher thermal stability of jute fiber. Sathish et al. [193] fabricated and tested the thermal properties of banana-kenaf fiber reinforced hybrid epoxy composite with different fiber orientation and volume fraction. It is concluded from the thermo gravimetric analysis that the composite with 45° orientation has better flame resistance than other composites. Pujari et al. [194] evaluated the thermal conductivity of the individual banana and jute fiber reinforced epoxy composites by varying the volume fraction of the fiber and compared the experimental results with the results obtained from the theoretical models (Hashin model, Series model, and Maxwell model). It is observed that there is a good agreement between experimental and theoretical results. Sreepathi et al. [195] measured the thermal conductivity of the jute fiber reinforced polyester composites and concluded that the thermal conductivity of unidirectional jute composites in fiber direction (longitudinal) is marginally higher than thermal conductivity of woven jute fabric composites in normal to the fabric (transverse) direction. Ahmad et al. [196] studied the thermal conductivity of chopped jute fiber reinforced epoxy composites with varying mass fraction (0.05-0.35) and fiber length (2-12 mm). They have concluded that the thermal conductivity of the composite decreases with an increase in the fiber content irrespective of the fiber length and the decreasing rate being highest for the fiber length of 2 mm followed by that for the fiber length of 6 and 12 mm.

2.5 On Micromechanical Analysis of Fiber Reinforced Composites

Mechanics of composites has developed during the latter part of the 20th century. Many micromechanical analyses based on both analytical and numerical solutions have been presented in the literature for predicting the mechanical and thermal properties of composite

materials reinforced with either unidirectional or short fibers or particles. Basic analytical approaches have been reported [197]–[199] to predict the composite materials properties, such as, strength, stiffness, and thermal conductivity. The behaviour of orthotropic unidirectional composite materials requires a convention to describe the material axes and is presented in Figure 2.3. Different micromechanical modeling techniques are presented in Figure 2.4.

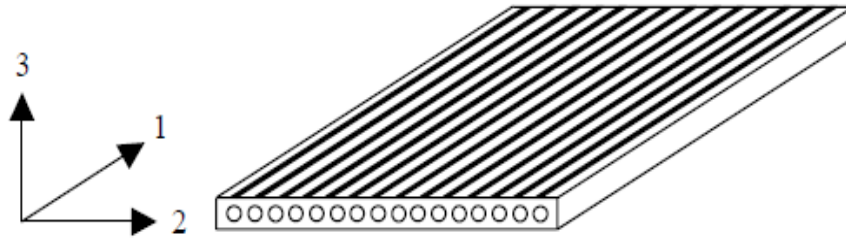


Figure 2.3: Axis system used for unidirectional laminae

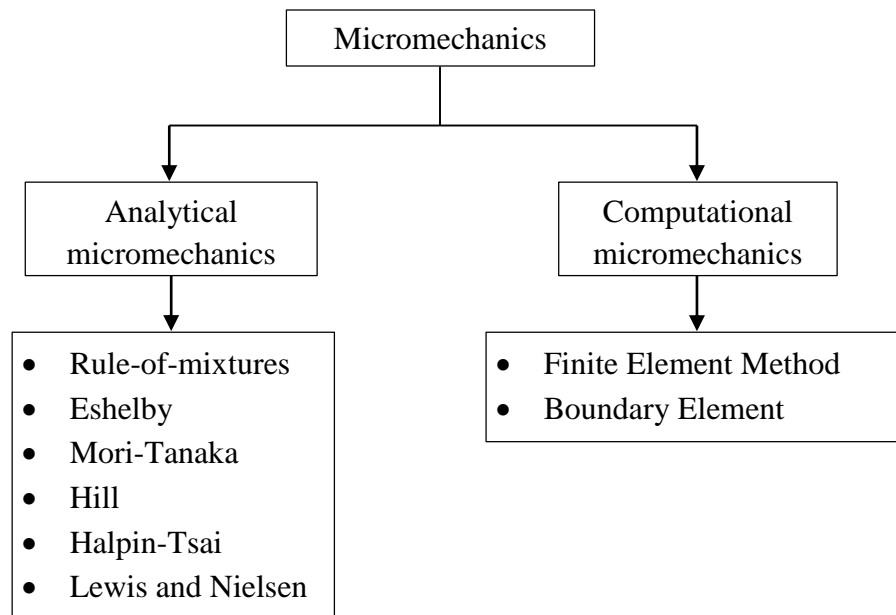


Figure 2.4: Different micromechanical modeling techniques [200]

2.5.1 Existing Analytical Models

In this section, various analytical models for evaluation of elastic and thermal properties of composite materials are reviewed. The methods comprise Voigt and Reuss approximations (rule of mixers), Halpin-Tsai model, and Lewis and Nielsen model and are discussed below:

2.5.1.1 Rule of Mixture

The general model to predict properties of a composite is the rule of mixture, which was first proposed by Voigt and Reuss to predict the mechanical properties of a composite in 1889. This model is also known as parallel or series model with respect to load. The longitudinal property of the composite can be calculated by using parallel model is given in equation 2.1

$$P_1 = P_f \Phi_f + P_m \Phi_m \quad (2.1)$$

Where, P_1 is the longitudinal property of the fiber composite. P_f and P_m are the material properties of fiber and matrix. The transverse property of composite can be calculated by using series model is given in equation 2.2.

$$(1/P_2) = (\Phi_f/P_f) + (\Phi_m/P_m) \quad (2.2)$$

Where, P_2 is the transverse property of the fiber composite in transverse direction.

2.5.1.2 Halpin-Tsai Model

Halpin and Tsai [201] have developed some simple and generalized semi-empirical equations to approximate the properties of composite materials considering the geometry of the reinforcing fiber used. These equations are simple and can be easily used in the design process. Furthermore, the predictions of these equations are good enough as long as the fiber volume fraction does not approach 1. The property of fiber reinforced composite can be calculated by using Halpin-Tsai model is given in equation 2.3.

$$\frac{P}{P_m} = \frac{1 + \xi \eta \Phi_f}{1 - \eta \Phi_f} \quad (2.3)$$

Where $\eta = (P_f/P_m) - 1 / (P_f/P_m) + \xi$

Where ξ is a parameter related to the fiber geometry, usually taking the value of $2L/d$ for longitudinal property of a composite and 2 when calculating the transverse property of a composite with cylindrical fibers [202], [203]. L and d are length and diameter of the fiber, respectively. The value of ξ must be in the range $0 \leq \xi \leq \infty$. When $\xi = 0$, the equation 2.3 becomes the series model described by equation 2.2, while for $\xi = \infty$, the parallel model described by equations 2.1 is replicated.

2.5.1.3 Lewis and Nielsen Model

Lewis and Nielsen [204] derived a semi-theoretical model by a modification of the Halpin-Tsai equation. Lewis and Nielsen include the effect of the shape of the particles and the

orientation or type of packing for a two phase system for calculating the material property. The longitudinal and transverse property of composite can be calculated by using Lewis and Nielsen model is given in equation 2.4.

$$\frac{P}{P_m} = \frac{1+\xi\eta\Phi_f}{1-\Psi\eta\Phi_f} \quad (2.4)$$

Where $\psi = 1 + \left(\frac{1-\phi_m}{\phi_m^2} \right) \times \Phi_f$. The values of ξ and ϕ_m for many geometric shapes and orientation are given in Tables 2.5 and 2.6.

Table 2.5: Value of ξ for various systems [205]

Type of dispersed phase	Direction	ξ
Cubes	Any	2.0
Spheres	Any	1.50
Aggregates of spheres	Any	$(2.5/\phi_m)-1$
Randomly oriented rods aspect ratio=2	Any	1.58
Randomly oriented rods aspect ratio=4	Any	2.08
Randomly oriented rods aspect ratio=6	Any	2.8
Randomly oriented rods aspect ratio=10	Any	4.93
Uniaxially oriented fibers	Parallel to fibers	$2L/D$
Uniaxially oriented fibers	Perpendicular to fibers	0.5

Table 2.6: Value of ϕ_m for various systems [205]

Shape of particle	Type of packing	ϕ_m
Spheres	Face centered cubic	0.7405
Spheres	Body centered cubic	0.60
Spheres	Simple cubic	0.524
Rods or fibers	Uniaxial hexagonal close	0.907
Rods or fibers	Uniaxial simple cubic	0.785
Rods or fibers	Uniaxial random	0.82
Rods or fibers	Three-dimensional random	0.52

2.5.2 On Elastic Properties of Composites

The fiber reinforced composite materials are generally transversely isotropic or orthotropic [206]. This property makes it challenging for the analysts to examine their behavior which is necessary for the design process of any structure. Few researchers have studied the effect of the fiber and matrix properties on the properties of the composite materials using micromechanical methods. Sun et al. [207] proposed a novel modeling approach for designing composite unit cells based on a reasoning Boolean operation. By using a series of Boolean operations they created composite unit cells representing 2D basket weave, 2D woven fabric, 3D unidirectional and 3D tri-axial braided composite. Tucker and Liang [208] provided a good overview on the micromechanical models used to predict the elastic moduli and Poisson's ratios of short fiber reinforced composites. The accuracy of these models is evaluated by comparison with numerical finite element results. They reported that the Mori-Tanaka model gives the most accurate predictions followed by Halpin-Tsai equations. The both square and hexagonal RVEs have been studied extensively by several researchers [209], [210]. Patnaik et al. [211] studied the micromechanical and thermal characteristics of glass fiber reinforced polymer composites and found that the experimental results are in good agreement with the finite element model based on representative area element approach. Babu et al. [212] studied the effective elastic modulus of hybrid composites by using micromechanical modeling based on the generalized method of cells. They also investigated the effect of microstructural parameters such as the concentration, aspect ratio and shape of fillers on elastic properties.

The finite element based homogenization method has been found to be useful for predicting effective material properties of fiber reinforced composites by using micromechanical analysis [213]–[215]. In periodic composite structure, it is not necessary to study the whole structure but only a unit cell or Square RVE and hexagonal RVE are analyzed for predicting elastic modulus. It is found that the square RVE predicts higher values of the elastic modulus than the hexagonal one but with considerable variation. Banerjee and Sankar [216] proposed a micromechanical analysis of hybrid composites with circular fibers in a hexagonal array to evaluate the stiffness and strength properties using FEM. The results were compared with existing empirical and semi empirical relations and found a good match within limits of computational error. Facca et al. [217] predicted the elastic modulus of different types of natural fiber reinforced high-density polyethylene composites by varying the volume fraction of the fibers and found that Halpin-Tsai model is the most accurate amongst others to predict the elastic modulus of natural fiber composites.

Bacarreza et al. [218] predicted the elastic properties of the plain and 3D woven composites using micromechanical modeling analysis. From this study, the problems in modeling are highlighted and recommendations are given for micromechanical analysis using the FEM. Mirbagheri et al. [219] evaluated the elastic modulus of the wood flour/kenaf fiber reinforced polypropylene composites at a fixed fiber loading of 40 wt.% and varying the relative weight ratio of the reinforcement. The investigation revealed that the Rule of hybrid mixture equation shows better with the experimental values than the Halpin–Tsai equation. Pal et al. [220] predicted the elastic properties of polypropylene fiber reinforced composite material by using RVE model. ANSYS software is used to model the composite with different volume fractions (10%, 17%, 27%, 40% and 50%) and found that there is a good agreement between finite element simulation results and the analytical results.

2.5.3 On Thermal Properties of Composites

A great deal of research work has been reported by various researchers on the thermal analysis of fiber reinforced composites. Most of them include the experimental determination of thermal conductivity of fiber reinforced polymer composites. Several researchers made their significant contribution in studying micromechanical thermal characteristics of composite materials. Many theoretical and semi empirical models have been proposed to predict the effective thermal conductivity of composite materials. Comprehensive review articles have discussed the applicability of many of these models [221]–[223]. Prediction of the thermal conductivity of unidirectional fiber reinforced composites along the fibers and normal to the fibers are reported by few reserchers [224]–[226]. Islam and Pramila [227] predicted the effective transverse thermal conductivity of fiber reinforced composites by using FEM. Four different sets of thermal boundary conditions were applied to the square and circular cross section fibers. Xiao et al. [228] developed a theoretical model for predicting the effective thermal conductivity of unidirectional fiber composite with square and hexagonal fiber geometry and observed that the results are in good agreement when the ratio of fiber and matrix is near to 1. Further increase in the volume fraction of fiber gives poorer agreement due to the local temperature gradient. Zou et al. [229] and Ascioğlu [230] used thermal–electrical analogy technique for developing analytical model to predict the transverse thermal conductivity of the unidirectional fiber reinforced composites. They considered thermal barrier between the fiber and matrix phases. The predicted results are found to be in good agreement with the existing analytical methods. Al-Sulaiman et al. [231] predicted the thermal conductivity of the constituents of fiber reinforced composite laminates using three empirical formulas. Grove [232] computed transverse thermal conductivity in

continuous unidirectional fiber reinforced composite materials using finite element and spatial statistical techniques for a range of fiber volume fraction up to 0.5. Lu [233] used boundary collocation scheme for evaluating the transverse effective thermal conductivity of 2-dimensional periodic arrays of long circular and square cylinders with square array and long circular cylinders with hexagonal array for a complete range of fiber volume fractions.

Liang and Li [234] developed a theoretical model of heat transfer in the polymer hollow micro-sphere composites based on the law of minimal thermal resistance and the equal law of the specific equivalent thermal conductivity. In another study, Liang and Li [235] studied the effects of the particle content and size on the effective thermal conductivity by using numerical analysis of heat-transfer process in hollow-glass-bead filled polymer composites. Sihn and Roy [236] reinvestigated both analytic and numerical models for the prediction of transverse thermal conductivity of laminated composites and observed that the results are significantly affected by the random fiber distributions, especially at high fiber volume fractions. Liu et al. [237] evaluated the transverse thermal conductivity of Manila hemp natural fiber using the theoretical method and FEM and found that the theoretical results shows good agreement with the experimental data. Ramani et al. [238] studied the thermal conductivity of polymer composites by FEM with parallelepiped and spherical fillers. They also considered the effect of microstructural characteristics on thermal conductivity such as interfacial thermal resistance, filler aspect ratio, filler dispersion, and volume fraction. Cao et al. [239] estimated the thermal conductivity of fiber composites through the RVEs with single and multiple fibers by using FEM based on homogenization technique. Agrawal and Satapathy [240] developed a mathematical model for estimating the effective thermal conductivity of particulate filled polymer hybrid composites and reported that the experimental results are in close approximation to the values predicted by the mathematical model. Haddadi et al. [241] studied the experimental and numerical analysis of thermal conductivity properties of date palm fiber composites by using guarded hot plate method and 3D finite element modelling and observed that the thermal conductivity is decreasing with increasing the fiber loading and the size of fillers has no significant effect on the results. Behzad and Sain [242] evaluated the in-plane and transverse thermal conductivities of hemp fiber reinforced polymer composites for different volume fractions of fiber. The experimental results were compared with finite element model and two theoretical models and found good agreement between the models and obtained results. Sahu et al. [243] established an analytical model to calculate the effective thermal conductivity of short banana fiber reinforced epoxy composites and found that the values obtained from the model proposed are in good agreement with the experimental values. Fu et al. [244] predicted the

thermal conductivity of short carbon fiber reinforced polymer composites by considering the effect of fiber orientation and fiber length.

2.6 The Knowledge Gap in Earlier Investigations

In spite of a number of research works reported in the past, there is a vast knowledge gap that needs a thorough and systematic research in this area of natural fiber reinforced polymer composites. An extensive literature survey presented above reveals that:

1. Although, the jute and banana based products has many low end applications such as in housing, packing, furniture and transportation, but its potential use in structural and thermal insulation application where synthetic fibers are widely used is less.
2. Most of the micromechanical studies are for composites reinforced with single fiber and very less work has been done on the synergistic effects of two or more kinds of fibers specifically natural fibers on the mechanical and thermal properties.
3. Though, some numerical and analytical models for estimation of thermal conductivity of single fiber reinforced composites are developed by few researchers, however there is no model exists for estimation of thermal conductivity of composites reinforced with hybrid fibers.
4. A number of research efforts have been devoted to the mechanical and thermal behaviour of fiber reinforced composites by either experimental or numerical. However, the comparison of both experimental and numerical analysis of hybrid composite materials are hardly been reported in the literature.
5. Though, some work has been done on mechanical and thermal behaviour of composites reinforced with banana or jute fiber, a possibility that the incorporation of both banana and jute in polymer matrix could provide a synergism in terms of improved physical, mechanical and thermal properties has not been addressed so far.

In view of the above, the present work is undertaken to investigate the physical, mechanical and thermal behaviour of epoxy and polyester matrix composites reinforced with banana and jute fibers.

2.7 Objectives of the Present Work

The knowledge gap in the existing literature summarized above has helped to set the objectives of this research work which are outlined as follows:

1. Fabrication of different sets of epoxy and polyester composites reinforced with banana and jute fibers in the form of unidirectional and short.

2. Development of theoretical models for estimation of thermal conductivity of the unidirectional and short fiber reinforced polymer hybrid composites.
3. To study the physical, mechanical and thermal properties of composites such as density, water absorption, tensile strength, tensile modulus, flexural strength, flexural modulus, inter-laminar shear strength, impact strength, hardness, thermal conductivity, specific heat and thermal diffusivity.
4. To study the effect of fiber loading and weight ratio on the physical, mechanical and thermal behaviour of the hybrid composites.
5. To study the elastic and thermal conductivity properties of the unidirectional and short fiber based hybrid composites by using micromechanical analysis using FEM.
6. Validation of proposed theoretical models and finite element results by comparing with the experimental results and results of existing analytical methods.

Chapter Summary

This chapter has provided:

- An exhaustive review of research work on various aspects of fiber reinforced polymer composites reported by previous investigators
- The knowledge gap in earlier investigations
- The objectives of the present work

The next chapter presents the development of theoretical models for estimating the transverse thermal conductivity of unidirectional fiber reinforced polymer hybrid composites and effective thermal conductivity of short fiber reinforced polymer hybrid composites.

Chapter 3

Development of Theoretical Models for Thermal Conductivity of Fiber Reinforced Hybrid Composites

This chapter presents the development of theoretical models for estimating the transverse thermal conductivity of unidirectional fiber reinforced hybrid composites and effective thermal conductivity of short fiber reinforced hybrid composites. It also gives an overview of the principles used for deriving the correlation for estimating the thermal conductivity of fiber reinforced hybrid composites.

3.1 Basic Principles

3.1.1 Background

The thermal conductivity is an important characterization of heat transfer properties of any materials. However, there are few studies on the characterization and measurement of the thermal conductivity for fiber reinforced composites. The heat transfer process and mechanisms in fiber reinforced hybrid composite materials are very complicated. It is quite important, to present some expressions or equations for calculating the thermal conductivity during heat transfer process in fiber reinforced hybrid composites.

3.1.2 Law of Minimal Thermal Resistance and Equal Law of Specific Equivalent Thermal Conductivity

In a composite system, heat conduction takes place along the path that offers minimum thermal resistance. From the law of minimal thermal resistance and the equal law of the specific equivalent thermal conductivity, when the heat conduction is only considered, specific equivalent thermal resistance of single element of the composite is considered equal to the total thermal resistance of the composite. The equivalent thermal conductivity of that single element is considered equal to the total thermal conductivity of the composite [245]. Therefore, the calculation of the equivalent thermal conductivity for composites can be attributed to the determination of the equivalent thermal conductivity of the element with the same specific equivalent thermal resistance. So, by following the above laws, once the

equivalent thermal conductivity of single element is calculated, the effective thermal conductivity of the complete composite system can be estimated.

3.2 Development of Theoretical Model for Unidirectional Fiber Reinforced Hybrid Composites

3.2.1 Nomenclature

The following symbols are used for the development of theoretical models for estimation of transverse thermal conductivity of unidirectional fiber reinforced hybrid composites:

a_1	side length of the unit cell in the direction of heat flow
r_{f1}, r_{f2}	radius of the fiber 1 and 2, respectively
k_m	thermal conductivity of matrix phase
k_{f1}, k_{f2}	thermal conductivity of fiber 1 and 2, respectively
A	cross-sectional area of element in the direction of heat flow
A_m	cross-sectional area of matrix phase in the direction of heat flow
A_{f1}, A_{f2}	cross-sectional area of fiber 1 and 2, respectively in the direction of heat flow
Q	heat flow through the cross-sectional area of the element
Q_m	heat flow through the cross-sectional area of matrix phase
Q_{f1}, Q_{f2}	heat flow through the cross-sectional area of fiber 1 and 2, respectively
Φ_{f1}, Φ_{f2}	volume fraction of fiber 1 and 2, respectively
V_c	volume of element under study
V_m	volume of matrix phase
V_{f1}, V_{f2}	volume of fiber 1 and 2, respectively
h_1, h_2, h_3, h_4	height of part 1, 2, 3 and 4, respectively of the element
k_1, k_2, k_3, k_4	thermal conductivity of part 1, 2, 3 and 4, respectively of the element
R	total thermal resistance of the element
R_1, R_2, R_3, R_4	thermal resistance of part 1, 2, 3 and 4, respectively
ΔT	temperature difference along the direction of heat flow

k_T	transverse thermal conductivity of the element under study
k_{eff}	effective thermal conductivity of the element under study

3.2.2 Generation of the Unit Cell

Generally, the factors affecting the thermal conductivity of fiber reinforced polymer composites are relatively more, such as fiber geometry, fiber length, nature of matrix, fiber loading as well as the distribution and dispersion pattern of the fibers in the matrix. Therefore, a detailed research into the heat transfer mechanisms, process, and their quantitative description is essential. The proposed model reports these in an effective manner for estimating the thermal conductivity of fiber reinforced composite material with a wide range of reinforcement concentration. In a real unidirectional fiber reinforced composites, the fibers are arranged randomly, and it is difficult to model random fiber arrangement. For simplicity reasons, most micromechanical models assume a periodic arrangement of fibers for which a unit cell can be isolated. The periodic fiber sequences commonly used are the square array and the hexagonal array. The schematic diagram of the unidirectional fiber reinforced hybrid composite where the fibers are arranged in the square array is shown in Figure 3.1.

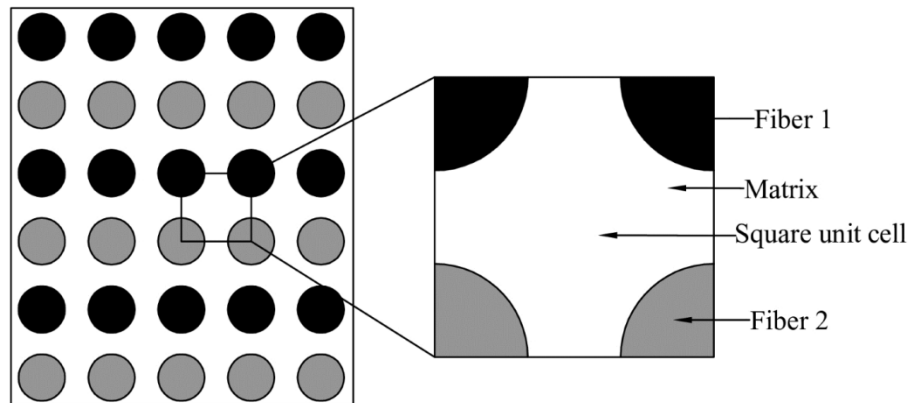


Figure 3.1: Arrangement of unidirectional hybrid fibers in a square array

A single unit cell is taken out from the square array of fiber composites for further study as shown in Figure 3.2. The unit cell having side length of a_1 and radius of fibers are r_{F1} and r_{F2} . In present study, the theoretical analysis of heat transfer in hybrid composite material is based on the following assumptions:

- The fibers are uniformly distributed in the matrix;
- Locally both the matrix and fibers are homogeneous and isotropic;

- (c) There is perfect bonding between fibers and matrix;
- (d) The composite material is free from voids;
- (e) The thermal contact resistance between the fiber and the matrix is negligible and
- (f) The temperature distribution along the direction of heat flow is linear.

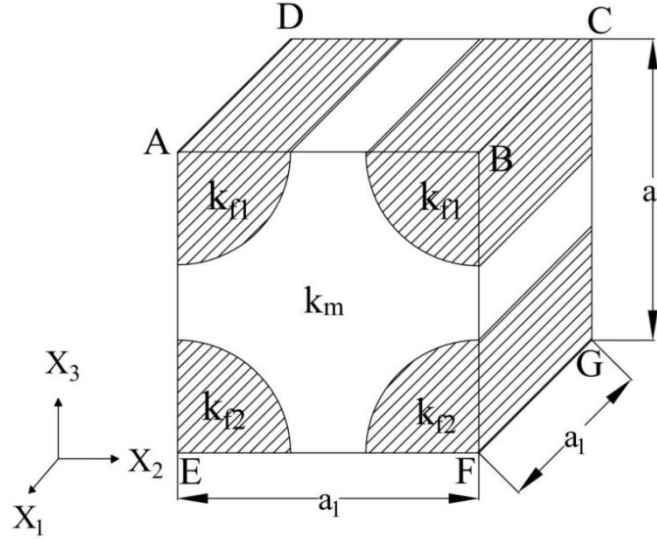


Figure 3.2: 3-Dimensional view of square unit cell

3.2.3 Heat Transfer Modeling

Figure 3.3 shows a series model of heat conduction through the square unit cell considered for the present study. The direction of heat flow is considered from top to bottom. The element is divided into four parts such as part 1, part 2, part 3 and part 4. Part 1 and part 4 represents the combination of fiber and matrix material while part 2 and part 3 represents the neat matrix. The thickness of part 2 and part 3 are h_2 and h_3 , respectively, where $h_2 = a_1/2 - r_{f1}$ and $h_3 = a_1/2 - r_{f2}$. Part 1 and part 4 having thickness of $h_1 = r_{f1}$ and $h_4 = r_{f2}$, respectively. The transverse thermal conductivity of the whole element is determined using the law of minimum thermal resistance and equal law of specific thermal conductivity. From the element under study, expressions for volume of composite and volume fraction of fibers can be represented as follows:

$$V_c = V_{f1} + V_{f2} + V_m \quad (3.1)$$

For fiber 1:

$$\Phi_{f1} = \frac{V_{f1}}{V_c} = \frac{\pi r_{f1}^2 a_1}{2a_1^3} \quad (3.2)$$

For fiber 2:

$$\Phi_{f2} = \frac{V_{f2}}{V_c} = \frac{\pi r_{f2}^2 a_1}{2a_1^3} \quad (3.3)$$

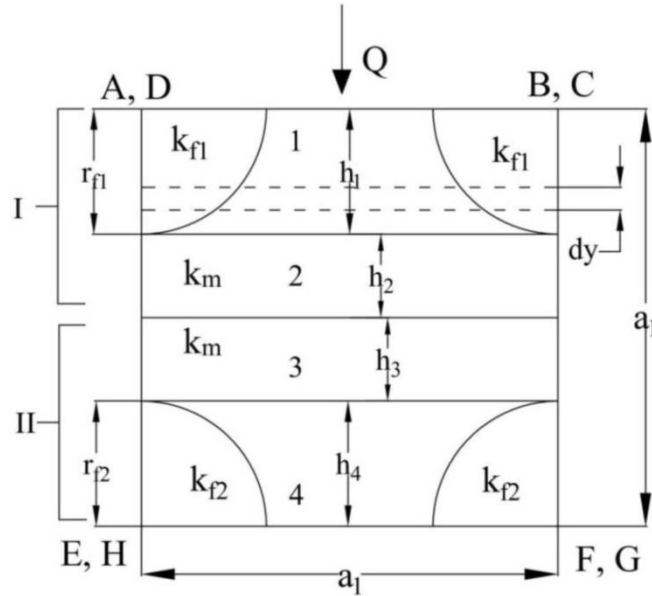


Figure 3.3: Series model of heat transfer in square unit cell

The heat transfer mechanism in fiber reinforced polymer composites are three types such as solid thermal conduction, heat radiation on the surface between neighboring fibers, as well as natural thermal convection. According to the past research work, the natural thermal convection will not occur when the fiber diameter is less than 4 mm [246], thus the natural thermal convection may be neglected. Furthermore, polymer composite works usually under lower temperature conditions where the proportion of the thermal radiation in the total heat transfer is very small; hence the thermal radiation effect is neglected. The heat transfer is occurred mainly by the mode of conduction. From the Fourier law of heat conduction, heat quantity can be expressed as:

$$Q = kA \frac{dT}{dx} \Rightarrow k = \frac{Q}{\left(\frac{dT}{dx}\right)A} \quad (3.4)$$

And the thermal resistance is expressed as:

$$R = \frac{dx}{kA} \quad (3.5)$$

Where, dx is the length of path followed by heat quantity. As already assumed that the temperature distribution along the direction of heat flow will be linear, thermal conductivity of each section can be calculated as:

For part 1 and part 4

This section consists of both the fiber and matrix phase and its thermal conductivity is the combined effect of both polymer and fiber material. Taking a thin piece with thickness of dy and applying Fourier's law of heat conduction, the thermal conductivity for part 1 and part 4 is calculated as:

For part 1

$$k_1 = \frac{Q_m + Q_{f1}}{\left(\frac{dT}{dy}\right)A} = \frac{k_m A_m}{A} + \frac{k_{f1} A_{f1}}{A} \quad (3.6)$$

For part 4

$$k_4 = \frac{Q_m + Q_{f2}}{\left(\frac{dT}{dy}\right)A} = \frac{k_m A_m}{A} + \frac{k_{f2} A_{f2}}{A} \quad (3.7)$$

Integrating equations (3.6) and (3.7) over the complete thickness, the equations (3.8) and (3.9) can be obtained as:

For part 1

$$k_1 = \int_{h_1} \frac{(k_m A_m / A + k_{f1} A_{f1} / A) dy}{h_1} = \frac{1}{h_1 A} (k_m V_m + k_{f1} V_{f1}) \quad (3.8)$$

For part 4

$$k_4 = \int_{h_4} \frac{(k_m A_m / A + k_{f2} A_{f2} / A) dy}{h_4} = \frac{1}{h_4 A} (k_m V_m + k_{f2} V_{f2}) \quad (3.9)$$

For part 2 and 3

Since, there is no fiber in the part 2 and part 3; the thermal conductivity of that region will be same as that of matrix material.

$$k_2 = k_3 = \int_{h_2} k_m \frac{dy}{h_2} = k_m \quad (3.10)$$

Similarly, the thermal resistance of the four parts is given as:

$$R_1 = \frac{h_1}{\frac{1}{h_1 A} (k_m V_m + k_{f1} V_{f1}) A} = \frac{h_1^2}{k_m V_m + k_{f1} V_{f1}} \quad (3.11)$$

$$R_2 = \frac{h_2}{k_m A} \quad (3.12)$$

$$R_3 = \frac{h_3}{k_m A} \quad (3.13)$$

$$R_4 = \frac{h_4}{\frac{1}{h_4 A} (k_m V_m + k_{f2} V_{f2}) A} = \frac{h_4^2}{k_m V_m + k_{f2} V_{f2}} \quad (3.14)$$

As the series model is considered for the heat transfer in the element, the transverse thermal conductivity of the composite is given by dividing the element into two parts I, and II. The thermal conductivity is calculated for its individual parts and then combined it for the series connection to obtain the transverse thermal conductivity. Figure 3.4 shows the series connection of thermal resistance.

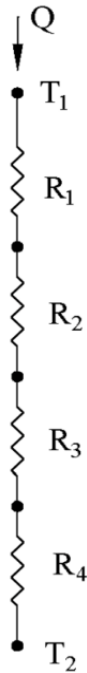


Figure 3.4: Series connection of thermal resistance

For part I

$$k_{\text{II}} = \frac{a_1/2}{RA} = \frac{a_1/2}{(R_1 + R_2)A} \quad (3.15)$$

For part II

$$k_{\text{III}} = \frac{a_1/2}{RA} = \frac{a_1/2}{(R_3 + R_4)A} \quad (3.16)$$

For part I

Substituting equations (3.11) and (3.12) in equation (3.15),

$$k_{\text{II}} = \frac{a_1}{2 \left(\frac{h_1^2}{k_m V_m + k_{f1} V_{f1}} + \frac{h_2}{k_m A} \right) A} \quad (3.17)$$

This can be written as,

$$k_{\text{II}} = \frac{1}{2 \left(\frac{h_1^2 a_1}{k_m V_m + k_{f1} V_{f1}} + \frac{h_2}{k_m a_1} \right)} \quad (3.18)$$

From Figure 3.3 it is clear that

$$h_1 = r_{f1}, \quad h_2 = \frac{a_1}{2} - r_{f1} \quad (3.19)$$

Substituting equation (3.19) in equation (3.18)

$$k_{\text{II}} = \frac{1}{2 \left(\frac{r_{f1}^2 a_1}{k_m V_m + k_{f1} V_{f1}} + \frac{a_1 - 2r_{f1}}{2k_m a_1} \right)} \quad (3.20)$$

Which otherwise can be written as,

$$k_{\text{II}} = \frac{1}{2 \left(\frac{r_{f1}^2 a_1}{k_m V_m + k_{f1} V_{f1}} + \frac{1}{2k_m} - \frac{r_{f1}}{2k_m a_1} \right)} \quad (3.21)$$

From equation (3.2) and Figure 3.3 it is clear that

$$a_1 = \left(\frac{\pi r_{f1}^2}{2\Phi_{f1}} \right)^{\frac{1}{2}}, \quad V_{f1} = \frac{\pi r_{f1}^2 a_1}{2}, \quad V_m = \left(r_{f1} a_1^2 - \frac{\pi r_{f1}^2 a_1}{2} \right) \quad (3.22)$$

Putting the above expressions in equation (3.21) and rearranging it, the final expression for part I can be written as:

$$k_{PI} = \frac{1}{2 \left[\frac{1}{2k_m} - \frac{1}{k_m} \left(\frac{2\Phi_{f1}}{\pi} \right)^{\frac{1}{2}} + \frac{2}{\pi \left(k_m \left(\left(\frac{2}{\pi\Phi_{f1}} \right)^{\frac{1}{2}} - 1 \right) + k_{f1} \right)} \right]} \quad (3.23)$$

For part II

By following similar procedure as for part I, the expression for the thermal conductivity of part II can be written as:

$$k_{PII} = \frac{1}{2 \left[\frac{1}{2k_m} - \frac{1}{k_m} \left(\frac{2\Phi_{f2}}{\pi} \right)^{\frac{1}{2}} + \frac{2}{\pi \left(k_m \left(\left(\frac{2}{\pi\Phi_{f2}} \right)^{\frac{1}{2}} - 1 \right) + k_{f2} \right)} \right]} \quad (3.24)$$

As the series model is considered for heat transfer in the element, the transverse thermal conductivity of composite is given by:

$$k_T = 2 \times \left(\frac{1}{k_{PI}} + \frac{1}{k_{PII}} \right)^{-1} \quad (3.25)$$

Finally, substituting equations (3.23) and (3.24) into equation (3.25), the transverse thermal conductivity of the unidirectional fiber reinforced hybrid composite is obtained as:

$$k_T = \left[\left(\frac{1}{2k_m} - \frac{1}{k_m} \left(\frac{2\Phi_{f1}}{\pi} \right)^{\frac{1}{2}} + \frac{2}{\pi \left(k_m \left(\left(\frac{2}{\pi\Phi_{f1}} \right)^{\frac{1}{2}} - 1 \right) + k_{f1} \right)} \right) + \left(\frac{1}{2k_m} - \frac{1}{k_m} \left(\frac{2\Phi_{f2}}{\pi} \right)^{\frac{1}{2}} + \frac{2}{\pi \left(k_m \left(\left(\frac{2}{\pi\Phi_{f2}} \right)^{\frac{1}{2}} - 1 \right) + k_{f2} \right)} \right) \right]^{-1} \quad (3.26)$$

The correlation given in equation (3.26) is thus an expression for estimation of transverse thermal conductivity of the unidirectional fiber reinforced hybrid composites in terms of the volume fraction of individual fibers, their respective intrinsic thermal conductivity values and the thermal conductivity of the base matrix. This correlation can be used for estimation of transverse thermal conductivity of any unidirectional fiber reinforced hybrid composite with similar structural arrangement.

3.3 Development of Theoretical Model for Short Fiber Reinforced Hybrid Composites

3.3.1 Generation of the Unit Cell

The nomenclature to derive the theoretical model for estimating the effective thermal conductivity for short fiber reinforced hybrid composite are same as those taken for the unidirectional fiber reinforced hybrid composites. The schematic diagram of the short fiber reinforced composite, where the fibers are arranged in the square pattern is shown in Figure 3.5.

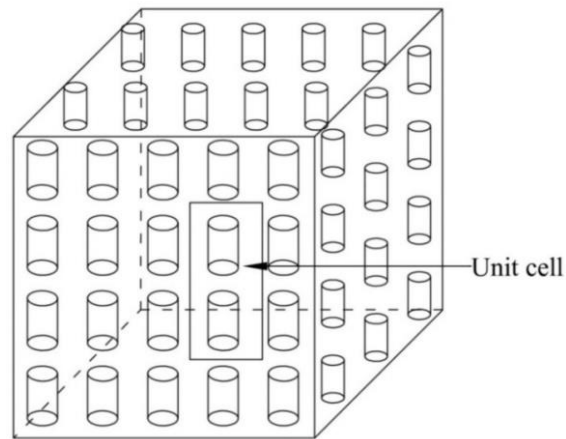


Figure 3.5: 3-Dimensional view of short fiber reinforced composite

A single unit cell is taken out from the square pattern of short fiber composites for further study as shown in Figure 3.6. The unit cell having side length of a_1 and radius of fibers are r_{f1} and r_{f2} . The assumptions taken to derive the mathematical correlation for estimating the effective thermal conductivity for hybrid filler reinforced polymer composite are same as those taken for unidirectional fiber reinforced polymer composites.

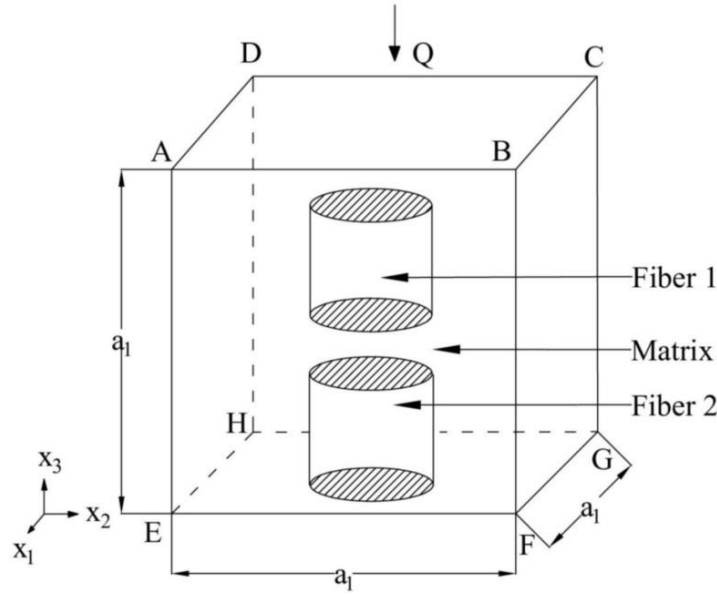


Figure 3.6: 3-Dimensional view of hybrid fiber square unit cell under study

3.3.2 Heat Transfer Modeling

Figure 3.7 shows a series model of heat conduction through the square unit cell considered for the present study. The element is divided into four parts, part 1 and part 3 represents the neat matrix while part 2 and part 4 represents the combination of fiber and matrix material; k_1 , k_2 , k_3 , and k_4 are the mean conductivity coefficient of respective parts; h_1 , h_2 , h_3 , and h_4 are the thickness of respective parts. The effective thermal conductivity of the whole element is determined using the law of minimum thermal resistance and equal law of specific thermal conductivity. From the element under study, expressions for volume of composite and volume fraction of fibers can be represented as follows:

$$V_c = V_{f1} + V_{f2} + V_m \quad (3.27)$$

For fiber 1:

$$\Phi_{f1} = \frac{V_{f1}}{V_c} = \frac{\pi r_{f1}^2 h_2}{a_1^3} \quad (3.28)$$

For fiber 2:

$$\Phi_{f2} = \frac{V_{f2}}{V_c} = \frac{\pi r_{f2}^2 h_4}{a_1^3} \quad (3.29)$$

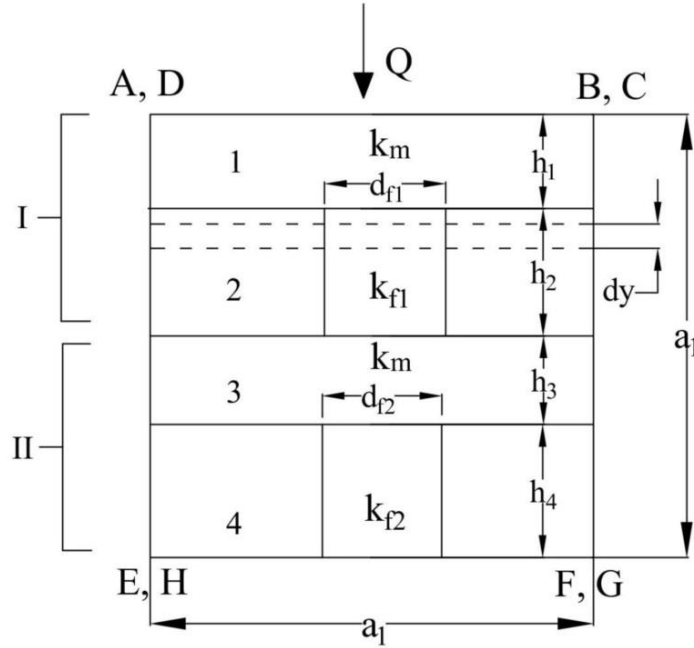


Figure 3.7: Series model of heat transfer in unit cell

For part 1 and 3

Since there is no fiber in the part 1 and part 3, the thermal conductivity of that region will be same as that of matrix material.

$$k_1 = k_3 = \int_{h_1} k_m \frac{dy}{h_1} = k_m \quad (3.30)$$

For part 2 and 4

This section consists of both the fiber and matrix phase and its thermal conductivity is the combined effect of matrix and fiber material. Taking a thin piece with thickness of dy and applying Fourier's law of heat conduction, the thermal conductivity for part 2 and part 4 is given as:

For part 2

$$k_2 = \frac{Q_m + Q_{f1}}{\left(\frac{dT}{dy}\right)_A} = \frac{k_m A_m}{A} + \frac{k_{f1} A_{f1}}{A} \quad (3.31)$$

For part 4

$$k_4 = \frac{Q_m + Q_{f2}}{\left(\frac{dT}{dy}\right)_A} = \frac{k_m A_m}{A} + \frac{k_{f2} A_{f2}}{A} \quad (3.32)$$

Integrating equations (3.31) and (3.32) over the complete thickness, we get equations (3.33) and (3.34).

For part 2

$$k_2 = \int_{h_2} \frac{(k_m A_m / A + k_{f1} A_{f1} / A) dy}{h_2} = \frac{1}{h_2 A} (k_m V_m + k_{f1} V_{f1}) \quad (3.33)$$

For part 4

$$k_4 = \int_{h_4} \frac{(k_m A_m / A + k_{f2} A_{f2} / A) dy}{h_4} = \frac{1}{h_4 A} (k_m V_m + k_{f2} V_{f2}) \quad (3.34)$$

Similarly, thermal resistance of the four parts is given as:

$$R_1 = \frac{h_1}{k_m A} \quad (3.35)$$

$$R_2 = \frac{h_2}{\frac{1}{h_2 A} (k_m V_m + k_{f1} V_{f1}) A} = \frac{h_2^2}{k_m V_m + k_{f1} V_{f1}} \quad (3.36)$$

$$R_3 = \frac{h_3}{k_m A} \quad (3.37)$$

$$R_4 = \frac{h_4}{\frac{1}{h_4 A} (k_m V_m + k_{f2} V_{f2}) A} = \frac{h_4^2}{k_m V_m + k_{f2} V_{f2}} \quad (3.38)$$

As the series model is considered for heat transfer in the element, the effective thermal conductivity of the composite is given by dividing the element into two parts I, and

II. The thermal conductivity is calculated for its individual parts and then combined it for the series connection to obtain the effective thermal conductivity of the element.

$$k_I = \frac{a_1/2}{RA} = \frac{a_1/2}{(R_1 + R_2)A} \quad (3.39)$$

$$k_{II} = \frac{a_1/2}{RA} = \frac{a_1/2}{(R_3 + R_4)A} \quad (3.40)$$

For part I

Substituting equations (3.35) and (3.36) in equation (3.39),

$$k_I = \frac{a_1}{2 \left(\frac{h_1}{k_m A} + \frac{h_2^2}{k_m V_m + k_{fl} V_{fl}} \right) A} \quad (3.41)$$

This can be written as,

$$k_I = \frac{1}{2 \left(\frac{h_1}{k_m a_1} + \frac{h_2^2 a_1}{k_m V_m + k_{fl} V_{fl}} \right)} \quad (3.42)$$

From equation (3.28) and Figure 3.7 it is clear that

$$h_1 = \frac{a_1}{2} - 2r_{fl}, \quad h_2 = 2r_{fl}, \quad a_1 = r_{fl} \left(\frac{2\pi}{\Phi_{fl}} \right)^{\frac{1}{3}}, \quad V_f = 2\pi r_{fl}^3, \quad V_m = 2(a_1^2 r_{fl} - \pi r_{fl}^3) \quad (3.43)$$

Putting the above expressions in equation (3.42) and rearranging it, the final expression for part I can be written as:

$$k_I = \frac{1}{2 \left(\frac{1}{2k_m} - \frac{1}{k_m \left(\frac{\pi}{4\Phi_{fl}} \right)^{\frac{1}{3}}} + \frac{\left(\frac{16\pi}{\Phi_{fl}} \right)^{\frac{1}{3}}}{k_m \left(\frac{2\pi}{\Phi_{fl}} \right)^{\frac{2}{3}} + \pi(k_{fl} - k_m)} \right)} \quad (3.44)$$

For part II

By following similar procedure as for part I, the expression for the thermal conductivity of part II can be written as:

$$k_{II} = \frac{1}{2 \left[\frac{1}{2k_m} - \frac{1}{k_m \left(\frac{\pi}{4\Phi_{f2}} \right)^{\frac{1}{3}}} + \frac{\left(\frac{16\pi}{\Phi_{f2}} \right)^{\frac{1}{3}}}{k_m \left(\frac{2\pi}{\Phi_{f2}} \right)^{\frac{2}{3}} + \pi(k_{f2} - k_m)} \right]} \quad (3.45)$$

As the series model is considered for heat transfer in the element, the effective thermal conductivity of composite is given by:

$$k_{eff} = 2 \times \left(\frac{1}{k_I} + \frac{1}{k_{II}} \right)^{-1} \quad (3.46)$$

Finally, substituting equations (3.44) and (3.45) into equation (3.46), the effective thermal conductivity of the short fiber reinforced hybrid composite is obtained as:

$$k_{eff} = \left[\left(\frac{1}{2k_m} - \frac{1}{k_m \left(\frac{\pi}{4\Phi_{f1}} \right)^{\frac{1}{3}}} + \frac{\left(\frac{16\pi}{\Phi_{f1}} \right)^{\frac{1}{3}}}{k_m \left(\frac{2\pi}{\Phi_{f1}} \right)^{\frac{2}{3}} + \pi(k_{f1} - k_m)} \right) + \left(\frac{1}{2k_m} - \frac{1}{k_m \left(\frac{\pi}{4\Phi_{f2}} \right)^{\frac{1}{3}}} + \frac{\left(\frac{16\pi}{\Phi_{f2}} \right)^{\frac{1}{3}}}{k_m \left(\frac{2\pi}{\Phi_{f2}} \right)^{\frac{2}{3}} + \pi(k_{f2} - k_m)} \right) \right]^{-1} \quad (3.47)$$

The correlation given in equation (3.47) is thus an expression for effective thermal conductivity of the short fiber reinforced hybrid composites in terms of the volume fraction of individual fibers, their respective intrinsic thermal conductivities and the thermal conductivity of the base matrix. This correlation can be used for estimation of effective thermal conductivity of any short fiber reinforced hybrid composite with similar structural arrangement.

Chapter Summary

This chapter has presented the development of theoretical models for estimating the transverse thermal conductivity of unidirectional fiber reinforced hybrid composites and effective thermal conductivity of short fiber reinforced hybrid composites. Heat transfer within a hybrid fiber reinforced polymer composite involves complex mechanisms; simplified theoretical models for such a process may appear inadequate unless its assessment against experimental results is made. So, for the validation of the proposed models, thermal

conductivity tests on the hybrid composites with various fiber concentrations are to be conducted.

The next chapter presents a description of materials used for fabrication of various hybrid composites under this study and the details of various tests carried out on them.

Chapter 4

Materials and Methods

This chapter describes the materials and methods used for processing and characterizing the hybrid composites under investigation. It presents the details of the tests related to the physical, mechanical, and thermal characterization of the prepared fiber reinforced polymer hybrid composites. This chapter also explores the micromechanical methods for predicting elastic and thermal properties of hybrid composites.

4.1 Materials

4.1.1 Matrix Material

4.1.1.1 Matrix Material - 1: (Epoxy)

Generally, the epoxy resins are being widely used for many advanced composites due to their excellent adhesion to wide variety of fibers, good performance at elevated temperatures, superior mechanical and electrical properties. In addition to that they have good chemical resistance and low shrinkage upon curing. Due to several advantages over the other thermoset polymers as mentioned above, epoxy (LY 556) is chosen as the matrix material for the present research work. Its common name is Bisphenol-A-Diglycidyl-Ether (BADGE or DGEBA) and it chemically belongs to the ‘epoxide’ family. It provides a solvent free room temperature curing system when it is combined with the hardener tri-ethylene-tetramine (TETA) which is an aliphatic primary amine with commercial designation as HY 951. The LY 556 epoxy resin and the corresponding hardener HY-951 are procured from Ciba Geigy, India Ltd. (Figure 4.1).



Figure 4.1: Epoxy resin and corresponding hardener

4.1.1.2 Matrix Material - 2: (Polyester)

The workhorse of another thermoset polymer is unsaturated polyester, which offers an attractive combination of low price, good cross linking tendency, excellent process ability and reasonably good properties when cured [247]. The unsaturated polyester resin of grade ECMALON 4411 is used as another matrix material for the present investigation. For a proper chemical reaction, methyl ethyl ketone peroxide and cobalt naphthenate are used as catalyst and accelerator respectively. The resin and the corresponding catalyst and accelerator are supplied by Ecmass resin (Pvt) Ltd., Hyderabad, India. Figure 4.2 shows the unsaturated polyester resin and corresponding catalyst and accelerator. Table 4.1 provides some of the important properties of epoxy and polyester.



Figure 4.2: Polyester resin and corresponding catalyst and accelerator

Table 4.1: Some important properties of matrix materials under investigation

Characteristic Property	Units	Epoxy	Polyester
Density	g/cm ³	1.15	1.13
Elongation	%	1.5	2.5
Thermal conductivity	W/m-K	0.363	0.2
Glass transition temperature	°C	104	55
Water absorption	%	0.1	0.1–0.3

4.1.2 Fiber Material

A great deal of work has been done on the use of various types of natural fibers as reinforcement in polymer composites by various researchers. Among various natural fibers, jute and banana fibers have the potential to be used as reinforcement in polymer composites

because of their advantages like low density, low cost, no health risk, high specific strength and modulus, renewability, easy availability and much lower energy requirement for processing. Due to the above mentioned advantages, these two materials in two different forms i.e. unidirectional and short fibers are selected as reinforcing material in the present research work.

4.1.2.1 Fiber Material - 1: (Banana Fiber)

Banana fiber is a waste product of banana cultivation. Banana belongs to the Musaceae family and there are nearly 300 species, but only 20 varieties are used for consumption. The main component of banana fiber is cellulose which leads to higher stiffness. Banana fibers used in present investigation are collected from the local sources. Figure 4.3 shows the unidirectional and short banana fiber used as reinforcement in the present work. Banana fiber has a density of 1.35 g/cm^3 and thermal conductivity of 0.09 W/m-K [19], [243].



Figure 4.3: Unidirectional and short banana fiber

4.1.2.2 Fiber Material - 2: (Jute Fiber)

Jute fiber is generally derived from the stem of a jute plant. Jute is the other natural fiber material that has been used as reinforcement in the present work. Jute is a lingo-cellulosic fiber because its major chemical constituents are lignin and cellulose. Jute fibers used in present investigation are procured from local sources. Figure 4.4 shows the unidirectional and short jute fiber used as reinforcement in the present work. Jute fiber has a density of 1.4 g/cm^3 and thermal conductivity of 0.036 W/m-K [192], [248].



Figure 4.4: Unidirectional and short jute fiber

4.2 Composite Fabrication

The fabrication of the epoxy and polyester based hybrid composites is done by conventional hand lay-up technique followed by light compression molding. Two different forms of fiber are taken for the study such as unidirectional and short. Composites are fabricated with five different fiber loadings (0 wt.%, 10 wt.%, 20 wt.%, 30 wt.%, and 40 wt.%) and by keeping the weight ratio of banana and jute fiber as 1:1, 1:3, and 3:1. The composition and designation of various composites fabricated using epoxy and polyester as the base matrices are presented in Tables 4.2 and 4.3 respectively. For epoxy based composites, the epoxy and hardener HY951 are mixed in a ratio of 10:1 by weight as recommended. For polyester based composites, the polyester resin is mixed with 1.5 wt.% of the catalyst and 1.5 wt.% of the accelerator for cure initiation. The arrangement of fibers in unidirectional fiber reinforced hybrid composites is schematically represented in Figures 4.5 (a–c). Figure 4.5 (a) represents the composite with 1:1 weight ratio of the banana and jute fiber. Figure 4.5 (b) represents the composite with 1:3 weight ratio of banana and jute fiber where the jute fiber as the skin material and banana fiber as the core material and it is in the reverse order for the composite with 1:3 weight ratio as shown in Figure 4.5 (c). For quick and easy removal of the composite material, a mold release sheet and mold release spray is used on the top and bottom of the wooden mold. Care is taken to avoid the formation of air bubbles during preparation. A moderate pressure of 0.1 MPa is applied from the top and then mold is

allowed to cure at room temperature for 48 hrs. After 48 hrs, the samples are taken out of the mold and cut into required size by diamond cutter for physical, mechanical and thermal tests. Figure 4.6 shows the fabricated composite sheets. The composite specimens as per ASTM standards are shown in Figure 4.7.

Table 4.2: Detailed designation and composition of epoxy based composites reinforced with unidirectional and short fibers

Composite designation		Composition
Unidirectional fiber (Set I)	Short fiber (Set III)	
CE1	SE1	Epoxy (100 wt.%)
CE2	SE2	Epoxy (90 wt.%) + Banana (5 wt.%) + Jute (5 wt.%)
CE3	SE3	Epoxy (80 wt.%) + Banana (10 wt.%) + Jute (10 wt.%)
CE4	SE4	Epoxy (70 wt.%) + Banana (15 wt.%) + Jute (15 wt.%)
CE5	SE5	Epoxy (60 wt.%) + Banana (20 wt.%) + Jute (20 wt.%)
CE6	SE6	Epoxy (90 wt.%) + Banana (2.5 wt.%) + Jute (7.5 wt.%)
CE7	SE7	Epoxy (80 wt.%) + Banana (5 wt.%) + Jute (15 wt.%)
CE8	SE8	Epoxy (70 wt.%) + Banana (7.5 wt.%) + Jute (22.5 wt.%)
CE9	SE9	Epoxy (60 wt.%) + Banana (10 wt.%) + Jute (30 wt.%)
CE10	SE10	Epoxy (90 wt.%) + Banana (7.5 wt.%) + Jute (2.5 wt.%)
CE11	SE11	Epoxy (80 wt.%) + Banana (15 wt.%) + Jute (5 wt.%)
CE12	SE12	Epoxy (70 wt.%) + Banana (22.5 wt.%) + Jute (7.5 wt.%)
CE13	SE13	Epoxy (60 wt.%) + Banana (30 wt.%) + Jute (10 wt.%)

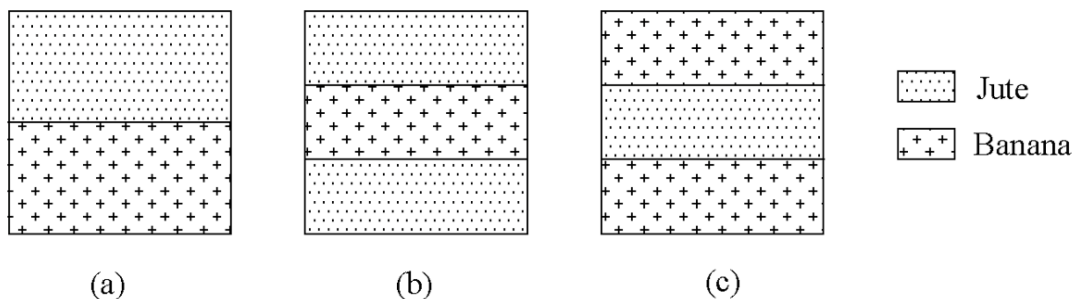


Figure 4.5: Arrangement of fibers in unidirectional hybrid composites with weight ratio of banana and jute fiber as (a) 1:1, (b) 1:3, and (c) 3:1

Table 4.3: Detailed designation and composition of polyester based composites reinforced with unidirectional and short fibers

Composite designation		Composition
Unidirectional fiber (Set II)	Short fiber (Set IV)	
CP1	SP1	Polyester (100 wt.%)
CP2	SP2	Polyester (90 wt.%) + Banana (5 wt.%) + Jute (5 wt.%)
CP3	SP3	Polyester (80 wt.%) + Banana (10 wt.%) + Jute (10 wt.%)
CP4	SP4	Polyester (70 wt.%) + Banana (15 wt.%) + Jute (15 wt.%)
CP5	SP5	Polyester (60 wt.%) + Banana (20 wt.%) + Jute (20 wt.%)
CP6	SP6	Polyester (90 wt.%) + Banana (2.5 wt.%) + Jute (7.5 wt.%)
CP7	SP7	Polyester (80 wt.%) + Banana (5 wt.%) + Jute (15 wt.%)
CP8	SP8	Polyester (70 wt.%) + Banana (7.5 wt.%) + Jute (22.5 wt.%)
CP9	SP9	Polyester (60 wt.%) + Banana (10 wt.%) + Jute (30 wt.%)
CP10	SP10	Polyester (90 wt.%) + Banana (7.5 wt.%) + Jute (2.5 wt.%)
CP11	SP11	Polyester (80 wt.%) + Banana (15 wt.%) + Jute (5 wt.%)
CP12	SP12	Polyester (70 wt.%) + Banana (22.5 wt.%) + Jute (7.5 wt.%)
CP13	SP13	Polyester (60 wt.%) + Banana (30 wt.%) + Jute (10 wt.%)



Figure 4.6: Fabricated composite sheets by hand lay-up technique



Figure 4.7: Composite specimens as per ASTM standards

4.3 Testing of Physical Properties

4.3.1 Density and Void Content

Density of a composite material is the most important factor for designing any light weight structural component and it mainly depends on the relative proportion of reinforcing and matrix materials. The theoretical density (ρ_{ct}) of the hybrid composites in terms of weight fractions of different constituents can be calculated from the following equation given by Agarwal and Broutman [249].

$$\rho_{ct} = \frac{1}{(W_{fb}/\rho_{fb}) + (W_{fj}/\rho_{fj}) + (W_m/\rho_m)} \quad (4.1)$$

Where, W and ρ represent the weight fraction and density, respectively. The suffixes fb, fj, m, and c stand for the banana fiber, jute fiber, matrix, and composite respectively. The actual density (ρ_{ce}) of the composite material can be determined experimentally by the Archimedes principle or water immersion technique as per ASTM D 792-91 standard. The void content

(V_v) of the composite material is determined as per ASTM D 2734-70 standard using the following equation (4.2).

$$V_v = \frac{\rho_{ct} - \rho_{ce}}{\rho_{ct}} \quad (4.2)$$

4.3.2 Water Absorption

Water absorption tests are conducted according to ASTM D 570-98, which investigates the increase of the composite weight after exposure to water. The specimen dimension of $60 \times 10 \times 4$ mm is used for the measurement of water absorption. The composite samples are dried at 65°C in oven and weighed before being submerged in distilled water at room temperature. The samples are removed from the water after 24 hr and wiped with a cotton cloth to measure the weight of specimen using a precise four-digit balance at a given immersion time. The specimens are weighed regularly from 24-288 hrs. The water absorption is calculated by the weight difference. The amount of water uptake (M_t) in the composite samples is measured at regular time intervals of time by using the following equation (4.3).

$$M_t(\%) = \frac{(W_t - W_0)}{W_0} \times 100 \quad (4.3)$$

Where, W_t is the weight of specimen at a given immersion time and W_0 is the oven dried weight.

4.3.3 Kinetics of Water Absorption

In order to study the mechanisms of water absorption, the kinetic parameters n and k , diffusion coefficient, sorption coefficient and permeability coefficient of different composite specimens are examined. Water absorption into the natural fiber composite materials is considered by three major mechanisms. First the diffusion of water molecules inside the microgaps between polymer chains; second the capillary transport of water molecules into the gaps and flaws at the interface between fibers and the polymer due to the incomplete wettability and impregnation; and finally transport of water molecules by micro cracks in the matrix, formed during the compounding process [250]–[252]. Though all the three mechanisms are active, the overall effect can be modeled conveniently considering the diffusion mechanism. There are three different kinds of diffusion behavior and they include Case 1: Fickian diffusion, in which the rate of diffusion is much less than that of the polymer segment mobility. The equilibrium inside the polymer is rapidly reached and it is maintained with independence of time. Case 2: non-Fickian or anomalous diffusion is relaxation control,

in which penetrant mobility is much greater than other relaxation processes. This diffusion is characterized by the development of a boundary between the swollen outer part and the inner glassy core of the polymer. The boundary advances at a constant velocity and the core diminishes in size until an equilibrium penetrant concentration is reached in whole polymer. Case 3: when anomalous diffusion occurs where the penetrant mobility and the polymer segment relaxation are comparable. It is then, an intermediate behavior between case 1 and 2 diffusion [253]. In order to investigate the type of diffusion mechanism, the absorption data have been fitted to the following equation (4.4), obtained from Fick law,

$$\log \frac{M_t}{M_m} = \log(k) + n \cdot \log(t) \quad (4.4)$$

Where, M_t is the moisture content at time t , M_m is the moisture content at the equilibrium and k and n are constants. The value of n indicates the type of transport mechanism and k indicates the interaction between the sample and water in addition to its structural characteristics of polymer network. The value of coefficient n shows different behavior between the three cases. For Fickian diffusion $n=1/2$, while for Case II $n=1$ and for anomalous diffusion n shows an intermediate value ($1/2 < n < 1$). The value of k provides an idea about the interaction of moisture with the material.

After calculating the kinetic parameters, the next step is the performance of an analysis of the transport coefficients of the epoxy and polyester based composites. The diffusion coefficient (D) is one of the important parameters of Fick's model and shows the ability of water molecules to penetrate inside the composite materials. The values of moisture diffusion coefficient can be calculated using the equation (4.5) from the initial slope of the plot of M_t/M_m against square root of time taken [254].

$$D = \pi \left[\frac{h}{4M_m} \right]^2 \left[\frac{M_2 - M_1}{\sqrt{t_2} - \sqrt{t_1}} \right]^2 \quad (4.5)$$

Where, M_m is the equilibrium moisture content, h is the thickness of the sample, t_1 and t_2 are the selected time points in the initial linear portion of curve and M_1 and M_2 are the moisture content at time t_1 and t_2 , respectively. Absorption coefficient is another important factor to determine the kinetics of water absorption behaviour. The permeability of water molecules through the composite depends on the absorption of water through the fibers. Therefore, the absorption coefficient is related to the equilibrium absorption of the penetrant and it is calculated by using the equation (4.6) [255].

$$S = \frac{w_m}{w_p} \quad (4.6)$$

Where, w_m is the mass of the solvent taken up at equilibrium swelling and w_p is the mass of the sample. The permeability coefficient (P) which represents the net effect of absorption and diffusion is given by the following relation [255].

$$P = D \times S \quad (4.7)$$

4.4 Testing of Mechanical Properties

4.4.1 Single Fiber Tensile Test

In order to determine the mechanical properties of the composite, it is important to know the individual fiber properties. The single fiber tensile test is performed to calculate the individual material properties of banana and jute fiber in accordance with ASTM D 3379-75. The embedded diameter of the fibers is measured by scanning electron microscope. Each fiber specimen is prepared by mounting on a stiff cardboard piece with gauge length of 50 mm. The ends of the fibers are glued on the cardboard with epoxy resin. The specimen for single fiber tensile test is shown in Figure 4.8. After curing, the specimens were taken out from the mould. Pull-out test is then conducted on Instron 1195 tensile testing machine at a cross head speed of 0.5 mm/min. The ultimate values of strength and percentage of strain in tension are obtained for ten specimens and the average of these is used to calculate the tensile modulus.

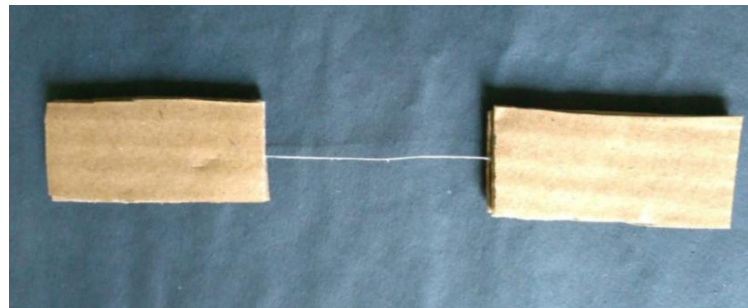


Figure 4.8: Specimen for single fiber tensile test

4.4.2 Tensile Properties

The ability of the material to stretch without breaking is termed as tensile strength. The testing process involves placing the test specimen in the testing machine and applying tension to it until it fractures. In the case of composite material, the tensile test is generally performed

on flat specimens. The ASTM standard test for tensile properties of fiber reinforced composites has the designation D3039-76. The dimensions of the specimen are 153 mm × 12.7 mm × 4 mm for longitudinal direction and 153 mm × 25.4 mm × 4 mm for transverse direction. In the present work, the tensile test is performed in universal testing machine Instron 1195 (Figure 4.9) at a cross head speed of 2 mm/min and the results are used to calculate the tensile modulus and tensile strength of the composite samples. The loading arrangement for the tensile test is shown in Figure 4.10 (a). For each composite type, three identical specimens are tested and the mean value is reported as the property of that composite.

4.4.3 Flexural Properties

The three-point bend test is carried out to obtain the flexural properties of all the composite samples. A flexural test imposes compressive stress on the concave side and tensile stress on the convex side of the composite specimen which causes a shear stress along the center line. The flexural strength of a composite is the maximum stress that it can withstand during bending before reaching the breaking point. The specimen bends and fractures when the load is applied at the middle of the beam. The flexural test is carried out on rectangular specimens of composite samples using universal testing machine Instron 1195 as per ASTM D 790. The dimensions of the specimen are 100 mm × 12.7 mm × 4 mm for longitudinal direction and 100 mm × 25.4 mm × 4 mm for transverse direction. The test is conducted using the load cell of 10kN at 2 mm/min rate of loading. The loading arrangement for the flexural test is shown in Figure 4.10 (b). For each composite type, three identical specimens are tested and the mean value is reported as the property of that composite. The flexural strength of the composite specimen is determined using the equation (4.8).

$$\frac{3PL}{2bt^2} \quad (4.8)$$

Where, P is the maximum load at failure (N), L is the span length of the sample (mm), and b and t are the width and thickness of the specimen (mm), respectively. Flexural modulus is calculated from equation (4.9).

$$\frac{mL^3}{4bt^3} \quad (4.9)$$

Where, m is the slope of the tangent to the initial straight-line portion of the load deflection curve (N/mm).



Figure 4.9 Universal testing machine (Instron 1195)

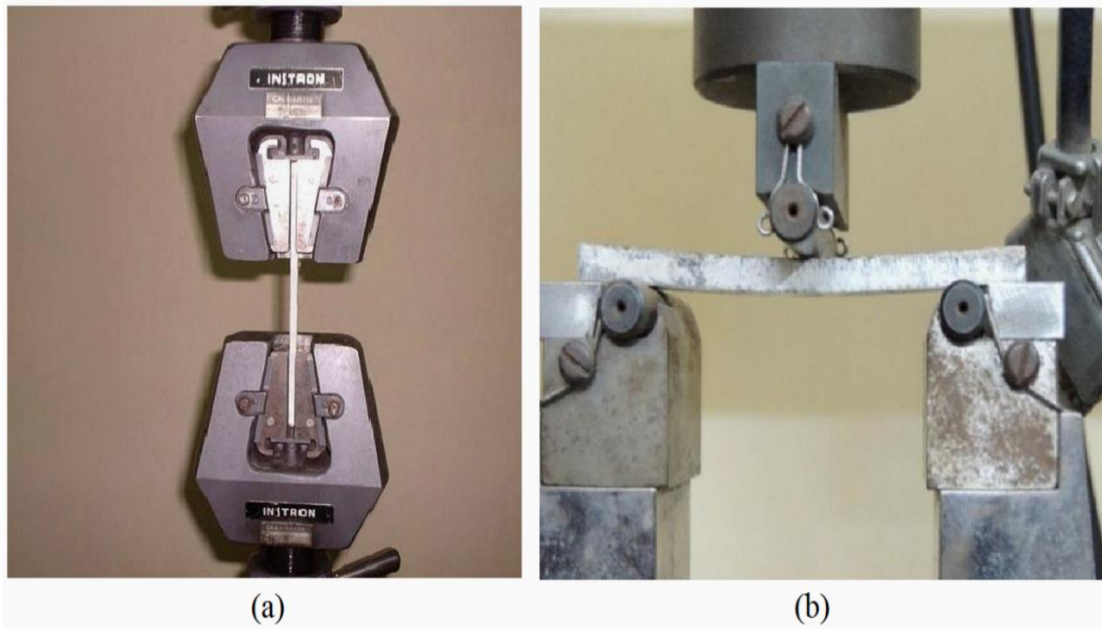


Figure 4.10 Loading arrangements for tensile and flexural tests

4.4.4 ILSS

The short beam shear tests are performed on the composite samples at room temperature to evaluate the value of ILSS. The test is conducted as per ASTM standard D 2344-84 using the

same universal testing machine Instron 1195. In this test, a short specimen with dimension of 45 mm × 10 mm × 4 mm is submitted to an apparatus at a crosshead speed of 2 mm/min. As the loading cylinder exerts a downward force, the specimen is subjected to normal (bending) and transverse shear stresses. By using a short beam, it is assumed that the beam is short enough to minimize bending stresses resulting in inter-laminar shear failure by cracking along a horizontal plane between the laminates. For each composite type, three identical specimens were tested, and the mean value is reported as the property of that composite. The ILSS of the composite specimen is determined using the equation (4.10).

$$\frac{3P}{4bt} \quad (4.10)$$

4.4.5 Impact Test

The energy required to fracture a standard test piece under an impact load is called impact energy. Low velocity instrumented impact tests are carried out on the composite specimens. The test is conducted as per ASTM standard D 256 by using Izod impact tester supplied by VEEKAY test lab, India. The dimension of the specimen is 64 mm × 12.7 mm × 4 mm and the test is accompanied on the unnotched specimens. The impact testing machine determines the impact strength of the material by shattering the specimen with a pendulum hammer, measuring the spent energy and relating it to the cross section of the specimen. The impact energy absorbed in breaking the hybrid composite specimen is recorded directly on the dial indicator.

4.4.6 Micro-Hardness

Hardness is a measure of material's resistance to permanent deformation or damage. In the present study, a Leitz micro-hardness tester (Figure 4.11) is used to measure the Vickers hardness number of the composite samples as per ASTM D785 test standard. A diamond indenter, in the form of a right pyramid with a square base and an angle 136° between opposite faces, is forced into the material under a load. The two diagonals X and Y of the indentation left on the surface of the material after removal of the load are measured and their arithmetic mean L is calculated. In the present study, the load considered as F = 24.54 N and Vickers hardness number is calculated using the equation (4.11).

$$H_v = 0.1889 \frac{F}{L^2} \quad (4.11)$$

$$\text{and } L = \frac{X+Y}{2}$$

Where, F is the applied load in N, L is the diagonal of square impression in mm, X is the horizontal length in mm and Y is the vertical length in mm. For each composite type, three identical specimens are tested and the mean value is reported as the property of that composite.



Figure 4.11: Experimental set up for micro-hardness test

4.4.7 Scanning Electron Microscopy

The surface morphology of the fiber reinforced hybrid composites together with the dispersion characteristics of the fibers in the matrix material have been studied using a scanning electron microscope JEOL JSM-6480LV as shown in Figure 4.12. The composite samples are mounted on stubs with silver paste. To enhance the conductivity of the samples, a thin film of platinum is vacuum-evaporated onto them before the micrographs are taken.

4.5 Testing of Thermal Properties

4.5.1 Thermal Conductivity

By definition, the thermal conductivity is the material property that describes the rate at which heat flows within a body for a given temperature change. Unitherm™ model 2022 thermal conductivity tester is generally used to measure the thermal conductivity of various materials, which include polymers, glasses, ceramics, rubbers, composites, few metals and other materials with medium to low thermal conductivity. In the present work, this instrument is used to measure the thermal conductivity of the composites based on guarded heat flow meter method. Disc type specimens of size 50 mm in diameter and 4 mm in

thickness are used for this purpose. This test is conducted in accordance with ASTM E1530-99 standards. The experimental set up of the Unitherm™ Model 2022 tester is shown in Figure 4.13.



Figure 4.12: Scanning electron microscope (JEOL JSM-6480LV)



Figure 4.13: Experimental set up of Unitherm™ 2022

4.5.1.1 Operating principle of Unitherm™ model 2022

The schematic view of the Unitherm™ model 2022 instrument is shown in Figure 4.14. The composite specimen is placed between two polished surfaces, under pneumatic load of 10 psi

at top portion of the stack. The top and bottom heater helps to maintain steady state heat transfer through the sample. A reference calorimeter is placed under the lower plate, which acts as a heat flux transducer. To avoid the excessive temperature from the system heat sink is used at the bottom. Each composite specimen is tested in the temperature range from 30 to 120°C. After reaching thermal equilibrium, the temperature difference across the sample is measured along with the output from the heat flow transducer. For steady state heat transfer, the user can divide the testing into different zones, called as set point temperatures.

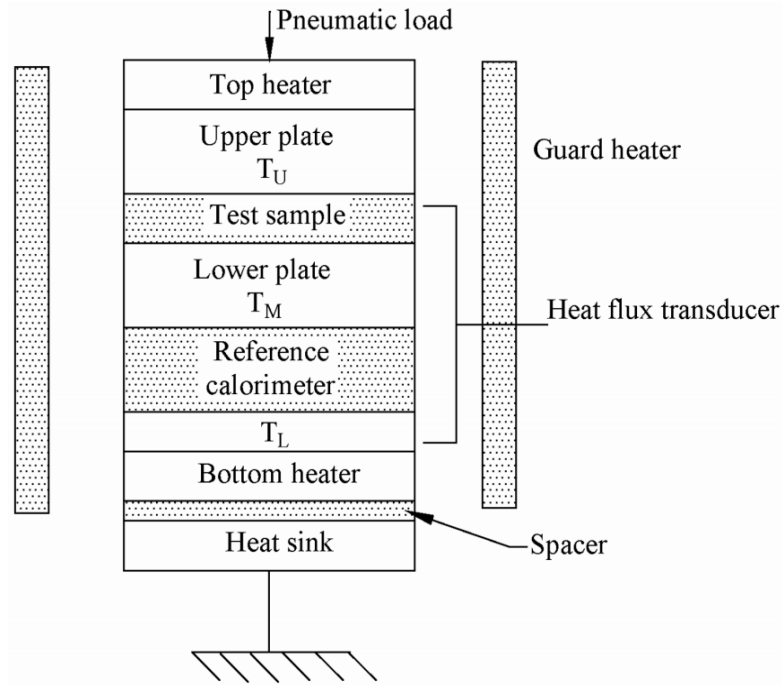


Figure 4.14: Experimental set up of Unitherm™ 2022

In the present work, the testing is divided into four temperature zones i.e. 30, 60, 90, and 120°C. For one-dimensional heat conduction the formula can be given as equation (4.12).

$$q = \frac{k(T_1 - T_2)}{L} \quad (4.12)$$

Where, q is the heat flux (W/m^2), k is the thermal conductivity ($\text{W}/\text{m}\cdot\text{K}$), $T_1 - T_2$ is the difference in temperature ($^{\circ}\text{C}$ or K), and L is the thickness of the sample (m). The thermal resistance of the composite sample is given as equation (4.13).

$$R = \frac{(T_1 - T_2)}{q} \quad (4.13)$$

Where, R is the resistance of the sample between hot and cold surfaces ($m^2\text{-K/W}$). From equations (4.12) and (4.13) the thermal conductivity can be written as equation (4.14).

$$k = \frac{L}{R} \quad (4.14)$$

In Unitherm™ 2022, heat flow transducers measure the value of heat flux q and temperature difference between upper and lower plate. Thus, thermal resistance between surfaces can be evaluated. Providing different thickness and known cross-sectional area as input parameters, the hybrid composite materials thermal conductivity can be calculated.

4.5.2 Differential Scanning Calorimeter and Thermogravimetry Analysis

Generally, differential scanning calorimeter (DSC) shows thermal transformation behavior of the sample. When the sample undergoes any transformation, it either releases energy (exothermic) or absorbs energy (endothermic). In this study, specific heat capacity is measured using DSC and the value is obtained using the following expression:

$$C_p = \frac{Q}{m \times \Delta T} \quad (4.15)$$

Where, C_p is the specified heat at constant pressure ($J/g \text{ } ^\circ\text{C}$), Q is the released or absorbed heat (J), m represents the mass (g), and ΔT is the temperature rise of specimen. The test is performed using a speed of heating $10^\circ\text{C}/\text{min}$ between 30 and 120°C . The thermal diffusivity is an important property in all problems involving a non-steady state heat transfer. The thermal diffusivity values of the composite samples are determined from the thermal conductivity, specific heat capacity and density values as given in equation (4.16).

$$\alpha = \frac{k}{\rho C_p} \quad (4.16)$$

Where, α is the thermal diffusivity of the sample (m^2/s), and k , ρ , and C_p are the thermal conductivity, specific heat capacity, and density, respectively.

The thermo gravimetric analysis (TGA) is the study of mass of the substance in a controlled atmosphere is recorded continuously as a function of temperature or time. As the temperature of the sample is increased, when the weights are plotted against temperature a curve characteristic of the substance is obtained. Such a curve is called a thermo gram or thermo gravimetric curve or thermal decomposition curve. The temperature of the phase transformation and the decomposition behaviour of the banana-jute fiber reinforced hybrid composites and the neat matrix materials are done by NETZSCH STA 449 C Jupiter®

equipment. The experimental set up of the NETZSCH STA 449 C Jupiter® is shown in Figure 4.15. Samples weighing approximately 10mg are subjected to pyrolysis in oxygen environment. The temperature range is taken from 30 to 600°C at a heating rate of 10°C/min. The mass loss is recorded in response to increasing temperature.



Figure 4.15: Experimental set up of NETZSCH STA 449 C Jupiter®

4.6 Micromechanical Methods for Hybrid Composites

4.6.1 Analytical Methods

The basic methods for predicting the elastic and thermal properties of composites materials are discussed in the literature review section as these form the basis of any homogenisation method applied to hybrid composites.

4.6.1.1 Rule of Hybrid Mixture Model

The well-known models that have been proposed and used to evaluate the properties of composites are the Voigt and Reuss model is also known as the rule of mixture model and inverse rule of mixture model. The rule of hybrid mixture is mathematical expressions which

gives the property of the composite in terms of the properties, quantity and arrangement of its constituents. The longitudinal property of the hybrid composite is calculated by using rule of hybrid mixture as given in equation (4.17).

$$P_1 = P_{fb} \Phi_{fb} + P_{fj} \Phi_{fj} + P_m \Phi_m \quad (4.17)$$

Where, P_1 is the longitudinal property of the hybrid composite in longitudinal direction. P_{fb} , P_{fj} , and P_m are the material properties of the banana fiber, jute fiber, and matrix, respectively. Similarly, Φ_{fb} , Φ_{fj} , and Φ_m are the volume fractions of the banana fiber, jute fiber, and matrix, respectively. The transverse property of hybrid composite is calculated by using rule of hybrid mixture as given in equation (4.18).

$$(1/P_2) = (\Phi_{fb}/P_{fb}) + (\Phi_{fj}/P_{fj}) + (\Phi_m/P_m) \quad (4.18)$$

Where, P_2 is the transverse property of the hybrid composite in transverse direction.

4.6.1.2 Geometric Mean Model

The geometric mean model [256], also known as Ratcliff empirical model gives the effective material property of the hybrid composite as given in equation (4.19).

$$P = P_{fb}^{\Phi_{fb}} \cdot P_{fj}^{\Phi_{fj}} \cdot P_m^{(1-(\Phi_{fb} + \Phi_{fj}))} \quad (4.19)$$

4.6.1.3 Halpin-Tsai Model

For the hybrid composites, a modification to the Halpin–Tsai equation (2.3) is proposed which incorporates the volume fractions of all the reinforcements. The longitudinal and transverse property of hybrid composite is calculated by using Halpin-Tsai model is shown in equation (4.20).

$$\frac{P}{P_m} = \left[\frac{1 + \xi(\eta_{fb} \Phi_{fb} + \eta_{fj} \Phi_{fj})}{1 - (\eta_{fb} \Phi_{fb} + \eta_{fj} \Phi_{fj})} \right] \quad (4.20)$$

Where, $\eta_{fb} = ((P_{fb}/P_m) - 1) / ((P_{fb}/P_m) + \xi)$ and $\eta_{fj} = ((P_{fj}/P_m) - 1) / ((P_{fj}/P_m) + \xi)$. Where, P represents the property of composite material listed in Table 4.4. ξ is a parameter that depends on the particular property being considered. For randomly oriented short fiber reinforced hybrid composites, the equations based on the Halpin–Tsai composite theory can be presented as the empirical equation (4.21).

$$P = \frac{3}{8}P_1 + \frac{5}{8}P_2 \quad (4.21)$$

Where, P_1 and P_2 are the predicted properties for short fiber composite in the longitudinal and transverse directions, respectively. The full description can be found in the literature [201].

Table 4.4: Traditional Halpin-Tsai parameters for fiber reinforced hybrid composites

P	P_{fb}	P_{fj}	P_m	ξ	Property
E_1	E_{fb}	E_{fj}	E_m	$2L/D$	Longitudinal modulus
E_2	E_{fb}	E_{fj}	E_m	2	Transverse modulus
G_{12}	G_{fb}	G_{fj}	G_m	1	In-plane shear modulus
k_1	k_{fb}	k_{fj}	k_m	$2L/D$	Longitudinal thermal conductivity
k_2	k_{fb}	k_{fj}	k_m	2	Transverse thermal conductivity

4.6.1.4 Lewis and Nielsen Model

For the hybrid composites, a modification to the Lewis and Nielsen model is proposed by incorporating the volume fractions of all the reinforcements. The properties of the hybrid composite are calculated by using Lewis and Nielsen model as given in equation (4.22).

$$\frac{P}{P_m} = \left[\frac{1 + \xi(\eta_{fb}\Phi_{fb} + \eta_{fj}\Phi_{fj})}{1 - \psi(\eta_{fb}\Phi_{fb} + \eta_{fj}\Phi_{fj})} \right] \quad (4.22)$$

Where, $\psi = 1 + \left(\frac{1 - \phi_m}{\phi_m^2} \right) \times (\Phi_{fb} + \Phi_{fj})$. The values of ξ and ϕ_m for different geometric shapes and orientation are already given in Tables 2.5 and 2.6.

4.6.2 Numerical Methods

The micromechanical analysis of composites is performed using commercial finite element analysis (FEA) software ANSYS. ANSYS is one of the most powerful FEA commercial software products that are widely used in automotive, aerospace, and other industries. This product is designed for solving wide variety of mechanical problems such as structural analysis, heat transfer, fluid flow problems and thermal-mechanical analysis as well as acoustic and electromagnetic problems. ANSYS can solve problems with heterogeneous components by assigning different geometries with different material properties. Thus it is very much suitable to perform mechanical and thermal analysis to predict the effective properties of unidirectional and short fiber reinforced hybrid composites using FEA.

Generally, in fiber reinforced composites, the fibers are distributed randomly with different resin contents in different local areas and the cross section of the fibers are not always circles with the same diameters. As a result, it will be difficult to predict the effective properties of fiber reinforced composites by using micromechanical analysis. In order to simplify the analysis, few assumptions are considered to all micromechanical models developed in the present work such as the fibers are uniformly distributed in the matrix, the fibers are having a circular cross section, locally both the matrix and fibers are homogeneous and isotropic, both the fiber and matrix are linear elastic, and there is perfect bonding between fibers and matrix and the composite body is free from voids [257]. These assumptions significantly reduce the complexity of calculation and make it possible to perform the analysis of unidirectional fiber reinforced composites with a RVE or unit cell. The micromechanical model considered in this work is established by the following five steps in ANSYS viz; generation of the RVE model, assigning material properties, selecting the appropriate elements and meshing, adding suitable boundary conditions, and applying mechanical and thermal loads.

Chapter Summary

This chapter has provided:

- The descriptions of the matrix and fiber materials used in this research.
- The details of fabrication of the composites.
- The various testing methods used for determining the physical, mechanical and thermal properties.
- The micromechanical methods for predicting the elastic and thermal properties of hybrid composites

The next chapter presents the results and discussion of the physical, mechanical and thermal behaviour of unidirectional fiber reinforced hybrid composites under this study.

Chapter 5

Results and Discussion – I

Unidirectional Fiber Reinforced Composites

This chapter presents the physical, mechanical and thermal behavior of the unidirectional banana-jute fiber reinforced epoxy and polyester based composites. The results of this chapter are divided into two parts. First part represents the elastic and thermal conductivity of unidirectional banana-jute fiber reinforced hybrid composites. The second part represents the physical, mechanical and thermal characteristics of unidirectional fiber reinforced hybrid composites.

5.1 Elastic and Thermal Conductivity of Unidirectional Fiber Reinforced Composites

This part of the chapter presents the micromechanical analysis for predicting the elastic and thermal conductivity of unidirectional fiber reinforced hybrid composites. The test results for elastic modulus and thermal conductivity of hybrid composites are investigated along the longitudinal and transverse direction. The results of the proposed theoretical model for calculation of transverse thermal conductivity are presented in this part of the thesis.

5.1.1 Development of Micromechanical Model in ANSYS

5.1.1.1 Generation of the RVE Model

In this work, square and hexagonal array type of fiber arrangements have been taken to study the effect of the fiber distribution on the final elastic and thermal conductivity of the hybrid composites [213], which are shown in Figures 5.1 (a) and (b), respectively. For simplicity reason, most micromechanical models assume a periodic arrangement of fibers for which a RVE or unit cell can be isolated. The RVE has the same properties and fiber volume fraction as the composite. A single RVE is taken out from the square and hexagonal array of composites for further study as shown in Figure 5.2.

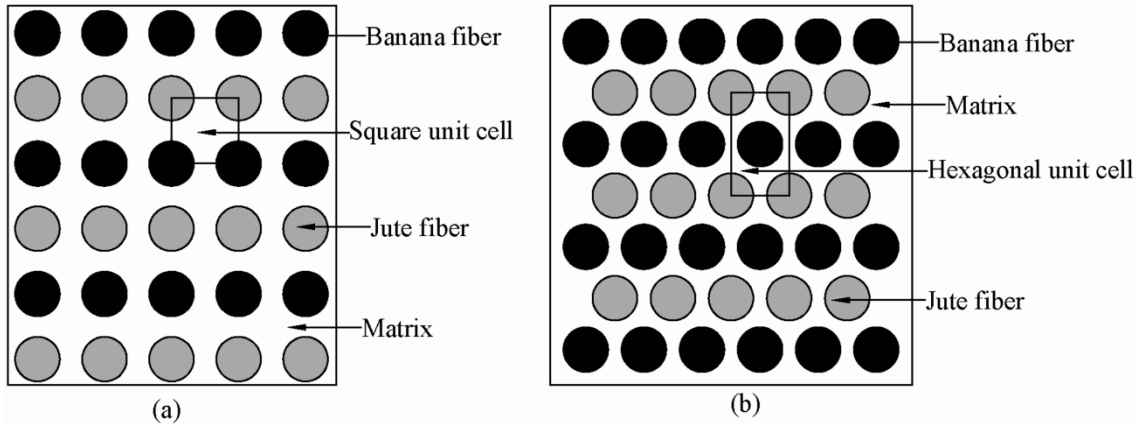


Figure 5.1: Arrangement of unidirectional fibers in (a) square array and (b) hexagonal array

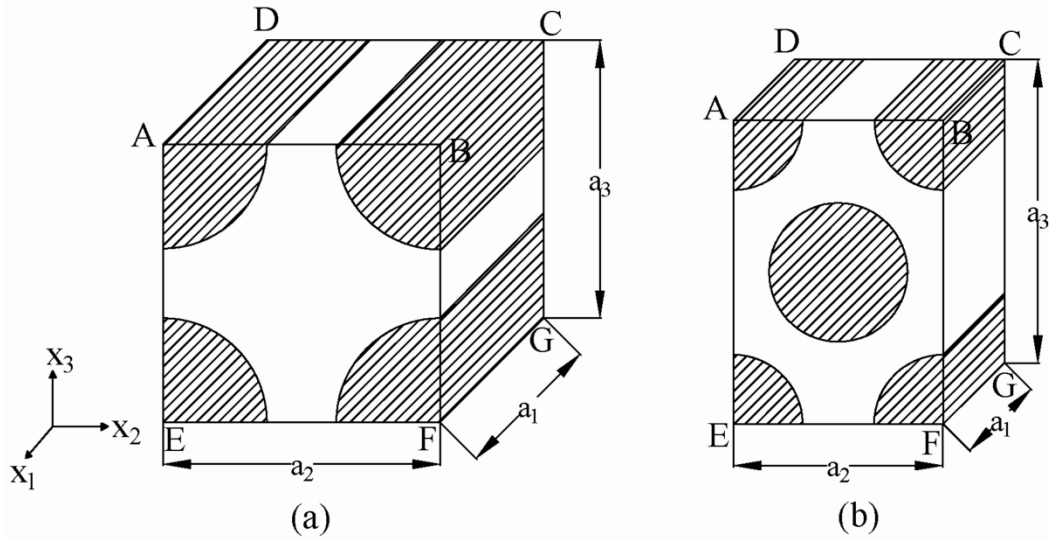


Figure 5.2: RVE of (a) square packing and (b) hexagonal packing

For a square RVE as shown in Figure 5.2 (a), the maximum theoretically achievable fiber volume fraction is 78.54%. In square RVE, the radius of fiber is calculated by using equation (5.1) [258].

$$\Phi_{fb} = \frac{\pi/2 r_{fb}^2 a_1}{a_1 a_2 a_3} \quad \text{and} \quad \Phi_{fj} = \frac{\pi/2 r_{fj}^2 a_1}{a_1 a_2 a_3} \quad (5.1)$$

Where, Φ_{fb} and Φ_{fj} are the volume fraction of banana fiber and jute fiber, respectively. Similarly, a_1 , a_2 , and a_3 are the length of square RVE and r_{fb} and r_{fj} are the radius of banana and jute fiber, respectively. In square RVE, the length of the side is same in all directions i.e., $a_1 = a_2 = a_3$. For a hexagonal RVE as shown in Figure 5.2 (b), the maximum theoretically

achievable fiber volume fraction is 90.69%. Obviously, with a hexagonal packing geometry a composite can be made more compact than with a square packing geometry. In hexagonal RVE, the radius of fiber is calculated by using equation (5.2).

$$\Phi_{fb} = \frac{\pi r_{fb}^2 a_1}{a_1 a_2 a_3} \quad \text{and} \quad \Phi_{fj} = \frac{\pi r_{fj}^2 a_1}{a_1 a_2 a_3} \quad (5.2)$$

Where $a_2 = 4a_3$ and $a_1 = a_2 \tan 60^\circ$. The length of the fiber is considered as $a_1 = 1.0 \times 10^{-5}$ m for the present analysis of square and hexagonal RVE. The radius of the banana fiber and jute fiber is calculated corresponds to the fiber loading ranging from 0 to 40 wt.%. Table 5.1 shows the volume fraction of banana and jute fibers at different fiber loading.

Table 5.1: Volume fraction of banana and jute fiber at different fiber loadings

Epoxy based composites				Polyester based composites			
Composite	Volume fraction of Banana (%)	Volume fraction of Jute (%)	Total volume fraction of fiber (%)	Composite	Volume fraction of Banana (%)	Volume fraction of Jute (%)	Total volume fraction of fiber (%)
CE1	0	0	0	CP1	0	0	0
CE2	4.330	4.175	8.505	CP2	4.261	4.109	8.370
CE3	8.806	8.492	17.298	CP3	8.679	8.369	17.048
CE4	13.423	12.943	26.366	CP4	13.250	12.776	26.026
CE5	18.228	17.577	35.805	CP5	18.023	17.379	35.402
CE6	2.167	6.268	8.435	CP6	2.132	6.168	8.300
CE7	4.410	12.758	17.168	CP7	4.346	12.573	16.919
CE8	6.727	19.462	26.189	CP8	6.640	19.210	25.850
CE9	9.144	26.452	35.596	CP9	9.041	26.153	35.194
CE10	6.490	2.086	8.576	CP10	6.386	2.053	8.439
CE11	13.189	4.239	17.428	CP11	12.998	4.178	17.176
CE12	20.086	6.456	26.542	CP12	19.828	6.373	26.201
CE13	27.253	8.760	36.013	CP13	26.948	8.662	35.610

5.1.1.2 Modeling

In order to evaluate the effective properties of hybrid composites, the finite element software package ANSYS is used. In the study of the micromechanics of fiber reinforced materials, it

is convenient to use an orthogonal coordinate system that has one axis aligned with the fiber direction. The axis x_1 is aligned with the fiber direction; the axis x_2 is in the plane of the RVE and perpendicular to the fibers and the axis x_3 is perpendicular to the plane of the RVE and is also perpendicular to the fibers as shown in Figure 5.2. A three dimensional element SOLID186 is used to determine elastic properties and is defined by 20 nodes having three degrees of freedom at each node i.e., translations in the nodal x_1 , x_2 , and x_3 directions. To determine the thermal conductivity, a three-dimensional quadratic brick element SOLID90 is used for discretization of the constituents and is defined by 20 nodes with a single degree of freedom i.e., temperature at each node. The meshed model of square and hexagonal RVE at 30 wt.% of fiber loading with different weight ratio of banana and jute fiber is shown in Figure 5.3.

5.1.1.3 Boundary Conditions for Evaluation of Elastic Properties

Composite materials can be represented as a periodic array of the RVEs. Therefore, the periodic boundary conditions must be applied to RVE models. Xia et al. [259], [260] have used an explicit unified form of periodic boundary conditions and used it in FEA of RVEs for unidirectional and angle-ply composite laminates. Since, the unidirectional and short fiber reinforced hybrid composite materials can also be envisaged as a periodical array of RVEs, so the periodic boundary conditions are adopted in the present analysis. For the sake of completeness, it is shortly summarized as follows: consider a periodic structure of unidirectional fiber reinforced composites consisting of periodic array of RVEs as shown in the Figure 5.1. It is chosen in a square and hexagonal shape to represent a more general RVE as show in Figure 5.2. The displacement field for the periodic structure can be expressed as equation (5.3) [261].

$$u_i(x_1, x_2, x_3) = \varepsilon_{ij}^0 x_j + u_i^*(x_1, x_2, x_3) \quad (5.3)$$

Where, x_j is the Cartesian coordinate of a material point and ε_{ij}^0 is the average strain over the RVE. The first term on the right hand side represents a linear distributed displacement field and the second term on the right side, $u_i^*(x_1, x_2, x_3)$ is a periodic function from one RVE to another. It represents a modification to the linear displacement field due to the heterogeneous structure of the composites. Since the periodic array of RVEs represents a continuous physical body, two continuity conditions must be satisfied at the boundaries of neighboring RVEs.

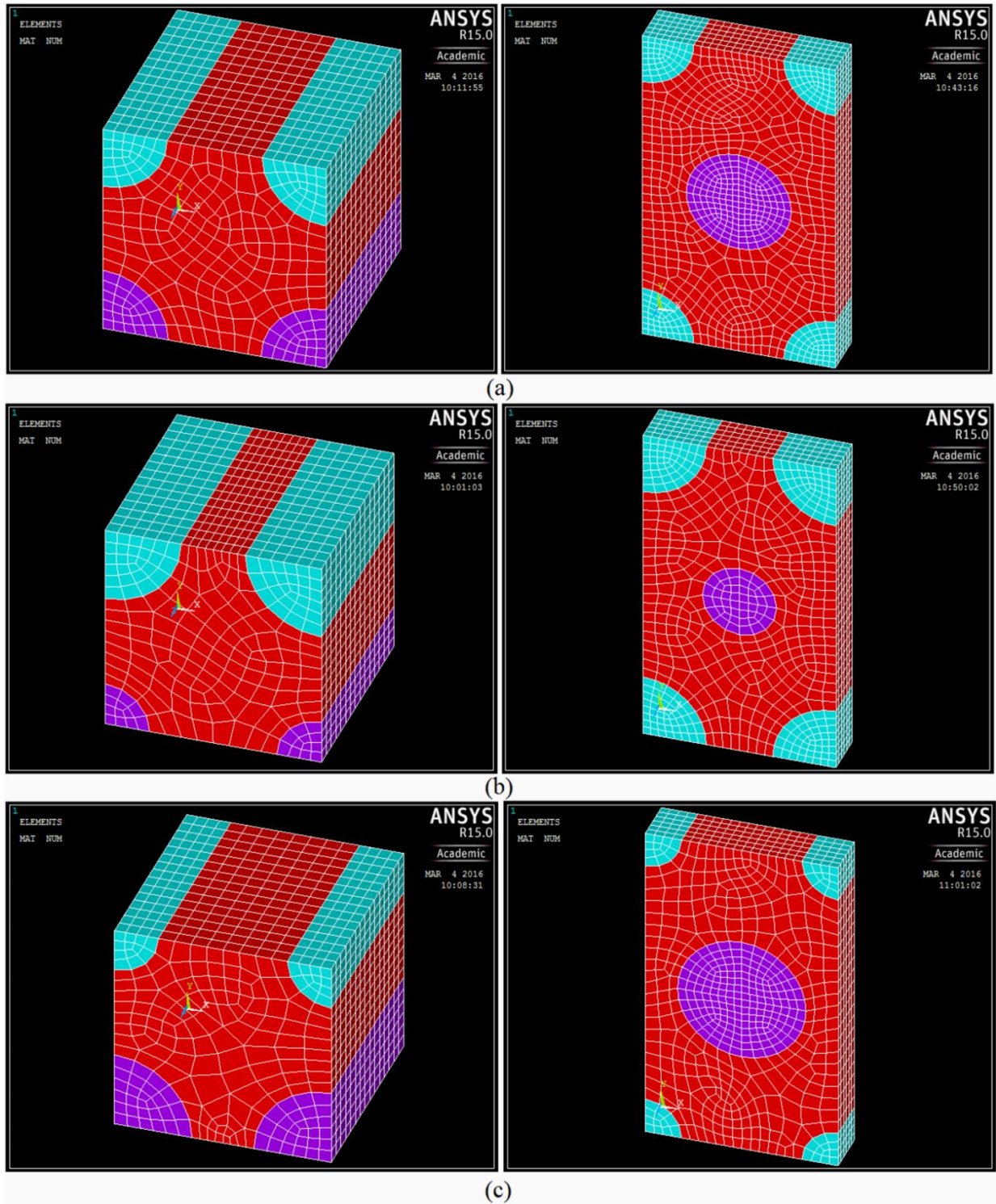


Figure 5.3: Meshed model of the square RVE and hexagonal RVE with weight ratio of banana and jute fiber as (a) 1:1, (b) 1:3, and (c) 3:1 at 30 wt.% of fiber loading

One condition is that the displacements must be continuous; it implies that each RVE in the composite has the same deformation mode and that there is no overlap or separation between neighboring RVEs after deformation. The second condition implies that the traction distributions at the opposite parallel boundaries of a RVE must be the same. In this manner, individual RVEs can be assembled as a physically continuous body. The displacement field in the equation (5.3) meets the first of the above requirements. However, it cannot be directly applied to the boundaries because the periodic part $u_i^*(x_1, x_2, x_3)$ is generally unknown. For any RVEs, the boundary surfaces always appear in parallel pairs. The displacements on a pair of parallel opposite boundary surfaces can be written as equations (5.4) and (5.5)

$$u_i^{k+} = \varepsilon_{ij}^0 x_j^{k+} + u_i^* \quad (5.4)$$

$$u_i^{k-} = \varepsilon_{ij}^0 x_j^{k-} + u_i^* \quad (5.5)$$

Where, index ‘+k’ means positive boundary surface and ‘-k’ means negative boundary surface of the k^{th} pair of a RVE. Since $u_i^*(x_1, x_2, x_3)$ is the same at the two parallel boundaries (periodicity), therefore, the difference between the equations (5.4) and (5.5) is:

$$u_i^{k+} - u_i^{k-} = \varepsilon_{ij}^0 (x_j^{k+} - x_j^{k-}) = \varepsilon_{ij}^0 \Delta x_j^k \quad (5.6)$$

The right hand side of equation (5.6) becomes constant with specified ε_{ij}^0 , since Δx_j^k are constants for each pair of the parallel boundary surfaces. Equation (5.6) can be readily applied as the nodal displacement constraint equation in FEA. It is assumed that the average mechanical properties of the RVE are equal to the average properties of the particular composite. From the numerical results, the stresses in different directions under the aforementioned boundary conditions are solved. The volume average of the stresses and strains are given by equation (5.7).

$$\begin{aligned} \bar{\sigma}_{ij} &= \frac{1}{V} \int_V \sigma_{ij} dV \\ \bar{\varepsilon}_{ij} &= \frac{1}{V} \int_V \varepsilon_{ij} dV \end{aligned} \quad (5.7)$$

Where, $\bar{\sigma}$ and $\bar{\varepsilon}$ are the average stresses and average strains and V is the volume of the RVE. The effective material coefficients can be calculated by using the constitutive equations of the material properties as the ratio of corresponding average stresses and average strains by applying the periodic boundary conditions. The most general form of the anisotropic

constitutive equations for homogeneous, elastic, composite materials is given by Hook's law as shown in equation (5.8).

$$\begin{Bmatrix} \sigma_1 \\ \sigma_2 \\ \sigma_3 \\ \sigma_4 \\ \sigma_5 \\ \sigma_6 \end{Bmatrix} \equiv \begin{Bmatrix} \sigma_{xx} \\ \sigma_{yy} \\ \sigma_{zz} \\ \tau_{yz} \\ \tau_{zx} \\ \tau_{xy} \end{Bmatrix} = \begin{bmatrix} C_{11} & C_{12} & C_{13} & C_{14} & C_{15} & C_{16} \\ C_{12} & C_{22} & C_{23} & C_{24} & C_{25} & C_{26} \\ C_{13} & C_{23} & C_{33} & C_{34} & C_{35} & C_{36} \\ C_{14} & C_{24} & C_{34} & C_{44} & C_{45} & C_{46} \\ C_{15} & C_{25} & C_{35} & C_{45} & C_{55} & C_{56} \\ C_{16} & C_{26} & C_{36} & C_{46} & C_{56} & C_{66} \end{bmatrix} \begin{Bmatrix} \varepsilon_{xx} \\ \varepsilon_{yy} \\ \varepsilon_{zz} \\ \gamma_{yz} \\ \gamma_{zx} \\ \gamma_{xy} \end{Bmatrix} \equiv \begin{Bmatrix} \varepsilon_1 \\ \varepsilon_2 \\ \varepsilon_3 \\ \varepsilon_4 \\ \varepsilon_5 \\ \varepsilon_6 \end{Bmatrix} \quad (5.8)$$

Where, σ_{ij} and τ_{ij} are normal and shear components of stress, respectively, ε_{ij} and γ_{ij} are the normal and shear components of strain, respectively, and C_{ij} is the symmetric stiffness matrix with 21 independent elastic constants. According to the behaviour, composites may be characterized as anisotropic, monoclinic, orthotropic and transversely isotropic. In present work, transversely isotropic characteristics have been considered for the fiber reinforced composite. A transversely isotropic material is a material whose effective properties are isotropic in one of its planes and the stiffness tensor is represented by using equation (5.9).

$$\begin{Bmatrix} \sigma_1 \\ \sigma_2 \\ \sigma_3 \\ \sigma_4 \\ \sigma_5 \\ \sigma_6 \end{Bmatrix} = \begin{bmatrix} C_{11} & C_{12} & C_{12} & 0 & 0 & 0 \\ C_{12} & C_{22} & C_{23} & 0 & 0 & 0 \\ C_{12} & C_{23} & C_{22} & 0 & 0 & 0 \\ 0 & 0 & 0 & \frac{1}{2}(C_{22}-C_{23}) & 0 & 0 \\ 0 & 0 & 0 & 0 & C_{66} & 0 \\ 0 & 0 & 0 & 0 & 0 & C_{66} \end{bmatrix} \begin{Bmatrix} \varepsilon_1 \\ \varepsilon_2 \\ \varepsilon_3 \\ \varepsilon_4 \\ \varepsilon_5 \\ \varepsilon_6 \end{Bmatrix} \quad (5.9)$$

Once σ_{ij} of a RVE are obtained for given ε_{ij} by equation (5.7), the C_{ij} can be determined by equation (5.9). Table 5.2 illustrates the six types of periodic boundary conditions used for obtaining each row of the stiffness matrix where the coordinates of the square RVE and hexagonal RVE are shown in Figure 5.2. After evaluating the stiffness matrix coefficients under the plane strain conditions, the longitudinal elastic modulus, transverse elastic modulus and in-plane shear modulus of the homogenized composite material are computed by equation (5.10) [258]. Figures 5.4 and 5.5 show the counter of stress and strain in square and hexagonal RVE with different weight ratio of banana and jute fiber at 30 wt.% of fiber loading.

$$\begin{aligned}
E_1 &= C_{11} - 2C_{12}^2 / (C_{22} + C_{23}) \\
E_2 = E_3 &= [C_{11}(C_{22} + C_{23}) - 2C_{12}^2] (C_{22} - C_{23}) / (C_{11}C_{22} - C_{12}^2) \\
G_{12} &= \frac{1}{2}(C_{22} - C_{23})
\end{aligned} \tag{5.10}$$

Table 5.2: Periodic boundary conditions for square and hexagonal RVE

Case	Constraint between ABEF and CDGH	Constraint between ADEH and BCFG faces	Constraint between ABCD and EFGH faces
$\varepsilon_{11}=1$	$u_1(x_1, a_1) - u_1(x_1, 0) = a_1$	$u_1(x_2, a_2) - u_1(x_2, 0) = 0$	$u_1(x_3, a_3) - u_1(x_3, 0) = 0$
	$u_2(x_1, a_1) - u_2(x_1, 0) = 0$	$u_2(x_2, a_2) - u_2(x_2, 0) = 0$	$u_2(x_3, a_3) - u_2(x_3, 0) = 0$
	$u_3(x_1, a_1) - u_3(x_1, 0) = 0$	$u_3(x_2, a_2) - u_3(x_2, 0) = 0$	$u_3(x_3, a_3) - u_3(x_3, 0) = 0$
$\varepsilon_{22}=1$	$u_1(x_1, a_1) - u_1(x_1, 0) = 0$	$u_1(x_2, a_2) - u_1(x_2, 0) = 0$	$u_1(x_3, a_3) - u_1(x_3, 0) = 0$
	$u_2(x_1, a_1) - u_2(x_1, 0) = 0$	$u_2(x_2, a_2) - u_2(x_2, 0) = a_2$	$u_2(x_3, a_3) - u_2(x_3, 0) = 0$
	$u_3(x_1, a_1) - u_3(x_1, 0) = 0$	$u_3(x_2, a_2) - u_3(x_2, 0) = 0$	$u_3(x_3, a_3) - u_3(x_3, 0) = 0$
$\varepsilon_{33}=1$	$u_1(x_1, a_1) - u_1(x_1, 0) = 0$	$u_1(x_2, a_2) - u_1(x_2, 0) = 0$	$u_1(x_3, a_3) - u_1(x_3, 0) = 0$
	$u_2(x_1, a_1) - u_2(x_1, 0) = 0$	$u_2(x_2, a_2) - u_2(x_2, 0) = 0$	$u_2(x_3, a_3) - u_2(x_3, 0) = 0$
	$u_3(x_1, a_1) - u_3(x_1, 0) = 0$	$u_3(x_2, a_2) - u_3(x_2, 0) = 0$	$u_3(x_3, a_3) - u_3(x_3, 0) = a_3$
$\gamma_{23}=1$	$u_1(x_1, a_1) - u_1(x_1, 0) = 0$	$u_1(x_2, a_2) - u_1(x_2, 0) = 0$	$u_1(x_3, a_3) - u_1(x_3, 0) = 0$
	$u_2(x_1, a_1) - u_2(x_1, 0) = 0$	$u_2(x_2, a_2) - u_2(x_2, 0) = 0$	$u_2(x_3, a_3) - u_2(x_3, 0) = a_3/2$
	$u_3(x_1, a_1) - u_3(x_1, 0) = 0$	$u_3(x_2, a_2) - u_3(x_2, 0) = a_2/2$	$u_3(x_3, a_3) - u_3(x_3, 0) = 0$
$\gamma_{13}=1$	$u_1(x_1, a_1) - u_1(x_1, 0) = 0$	$u_1(x_2, a_2) - u_1(x_2, 0) = 0$	$u_1(x_3, a_3) - u_1(x_3, 0) = a_3/2$
	$u_2(x_1, a_1) - u_2(x_1, 0) = 0$	$u_2(x_2, a_2) - u_2(x_2, 0) = 0$	$u_2(x_3, a_3) - u_2(x_3, 0) = 0$
	$u_3(x_1, a_1) - u_3(x_1, 0) = a_1/2$	$u_3(x_2, a_2) - u_3(x_2, 0) = 0$	$u_3(x_3, a_3) - u_3(x_3, 0) = 0$
$\gamma_{12}=1$	$u_1(x_1, a_1) - u_1(x_1, 0) = 0$	$u_1(x_2, a_2) - u_1(x_2, 0) = a_2/2$	$u_1(x_3, a_3) - u_1(x_3, 0) = 0$
	$u_2(x_1, a_1) - u_2(x_1, 0) = a_1/2$	$u_2(x_2, a_2) - u_2(x_2, 0) = 0$	$u_2(x_3, a_3) - u_2(x_3, 0) = 0$
	$u_3(x_1, a_1) - u_3(x_1, 0) = 0$	$u_3(x_2, a_2) - u_3(x_2, 0) = 0$	$u_3(x_3, a_3) - u_3(x_3, 0) = 0$

5.1.1.4 Boundary Conditions for Evaluation of Thermal Conductivity

The application of thermal boundary conditions plays a significant role in determining the heat transfer and thermal conductivity. One-dimensional steady state heat transfer simulations are performed by using FEA to predict thermal conductivity of the hybrid composite material along the longitudinal and transverse direction. As the model generated represents a RVE in the composite, therefore a homogenization scheme is used to define the thermal conductivity of composites along the longitudinal and transverse direction. The thermal conditions can be represented by the equation (5.11).

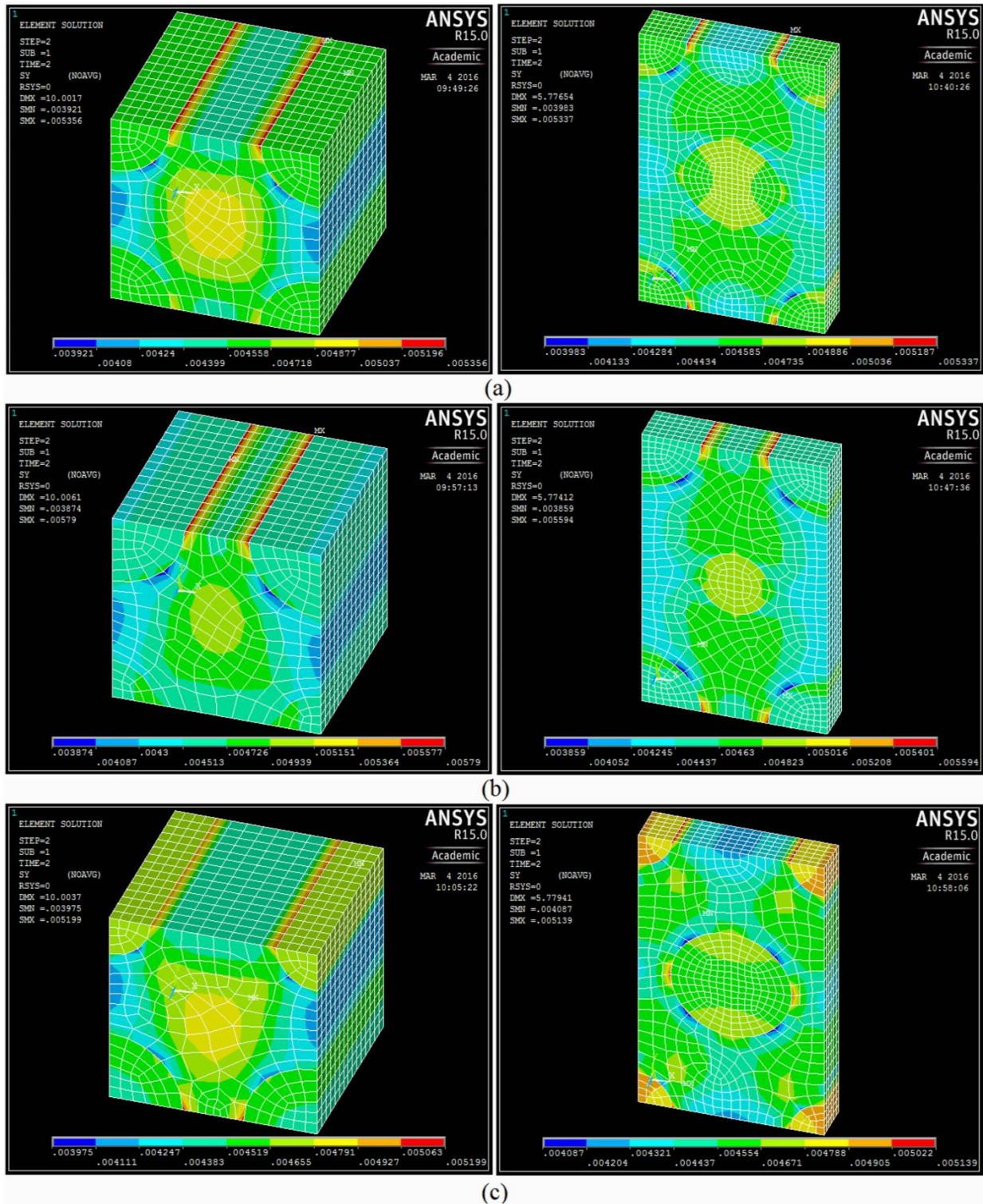


Figure 5.4: Counter of stress in square RVE and hexagonal RVE with weight ratio of banana and jute fiber as (a) 1:1, (b) 1:3, and (c) 3:1 at 30 wt.% of fiber loading

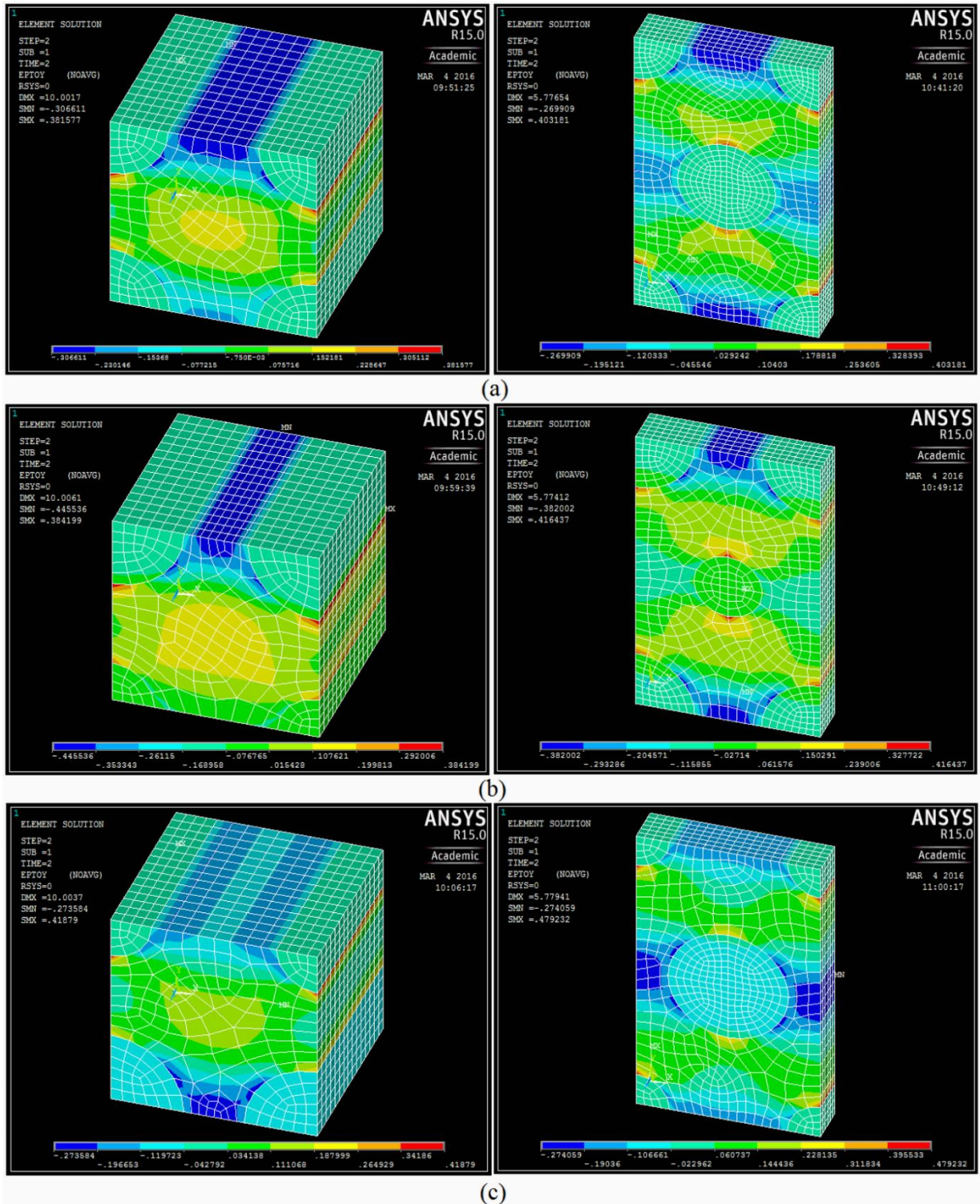


Figure 5.5: Counter of strain in square RVE and hexagonal RVE with weight ratio of banana and jute fiber as (a) 1:1, (b) 1:3, and (c) 3:1 at 30 wt.% of fiber loading

$$\begin{pmatrix} q_{x_1} \\ q_{x_2} \\ q_{x_3} \end{pmatrix} = \begin{bmatrix} k_{x_1x_1} & k_{x_1x_2} & k_{x_1x_3} \\ k_{x_2x_1} & k_{x_2x_2} & k_{x_2x_3} \\ k_{x_3x_1} & k_{x_3x_2} & k_{x_3x_3} \end{bmatrix} \begin{pmatrix} \frac{\partial T}{\partial a_1} \\ \frac{\partial T}{\partial a_2} \\ \frac{\partial T}{\partial a_3} \end{pmatrix} \quad (5.11)$$

The prescribed boundary conditions with the direction of heat flow for the conduction problem is shown in Figure 5.2. To calculate the longitudinal thermal conductivity, the temperature at the nodes along the surface ABEF is kept at T_1 ($=120^\circ\text{C}$) and the corresponding surface CDGH is kept at T_2 ($=30^\circ\text{C}$) in order to maintain the temperature difference of 90°C . In the second instance, to calculate the transverse thermal conductivity, one wall ABCD of the RVE is kept at T_1 ($=120^\circ\text{C}$) and the corresponding wall EFGH of the RVE is kept at T_2 ($=30^\circ\text{C}$) in order to maintain the temperature difference of 90°C . The other surfaces parallel to the direction of the heat flow are assumed to be adiabatic. The temperature at the inside domain and on the other boundaries are not apprehended. Thereafter, the finite element program package ANSYS is used to obtain the heat rate by using these temperature gradients. The thermal conductivity of hybrid composite is established from the fundamental heat conduction law, found by Fourier's, which states that the heat flux is proportional to the temperature gradient [262]. The longitudinal thermal conductivity of the hybrid composite is calculated by using equation (5.12).

$$k_1 = \frac{q_1}{\Delta T/a_1} \quad (5.12)$$

$$q_1 = \frac{Q_1}{A}$$

Where, ΔT is the temperature difference across the thickness (a_1) of the composite, Q_1 is the heat rate along the longitudinal direction obtained as result from simulation in W, q_1 is the heat flux in longitudinal direction in W/m^2 , A is the cross-sectional area across the flux in m^2 and k_1 is the longitudinal thermal conductivity of the hybrid composite in $\text{W}/\text{m}\cdot\text{K}$. The temperature distribution along the longitudinal direction in square and hexagonal RVE at 30 wt.% of fiber loading is shown in Figure 5.6. The transverse thermal conductivity of the hybrid composite is calculated by using equation (5.13).

$$k_2 = k_3 = \frac{q_3}{\Delta T/a_3} \quad (5.13)$$

$$q_3 = \frac{Q_3}{A}$$

Where, ΔT is the temperature difference across the thickness (a_3) of the composite, Q_3 is the heat rate along the transverse direction obtained as result from simulation in W, q_3 is the heat flux in transverse direction in W/m^2 , A is the cross-sectional area across the flux in m^2 and K_3 is the transverse thermal conductivity of the hybrid composite in $W/m-K$. Figure 5.7 shows the temperature distribution along the transverse direction in square and hexagonal RVE at 30 wt.% of fiber loading.

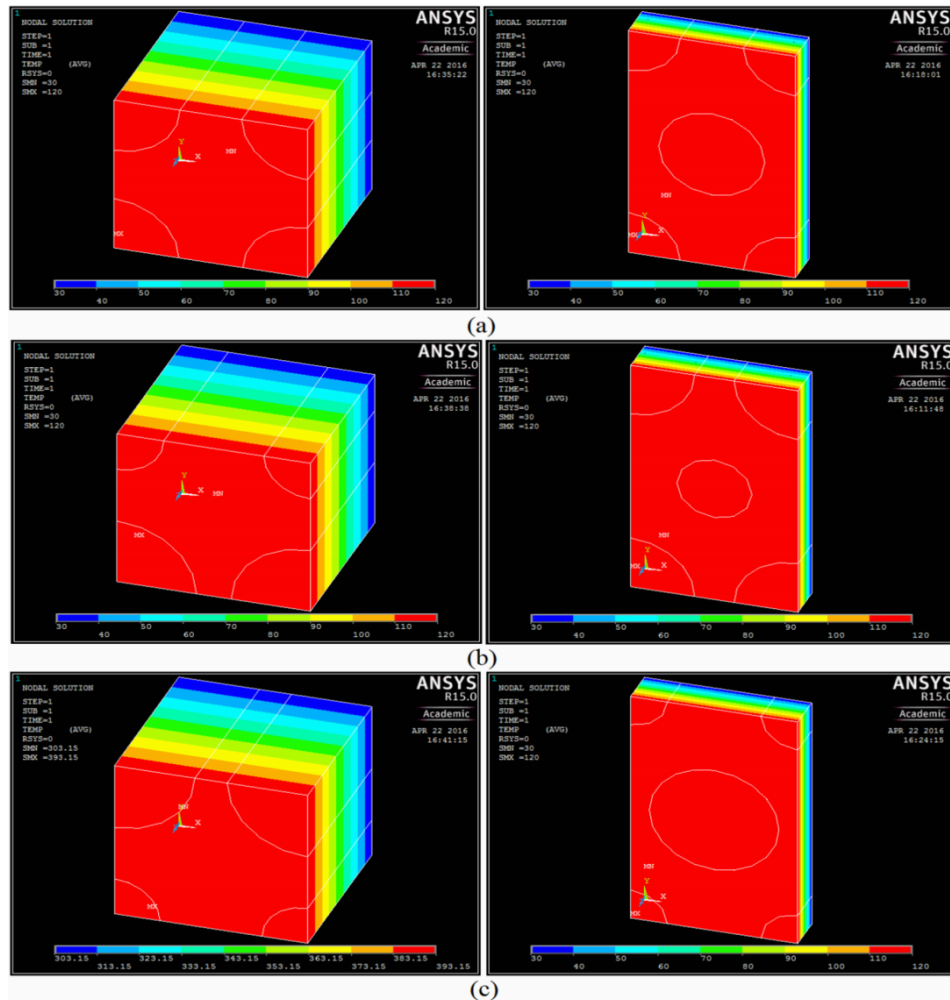


Figure 5.6: Longitudinal temperature distribution in square RVE and hexagonal RVE with weight ratio of banana and jute fiber as (a) 1:1, (b) 1:3, and (c) 3:1 at 30 wt.% of fiber loading

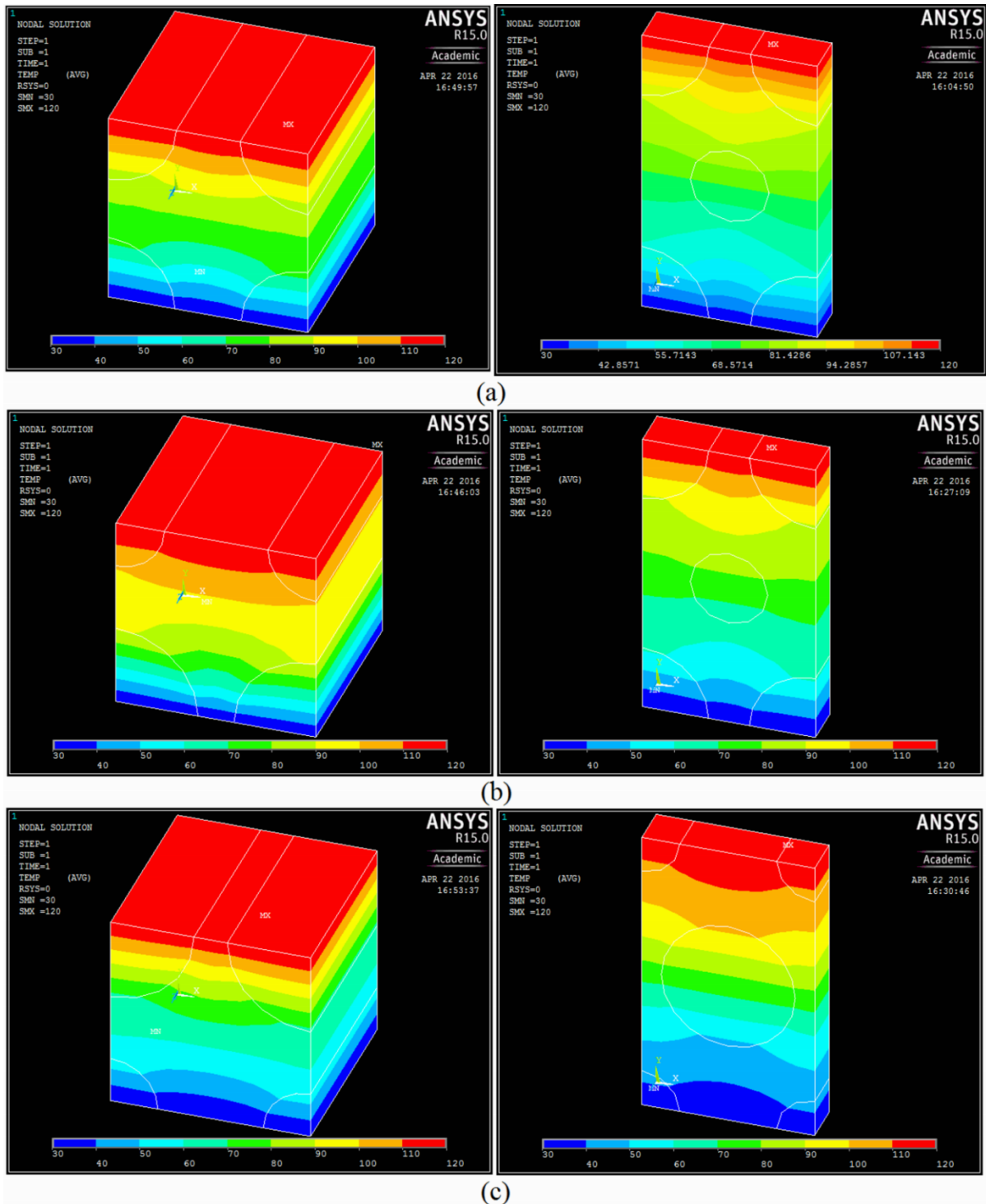


Figure 5.7: Transverse temperature distribution in square RVE and hexagonal RVE with weight ratio of banana and jute fiber as (a) 1:1, (b) 1:3, and (c) 3:1 at 30 wt.% of fiber loading

5.1.2 Elastic Properties of Unidirectional Fiber Reinforced Hybrid Composites

Tensile testing is performed to evaluate the longitudinal and transverse elastic modulus of composite specimens using the procedure described in section 4.4.2. The relationship between the applied force and elongation is linear behaviour until the point of sudden failure is observed in all cases. Failure is noted to occur in a violent manner, involving fiber breakage and the presence of cracks. The linear region obeys the Hook's law where the stress to the strain is a constant. The constant is the slope of the line in this region where the stress is proportional to the strain and is called elastic modulus. The different composite samples are tested in the universal testing machine Instron 1195 and the samples are left to break till the ultimate modulus and strength occurs. The numerical and analytical solutions for the longitudinal and transverse elastic modulus of composites are calculated and compared with experimental results at different fiber loading and weight ratio. In addition, the tensile properties of individual banana and jute fibers are also presented.

5.1.2.1 Tensile Modulus of Banana and Jute Fiber

The single fiber tensile test is performed for ten fiber specimens and the average of these is used to calculate the tensile modulus. The tensile modulus of the banana and jute fiber were determined using the cross-sectional area with the diameter of the fiber obtained using the microscopy method. The stress-strain curves of banana and jute fiber obtained at 50 mm gage length are shown in Figures 5.8 and 5.9. The result shows that the banana and jute fiber have an average tensile modulus of 6.2 ± 0.87 GPa and 8.5 ± 0.59 GPa, respectively.

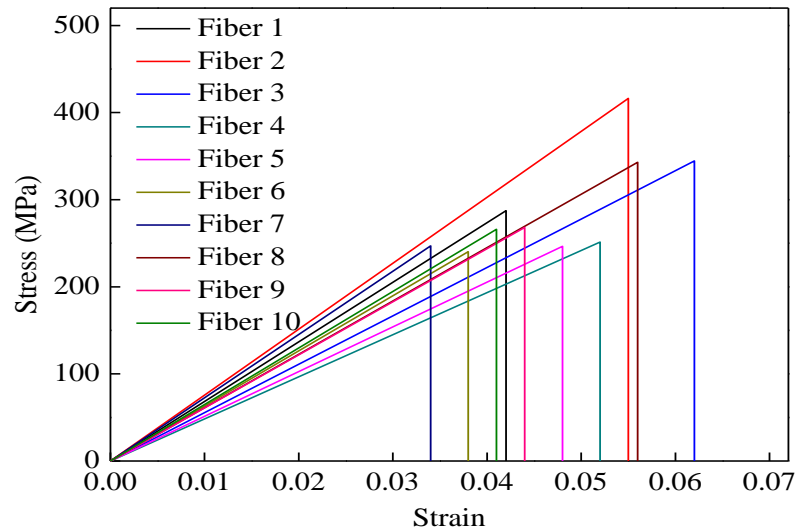


Figure 5.8: Stress-strain curves for banana fiber specimens

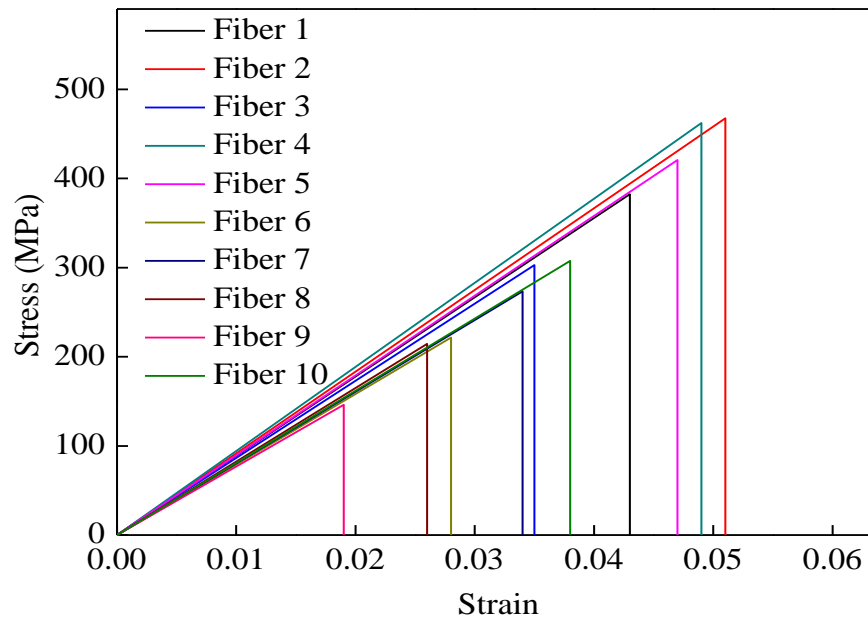


Figure 5.9: Stress-strain curves for jute fiber specimens

5.1.2.2 Longitudinal Elastic Modulus of Composites

Longitudinal elastic modulus can be defined as the ratio of longitudinal stress to the longitudinal strain. It is the response of material during the application of load parallel to the fiber direction. In longitudinal loading, the unidirectional fiber reinforced composites affected by the failure of fiber and the yield of matrix. Matrix yielding is a gradual process and as the applied longitudinal load increases the yield region expands progressively. The effect of fiber loading and weight ratio on longitudinal elastic modulus values of the epoxy and polyester based composites are shown in Figures 5.10 and 5.11, respectively. It may be noted that, the elastic modulus of the neat epoxy and polyester resin are 3.14 GPa and 1.48 GPa, respectively. The elastic modulus of the composites increases continuously as the fiber loading increases in both the epoxy and polyester based composites. This observation is rather common due to the incorporation of stiff lignocellulose fibers such as banana and jute in to the polymer matrix. Similar trend of increase in longitudinal elastic modulus values with increase in fiber loading is reported by the past researchers [112], [263]. Composite at 40 wt.% of fiber loading with weight ratio of banana and jute fiber of 1:3 shows the maximum elastic modulus than the other weight ratios. Generally, the jute fiber has higher elastic modulus than that of banana fiber. Hence, it would be expected that hybrid composites containing greater proportions of jute fiber have higher elastic modulus. For epoxy based composites, the longitudinal elastic modulus increases from 3.14 GPa at 0 wt.% fiber loading to 4.21 GPa, 4.29 GPa and 4.709 GPa at 40 wt.% fiber loading with weight ratio of banana and jute fiber as 1:1, 1:3, and 3:1, respectively. Similarly, for polyester based composites, the

longitudinal elastic modulus increases from 1.48 GPa at 0 wt.% fiber loading to 3.22 GPa, 3.37 GPa and 2.92 GPa at 40 wt.% fiber loading with weight ratio of banana and jute fiber as 1:1, 1:3, and 3:1, respectively.

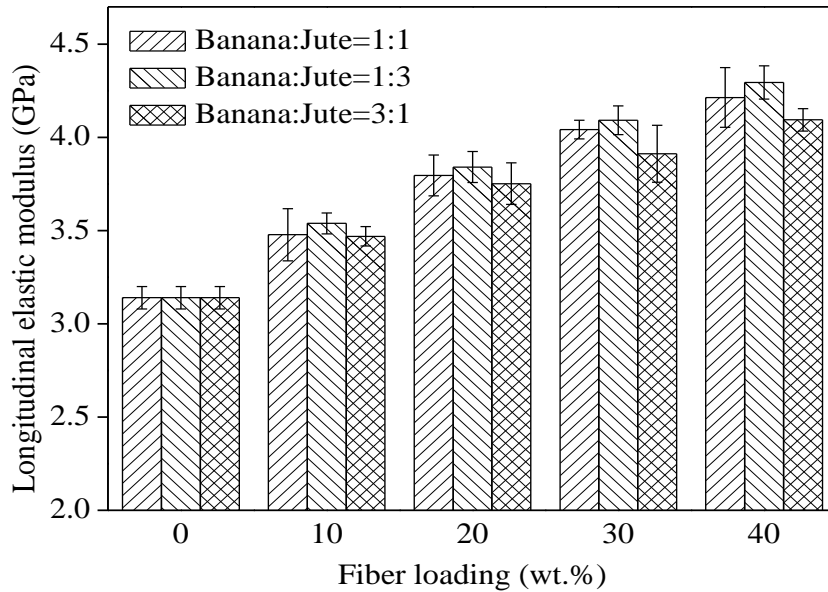


Figure 5.10: Effect of fiber loading and weight ratio on longitudinal elastic modulus of epoxy based hybrid composites

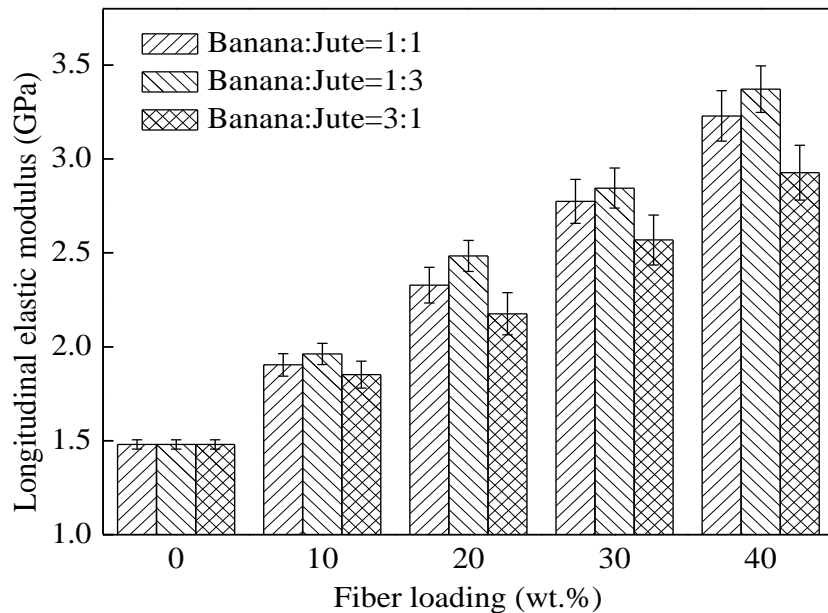


Figure 5.11: Effect of fiber loading and weight ratio on longitudinal elastic modulus of polyester based hybrid composites

A comparison of experimental longitudinal elastic modulus values of epoxy based hybrid composites with the predicted values using rule of hybrid mixture, Halpin–Tsai, Lewis and Nielsen models along with the results of FEA are presented in Figures 5.12 to 5.14 at different weight ratio of banana and jute fiber. The corresponding results for polyester based composites are shown in Figures 5.15 to 5.17. The similar trend of increase in elastic modulus with the increase in fiber loading is observed for all the cases. Among all micromechanical models, rule of hybrid mixture presents the upper bound of the elastic modulus, where it shows a clear difference with the experimental results. By comparing the experimental results and the results of rule of hybrid mixture model, the maximum relative error is found as 12.61% and 10.97% for epoxy and polyester based hybrid composites, respectively. Whereas, the maximum relative error between the experimental results and results of Lewis and Nielsen model are found to be 5.26% and 29.71% for epoxy and polyester based composites, respectively. It is also observed that the experimental results are close to the predicted value obtained using Halpin-Tsai model with the maximum relative error of 3.77% and 18.35% for epoxy and polyester based hybrid composites, respectively. Thus, it is suggested that Halpin–Tsai model is more suitable to predict longitudinal elastic modulus of natural fiber reinforced hybrid composites than the other analytical predictions. Also, the elastic modulus of natural fiber reinforced polymer composites predicted by Halpin–Tsai model has been found to agree well with the experimental modulus by previous researchers [217], [264].

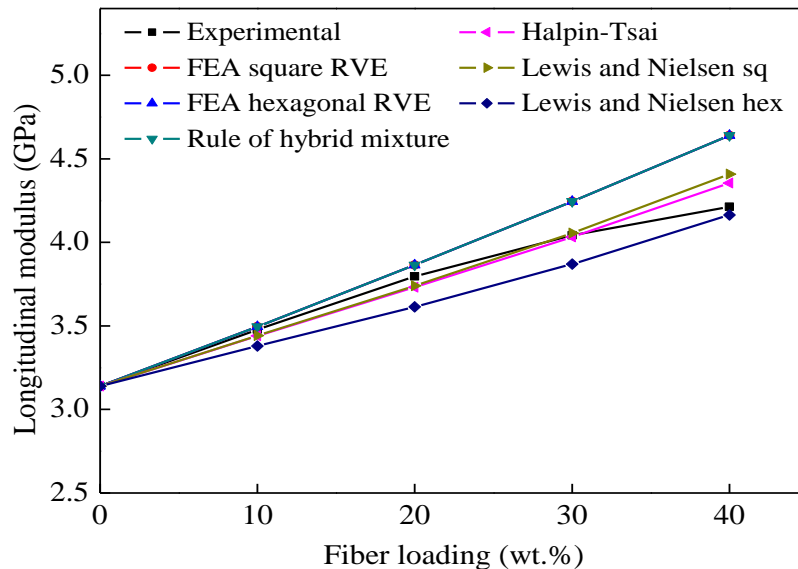


Figure 5.12: Comparison of longitudinal elastic modulus values of epoxy based composites with the weight ratio of banana and jute fiber as 1:1

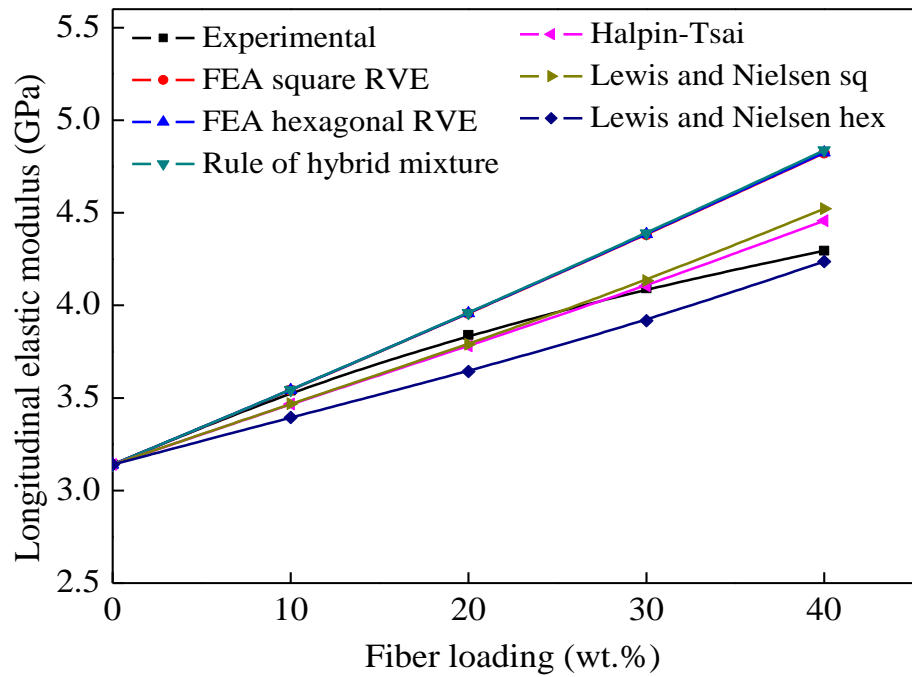


Figure 5.13: Comparison of longitudinal elastic modulus values of epoxy based composites with the weight ratio of banana and jute fiber as 1:3

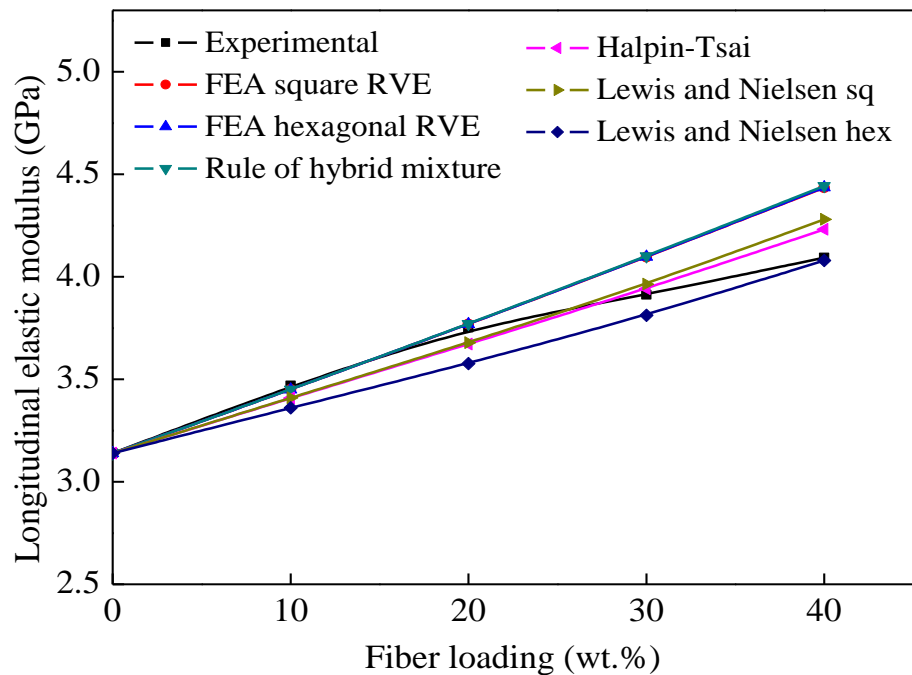


Figure 5.14: Comparison of longitudinal elastic modulus values of epoxy based composites with the weight ratio of banana and jute fiber as 3:1

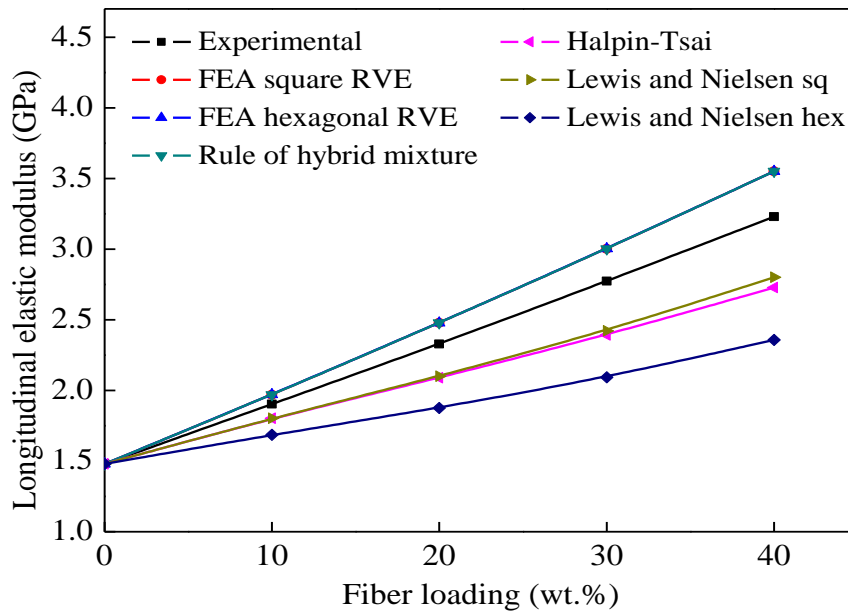


Figure 5.15: Comparison of longitudinal elastic modulus values of polyester based composites with the weight ratio of banana and jute fiber as 1:1

In the numerical analysis, square and hexagonal RVE models are considered for each fiber loading, and subjected to longitudinal tensile deformation along the x_1 axis of coordinate. The ensemble average of the effective material properties at each volume fraction are considered as effective material properties of the total composite at that particular volume fraction. It is clear from the figures that the longitudinal elastic modulus obtained from FEA square RVE and FEA hexagonal RVE are in good agreement with the rule of hybrid mixture results. In addition, the numerical results are reasonably fitted to experimental results. It can be observed that the differences between FEA and experimental results for epoxy and polyester based hybrid composites are very much within the acceptable limits which proves the consistency of FEA in predicting the longitudinal elastic modulus. Thus, it can be inferred that FEA can be used effectively to predict longitudinal elastic modulus of unidirectional fiber reinforced hybrid composites with square RVE and hexagonal RVE in similar conditions. Generally, in experimental investigation it is observed that the volume fraction of voids increases with the increase in fiber loading. Similarly, the fiber-fiber interaction, surface irregularities of the fiber and non-uniformity of the fiber are also affects the composite properties [265]. However, these factors are not considered for any of the models i.e. both the numerical and analytical models used in this study. For the above reason, there may be the deviation between the experimental results and results of analytical and numerical models.

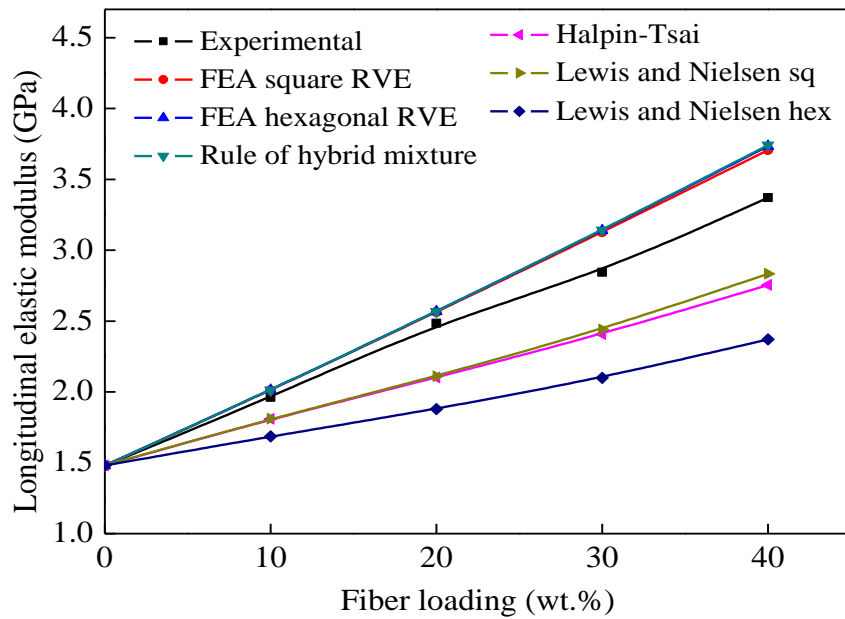


Figure 5.16: Comparison of longitudinal elastic modulus values of polyester based composites with the weight ratio of banana and jute fiber as 1:3

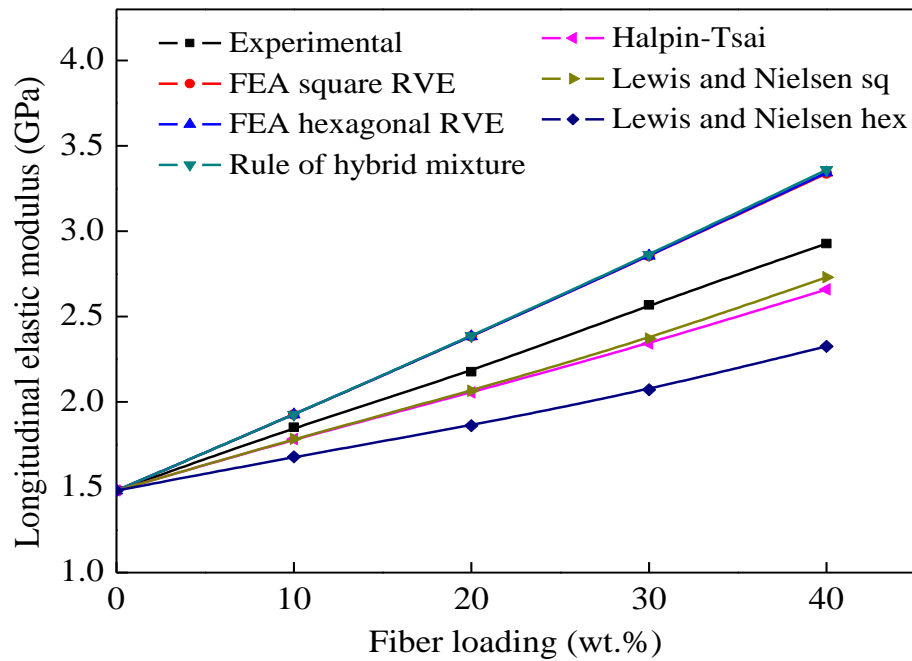


Figure 5.17: Comparison of longitudinal elastic modulus values of polyester based composites with the weight ratio of banana and jute fiber as 3:1

5.1.2.3 Transverse Elastic Modulus of Composites

The transverse elastic modulus can be defined as the ratio of transverse stress to the transverse strain. Generally, it is the response of material during the application of load perpendicular to the fiber direction. The influence of fiber loading and weight ratio on the transverse elastic modulus of epoxy and polyester based composites are shown in Figures 5.18 and 5.19 respectively. It is observed from the figures that the transverse elastic modulus increases with the increase in fiber loading up to 30 wt.%, beyond which the modulus decreases. At higher fiber loading, the possibility of fiber agglomeration, and presence of voids results in the hybrid composite which leads to decrease in stress transfer between the fiber and the matrix [265].

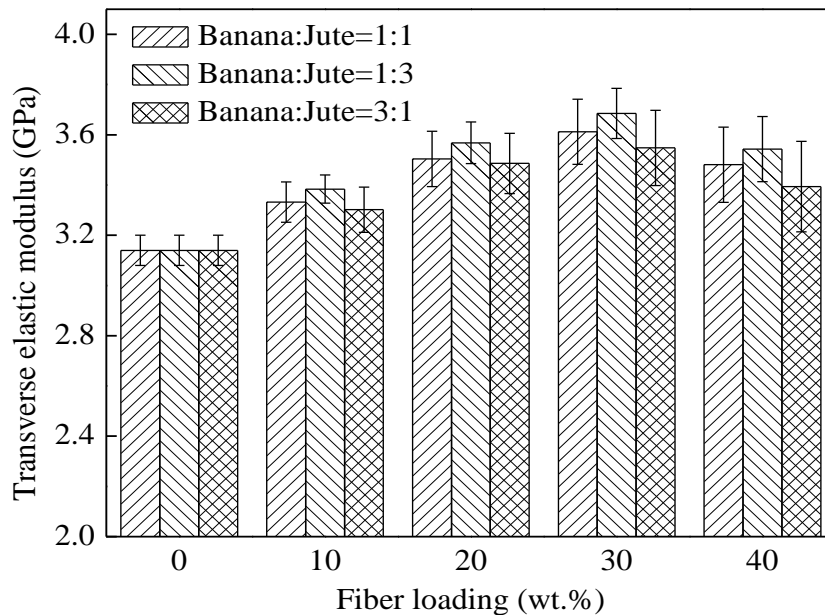


Figure 5.18: Effect of fiber loading and weight ratio on transverse elastic modulus of epoxy based hybrid composites

For epoxy based composites at 30 wt.% of fiber loading, the transverse elastic modulus of the composites increased by 15%, 17.3%, and 12.9% with the weight ratio of banana and jute fiber as 1:1, 1:3, and 3:1 respectively, as compared to the neat epoxy. Similarly, in polyester based composites at 30 wt.% fiber loading, the transverse elastic modulus is found to be increased by 41.6%, 43.7%, and 33.9% with the weight ratio of banana and jute fiber as 1:1, 1:3, and 3:1 respectively, as compared to the neat polyester. It can be seen from figures that the hybrid composites have lower elastic modulus in the transverse direction as compared to the longitudinal direction. This may be due to the fact

that the longitudinal elastic modulus of the hybrid composites is controlled by the fiber properties in longitudinal direction and the transverse elastic modulus is controlled by the matrix properties in transverse direction. Similar observations have also been reported by previous researchers [266].

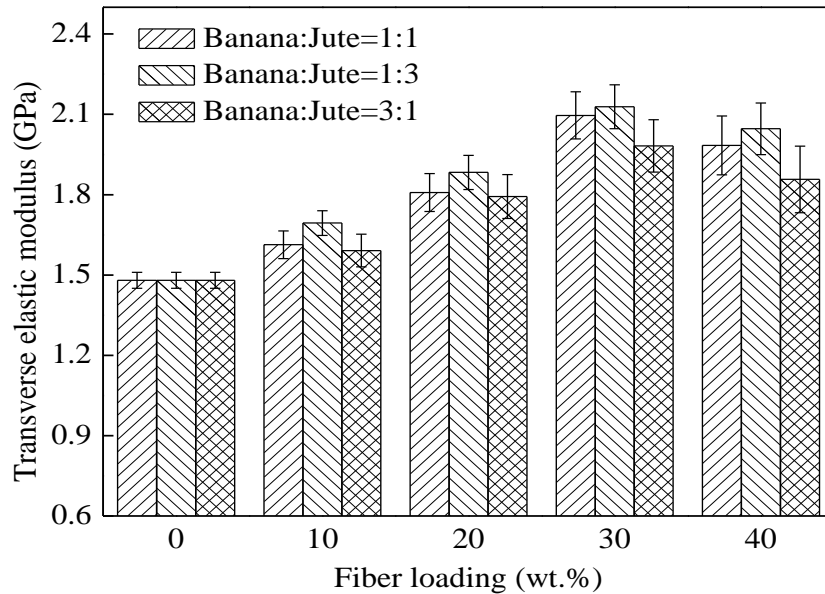


Figure 5.19: Effect of fiber loading and weight ratio on transverse elastic modulus of polyester based hybrid composites

The numerical prediction of the transverse elastic modulus in unidirectional hybrid composites seems more difficult than the longitudinal elastic modulus. In the square and hexagonal RVE in Figure 5.2, the x_2 and x_3 directions are represented to be transverse to the fibers. The transverse elastic modulus in x_2 direction and x_3 direction are supposed to be the same. Thus, the same numerical solution to evaluate E_2 has been adopted to calculate E_3 . Figures 5.20 to 5.22 shows the comparison of experimental results and results obtained using analytical and numerical models for transverse elastic modulus of epoxy based composites at different weight ratios of banana and jute fiber. The corresponding results of polyester based composites are shown in Figures 5.23 to 5.25. It is observed from the figures that the analytical and numerical results are matched well with the experimental values at low fiber loading (less than 30 wt.%) due to the uniform stress distribution in the composites through the well-dispersed matrix. But at higher fiber loading, due to the presence of voids, the applied load may not be evenly distributed between the fibers. So that at higher fiber loading the experimental results deviates from the analytical and numerical values [106]. It is

interesting to notice the difference between the results from the FEA square RVE and FEA hexagonal RVE.

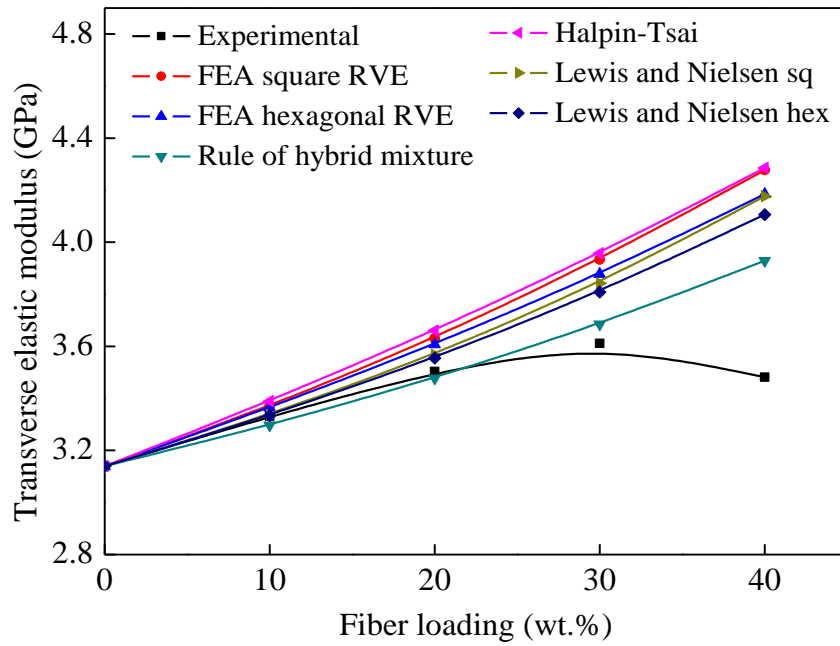


Figure 5.20: Comparison of transverse elastic modulus values of epoxy based composites with the weight ratio of banana and jute fiber as 1:1

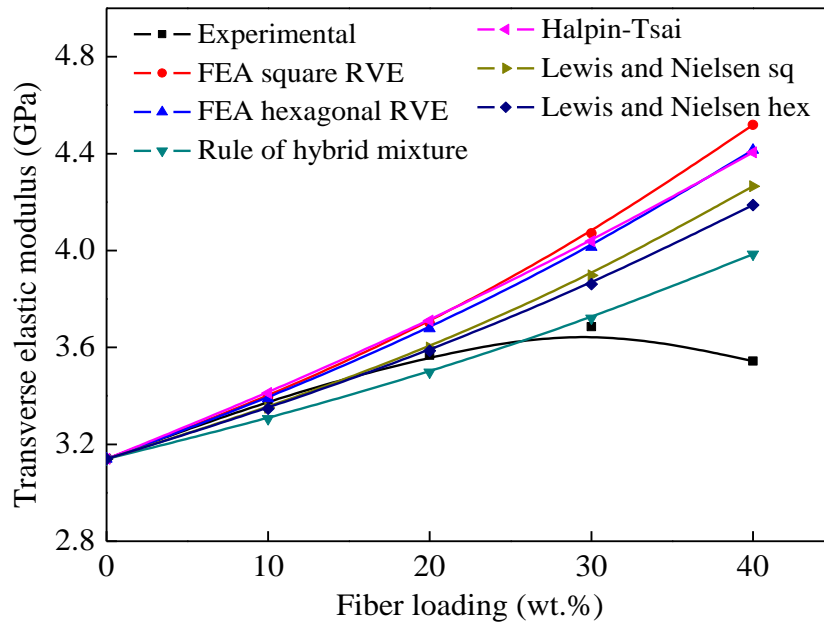


Figure 5.21: Comparison of transverse elastic modulus values of epoxy based composites with the weight ratio of banana and jute fiber as 1:3

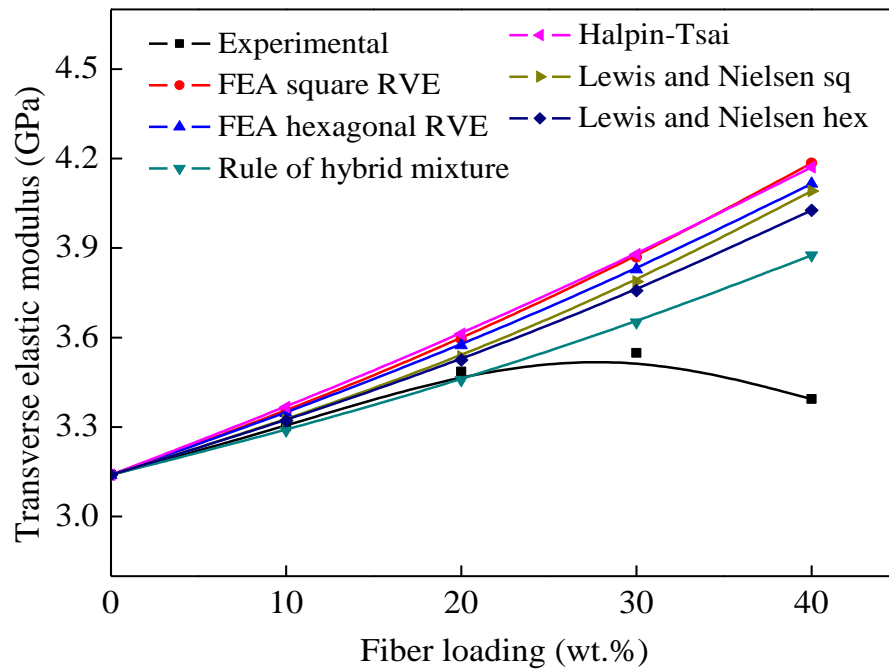


Figure 5.22: Comparison of transverse elastic modulus values of epoxy based composites with the weight ratio of banana and jute fiber as 3:1

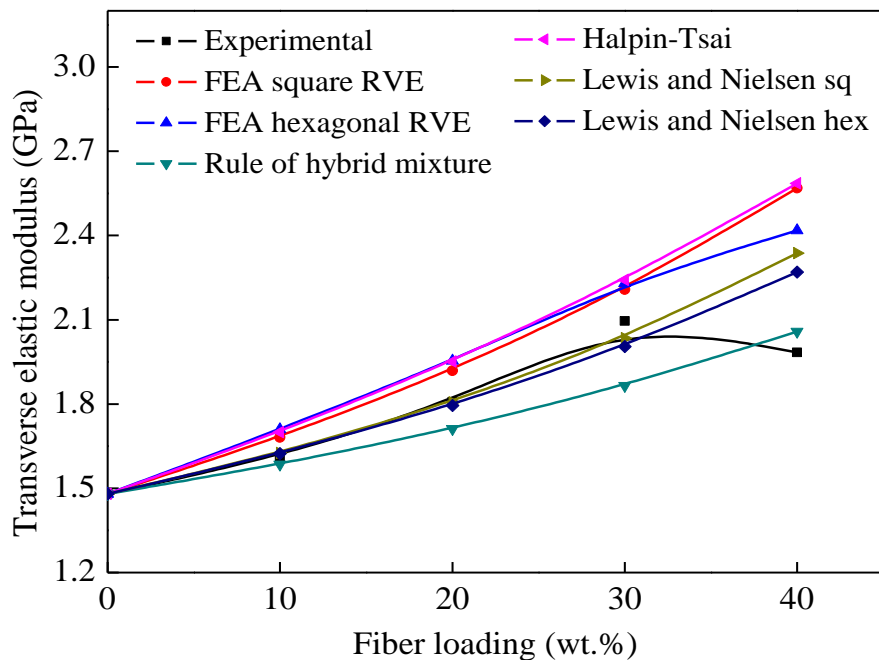


Figure 5.23: Comparison of transverse elastic modulus values of polyester based composites with the weight ratio of banana and jute fiber as 1:1

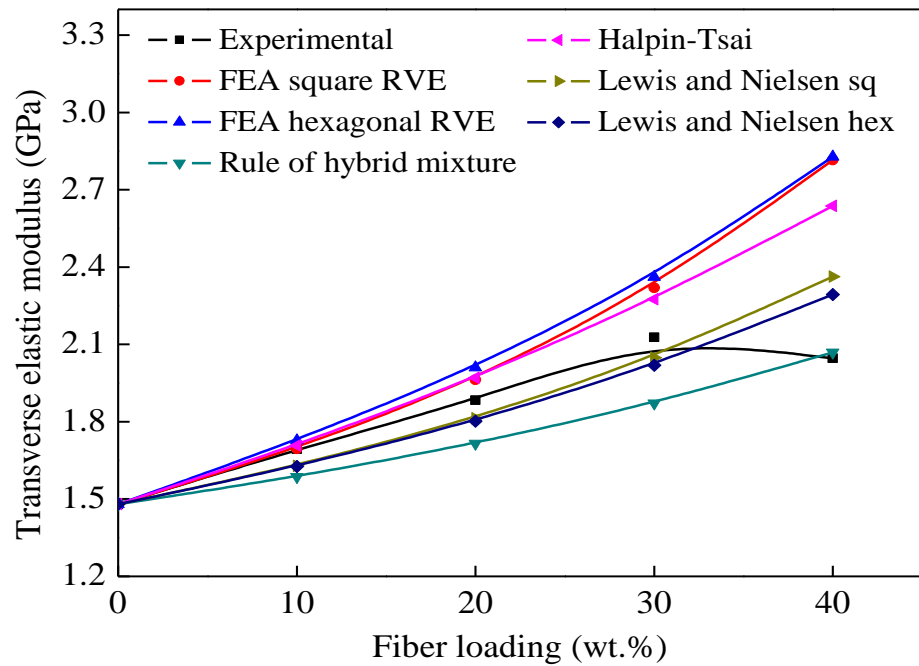


Figure 5.24: Comparison of transverse elastic modulus values of polyester based composites with the weight ratio of banana and jute fiber as 1:3

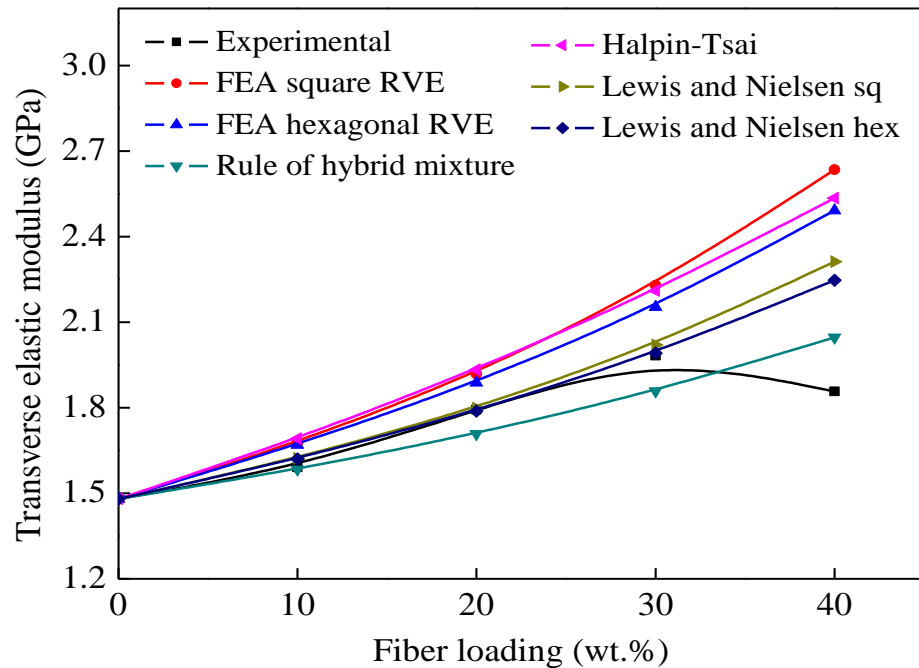


Figure 5.25: Comparison of transverse elastic modulus values of polyester based composites with the weight ratio of banana and jute fiber as 3:1

The transverse elastic modulus obtained from the FEA square RVE tends to be higher than that from the FEA hexagonal RVE. However, the difference is marginal and this behavior is consistent with the results reported by Kari [267]. The results obtained from FEA hexagonal RVE are in good agreement with the analytical methods as compared to FEA square RVE. By comparing the FEA square RVE and experimental results at 30 wt.% of fiber loading, the maximum relative error is found to be 10.47% and 9.02% for epoxy and polyester hybrid composites, respectively. Similarly, by comparing the FEA hexagonal RVE and experimental results, the maximum relative error is found to be of 7.89% and 8.62% for epoxy and polyester hybrid composites, respectively.

5.1.2.4 In-plane Shear Modulus of Hybrid Composites

In-plane shear modulus of material is the ratio of shear stress to the shear strain in longitudinal direction. The shear modulus of the constituent materials is calculated by using the equation (5.14).

$$G_p = \frac{E_p}{2(1 + \nu_p)} \quad (5.14)$$

Where, G_p , E_p , and ν_p are the shear modulus, Young's modulus and Poisson's ratio of constituent material, respectively. The Young's modulus of banana fiber, jute fiber, epoxy and polyester matrix are considered as 6.2 GPa, 8.5 GPa, 3.14 GPa and 1.48 GPa, respectively. Similarly, the Poisson's ratio of banana fiber, jute fiber, epoxy and polyester matrix are considered as 0.38, 0.36, 0.39 and 0.46, respectively [268]. The comparison of in-plane shear modulus of the epoxy based composites are shown in Figures 5.26 to 5.28, whereas polyester based composites are shown in Figures 5.29 to 5.31. It is observed from the figures that the in-plane shear modulus of the composites increases continuously as the fiber loading increases in both the epoxy and polyester based composites. It is also evident that the FEA results are in good agreement with the analytical methods. Agreement is obvious while discrepancy is purely due to the differences in the assumptions taken like fiber arrangement, square and hexagonal packing. The in-plane shear modulus value predicted by the FEA hexagonal RVE are in good agreement with those by the theoretical models. Among all the analytical models, rule of hybrid mixture shows the lower bound of the in-plane shear modulus and it shows a clear difference with the FEA results. By comparing the FEA hexagonal RVE results and the rule of hybrid mixture model, the maximum relative error is found to be 9.52% and 22.71% for epoxy and polyester based composites, respectively, whereas the maximum relative error for Halpin-Tsai model is found to be 9.45% and 15.32% for epoxy and polyester based composites, respectively. The FEA hexagonal results are close

to the predicted values using Lewis and Nielsen model within the maximum relative error of 3.06% and 11.39% for epoxy and polyester based composites, respectively. Thus, it is suggested that a Lewis and Nielsen model is more suitable to predict in-plane shear modulus of natural fiber reinforced hybrid composites than the other analytical predictions.

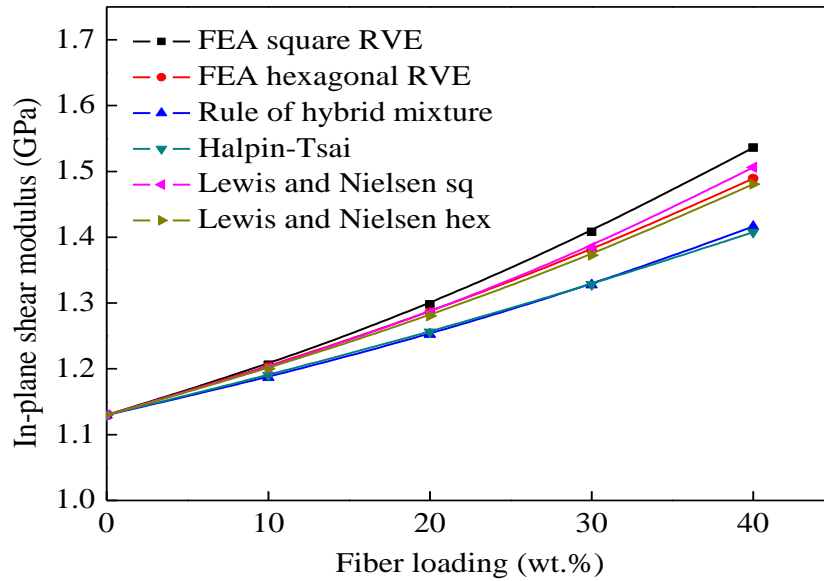


Figure 5.26: Comparison of in-plane shear modulus value of epoxy based composites with the weight ratio of banana and jute fiber as 1:1

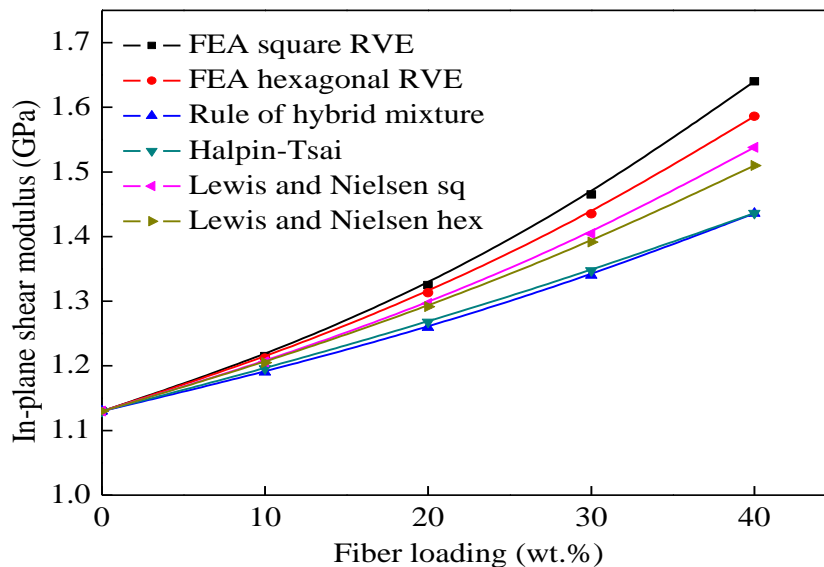


Figure 5.27: Comparison of in-plane shear modulus value of epoxy based composites with the weight ratio of banana and jute fiber as 1:3

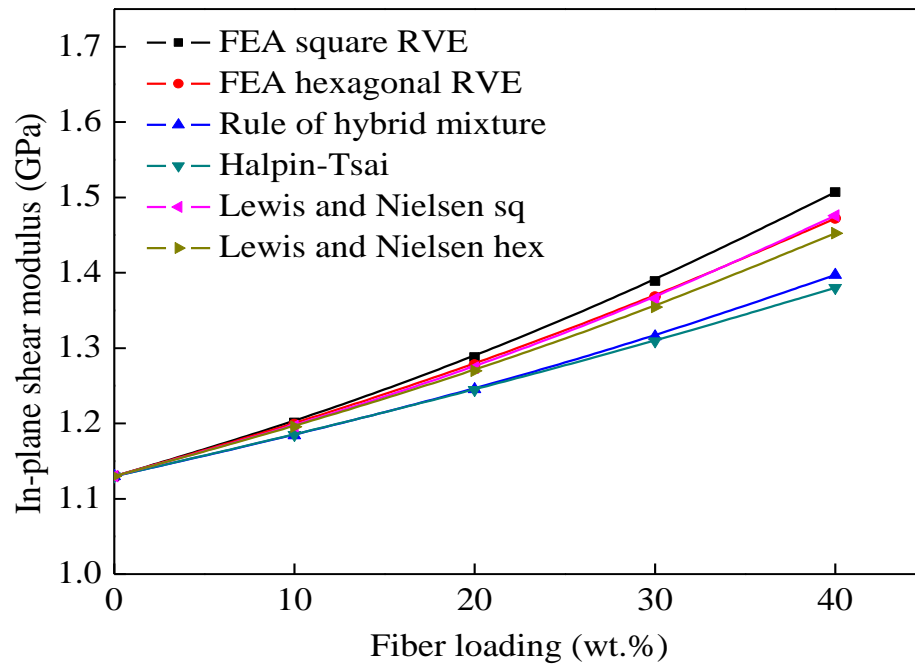


Figure 5.28: Comparison of in-plane shear modulus value of epoxy based composites with the weight ratio of banana and jute fiber as 3:1

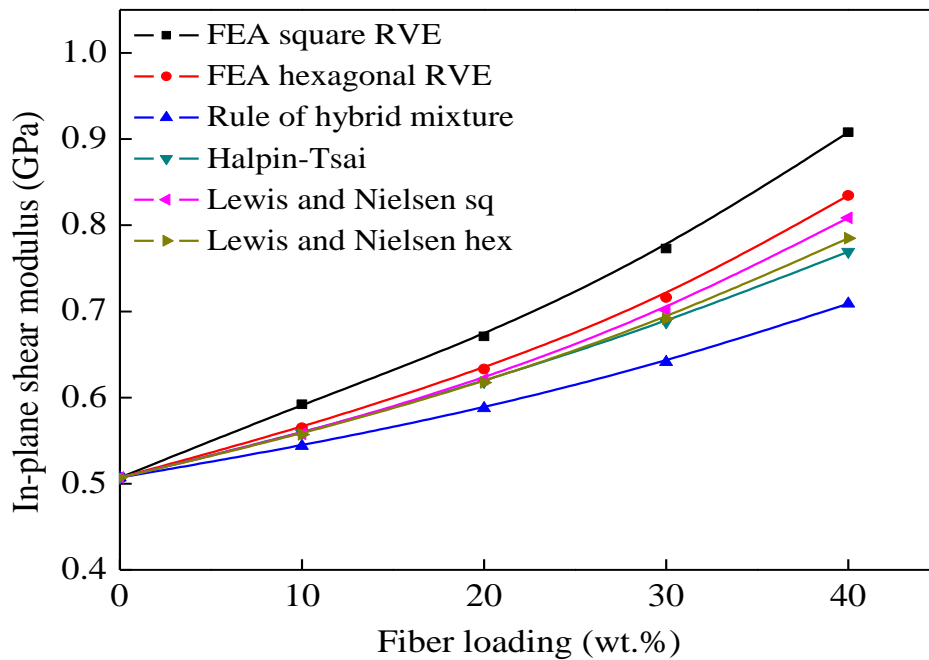


Figure 5.29: Comparison of in-plane shear modulus values of polyester based composites with the weight ratio of banana and jute fiber as 1:1

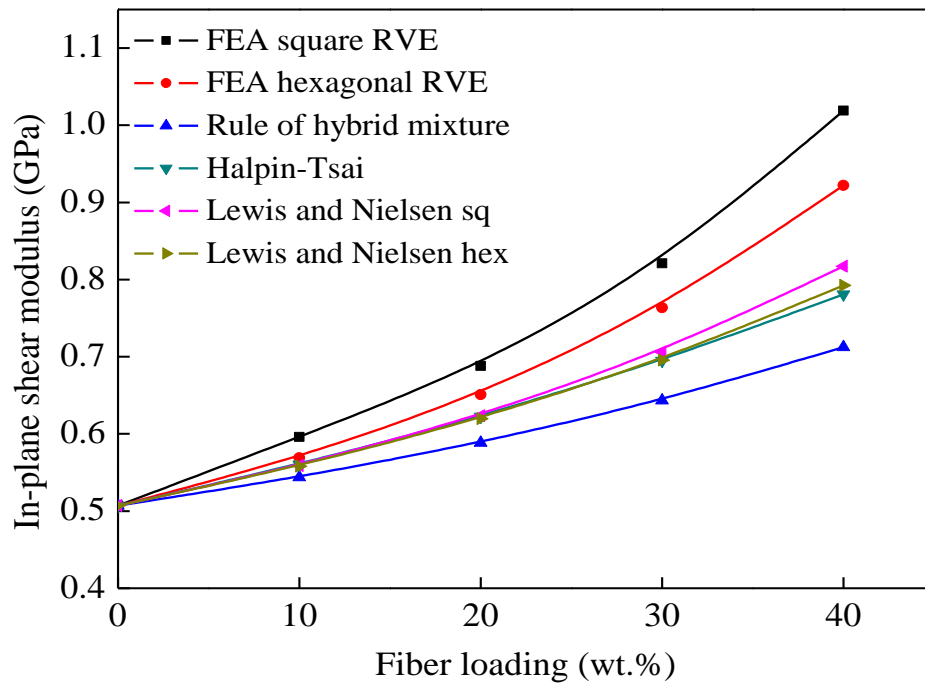


Figure 5.30: Comparison of in-plane shear modulus values of polyester based composites with the weight ratio of banana and jute fiber as 1:3

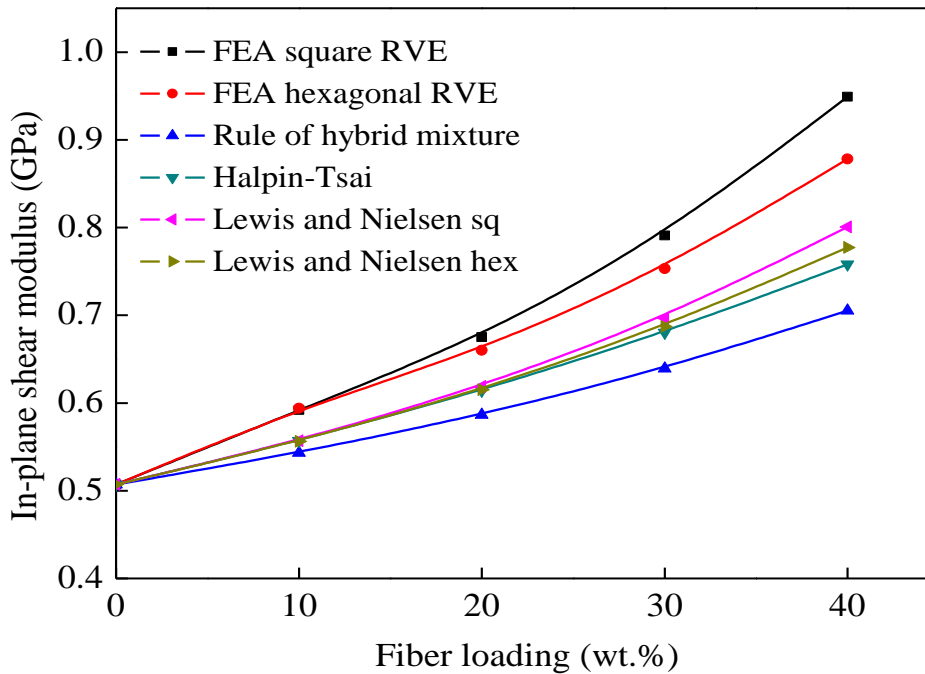


Figure 5.31: Comparison of in-plane shear modulus values of polyester based composites with the weight ratio of banana and jute fiber as 3:1

5.1.3 Thermal Conductivity of Unidirectional Fiber Reinforced Hybrid Composites

Longitudinal and transverse thermal conductivity of epoxy and polyester based composites reinforced with unidirectional banana and jute fibers were evaluated theoretically, numerically and experimentally. In addition, the interpretation and comparison of thermal conductivity obtained from different methods for hybrid composites with different fiber loading and weight ratio are presented.

5.1.3.1 Effect of Temperature on Thermal Conductivity of Composites

Thermal conductivity is considered as one of the most important heat transfer property of composite material and may differ from one material to another. It is influenced by many parameters such as fiber orientation, specific gravity of fiber, voids, fiber volume percentage, moisture content and conductivity properties of both the fiber and matrix. Longitudinal and transverse thermal conductivity of the hybrid composites are properties of the material to conduct heat in parallel and perpendicular to the direction of the fibers, respectively. The longitudinal and transverse thermal conductivity of epoxy based composites as a function of temperature from 30°C to 120°C are shown in Figures 5.32 and 5.33, whereas polyester based composites are shown in Figures 5.34 and 5.35. It can be observed from the figures that the longitudinal thermal conductivity values of banana-jute fiber reinforced hybrid composites shows higher than the transverse thermal conductivity values. As it is obvious, there is a significant difference in thermal conductivity values in the longitudinal and transverse direction of the fiber. Since, natural fibers consist of crystalline cellulose lattice that are radially arranged around its axis, they are highly anisotropic, which give higher heat flow path along the axis compare with across the axis. Moreover, the number of fiber walls in longitudinal direction would be much less than the number of fiber walls in transverse direction [242]. Therefore, there are more fiber walls to cross in the transverse direction and consequently more resistance to the heat flow. A similar observation in case of sisal/glass fiber reinforced composite is also reported by Kalaprasad et al. [161]. As the temperature increases, the thermal conductivity of all the composite samples increases because the vibration of the phonons is the thermal carrier and the moisture in the natural fiber begins to evaporate and escapes from the sample [162]. The results show that the thermal conductivity of the epoxy based composites are higher than that of the polyester based composites due to the higher thermal conductivity of epoxy resin.

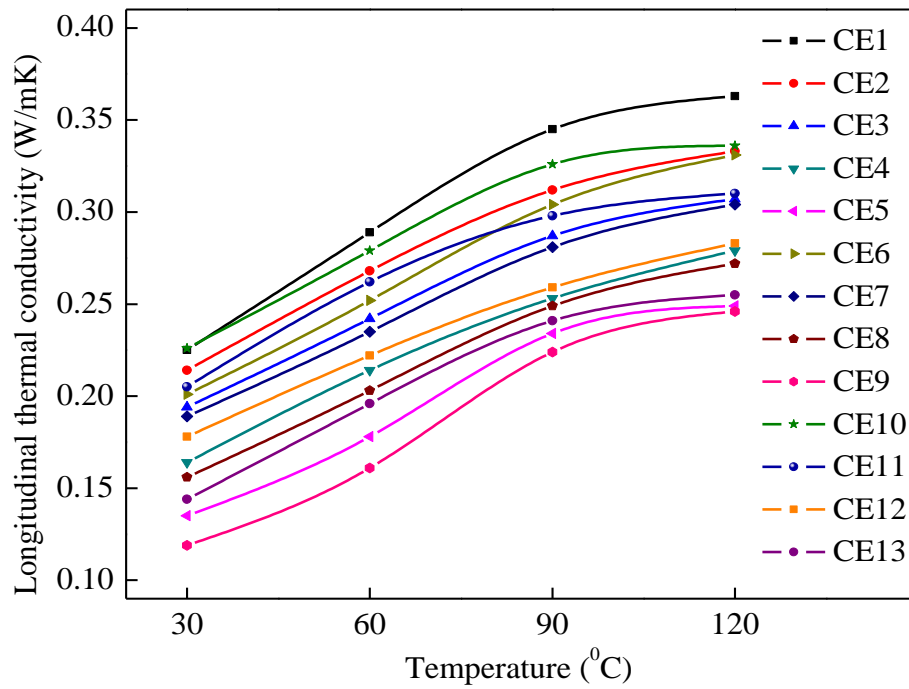


Figure 5.32: Effect of temperature on longitudinal thermal conductivity of epoxy based hybrid composites

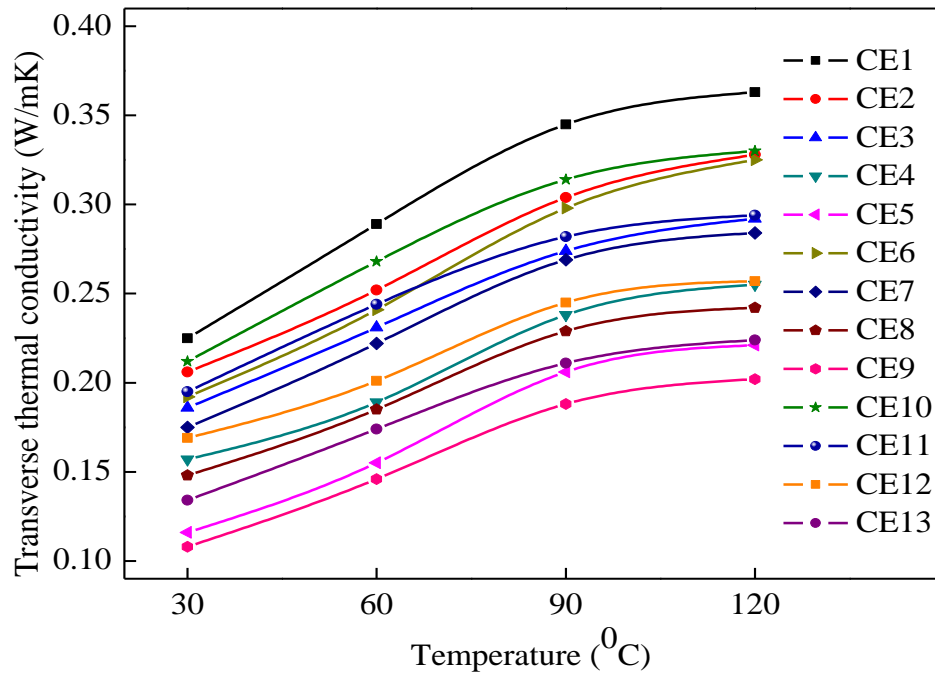


Figure 5.33: Effect of temperature on transverse thermal conductivity of epoxy based hybrid composites

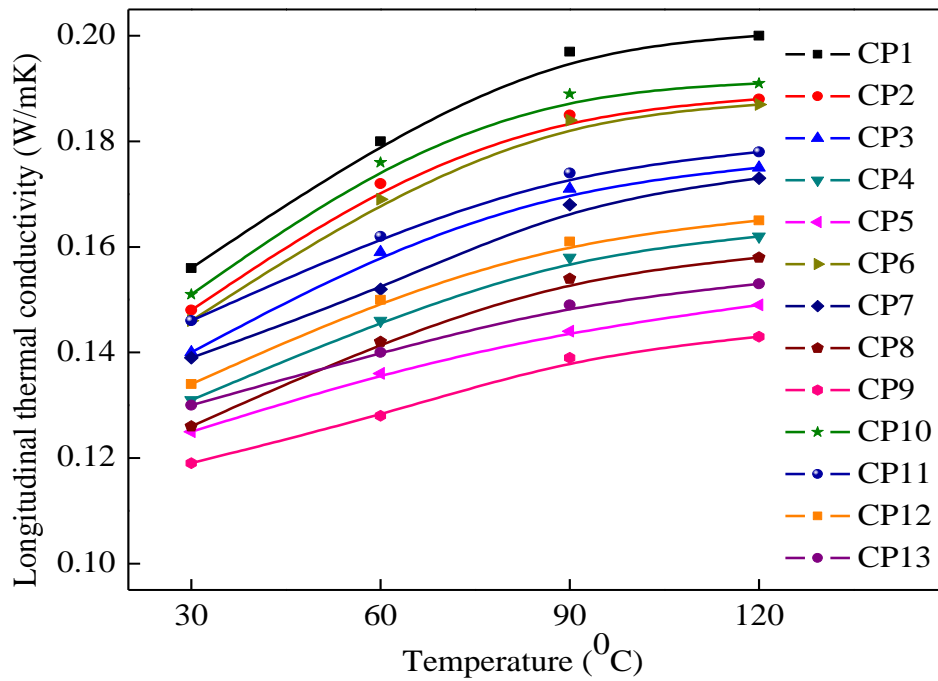


Figure 5.34: Effect of temperature on longitudinal thermal conductivity of polyester based hybrid composites

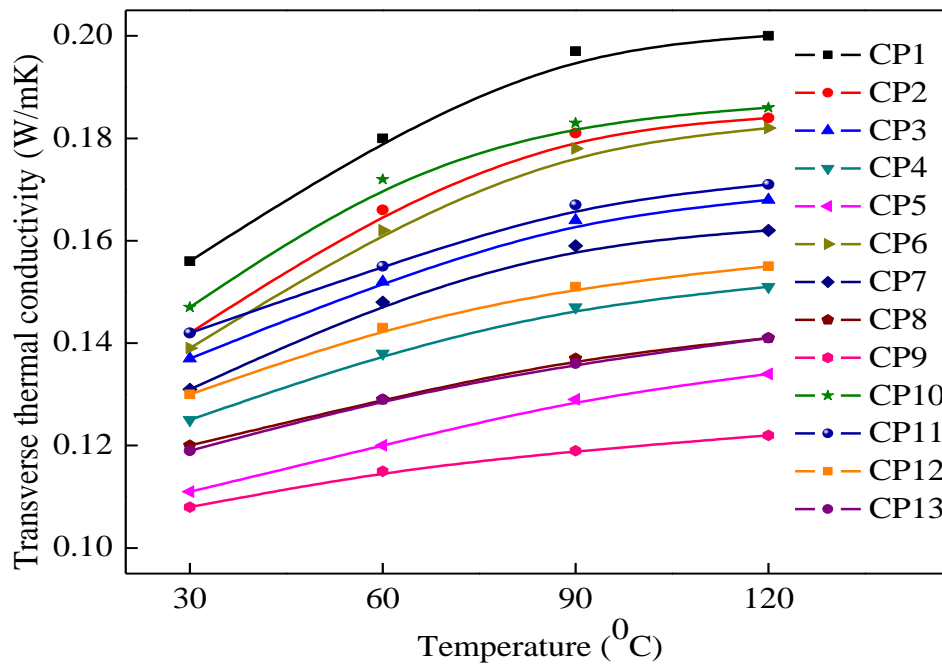


Figure 5.35: Effect of temperature on transverse thermal conductivity of polyester based hybrid composites

5.1.3.2 Longitudinal Thermal Conductivity of Composites

The influence of fiber loading and weight ratio on longitudinal thermal conductivity of epoxy and polyester based composites are shown in Figures 5.36 and 5.37. The thermal conductivity values of both the natural fibers used in this work are much lower than that of the neat polymer material. Therefore, the addition of these natural fibers to polymer matrix is expected to decrease the thermal conductivity of hybrid composites. When the banana and jute fibers are added to the polymer matrix, the gap between the polymer matrix and natural fibers are reduces. As a result of which the overall thermal resistance offered to heat flow becomes relatively more and consequently the thermal conductivity of the composite material decreases.

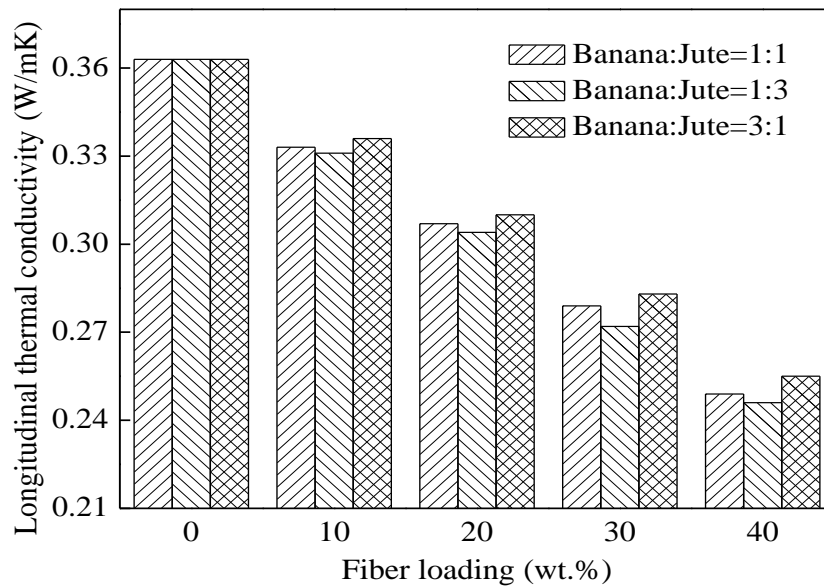


Figure 5.36: Effect of fiber loading and weight ratio on longitudinal thermal conductivity of epoxy based composites

It is evident from the figures that with the addition of banana and jute fibers, irrespective of the weight ratio, there is always a reduction in the heat conduction capability of the hybrid composites. However, it is found that this reduction is more in case of composites with weight ratio of banana and jute fiber as 1:3. The longitudinal thermal conductivity values for epoxy based composites with 40 wt.% of fiber loading and weight ratio of banana and jute fiber as 1:1, 1:3, and 3:1 are found to be 0.249 W/m-K, 0.246 W/m-K and 0.255 W/m-K, respectively. The thermal conductivity of the composites with weight ratio of banana and jute fiber as 1:1, 1:3 and 3:1 is decreased by 31.40%, 32.23% and 29.75%, respectively at the maximum fiber loading over the neat epoxy. Similarly, in

polyester based composites at 40 wt.% of fiber loading, the longitudinal thermal conductivity values are found to be decreased by 25.5%, 28.5%, and 23.5% with the weight ratio of banana and jute fiber as 1:1, 1:3, and 3:1 respectively, as compared to the neat polyester.

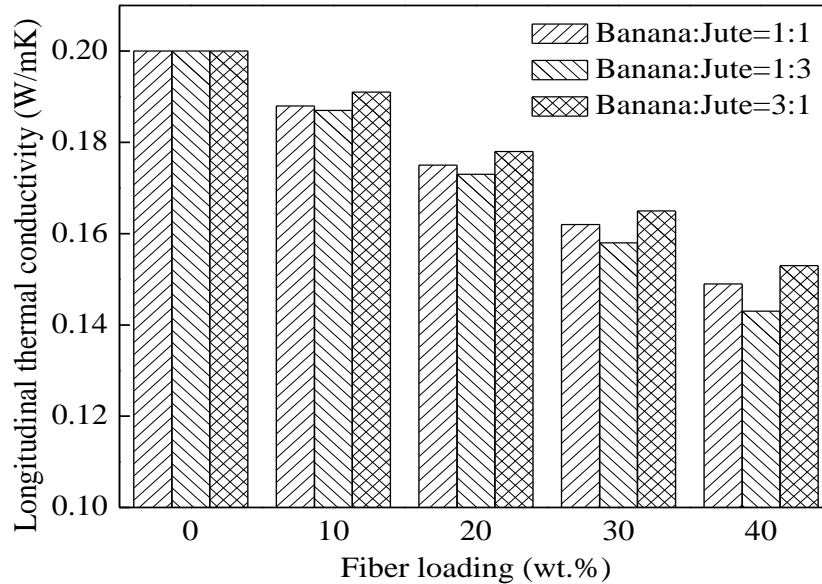


Figure 5.37: Effect of fiber loading and weight ratio on longitudinal thermal conductivity of polyester based composites

The experimental longitudinal thermal conductivity values of epoxy and polyester based composites are compared with the analytical and numerical results and as shown in Figures 5.38 to 5.40. The corresponding comparisons of polyester based composites are shown in Figures 5.41 to 5.43. The comparison graphs show that there is a discrepancy between the FEA results and the experimental results and results obtained from the FEA are higher than the experimental values. This is attributed to certain assumptions that are made for the numerical analysis for simplification of the problem. In the numerical analysis, the distribution of banana and jute fibers in the matrix material are supposed to be in an arranged manner, whereas the fibers are discrete in the matrix are actually randomly distributed. In experimental work, the volume fraction of voids present in the hybrid composite material is a very important factor which affects its thermal conductivity. However, it is encouraging to note that the finite element results are close approximation with the analytical and experimental results within an acceptable range of error. The finite element results are exactly obeying the rule of hybrid mixture model. Therefore, rule of hybrid mixture is generally accepted as the exact solution for the longitudinal thermal conductivity of fiber reinforced hybrid composites with isotropic constituents. It is seen that the numerical results,

measured values and all the theoretical models except for the Lewis and Nielsen hexagonal model are close to each other up to 20 wt.% of fiber loading.

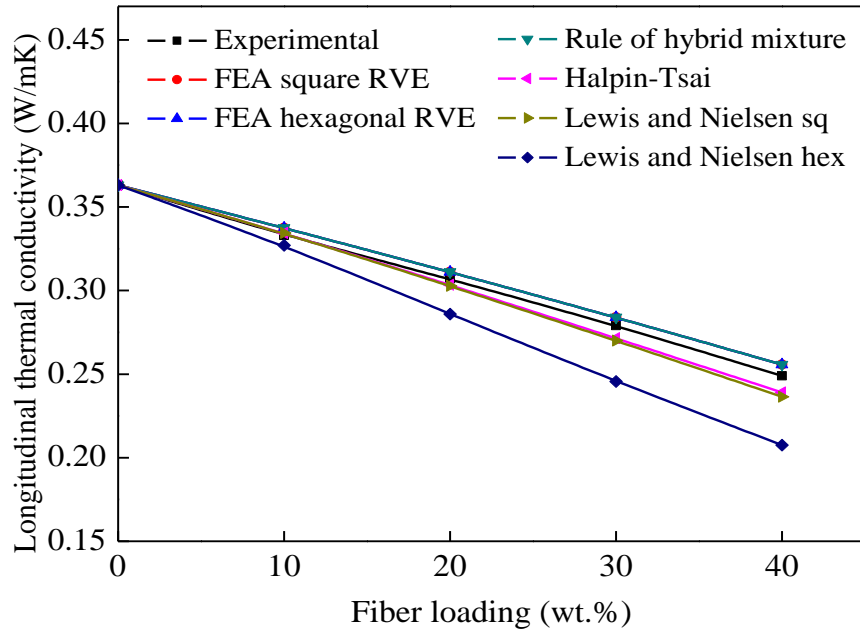


Figure 5.38: Comparison of longitudinal thermal conductivity values of epoxy based composites with the weight ratio of banana and jute fiber as 1:1

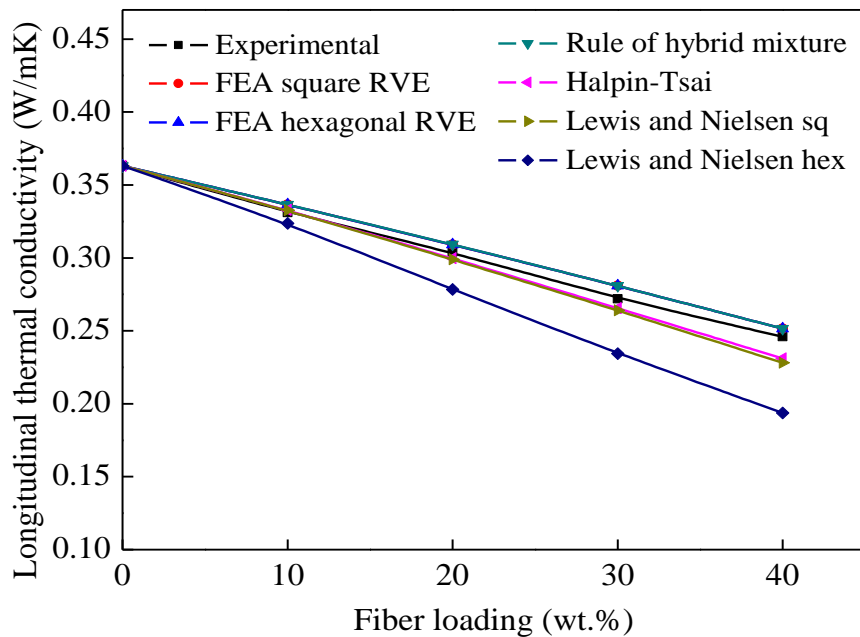


Figure 5.39: Comparison of longitudinal thermal conductivity values of epoxy based composites with the weight ratio of banana and jute fiber as 1:3

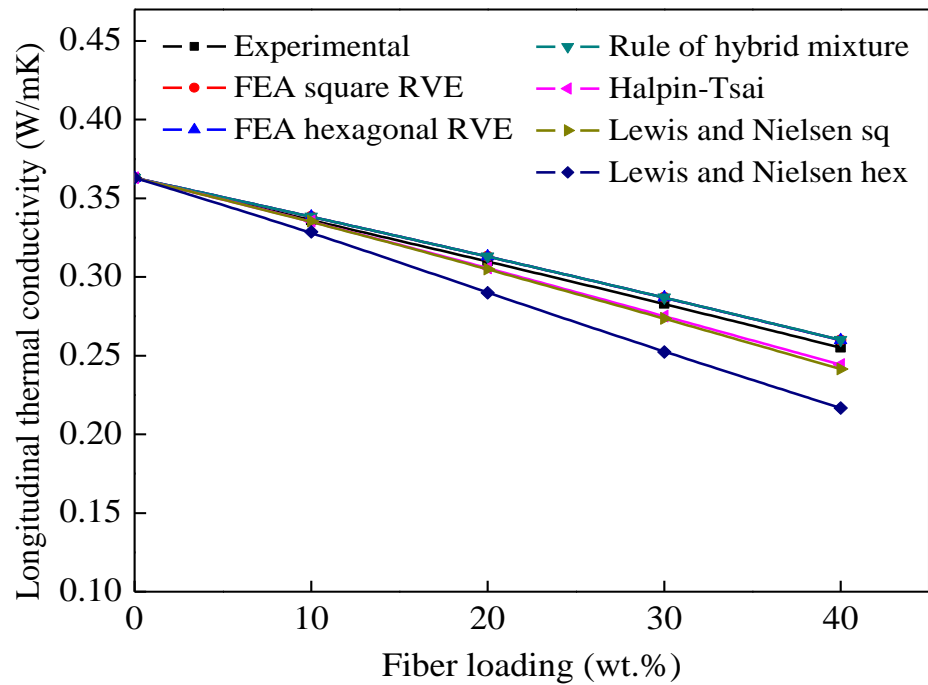


Figure 5.40: Comparison of longitudinal thermal conductivity values of epoxy based composites with the weight ratio of banana and jute fiber as 3:1

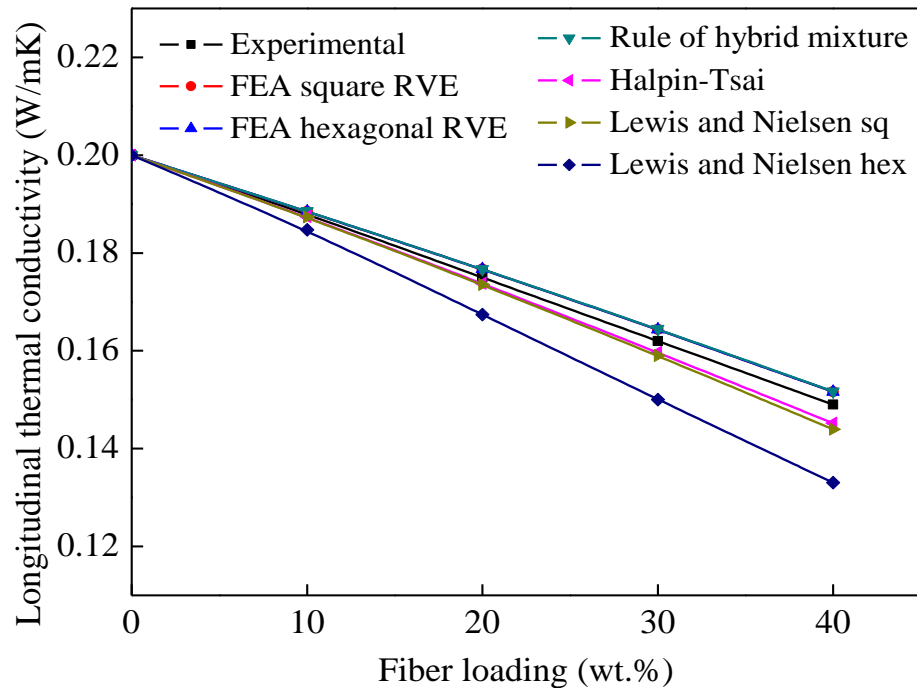


Figure 5.41: Comparison of longitudinal thermal conductivity values of polyester based composites with the weight ratio of banana and jute fiber as 1:1

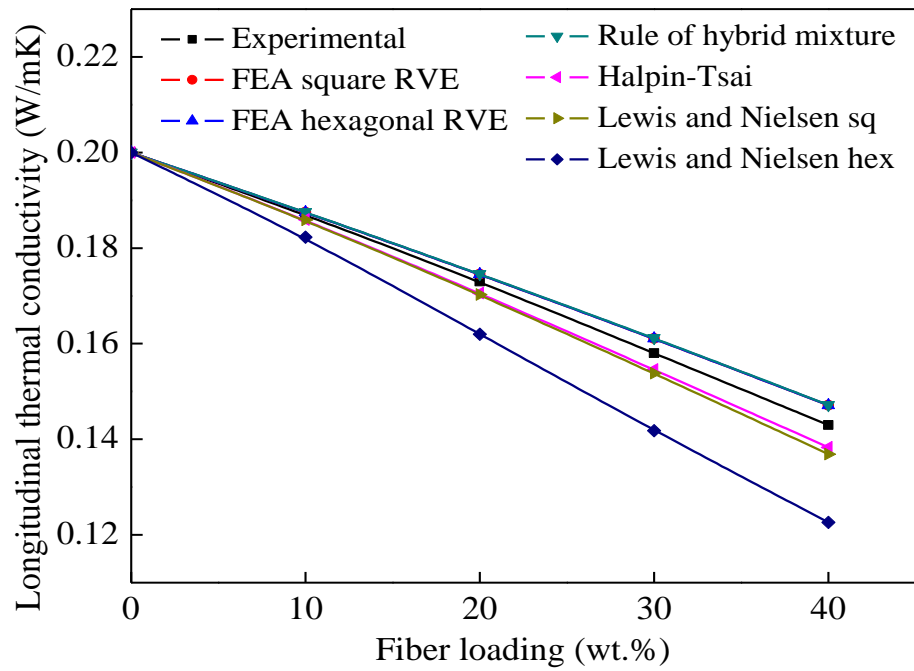


Figure 5.42: Comparison of longitudinal thermal conductivity values of polyester based composites with the weight ratio of banana and jute fiber as 1:3

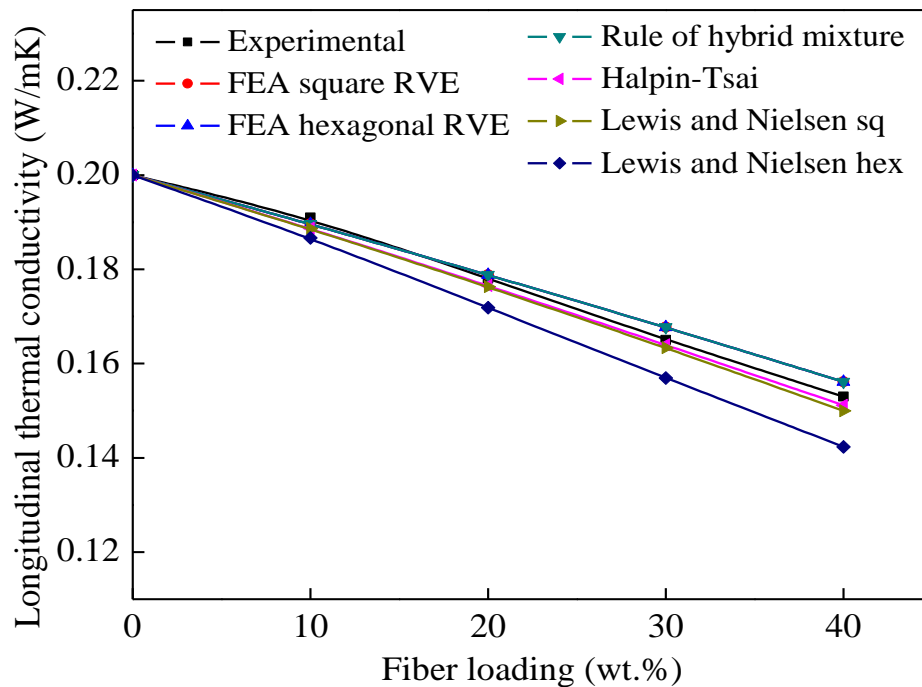


Figure 5.43: Comparison of longitudinal thermal conductivity values of polyester based composites with the weight ratio of banana and jute fiber as 3:1

5.1.3.3 Transverse Thermal Conductivity of Composites

Determination of transverse thermal conductivity by using proposed theoretical model:

In this study, a micromechanical model has been developed to study the transverse thermal conductivity of the fiber reinforced hybrid composites. The proposed heat transfer model has been based on law of minimal thermal resistance and equal law of specific equivalent thermal conductivity, in which heat is considered to be applied in only one direction. Transverse thermal conductivity values of the hybrid composites have also been estimated theoretically by using the correlation given in equation (3.26) derived on the basis of the one-dimensional heat conduction model proposed in this work. The details of model development have already been described in Chapter 3. The proposed correlation for the present analysis is as follows:

$$k_T = \left[\left(\frac{1}{2k_m} - \frac{1}{k_m} \left(\frac{2\Phi_{fb}}{\pi} \right)^{\frac{1}{2}} + \frac{2}{\pi \left(k_m \left(\left(\frac{2}{\pi\Phi_{fb}} \right)^{\frac{1}{2}} - 1 \right) + k_{fb} \right)} \right) + \left(\frac{1}{2k_m} - \frac{1}{k_m} \left(\frac{2\Phi_{fj}}{\pi} \right)^{\frac{1}{2}} + \frac{2}{\pi \left(k_m \left(\left(\frac{2}{\pi\Phi_{fj}} \right)^{\frac{1}{2}} - 1 \right) + k_{fj} \right)} \right) \right]^{-1} \quad (5.15)$$

Where, k_{fb} , k_{fj} and k_m are the respective heat conductivity of the banana fiber, jute fiber and matrix material, Φ_{fb} , Φ_{fj} and Φ_m are the respective volume fraction of the banana fiber, jute fiber and matrix material respectively. The effect of fiber loading and weight ratio on transverse thermal conductivity of epoxy and polyester based composites are shown in Figures 5.44 and 5.45 respectively. It is observed from the figures that the transverse thermal conductivity values of the composites decrease with the increase in fiber loading due to the lower thermal conductivity of fiber. For epoxy based composites with 40 wt.% of fiber loading and weight ratio of banana and jute fiber as 1:1, 1:3, and 3:1 exhibits transverse thermal conductivity values of 0.221 W/m-K, 0.202 W/m-K and 0.224 W/m-K, respectively. The thermal conductivity of the hybrid composites with weight ratio of banana and jute fiber as 1:1, 1:3 and 3:1 is decreased by 39.11%, 44.35% and 38.29%, respectively at the maximum fiber content over the pure epoxy. Similarly, in polyester based composites at 40 wt.% of fiber loading, the hybrid composites exhibit the transverse thermal conductivity values of 0.134 W/m-K, 0.122 W/m-K and 0.141 W/m-K, with weight ratio of banana and jute fiber as 1:1, 1:3, and 3:1, respectively. The transverse thermal conductivity values are

found to be decreased by 33%, 39%, and 29.5% with the weight ratio of banana and jute fiber as 1:1, 1:3, and 3:1 respectively, as compared to the neat polyester.

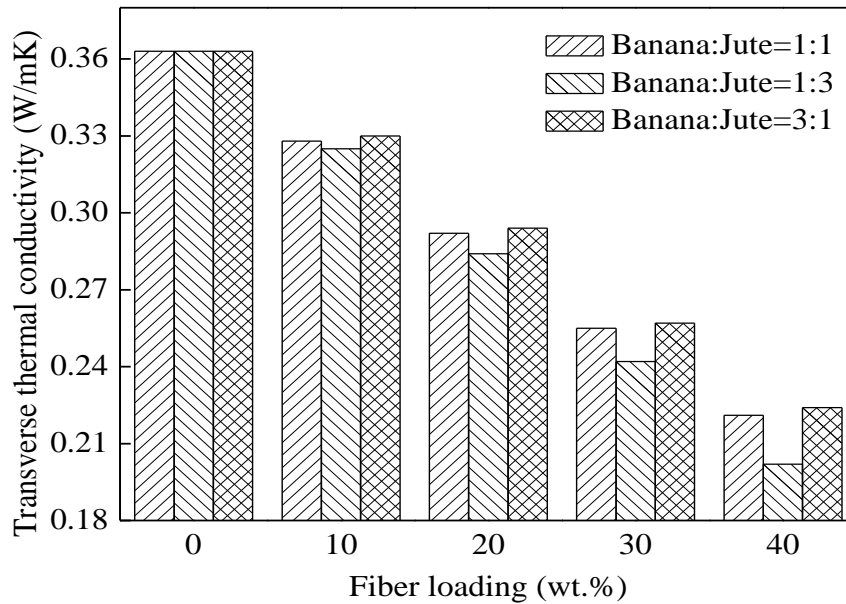


Figure 5.44: Effect of fiber loading and weight ratio on transverse thermal conductivity of epoxy based hybrid composites

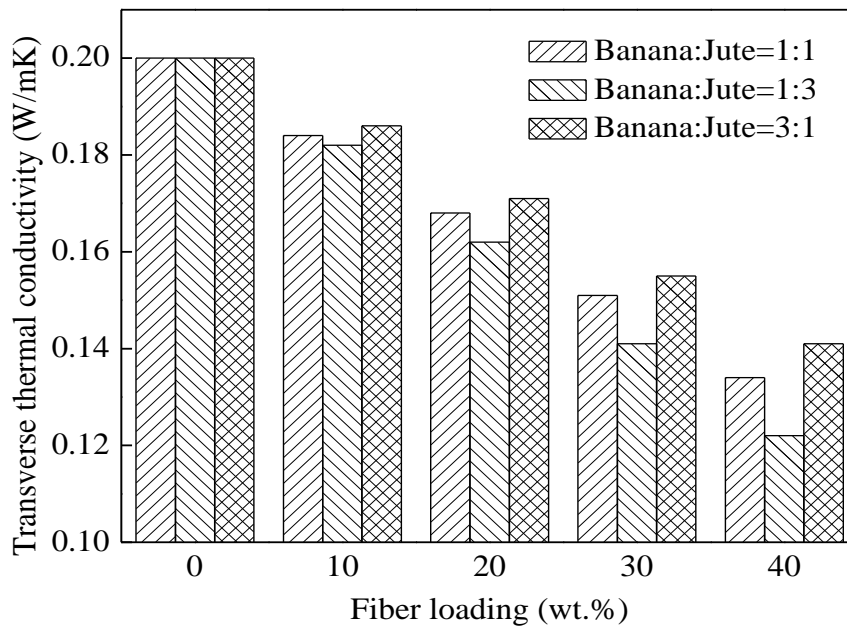


Figure 5.45: Effect of fiber loading and weight ratio on transverse thermal conductivity of polyester based hybrid composites

The comparisons of experimental results with the analytical and numerical results along with the results obtained from the proposed model are shown in Figures 5.46 to 5.48. The corresponding comparison results for polyester based composites are shown in Figures 5.49 to 5.51. It can be seen from the figures that the results achieved from the proposed model are in good agreement with the experimental, FEA as well as existing analytical models. However, the deviation of experimental and results of proposed model may be due to the assumptions taken while deriving the micromechanical model, as fibers are uniformly distributed in the matrix and composite is free from voids results in more systematic decrease in transverse thermal conductivity values in case of proposed model. In experimental investigation, the hybrid fibers arrangement is not a regular periodic array as assumed but very much randomly distributed in the matrix. With increasing the fiber loading, this randomness causes some fibers to be in contact with other fibers and hence a higher thermal resistance and a lower thermal conductivity for the hybrid composites are attained. The other influences which may also contribute to this are the non-homogeneity of the matrix material and experimental imprecisions. Sihn and Roy [236] developed a periodic arrangement and randomly distributed models for measuring transverse thermal conductivity. The randomly distributed model has shown a better agreement with the experimental data than the other periodic models.

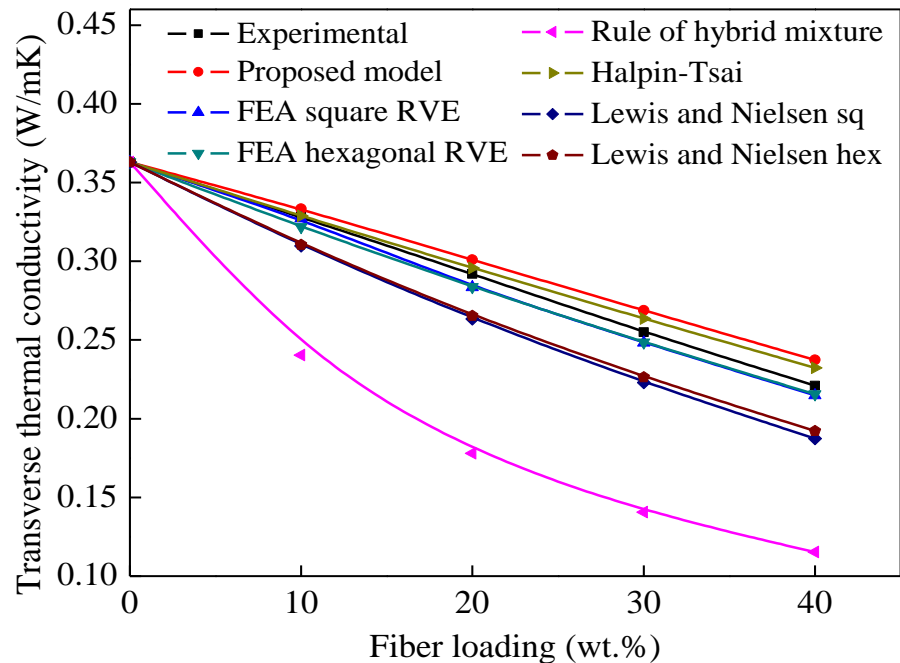


Figure 5.46: Comparison of transverse thermal conductivity values of epoxy based composites with the weight ratio of banana and jute fiber as 1:1

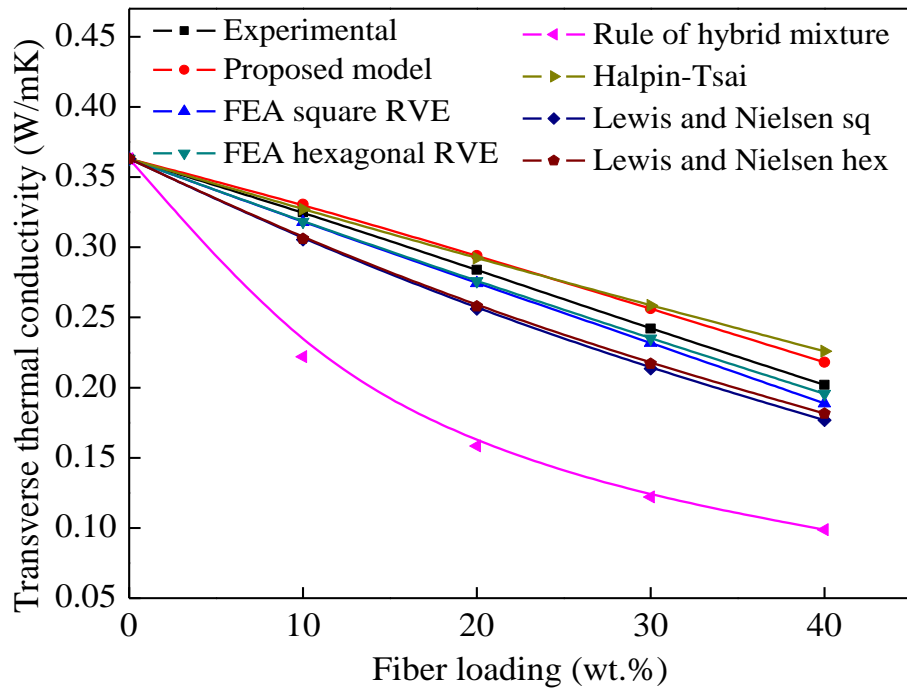


Figure 5.47: Comparison of transverse thermal conductivity values of epoxy based composites with the weight ratio of banana and jute fiber as 1:3

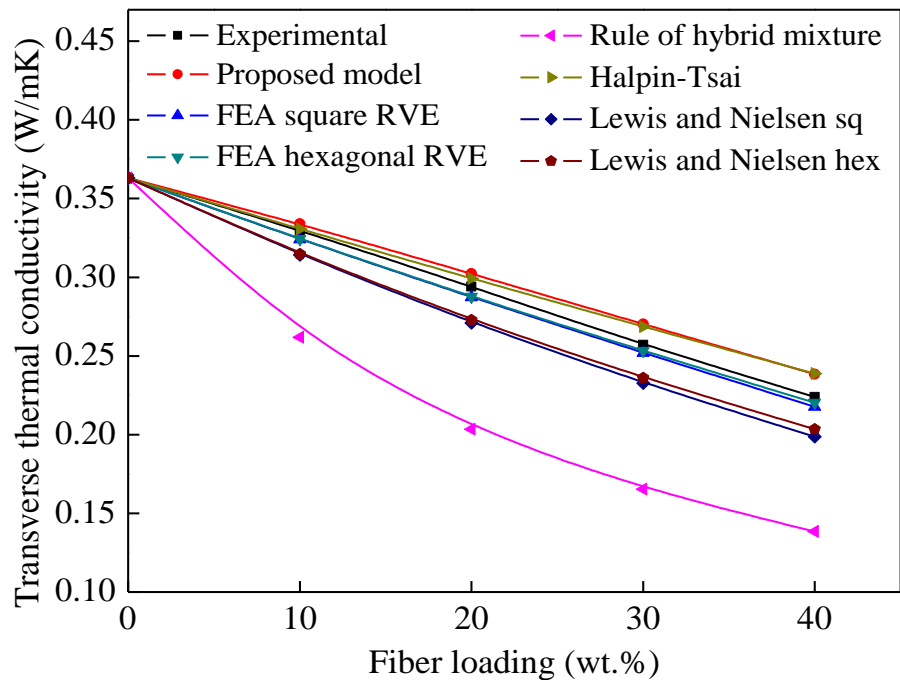


Figure 5.48: Comparison of transverse thermal conductivity values of epoxy based composites with the weight ratio of banana and jute fiber as 3:1

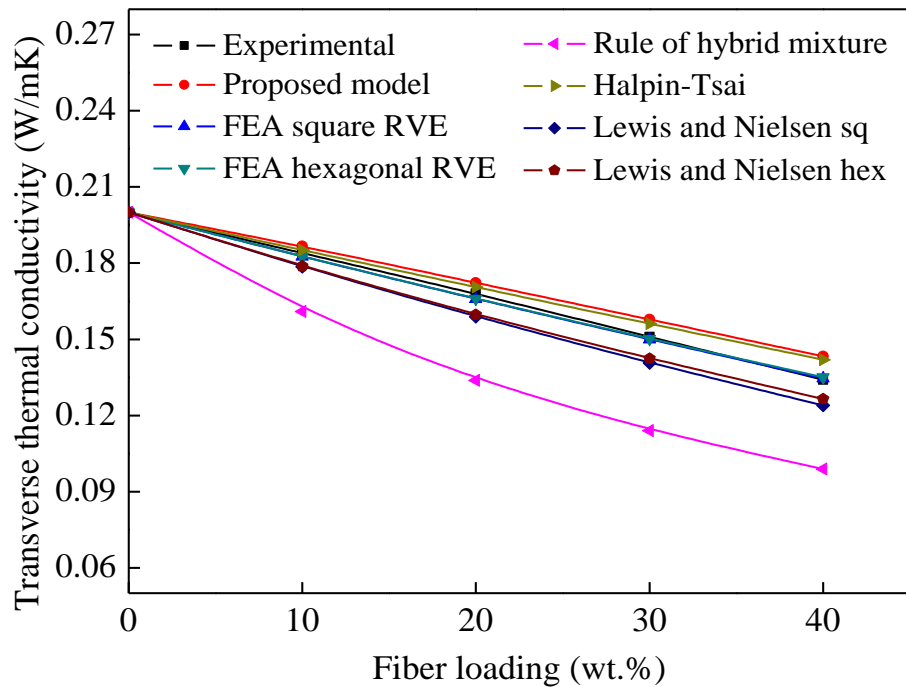


Figure 5.49: Comparison of transverse thermal conductivity values of polyester based composites with the weight ratio of banana and jute fiber as 1:1

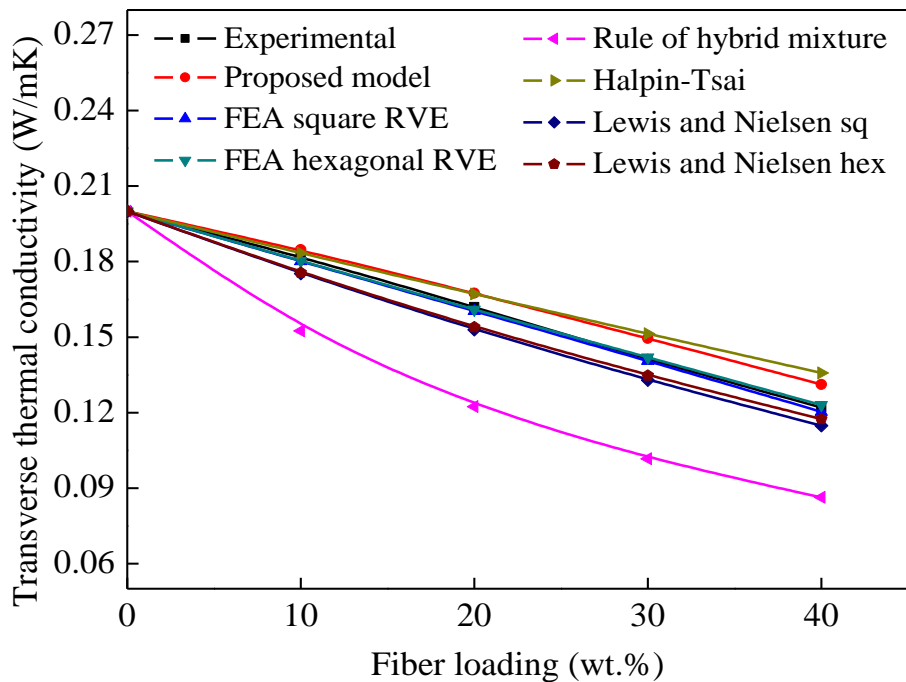


Figure 5.50: Comparison of transverse thermal conductivity values of polyester based composites with the weight ratio of banana and jute fiber as 1:3

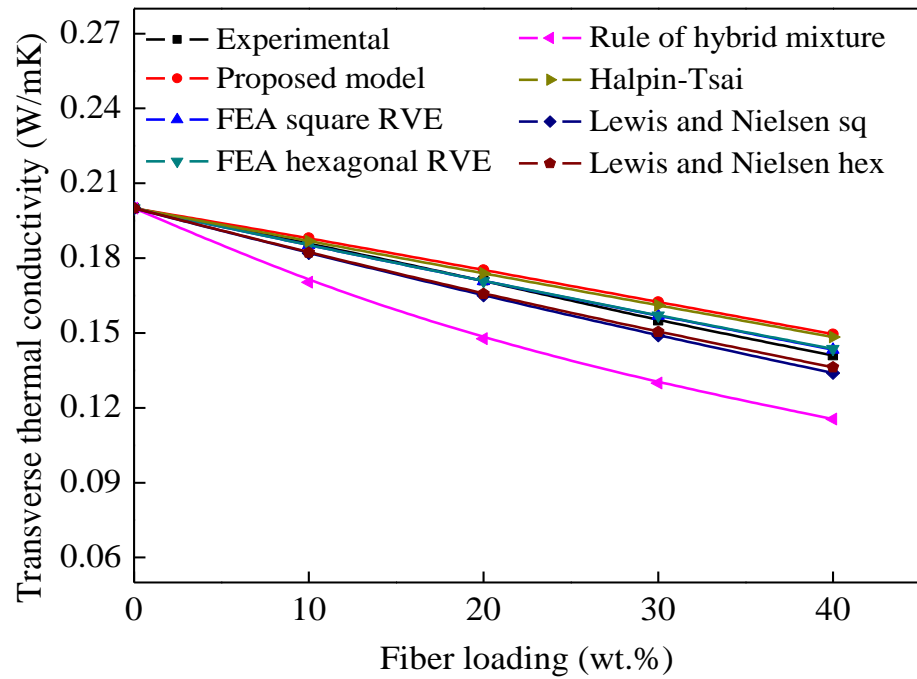


Figure 5.51: Comparison of transverse thermal conductivity values of polyester based composites with the weight ratio of banana and jute fiber as 3:1

The deviation can be attributed to the fact that the numerical analysis does not take interfacial thermal barrier resistance into account which strongly affects the thermal conductivity of composites. The assumption for proposed model (equation 5.15) is that there is no thermal contact resistance between the reinforcement and matrix. However, the fiber surface is covered by a different matrix. These can give a thermal contact resistance to heat flow. The effect of thermal contact resistance has also been observed in case of transverse thermal conductivity of unidirectional fiber composites studied by Zou et al. [229]. In their study, a proper thermal resistance is included in a theoretical model for a more accurate prediction of transverse thermal conductivity with experimental results. Tables 5.3 and 5.4 presents the percentage errors associated with the transverse thermal conductivity values of epoxy and polyester based composites obtained from different models/correlations with respect to the corresponding measured values. It may be noted that the error associated with the theoretical models are quite high whereas those associated with proposed model with respect to the measured values lie within a nominal acceptable range of just 0-7.3%. From the Tables 5.3 and 5.4 it is clear that the percentage error for the FEA square RVE and FEA hexagonal RVE values with the experimental values of the epoxy based composites are 0-7% and 0-3.5% respectively, whereas the polyester based composites are 0-1.7% and 0-1.9%

respectively. The reason for this marginal deviation is because of the assumptions taken while deriving the correlation.

Table 5.3: Percentage errors associated with the transverse thermal conductivity values of epoxy based composites obtained from different models

Composite	Experimental value (W/m-K)	Percentage errors						
		Proposed model	FEA square RVE	FEA hexagonal RVE	Rule of hybrid mixture	Halpin -Tsai	Lewis and Nielsen sq	Lewis and Nielsen hex
CE1	0.363	0	0	0	0	0	0	0
CE2	0.328	1.560	0.244	1.958	36.495	0.249	5.877	5.674
CE3	0.292	2.990	2.998	2.961	63.974	1.240	10.869	10.073
CE4	0.255	5.098	2.739	2.657	81.439	3.260	14.375	12.652
CE5	0.221	6.829	2.838	2.552	91.746	4.855	17.921	14.956
CE6	0.325	1.723	2.169	2.104	46.389	0.624	6.397	6.177
CE7	0.284	3.434	3.460	2.973	79.365	2.816	10.915	10.067
CE8	0.242	5.579	4.355	2.934	98.121	6.422	13.281	11.472
CE9	0.202	7.339	6.991	3.324	104.786	10.554	14.247	11.218
CE10	0.330	1.197	1.820	1.789	26.031	0.181	5.029	4.843
CE11	0.294	2.745	2.367	2.225	44.579	1.711	8.514	7.789
CE12	0.257	4.885	1.984	1.500	55.453	4.321	10.443	8.885
CE13	0.224	6.040	2.846	1.679	61.822	6.184	12.769	10.101

Table 5.4: Percentage errors associated with the transverse thermal conductivity values of polyester based composites obtained from different models

Composite	Experimental value (W/m-K)	Percentage errors						
		Proposed model	FEA square RVE	FEA hexagonal RVE	Rule of hybrid mixture	Halpin -Tsai	Lewis and Nielsen sq	Lewis and Nielsen hex
CP1	0.2	0	0	0	0	0	0	0
CP2	0.184	1.446	0.631	0.634	14.368	0.606	3.029	2.884
CP3	0.168	2.495	0.988	0.937	25.536	1.465	5.773	5.204
CP4	0.151	4.309	0.287	0.150	32.403	3.306	7.320	6.077
CP5	0.134	6.489	0.912	1.209	35.576	5.625	8.087	5.952
CP6	0.182	1.461	1.042	0.969	19.393	0.767	3.830	3.663
CP7	0.162	3.283	1.032	0.671	32.441	3.091	5.897	5.250
CP8	0.141	5.685	0.308	0.685	38.801	6.817	6.065	4.684
CP9	0.122	7.012	1.431	0.891	41.323	10.097	6.265	3.925
CP10	0.186	1.063	0.456	0.453	9.214	0.452	2.214	2.092
CP11	0.171	2.452	0.123	0.101	15.793	1.644	3.669	3.190
CP12	0.155	4.556	1.210	1.299	19.319	3.771	4.038	2.995
CP13	0.141	5.685	1.620	1.828	22.117	4.973	5.269	3.452

5.2 Physical, Mechanical and Thermal Behaviour of Unidirectional Fiber Reinforced Composites

This part of the chapter presents the measured values of various physical, mechanical and thermal properties of the epoxy and polyester based unidirectional fiber reinforced hybrid composites. The relative effects of fiber loading and different weight ratios of fiber on composite properties have been discussed.

5.2.1 Physical Properties

Evaluation of the physical properties of any new material is necessary both from the viewpoints of practical application and scientific understanding. In the present research work, a property data has been produced by conducting tests under controlled laboratory conditions to evaluate physical property i.e. density and water absorption of fabricated hybrid composites.

5.2.1.1 Density and Void Content

Density is a material property which is of prime importance in several weight sensitive applications. Thus, in many such applications polymer composites are found to replace conventional metals and materials primarily for their low densities. Density of a composite depends on the relative proportion of the reinforcement and matrix. The density values of neat epoxy and polyester resins measured by Archimedes method are found to be 1.15 g/cm^3 and 1.10 g/cm^3 , respectively. Further, the density values of their hybrid composites are also measured by the same principle. The theoretical and the measured densities along with the corresponding void content for unidirectional banana-jute fiber reinforced epoxy and polyester based composites are presented in Tables 5.5 and 5.6, respectively. It is seen that the theoretical density of all the sets of hybrid composites increases with the increase in fiber loading as expected due to the fact that the density values of jute (1.4 g/cm^3) and banana (1.35 g/cm^3) fibers used in this work are higher than those of the base matrices. It may be noted that the hybrid composite density values calculated by theoretically are not equal to the experimentally measured values. The reason for this is, while calculating the theoretical density using equation (4.1); it has been assumed that the composites are free from voids and defects, while in actual practice, fabrication of composites unavoidably gives rise to a certain amount of voids within the composite material.

Table 5.5: Theoretical and measured densities of the epoxy based composites

Weight ratio of banana and jute fiber	Composite	Theoretical density (g/cm ³)	Measured density (g/cm ³)	Void content (%)
	CE1	1.150	1.146	0.348
1:1	CE2	1.169	1.157	1.027
	CE3	1.189	1.165	2.019
	CE4	1.209	1.173	2.978
	CE5	1.230	1.182	3.903
1:3	CE6	1.170	1.159	0.940
	CE7	1.191	1.170	1.763
	CE8	1.212	1.180	2.641
	CE9	1.230	1.187	3.496
3:1	CE10	1.168	1.153	1.284
	CE11	1.187	1.157	2.528
	CE12	1.206	1.166	3.317
	CE13	1.226	1.176	4.079

Table 5.6: Theoretical and measured densities of the polyester based composites

Weight ratio of banana and jute fiber	Composite	Theoretical density (g/cm ³)	Measured density (g/cm ³)	Void content (%)
	CP1	1.100	1.095	0.454
1:1	CP2	1.122	1.107	1.336
	CP3	1.145	1.113	2.794
	CP4	1.170	1.122	4.102
	CP5	1.195	1.117	6.527
1:3	CP6	1.123	1.110	1.157
	CP7	1.147	1.119	2.441
	CP8	1.172	1.128	3.754
	CP9	1.199	1.127	6.005
3:1	CP10	1.121	1.106	1.338
	CP11	1.144	1.109	3.059
	CP12	1.167	1.116	4.370
	CP13	1.191	1.108	6.969

For epoxy based composites (i.e. Set I), it is found that with the increase in banana and jute fiber loading from 0 to 40 wt.%, the density increases by 3.14%, 3.57% and 2.61% for composites with weight ratio of banana and jute fiber as 1:1, 1:3, and 3:1, respectively. Similarly, a substantial rise in density by about 2.0%, 2.92% and 1.18% is observed as the fiber content in polyester based composites (Set II) increased from 0 to 40 wt.% with weight ratio of banana and jute fiber as 1:1, 1:3, and 3:1, respectively. From the Table 5.5 and Table 5.6, it is observed that the void content increases with the fiber loading. This may be attributed to poor interaction/adhesion between the fiber and matrix materials. The natural fibers consist of lumens in its cellular structure which acts as void. It means such fiber carries these voids naturally. Thus, it may be the reason of increase in void content with the increase in fiber loading. The similar trend of increase in void content with the increase in fiber loading is also reported by previous researchers [183]. In composite materials, voids may occur in the fiber lumens or at the fiber/matrix interface. It is also observed that the void content is less for composites with weight ratio of banana and jute fiber as 1:3 i.e. composites with greater percentage of jute fiber. This may be due to the smaller lumen of jute fiber, good fiber/matrix interface bonding and complete wetting of jute fiber by matrix material. Similar trend of results observed by Jawaid et al. [269] for oil palm empty fruit bunch and jute fiber reinforced epoxy composites.

5.2.1.2 Water Absorption

Water absorption test is done to determine the percentage of water absorbed under specified conditions. The water resistance of the hybrid composites is an important parameter mainly when natural fiber is used and it depends on the ability of the fibers to absorb water due to the presence of hydroxyl bonding, volume fraction of voids, fiber loading, humidity, temperature and viscosity of matrix [270]. The effect of fiber loading and weight ratio on the water absorption of the unidirectional banana-jute fiber reinforced epoxy and polyester based hybrid composites with increase in immersion time are shown in Figures 5.52 and 5.53. It is observed that the water absorption percentage of hybrid composites increases with increase in fiber loading. The reason for the increase in water absorption percentage may be due to the higher hydrophilic nature of cellulosic fibers, presence of voids and micro cracks present inside the composite [184]. Similar trend is also observed by previous researchers for *Lantana camara* and jute fiber reinforced epoxy composites [139], [271]. It is also observed that the increase in water absorption is more in the beginning and then gradually increases day by day and finally becomes stabilize at around 216 hrs for epoxy based composites and 240 hrs for polyester based composites.

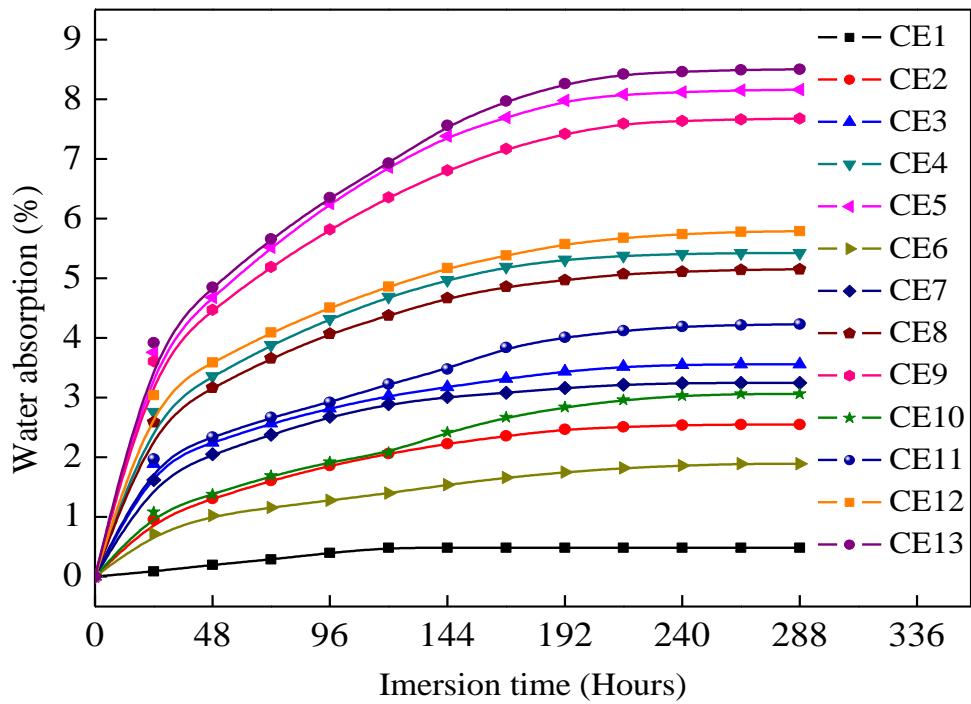


Figure 5.52: Variation of water absorption of unidirectional fiber reinforced epoxy based composites with immersion time

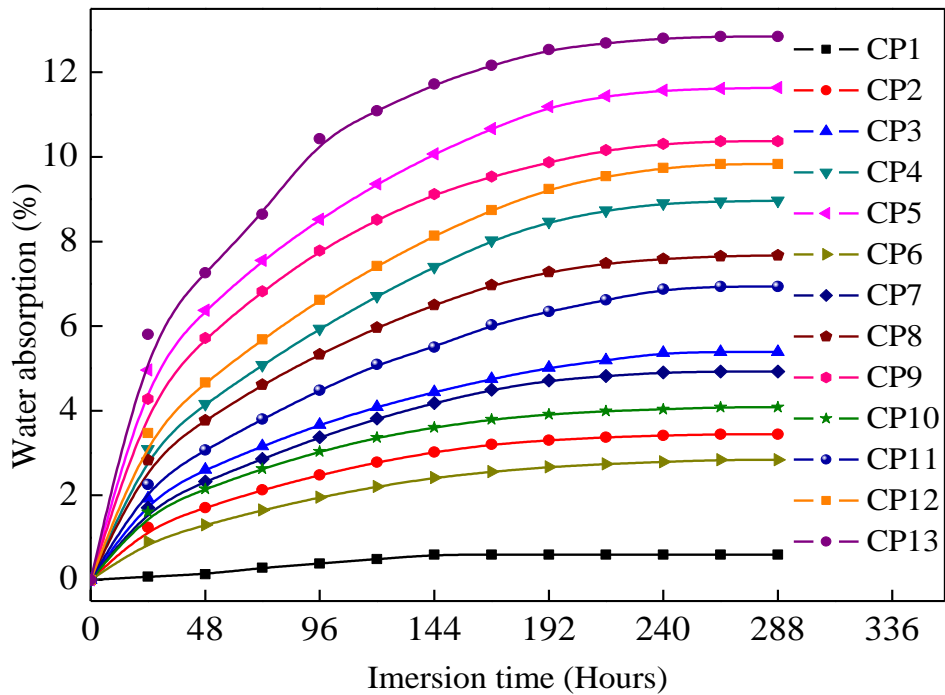


Figure 5.53: Variation of water absorption of unidirectional fiber reinforced polyester based composites with immersion time

After this time period, no significant changes in weights of hybrid composite samples are observed. The neat epoxy and polyester composite shows the lowest water absorption of 0.48% and 0.59%, respectively. This is because of the resin acts as water resistant matrix. For epoxy based composites at 40 wt.% of fiber loading, the maximum water absorption is found to be 8.49% for composite with the weight ratio of banana and jute fiber as 3:1. For the composite at same fiber loading (i.e. 40 wt.%), with the weight ratio of banana and jute fiber as 1:3 shows less water absorption of 7.67% as compared to the other two types. Similarly, for polyester based composites at 40 wt.% of fiber loading, with the weight ratio of banana and jute fiber as 1:3 shows less water absorption of 10.37% as compared to the other two types. By adding more percentage of jute fiber, the water uptake of the hybrid composites decreases. Generally, jute fiber has better aspect ratio, lowest sorption and highest density than banana fiber resulting in lower water absorption capability to the composite made of higher weight ratio jute fiber [272]. From the figures, the highest water absorption percentage is observed for composites with maximum content of banana fiber. The reason may be due to the banana fibers contain abundant polar hydroxide groups, which result in a high water absorption level compared to the jute fiber. The rate of water absorption is greatly influenced by the materials density and void content [180], [273].

5.2.1.3 Transport Coefficients in Water Absorption

The transport coefficients are determined for both the epoxy and polyester based composites. The values of n and k are determined from the slope and intercept of log plot of M_t/M_m versus time which can draw from experimental results. The coefficients n and k resulting from the fitting of formulations at different fiber loading and weight ratio of epoxy and polyester based composites are presented in Table 5.7. It is found from the Table 5.7 that the values of n are close to 0.5 for all composite types. Consequently, it can be concluded that the water absorption of the all hybrid composites follows the Fickian diffusion behavior [253]. Tables 5.8 and 5.9 summarizes the maximum water uptake (M_m), diffusion coefficient (D), sorption coefficient (S) and permeability coefficient (P) values of the epoxy and polyester based composites. The diffusion coefficient is found to be increased with the increase in fiber loading for both epoxy and polyester based composites. These phenomena are due to inherent hydrophilic nature of the fibers. The diffusion coefficient for the neat epoxy and polyester is only 3.68×10^{-6} and 4.11×10^{-6} , respectively. Higher diffusion coefficient values might also indicate higher void content in the composite and hence water can easily diffuse into the composites through the voids.

Table 5.7: The dependence of moisture sorption constant n and k for all formulations

Unidirectional fiber reinforced epoxy composites			Unidirectional fiber reinforced polyester composites		
Composite	n	k (g/g min ²)	Composite	n	k (g/g min ²)
CE1	0.914	5.206	CP1	1.082	6.200
CE2	0.471	2.751	CP2	0.498	2.907
CE3	0.296	1.743	CP3	0.471	2.775
CE4	0.332	1.942	CP4	0.495	2.917
CE5	0.379	2.219	CP5	0.398	2.343
CE6	0.413	2.451	CP6	0.545	3.187
CE7	0.343	1.992	CP7	0.506	2.972
CE8	0.331	1.936	CP8	0.471	2.761
CE9	0.359	2.108	CP9	0.419	2.453
CE10	0.459	2.738	CP10	0.455	2.655
CE11	0.336	2.008	CP11	0.511	3.024
CE12	0.301	1.776	CP12	0.481	2.834
CE13	0.371	2.175	CP13	0.401	2.332

Table 5.8: Values of maximum water uptake, diffusion coefficient, sorption coefficient, and permeability coefficient for unidirectional fiber reinforced epoxy composites

	Maximum water uptake (%)	Diffusion coefficient (mm ² /sec) × 10 ⁻⁶	Sorption coefficient (g/g)	Permeability coefficient (mm ² /sec) × 10 ⁻⁷
CE1	0.4866	3.6811	0.0049	0.1791
CE2	2.5495	4.3568	0.0254	1.1093
CE3	3.5587	4.6155	0.0354	1.6358
CE4	5.4193	5.3638	0.0542	2.9068
CE5	8.1591	6.1333	0.0814	4.9959
CE6	1.8889	3.9436	0.0189	0.7455
CE7	3.2487	4.5021	0.0323	1.4569
CE8	5.1480	4.9320	0.0515	2.5390
CE9	7.6792	5.1270	0.0767	3.9362
CE10	3.0591	4.7231	0.0304	1.4382
CE11	4.2292	4.9339	0.0422	2.0831
CE12	5.7884	5.8377	0.0578	3.3781
CE13	8.4986	7.3235	0.0849	6.2192

It is found that the composites with weight ratio of banana and jute fiber as 1:3 shows better resistance towards water absorption than the other two types. With better bonding between the jute fibers and matrix, the velocity of the diffusional processes decreases since there are fewer gaps in the interfacial region. Hybrid composites with weight ratio of banana and jute fiber as 3:1 show the highest diffusion coefficient values. The values obtained for the transport coefficients are in good agreement with the results reported by the previous researchers [137], [140], [274]. The values of sorption coefficient are observed to be increased with the increase in the fiber loading for both epoxy and polyester based composites and is related to the equilibrium sorption of the water. The permeability coefficient is a function of diffusion coefficient and sorption coefficient. The values of permeability coefficient of the hybrid composites having different fiber loading and weight ratio are presented in Tables 5.8 and 5.9. It is evident from the results that the permeability coefficient follows the same trend as that of diffusion coefficient and sorption coefficient. This phenomenon can be explained by the fact that, in a high moisture environment, micro cracks may develop on the surface of the composite material. As cracks develop, peeling and surface dissolution of the composite may be possible [275].

Table 5.9: Values of maximum water uptake, diffusion coefficient, sorption coefficient, and permeability coefficient for unidirectional fiber reinforced polyester composites

	Maximum water uptake (%)	Diffusion coefficient ($\text{mm}^2/\text{sec}) \times 10^{-6}$	Sorption coefficient (g/g)	Permeability coefficient ($\text{mm}^2/\text{sec}) \times 10^{-7}$
CP1	0.5953	4.1177	0.0059	0.2451
CP2	3.4394	4.8695	0.0343	1.6748
CP3	5.3898	5.6732	0.0538	3.0578
CP4	8.9673	6.0810	0.0896	5.4531
CP5	11.6358	6.7569	0.1163	7.8623
CP6	2.8358	4.5117	0.0283	1.2794
CP7	4.9264	4.9708	0.0492	2.4488
CP8	7.6717	5.3645	0.0767	4.1155
CP9	10.3714	5.8835	0.1037	6.1020
CP10	4.0840	5.1252	0.0408	2.0931
CP11	6.9381	5.8187	0.0693	4.0370
CP12	9.8285	6.5651	0.0982	6.4526
CP13	12.8464	8.0684	0.1284	10.3651

5.2.2 Mechanical Properties

5.2.2.1 Tensile Properties

The tensile strength of fiber reinforced composite depends on the ability to transfer the stress from fiber to matrix and the fiber-matrix interface [276]. In this work, the longitudinal and transverse tensile strength of all epoxy and polyester based hybrid composite specimens are evaluated. The results of the longitudinal tensile strength as a function of fiber loading for both epoxy and polyester based hybrid composites are shown in Figures 5.54 and 5.55, respectively. It is noticed that with addition of banana and jute fibers, the longitudinal tensile strength of composites increases. However, a further increase in fiber loading up to 40 wt.%, the longitudinal tensile strength decreases due to an increase in fiber-fiber interactions and cause difficulties in dispersion [72]. In comparison of epoxy and polyester composites, epoxy based hybrid composites shows higher tensile strength value. The ultimate longitudinal tensile strength of banana-jute fiber reinforced epoxy composites with weight ratio of banana and jute fiber as 1:1, 1:3, and 3:1 are 64.75 MPa, 84.48 MPa, and 60.83 MPa, respectively at 30 wt.% of fiber loading. Similarly, for polyester based composites at 30 wt.% of fiber loading, the tensile strength is found to be increased as compared to the neat polyester by 180%, 222%, and 155% with the weight ratio of banana and jute fiber as 1:1, 1:3, and 3:1, respectively. The results of the transverse tensile strength as a function of fiber loading for both epoxy and polyester based hybrid composites are shown in Figures 5.56 and 5.57, respectively. It is evident from the figures that the transverse tensile strength of epoxy and polyester based hybrid composites increases continuously up to 20 wt.% of fiber loading and then decreases when the fiber loading further increases. Generally, the transverse tensile strength of the composite is mainly controlled by the matrix tensile strength and the fiber/matrix interfacial strength. Generally, much stiffer fibers act like rigid inclusions in the matrix under transverse loading and the fibril separation is easy for the natural fibers. This can reduce the transverse tensile strength. The maximum transverse tensile strength for the epoxy based composites at 20 wt.% of fiber loading with the weight ratio of 1:1, 1:3 and 3:1 are found to be 41.82 MPa, 43.65 MPa and 39.63 MPa, respectively. Similarly, the corresponding values for polyester based composites at 20 wt.% of fiber loading are found to be 31.9 MPa, 35.06 MPa and 29.50 MPa, respectively.

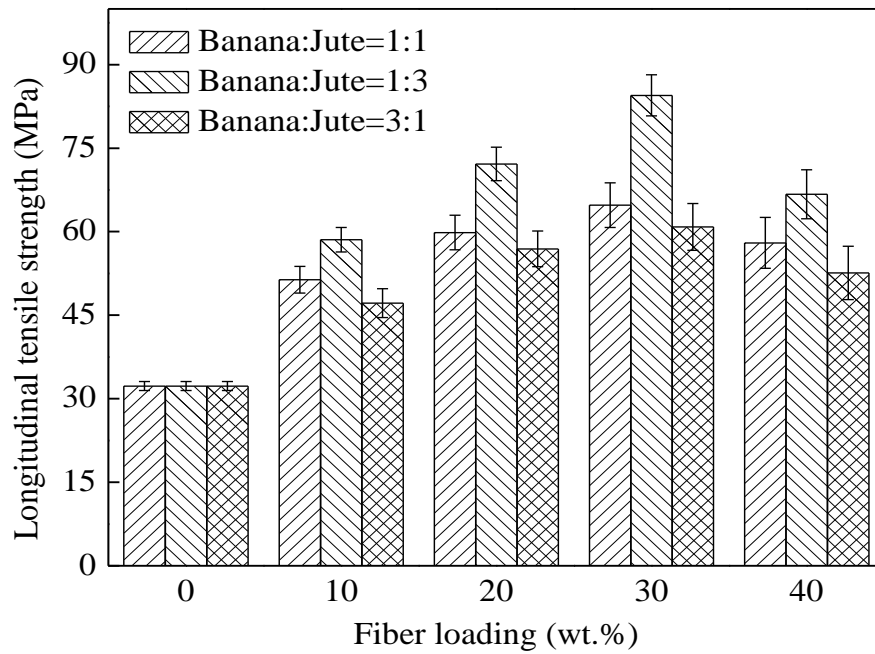


Figure 5.54: Effect of fiber loading and weight ratio on longitudinal tensile strength of epoxy based hybrid composites

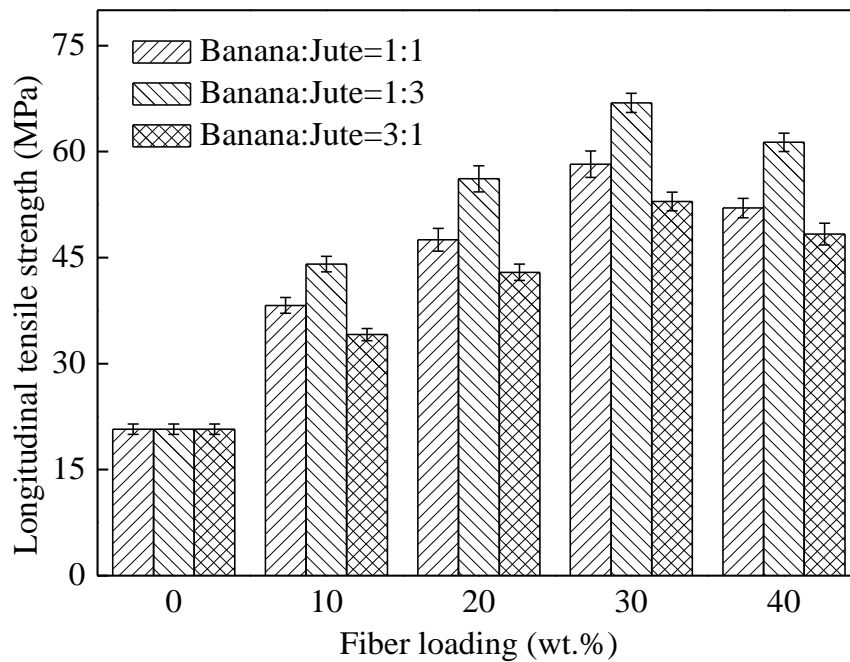


Figure 5.55: Effect of fiber loading and weight ratio on longitudinal tensile strength of polyester based hybrid composites

The tensile strength of composites is more pronounced for longitudinally oriented samples and much higher values of tensile strength is also observed as compared to the transversally oriented composite specimens. It has been well established in literature that when fibers are longitudinally oriented, the fibers are aligned parallel to the direction of load and the fibers transfer stress uniformly [277]. In transversely oriented, the fibers are aligned perpendicular to the direction of load and they cannot take part in stress transfer. Other researches have also observed that the tensile strength of composite improves when the fiber orientation is parallel to the loading direction compared to the other two mutually perpendicular directions. The maximum reinforcement and strength is achieved along the direction of fiber alignment, whereas in transverse direction, reinforcement is low because the fibers act as inclusions that prevent the distribution of stresses throughout the matrix [278], [279]. It is also observed that the longitudinal and transverse tensile strength is higher when the weight ratio of banana and jute fiber as 1:3. The increase in tensile strength of composite at this weight ratio is attributed to the reason that jute fibers are stronger and stiffer than banana fibers.

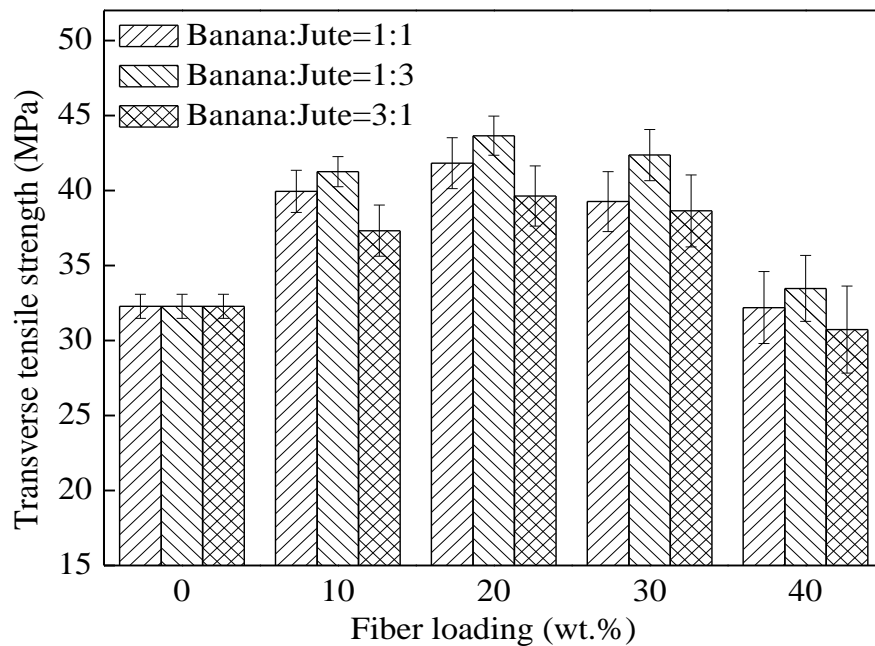


Figure 5.56: Effect of fiber loading and weight ratio on transverse tensile strength of epoxy based hybrid composites

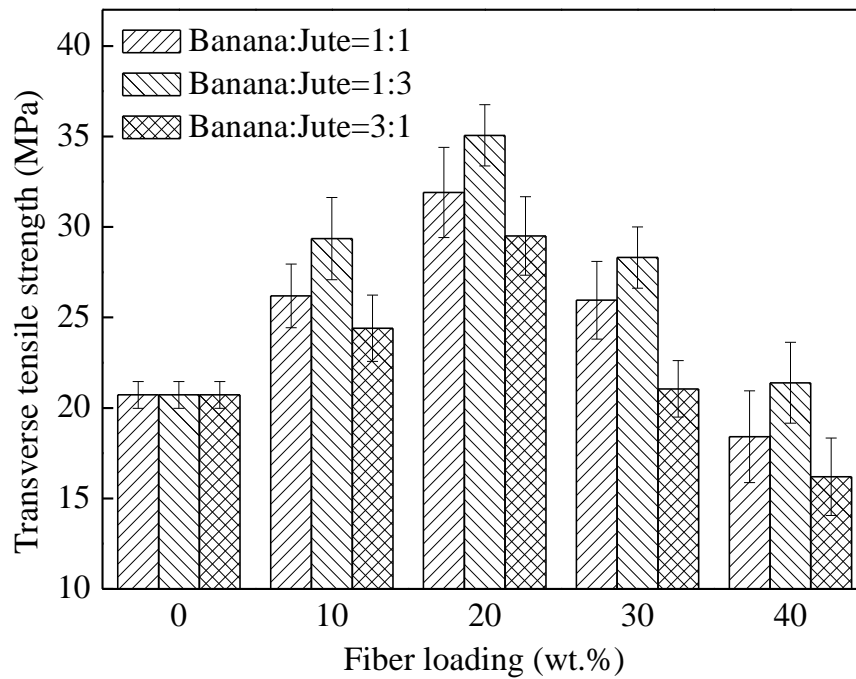


Figure 5.57: Effect of fiber loading and weight ratio on transverse tensile strength of polyester based hybrid composites

5.2.2.2 Flexural Properties

In the present work, the flexural properties such as flexural strength and modulus of the banana-jute fiber reinforced epoxy and polyester based hybrid composites are investigated along the longitudinal and transverse direction. In flexural loading, the composite samples are subjected to tension, compression and shear stresses [280]. The effect of fiber loading and weight ratio on the longitudinal flexural strength values of the epoxy and polyester based composites are shown in Figures 5.58 and 5.59 respectively, whereas the longitudinal flexural modulus are shown in Figures 5.60 and 5.61, respectively. It is noticeable that the incorporation of banana and jute fibers into the matrix, the longitudinal flexural properties of the composites increases up to 30 wt.% of fiber loading and then decreases at 40 wt.% fiber loading. The decrease in flexural properties while increasing fiber loading may be due to the fiber to fiber contact increases, the possibility of micro void formation is more, and deterioration of fiber and matrix adhesion. For epoxy based composites, the flexural strength increases with the increase in fiber loading from 46.32 MPa at 0 wt.% of fiber loading to 104.2 MPa, 125.1 MPa and 98.77 MPa at 30 wt.% fiber loading with weight ratio of banana and jute fiber as 1:1, 1:3, and 3:1, respectively. Similarly, for polyester based composites, the flexural strength increases with the increase in fiber loading from 41.19 MPa at 0 wt.% fiber

loading to 88.06 MPa, 94.30 MPa and 80.13 MPa at 30 wt.% fiber loading with weight ratio of banana and jute fiber as 1:1, 1:3, and 3:1, respectively. The longitudinal flexural modulus of the composites shows a similar trend as the flexural strength. The flexural modulus of neat epoxy and polyester resins are found to be 3.32 GPa and 1.616 GPa, respectively. For epoxy based composites, the flexural modulus of composite is found to be 124%, 137% and 104% greater than that of the neat epoxy resin with weight ratio of banana and jute fiber as 1:1, 1:3, and 3:1, respectively. Similarly, a substantial rise in flexural modulus of about 126%, 160% and 106% is observed as the fiber content in polyester increased from 0 to 30 wt.% with weight ratio of banana and jute fiber as 1:1, 1:3, and 3:1, respectively. The effect of fiber loading and weight ratio on the transverse flexural strength values of the epoxy and polyester based composites are shown in Figures 5.62 and 5.63, respectively, whereas the transverse flexural modulus are shown in Figures 5.64 and 5.65, respectively. The transverse flexural properties of the hybrid composites are increased up to 10 wt.% of fiber loading and then a gradual drop is observed. The reduction in the flexural properties of the hybrid composites is may be due to the alignment of fibers, weak interfacial bonding between fiber-matrix and ineffective wetting of the fibers by the matrix. A similar observation in case of short random oil palm fiber reinforced epoxy composites is also reported by Yusoff et al. [281].

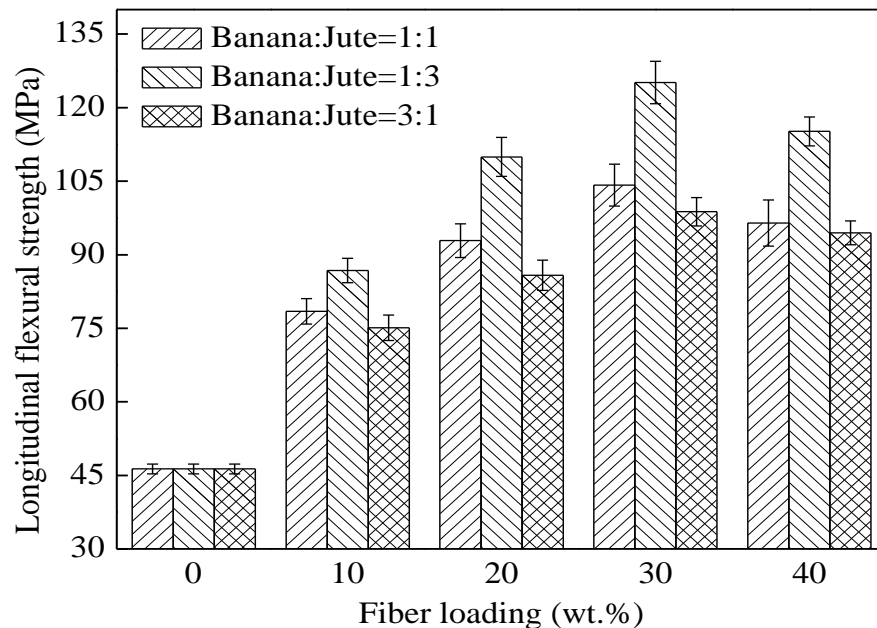


Figure 5.58: Effect of fiber loading and weight ratio on longitudinal flexural strength of epoxy based hybrid composites

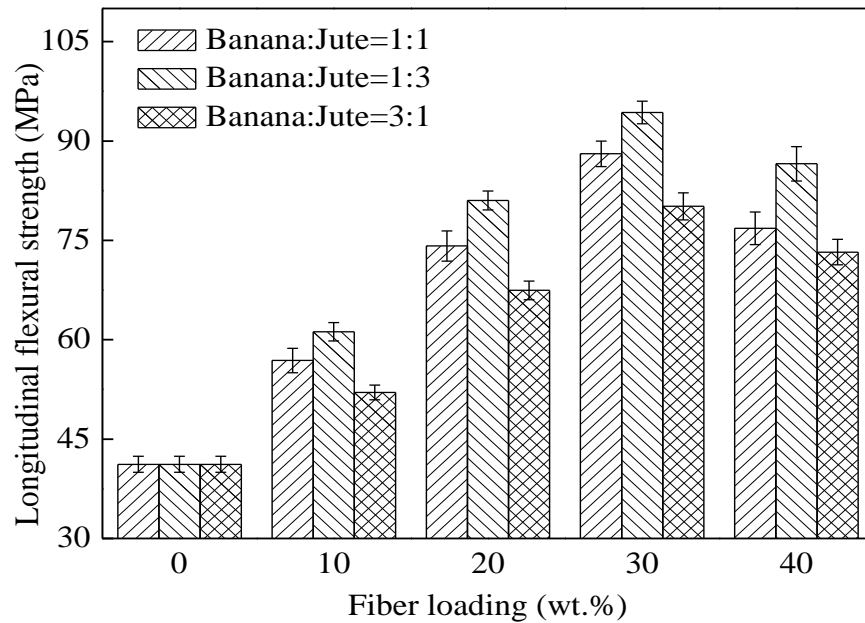


Figure 5.59: Effect of fiber loading and weight ratio on longitudinal flexural strength of polyester based hybrid composites

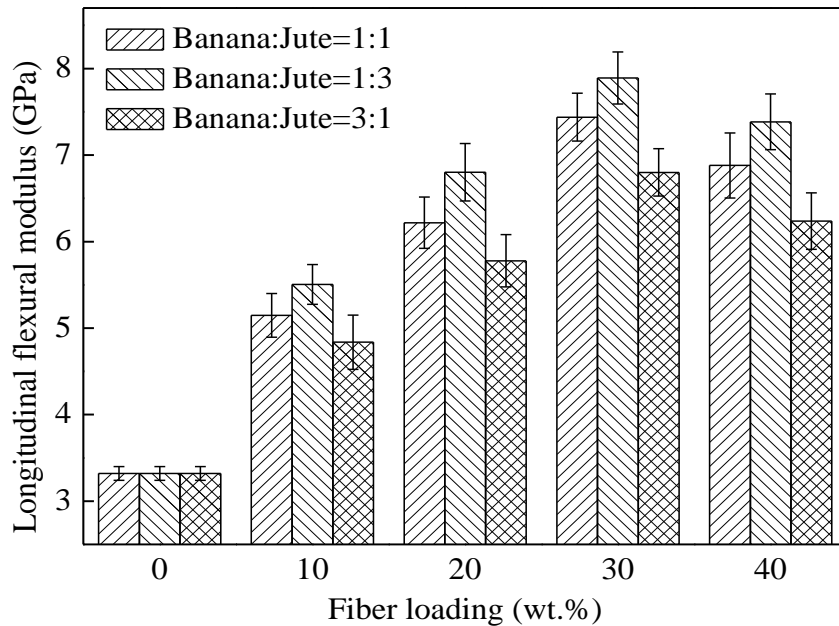


Figure 5.60: Effect of fiber loading and weight ratio on longitudinal flexural modulus of epoxy based hybrid composites

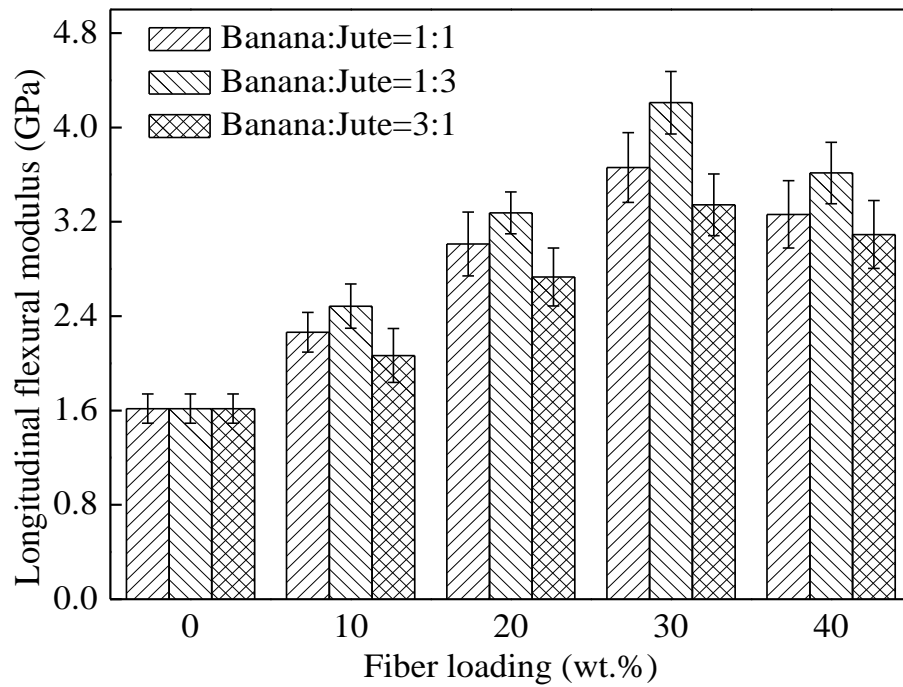


Figure 5.61: Effect of fiber loading and weight ratio on longitudinal flexural modulus of polyester based hybrid composites

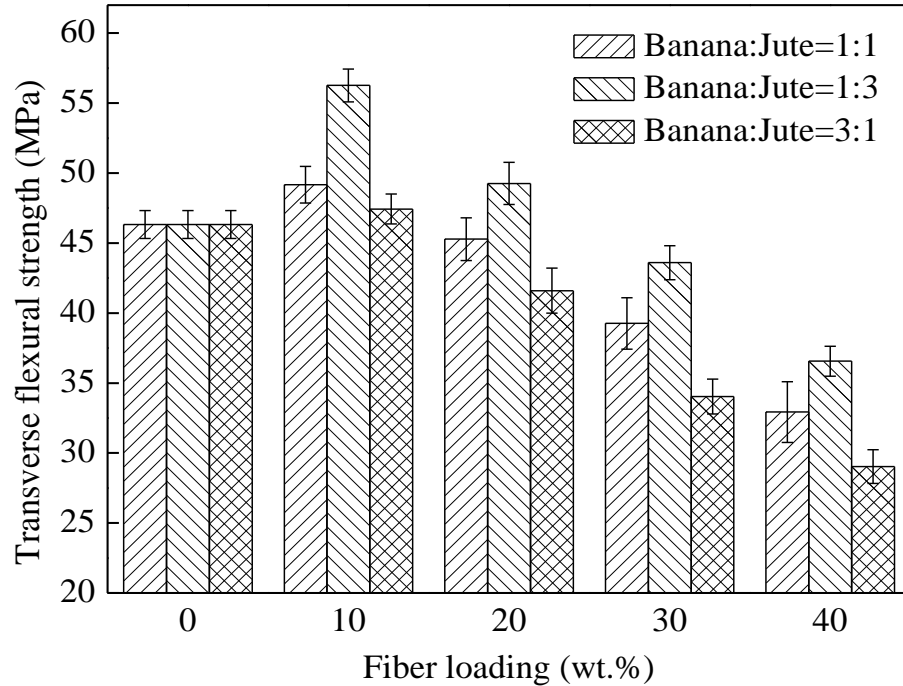


Figure 5.62: Effect of fiber loading and weight ratio on transverse flexural strength of epoxy based hybrid composites

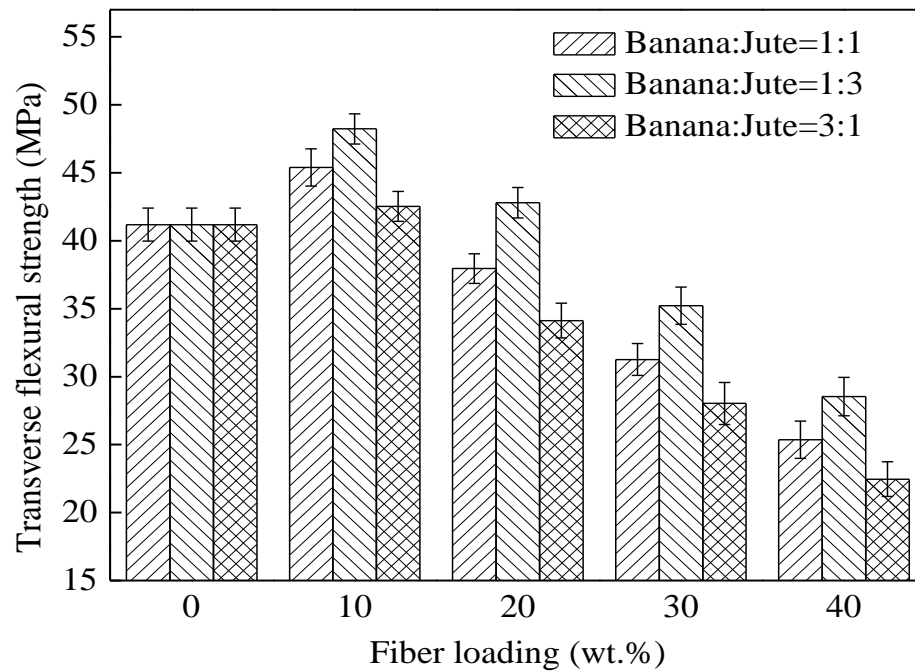


Figure 5.63: Effect of fiber loading and weight ratio on transverse flexural strength of polyester based hybrid composites

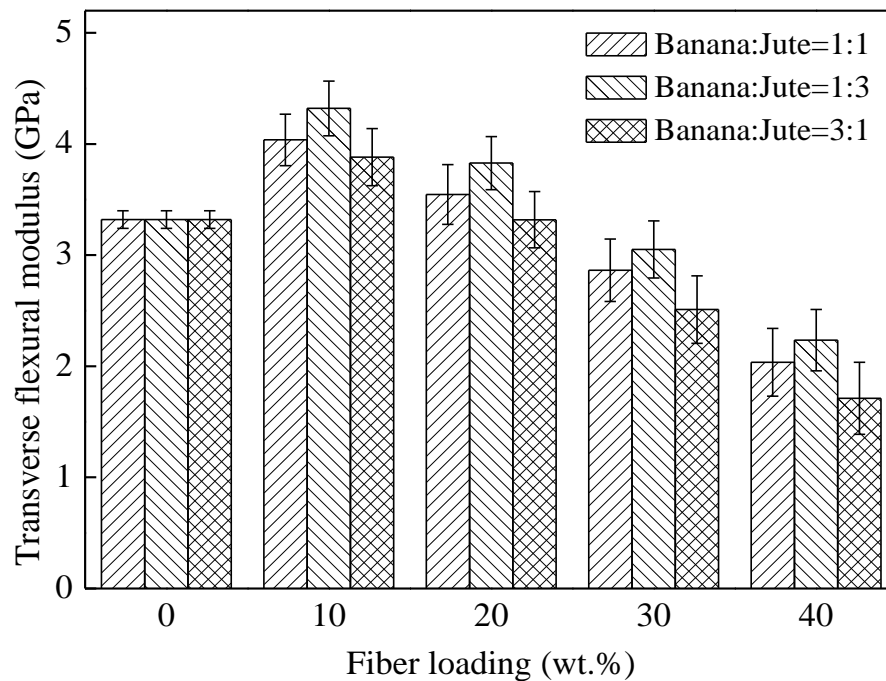


Figure 5.64: Effect of fiber loading and weight ratio on transverse flexural modulus of epoxy based hybrid composites

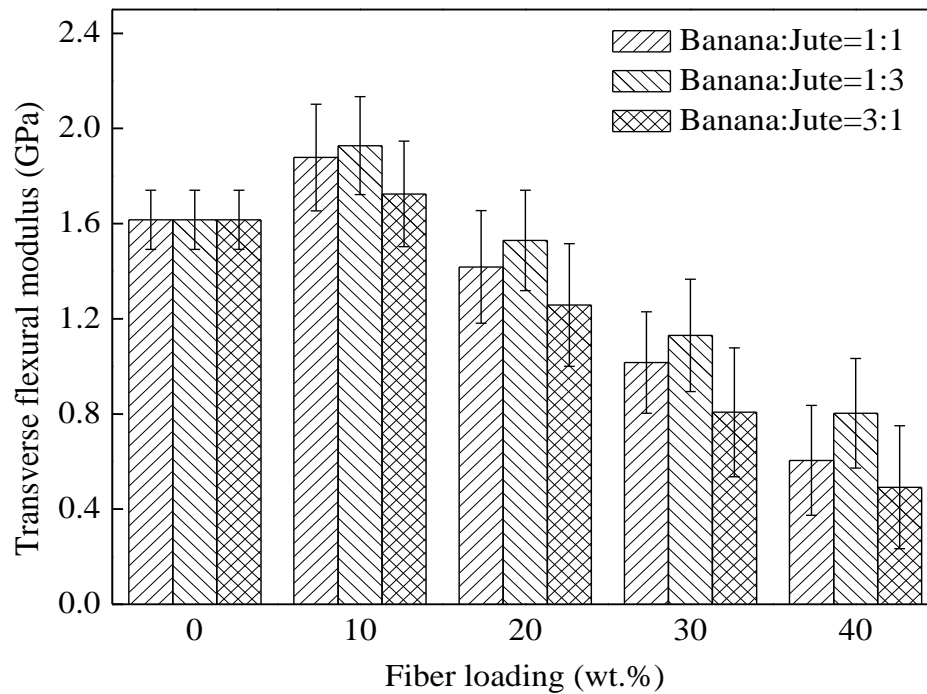


Figure 5.65: Effect of fiber loading and weight ratio on transverse flexural modulus of polyester based hybrid composites

It is observed from the figures that composites with the weight ratio of banana and jute fiber as 1:3 exhibits higher flexural properties compared to composite with the weight ratio of 1:1 and 1:3. In bending, the bottom layer of the composite subjected to tension and top layer subjected to compression and middle layer is subjected to shear. From this theory, it can be justified that the main load carrying members are skin in hybrid composite and hence skin layers should be made of high flexural strength fibers so that it withstands high load and hence improves the properties of the hybrid composite. Similar trend of higher flexural properties of hybrid composite due to the position of high strength material in the outer layer and low strength material as core material has also been reported by few researchers [92], [97], [282]. In a similar study, performed on oil palm/jute hybrid composites, a jute-oil palm-jute composite shows better flexural properties than oil palm-jute-oil palm hybrid composite [283].

5.2.2.3 ILSS

The ILSS is defined as the resistance of a layered composite to internal forces that tend to induce relative motion parallel to, and between the layers. The variation of ILSS of epoxy and polyester based composites with fiber loading and weight ratio are presented in Figures 5.66 and 5.67. In comparison to neat resin, the hybrid composite specimens show a

considerable improvement in ILSS. The ILSS of hybrid composites is increasing with the addition of fiber up to 30 wt.% and is decreasing with further increase in fiber loading up to 40 wt.%. The reduction of ILSS at higher fiber loading may be due to the formation of voids in the matrix which is generally located at the inter-laminar region of composites. The constituent materials, the fiber loading, the bonding between fiber and matrix, void content and the fiber orientation are the important parameters which govern the ILSS of the hybrid composites [284], [285]. In comparison of epoxy and polyester based composites, epoxy based hybrid composites shows higher ILSS than polyester based hybrid composites. This may be because of higher tensile strength of epoxy than polyester and better bond of epoxy with banana and jute fibers. Similar trend of increase in ILSS values of glass/ramie reinforced polyester composites with the increase in fiber volume fraction up to 31 vol.% is also reported by Romanzini et al. [124]. The ILSS of the neat epoxy is found to be 6.92 MPa and is increased to 18.57 MPa, 20.53 MPa, and 17.37 MPa with addition of 30 wt.% of fiber loading with weight ratio of banana and jute fiber as 1:1, 1:3, and 3:1, respectively. Similarly, the ILSS of the neat polyester is found to be 4.05 MPa and is increased to 14.47 MPa, 16.16 MPa, and 13.21 MPa with addition of 30 wt.% of fiber loading with weight ratio of banana and jute fiber as 1:1, 1:3, and 3:1, respectively. It can be seen that the weight ratio of banana and jute fiber as 1:3 possessed the highest ILSS compared with those of 1:1 and 3:1.

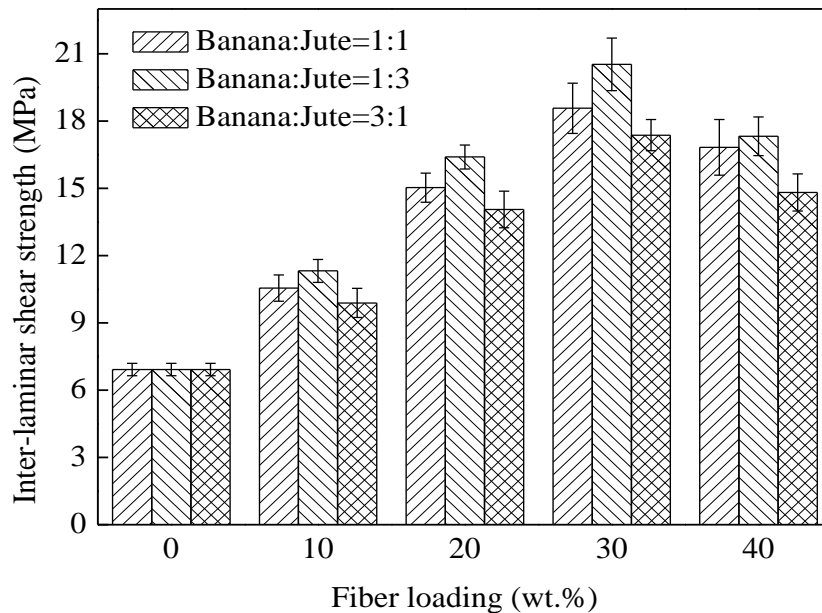


Figure 5.66: Effect of fiber loading and weight ratio on inter-laminar shear strength of epoxy based hybrid composites

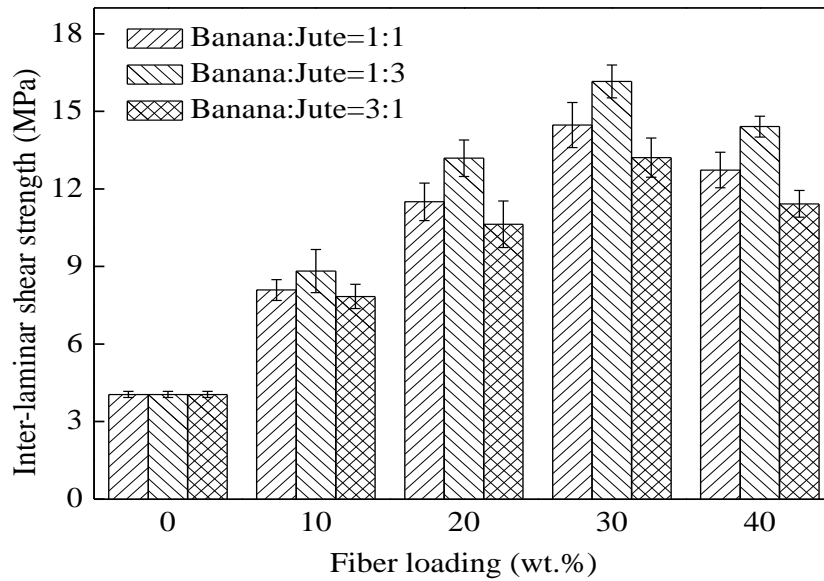


Figure 5.67: Effect of fiber loading and weight ratio on inter-laminar shear strength of polyester based hybrid composites

5.2.2.4 Impact Energy

Generally, impact tests are done for studying the toughness of a material. A material's toughness is a factor of its ability to absorb energy during plastic deformation. Matrix fracture, fiber breakage, fiber-matrix debonding, inter-layer delamination and fiber pull-out are the impotent factors of the impact failure of composites [286], [287]. In fiber reinforced composites, the reinforcement plays an important role in the impact energy of the composites as they interact with the crack formation in the matrix and act as a stress transferring medium. The effect of fiber loading and weight ratio on the impact energy of the epoxy and polyester based composites are shown in Figures 5.68 and 5.69, respectively. It is observed from the figures that the impact energy of the composites increases with an increase in the fiber loading. The reason may be due to the fact that when fiber loading is increases, more energy will have to be used up to break the coupling between the fibers. The impact energy of the epoxy based hybrid composites is much higher than those of the polyester based hybrid composites. The impact energy of the neat epoxy is found to be 1.01 J. The maximum impact energy absorbed by the epoxy based composites with weight ratio of banana and jute fiber as 1:1, 1:3, and 3:1 is found to be 3.56 J, 3.37 J and 3.77 J, respectively at 40 wt.% of fiber loading. Similarly, in case of polyester based hybrid composites at 40 wt.% of fiber loading, the impact energy is found to be 2.41 J, 2.28 J and 2.55 J with the weight ratio of banana and jute fiber as 1:1, 1:3, and 3:1, respectively.

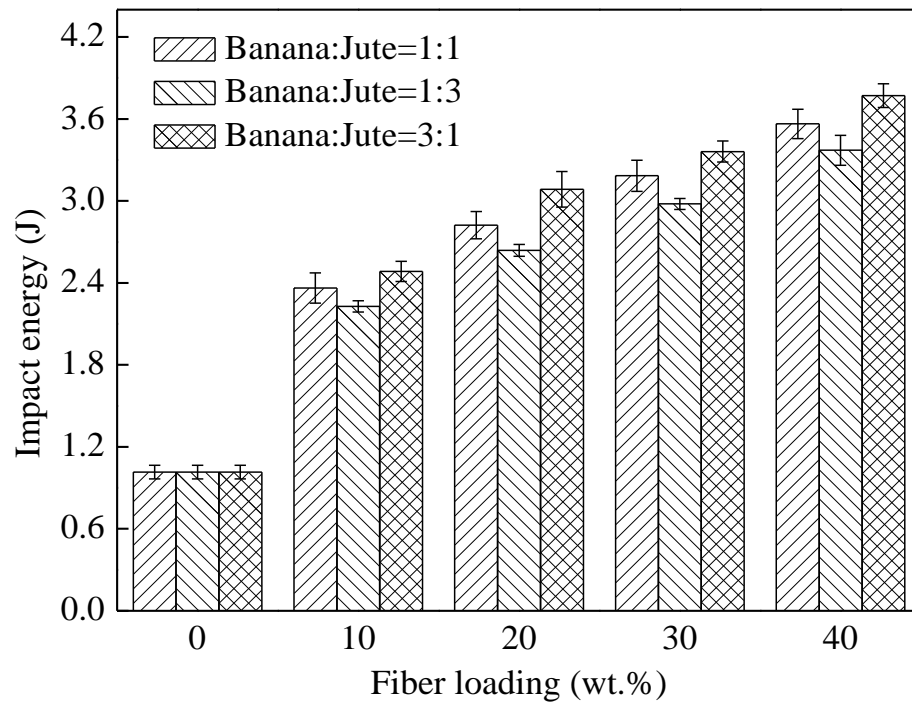


Figure 5.68: Effect of fiber loading and weight ratio on impact energy of epoxy based hybrid composites

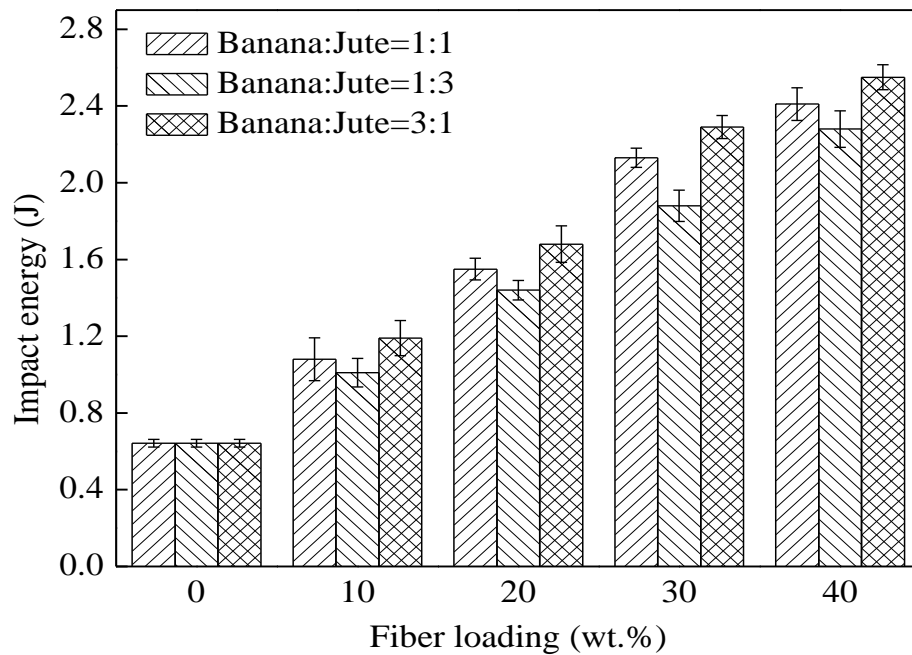


Figure 5.69: Effect of fiber loading and weight ratio on impact energy of polyester based hybrid composites

By adding the cellulose fibers in matrix, the drawbacks of matrix material such as surface cracking, brittle behavior and shrinkage during curing are eliminated. The similar trend is also observed by previous researchers on jute fiber reinforced polyester composites [288]. From the figures it can be also be observed that, composite with weight ratio of the banana and jute as 3:1 shows better impact properties than the other weight ratio. When banana fiber is used as an outer layer and jute fiber as a core, the impact energy is considerably improved for epoxy and polyester based hybrid composites due to the banana fiber, which has higher fracture toughness than jute fiber, and is present on one side of the hybrid composite [283], [289], [290]. The effect of the weight ratio does not have positive trend on the impact energy as obtained in the tensile and flexural properties.

5.2.2.5 Micro-Hardness

Hardness is considered as one of the most important factors of a composite material as it indicates the ability of the composite material to resist to the permanent deformation or damage. In the present work, micro-hardness of the composites is studied by applying indentation load normal to fiber length and diameter. The effect of fiber loading and weight ratio on hardness values of the epoxy and polyester based composites are shown in Figures 5.70 and 5.71 respectively. It is observed from the figures that with the increase in fiber loading, micro-hardness of the composites increases irrespective of the reinforcement and matrix type.

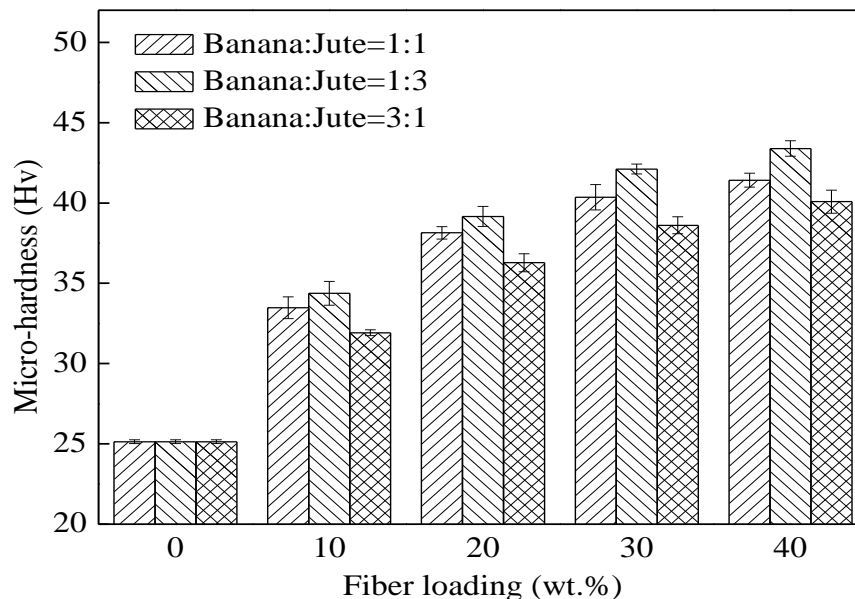


Figure 5.70: Effect of fiber loading and weight ratio on micro-hardness of epoxy based hybrid composites

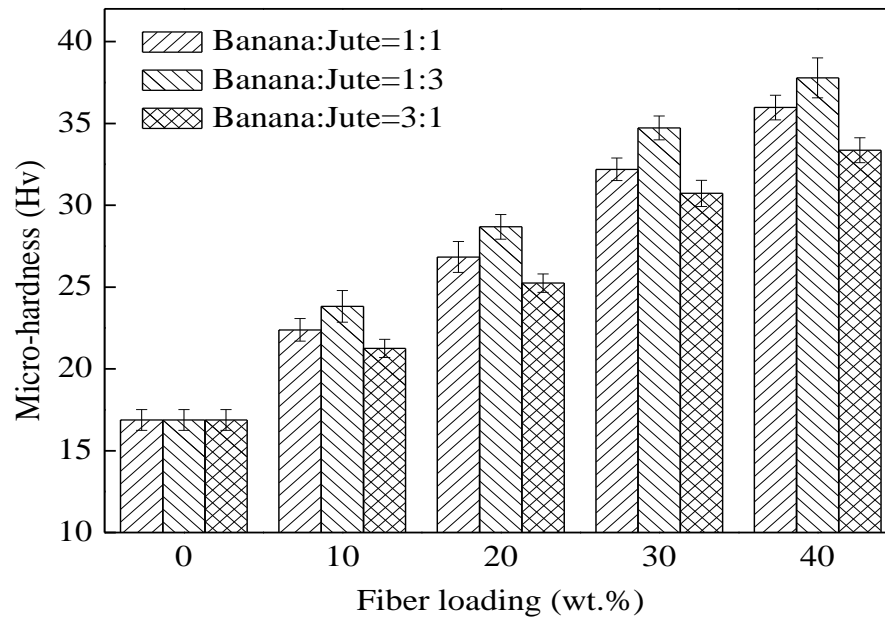


Figure 5.71: Effect of fiber loading and weight ratio on micro-hardness of polyester based hybrid composites

This may be attributed to compressive force applied during hardness testing which press the reinforcement and matrix together which result in decrease in indentation and effective transfer of load. In general, the fibers that increases the tensile modulus of composites is also increases the hardness of composites. This is because hardness is a function of relative fiber volume and modulus [134]. For epoxy based composites, the neat epoxy has the minimum hardness value of 25.13 Hv. The composites reinforced with 40 wt.% of fiber loading with weight ratio of banana and jute fiber as 1:1, 1:3, and 3:1 exhibits maximum hardness value of 41.42 Hv, 43.39 Hv and 40.08 Hv, respectively. The addition of reinforcement content increases the resistance strength of matrix to plastic deformation. The results are found to be in close conjunction with all weight ratio of the fiber. Similarly, for polyester based composites, with the increase in fiber loading, the micro-hardness value is found to be increasing although the rate of improvement is not as high as in the case of epoxy based composites. This difference in hardness is obvious as the epoxy resin is much harder than polyester. It is observed from the figure that the hardness of neat polyester is 16.88 Hv. With the addition of 40 wt.% of fiber loading, the micro-hardness of polyester based composite improves to 113%, 123% and 97% with corresponding weight ratio of banana and jute fiber as 1:1, 1:3, and 3:1, respectively. Among all the composites under this investigation, composites with weight ratio of banana and jute fiber as 1:3 shows the highest micro-hardness, compared with weight ratio of banana and jute fiber as 1:1 and 3:1. This may

be due to the brittle nature of the lignocellulosic fiber [291]. A similar trend of increase in hardness value with the increase in fiber loading is also observed by few researchers [135], [292].

5.2.2.6 Surface Morphology

It is well known that the properties of the composite material are mainly depends on the bonding between the reinforcement and the matrix. In order to evaluate the fiber-matrix bonding, the microstructure of the fibers and the dispersion of the banana and jute fibers in the matrix material are observed under scanning electron microscope. The cross-sectional view of banana and jute fiber is shown in Figure 5.72. These micrographs confirm the cylindrical shape of the fibers used as reinforcement in the matrix body. It is evident from Figure 5.72 (a) that the surface of the banana fiber is porous and is covered with a layer of waxy and pithy substances. It can be observed from the Figure 5.72 (b) that jute fiber has compact structure and the filaments are packed together due to the intercellular binding materials such as waxes and hemicelluloses. Generally, the jute fiber strength and its mechanical property is more due to the lowest porosity and close packing of cellulose chain. That is why, composites with weight ratio of banana and jute fiber as 1:3 shows better properties as compared to others.

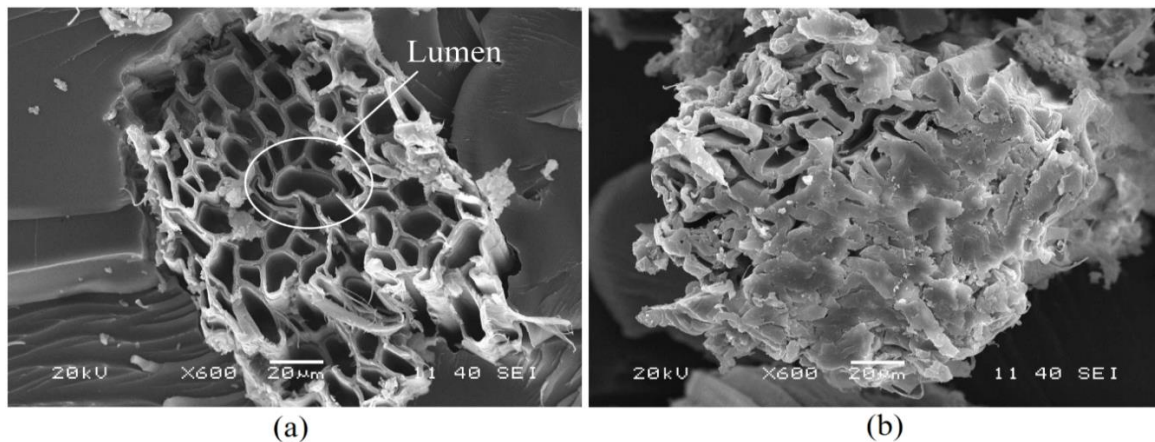


Figure 5.72: Scanning electron micrographs for cross-sectional views of (a) banana fiber, and (b) jute fiber

The scanning electron micrographs of longitudinal direction view of banana and jute fibers are shown in Figure 5.73. It is clear from the image that the average diameter of jute fiber is around 80-90 micron (Figure 5.73(a)) and banana fiber is around 170-190 micron (Figure 5.73 (b)). Figure 5.74 shows the morphological cross-section of neat epoxy and composite reinforced with different weight ratio of banana and jute fiber.

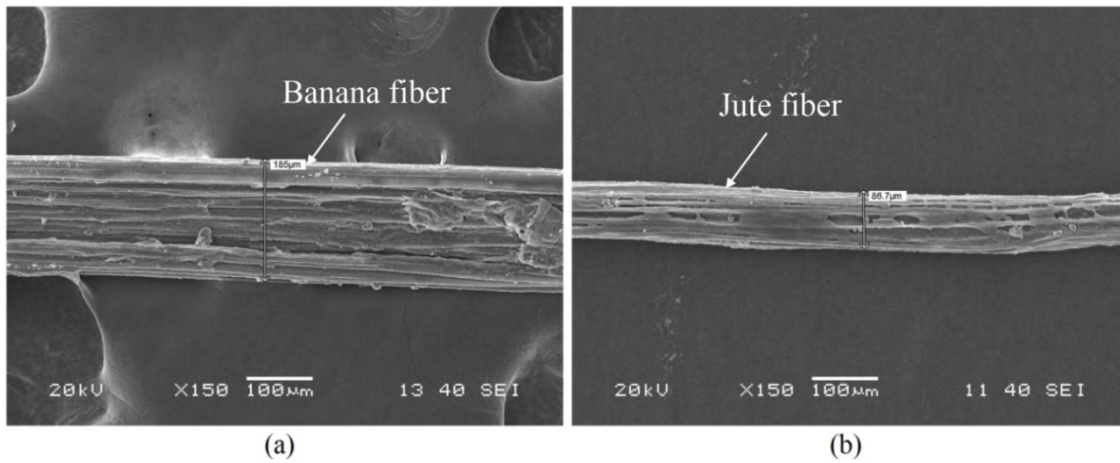


Figure 5.73: Scanning electron micrographs in longitudinal direction of (a) banana fiber, and (b) jute fiber

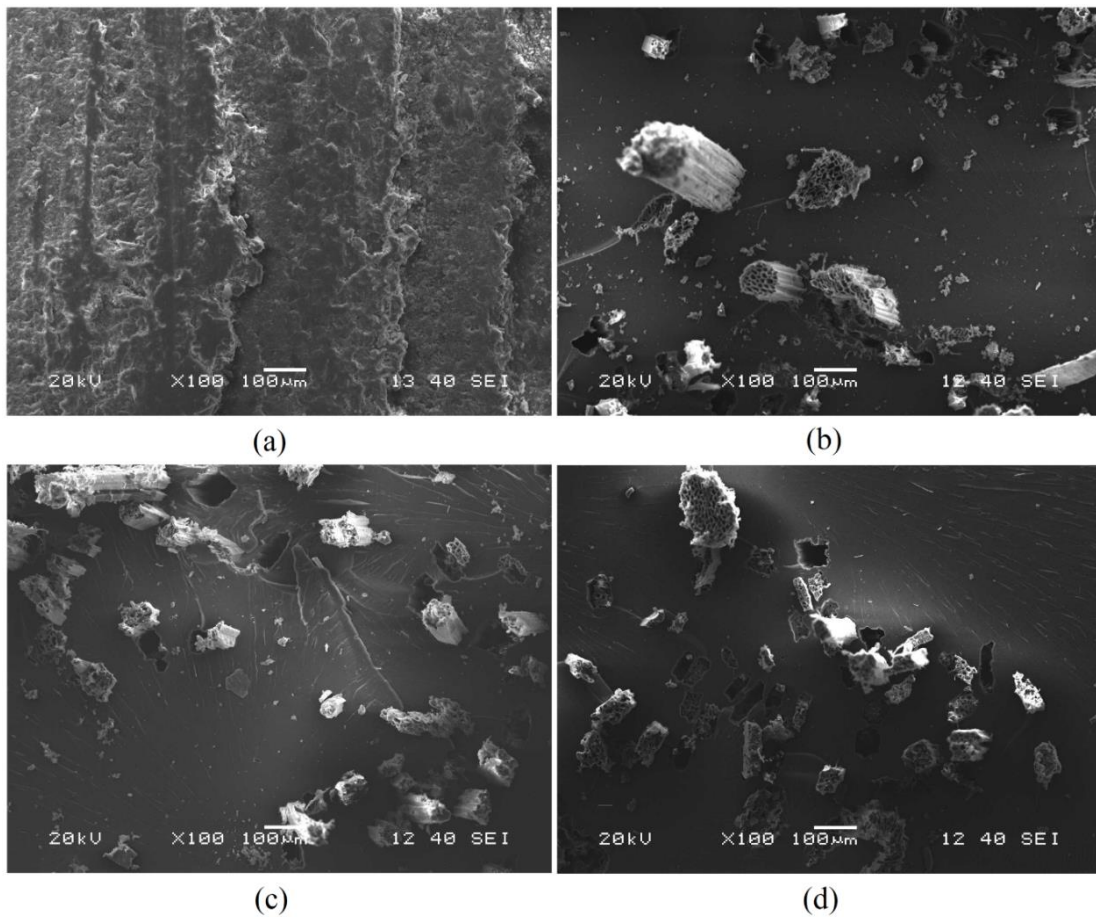


Figure 5.74: Scanning electron micrographs of morphological cross-section of (a) neat epoxy and the composites with weight ratio of banana and jute fiber as (b) 1:1, (c) 1:3 and (d) 3:1

All the micrographs are taken for composites with fiber loading of 30 wt. %. The morphological structure of the neat epoxy is presented in Figure 5.74 (a). From the figure, no pulling and stretching of polymer on the surface of epoxy composite is observed, but there is a sharp cut surface due to brittle nature of epoxy composite. The brittle nature of the neat polymer composite is studied and conformed by many researchers [90], [293]. Figure 5.74 (b), (c), and (d) shows the composites with weight ratio of banana and jute fiber as 1:1, 1:3, and 3:1, respectively. From the figures it is observed that the distributions of banana and jute fibers in the matrix material are more or less uniform and further increase of fiber loading beyond 30 wt.%, reduces the inter fiber distance upto the limit that fibers start to interfere with each other, which may decrease the properties of the fiber as well as the composites.

Scanning electron microscopy images for the tensile fracture of the unidirectional banana-jute fiber reinforced epoxy based composite are compared with the 30 wt.% and 40 wt.% fiber loading and the weight ratio of banana and jute fiber as 1:1. Figures 5.75 (a) and 5.75 (b) shows the micrograph of a fractured specimen after tensile test of banana-jute fiber reinforced epoxy composite along the longitudinal direction at 30 wt.% and 40 wt.% of fiber loading, respectively. It can be clearly observed from the Figure 5.75 (a) that there is a good interfacial bonding between the fiber and the matrix at 30 wt.% of fiber loading that leads to better strength properties of the composites. Fiber breakage, fiber pull out, and voids or air entrapments are observed in Figure 5.75 (b), which are a result of weak interfacial bonding between the fiber and matrix at 40 wt.% of fiber loading.

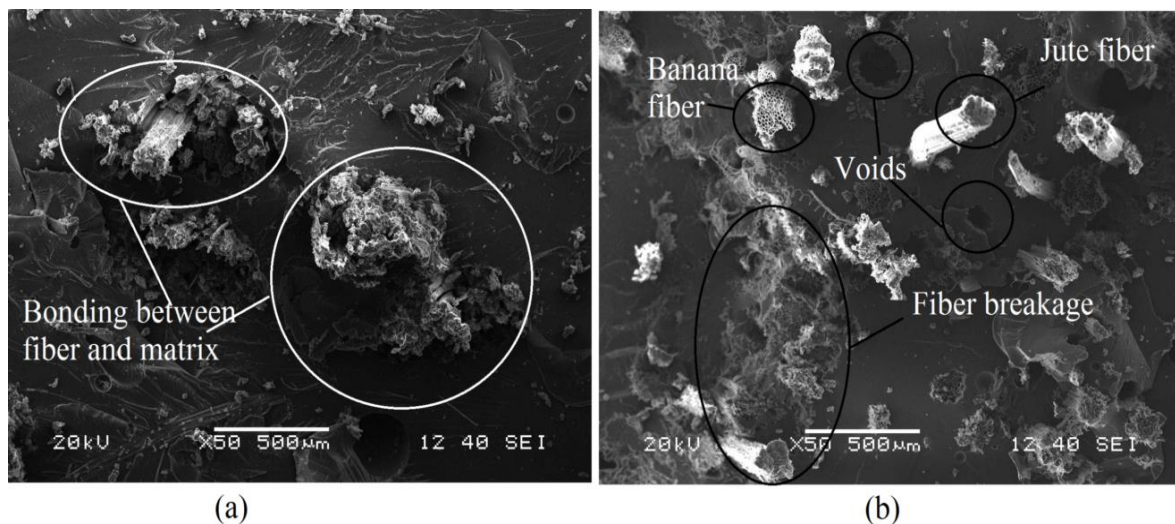


Figure 5.75: Tensile fracture surfaces of banana-jute epoxy based composites along the longitudinal direction with the weight ratio of banana and jute fiber as 1:1 (a) 30 wt.% fiber loading and (b) 40 wt.% fiber loading

Figure 5.76 (a) and (b) shows the micrographs of a fractured specimen of banana-jute fiber composite after tensile test along the transverse direction. A good adhesion is clearly observed for composites with 30 wt.% fiber loading in Figure 5.76 (a). However, it is evident from the Figure 5.76 (b) that the surface with fiber pull out, fracture and crack propagation in the matrix at 40 wt.% of fiber loading which leads to the poor mechanical properties of the composites.

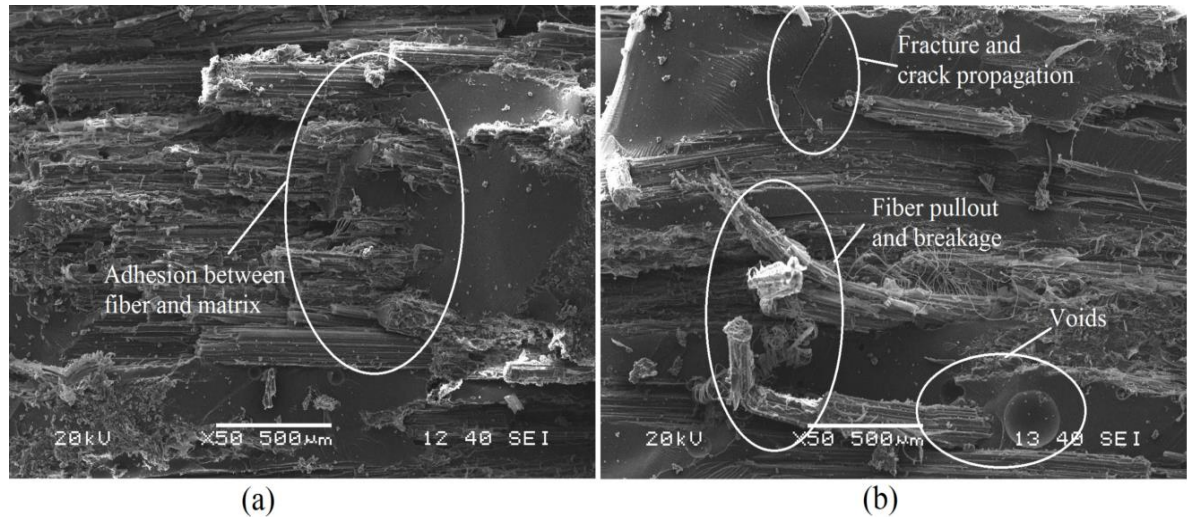


Figure 5.76: Tensile fracture surfaces of banana-jute epoxy based composites along the transverse direction with the weight ratio of banana and jute fiber as 1:1 (a) 30 wt.% fiber loading and (b) 40 wt.% fiber loading

5.2.3 Thermal Properties

5.2.3.1 Specific Heat and Thermal Diffusivity

Generally, the incorporation of hybrid fibers changes the thermal properties of the polymer composites. The fiber orientation, dispersion of the fibers, relative modulus of the fibers and polymer, and fiber aspect ratio affect the thermal properties of the hybrid composites. Specific heat capacity of material is the quantity of heat required to change the temperature of unit mass of the substance. The specific heat capacities of neat polymers and hybrid composites are measured at a maximum temperature of 120°C using DSC and listed in Table 5.10. As can be seen, the specific heat of the test materials decreased gradually with the increase in fiber loading in both the epoxy and polyester based composites. This behavior of composite is attributed to the lower specific heat capacity of the natural fibers. The physical significance of thermal diffusivity is associated with the propagation of heat into the medium during changes of temperature with time.

Table 5.10: Specific heat and thermal diffusivity of the unidirectional fiber reinforced composites

Unidirectional fiber reinforced epoxy composites				Unidirectional fiber reinforced polyester composites			
Composite	Specific heat (kJ/kg-K)	Longitudinal thermal diffusivity ($\times 10^{-7}$) (m ² /s)	Transverse thermal diffusivity ($\times 10^{-7}$) (m ² /s)	Composite	Specific heat (kJ/kg-K)	Longitudinal thermal diffusivity ($\times 10^{-8}$) (m ² /s)	Transverse thermal diffusivity ($\times 10^{-8}$) (m ² /s)
CE1	3.02	1.049	1.049	CP1	2.68	6.815	6.815
CE2	2.78	1.035	1.020	CP2	2.56	6.633	6.492
CE3	2.61	1.009	0.961	CP3	2.39	6.578	6.315
CE4	2.43	0.979	0.895	CP4	2.24	6.445	6.008
CE5	2.25	0.936	0.831	CP5	2.04	6.538	5.880
CE6	2.85	1.002	0.984	CP6	2.62	6.430	6.258
CE7	2.72	0.955	0.893	CP7	2.46	6.284	5.885
CE8	2.50	0.922	0.821	CP8	2.32	6.037	5.387
CE9	2.29	0.905	0.743	CP9	2.11	6.013	5.130
CE10	2.73	1.068	1.049	CP10	2.54	6.798	6.621
CE11	2.56	1.047	0.993	CP11	2.37	6.772	6.506
CE12	2.42	1.003	0.911	CP12	2.23	6.630	6.228
CE13	2.23	0.973	0.854	CP13	2.01	6.869	6.331

The lesser the thermal diffusivity, more the time required for heat to penetrate into the solid [148]. The thermal diffusivity values of the hybrid composites are calculated using equation (4.16) and shown in Table 5.10. The thermal diffusivity of the hybrid composites decreases with increase in the fiber loading. This means that the hybrid composites containing banana and jute fiber will require a longer time to be heated or cooled than the neat epoxy. The similar trend of results is also observed by previous researchers for flax and sisal fiber reinforced composites [160], [161]. The results obtained in the present study indicate that fiber loading has a great influence on the specific heat capacity and thermal diffusivity values. However, the influence of weight ratio of the fibers on specific heat and thermal diffusivity values given in Table 5.10 is negligible. This is mainly due to the high uncertainty bounds obtained for these two thermal parameters. It is also observed that the

diffusivity is proportional to thermal conductivity results. It is an added advantage especially in building materials to increase the fire resistance.

Chapter Summary

This chapter has provided:

- The results of the micromechanical analysis and experiments conducted to evaluate the elastic properties and thermal conductivity of the unidirectional banana-jute fiber reinforced hybrid composites under study
- The validation of proposed model for transverse thermal conductivity of unidirectional reinforced hybrid composites developed in Chapter 3 of this thesis through results obtained by micromechanical analysis and experimental results
- The results of the physical, mechanical and thermal behaviour of unidirectional banana-jute fiber reinforced hybrid composites.
- The effect of fiber loading and weight ratio on the physical, mechanical and thermal behaviour of unidirectional banana-jute fiber reinforced hybrid composites.

The next chapter presents the results and discussion of the physical, mechanical and thermal behaviour of short fiber reinforced hybrid composites under this study.

Chapter 6

Results and Discussion – II

Short Fiber Reinforced Composites

This chapter presents the physical, mechanical and thermal behaviour of the short banana-jute fiber reinforced epoxy and polyester based composites. The results of this chapter are divided into two parts. Part-1 represents the micromechanical analysis of short fiber reinforced hybrid composites for predicting the elastic properties and thermal conductivity. Part-2 represents the physical, mechanical and thermal properties of the short fiber reinforced hybrid composites.

6.1 Elastic and Thermal Conductivity of Short Fiber Reinforced Composites

This part of the chapter presents the micromechanical analysis for predicting the effective elastic properties and thermal conductivity of the short fiber reinforced hybrid composites. The result of the proposed theoretical model for calculation of effective thermal conductivity is also presented in this part of the thesis.

6.1.1 Development of Micromechanical Model in ANSYS

6.1.1.1 Generation of the RVE Model

In short fiber reinforced composites, the fibers are arranged randomly and hence it is difficult to model the random arrangement. For simplicity, most of the micromechanical models assume a periodic arrangement of fibers in which a RVE can be isolated. Figure 6.1 (a) shows the schematic diagram of the short fiber reinforced composite. A single RVE is taken out from the square pattern of short fiber composites for further study as shown in Figure 6.1 (b). The relation between the volume fraction of fiber and the radius of fiber is given in equation (6.1)

$$\Phi_{fb} = n_b \times \frac{\pi r_{fb}^2 l_b}{a_1 a_2 a_3} \quad \text{and} \quad \Phi_{fj} = n_j \times \frac{\pi r_{fj}^2 l_j}{a_1 a_2 a_3} \quad (6.1)$$

Where, Φ_{fb} and Φ_{fj} are the volume fraction of banana fiber and jute fiber, respectively; n_b and n_j are the number of banana and jute fibers, respectively. Similarly, a_1 , a_2 , and a_3 are the side length of square RVE, l_b and l_j are the length of the banana and jute fiber, respectively; and r_{fb} and r_{fj} are the radius of banana and jute fiber, respectively. In order to perform the micromechanical analysis, three-dimensional physical models with cylinders in cube (fibers in polymer) have been used to simulate the RVE of composite materials at different fiber loading and weight ratio. In the study of the micromechanics of fiber reinforced materials, it is convenient to use an orthogonal coordinate system that has one axis aligned with the fiber direction. The axis x_3 is aligned with the fiber direction; the axis x_2 is perpendicular to the plane of the unit cell and is also perpendicular to the fibers, and the axis x_1 is in the plane of the unit cell and perpendicular to the fibers as shown in Figure 6.1 (b). Dimensions considered for the analysis are $a_1=10 \mu\text{m}$. The radius of the banana fiber and jute fiber are calculated corresponds to the fiber loading ranging from 0 to 40 wt.% using equation (6.1). A three dimensional elements SOLID186 and SOLID90 are used to determine the elastic properties and thermal conductivity. The meshed model of square RVE at 30 wt.% of fiber loading with different weight ratio of banana and jute fiber is shown in Figure 6.2.

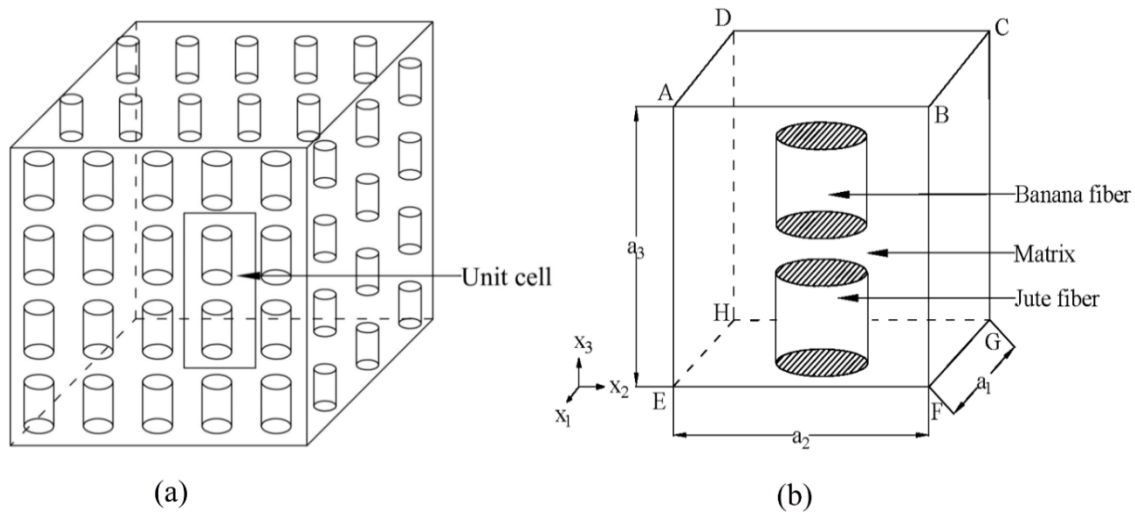


Figure 6.1: (a) Arrangement of short fibers and (b) RVE of short fibers in square packing

6.1.1.2 Boundary Conditions for Evaluation of Elastic Properties

The boundary conditions for the short fiber reinforced hybrid composites are similar to the unidirectional fiber reinforced hybrid composites. After evaluating the stiffness matrix coefficients under the plane strain conditions, the effective elastic modulus and shear modulus of the homogenized composite material can be computed by using equation (6.2).

Figures 6.3 and 6.4 show the counter of stress and strain in square RVE with different weight ratio of banana and jute fiber at 30 wt.% of fiber loading.

$$E = C_{11} - 2C_{12}^2 / (C_{22} + C_{23})$$

$$G = \frac{1}{2}(C_{22} - C_{23}) \quad (6.2)$$

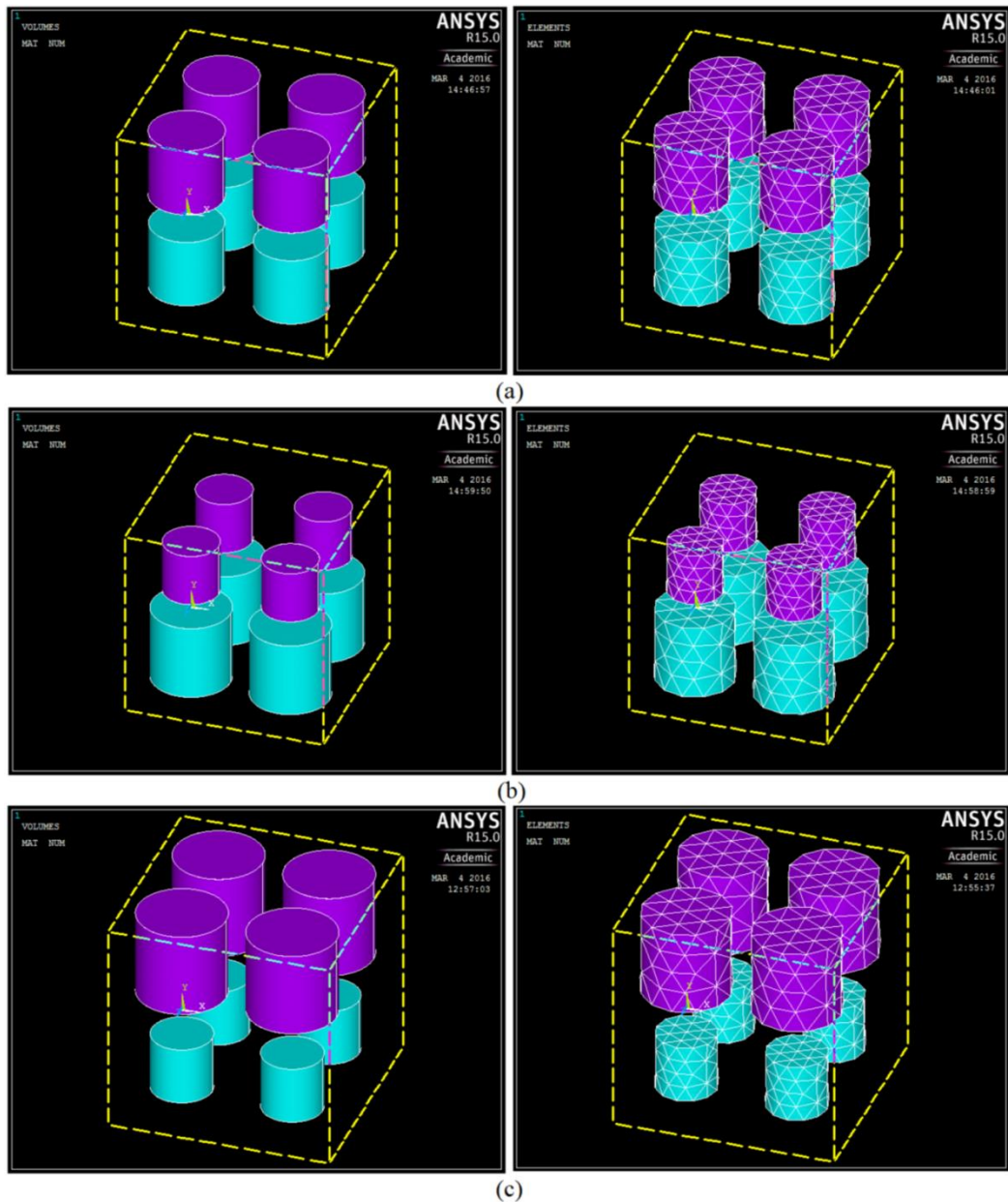


Figure 6.2: Finite element and meshed model of the RVE with weight ratio of banana and jute fiber as (a) 1:1, (b) 1:3, and (c) 3:1 at 30 wt.% of fiber loading

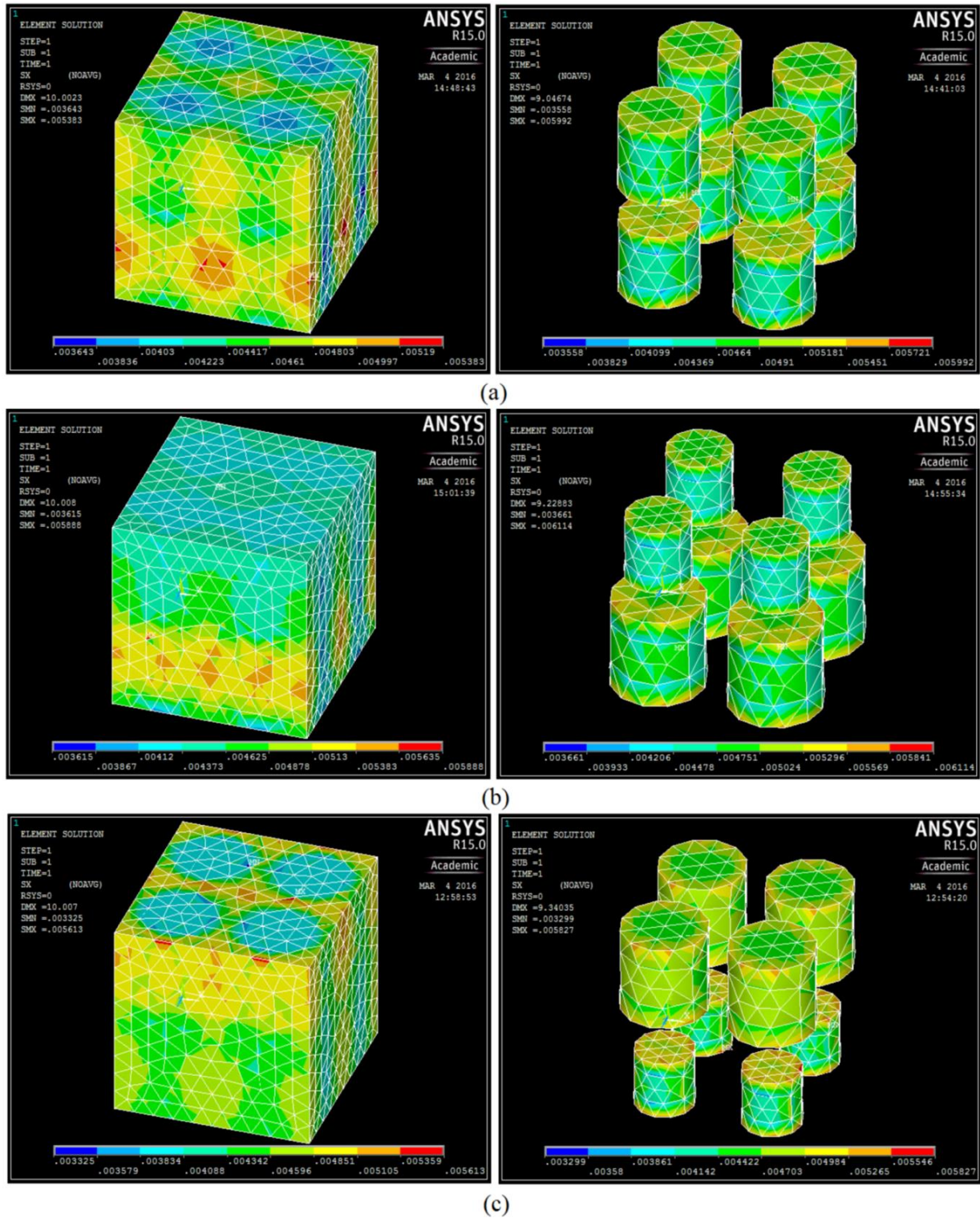


Figure 6.3: Counter of stress in RVE with weight ratio of banana and jute fiber as (a) 1:1, (b) 1:3, and (c) 3:1 at 30 wt.% of fiber loading

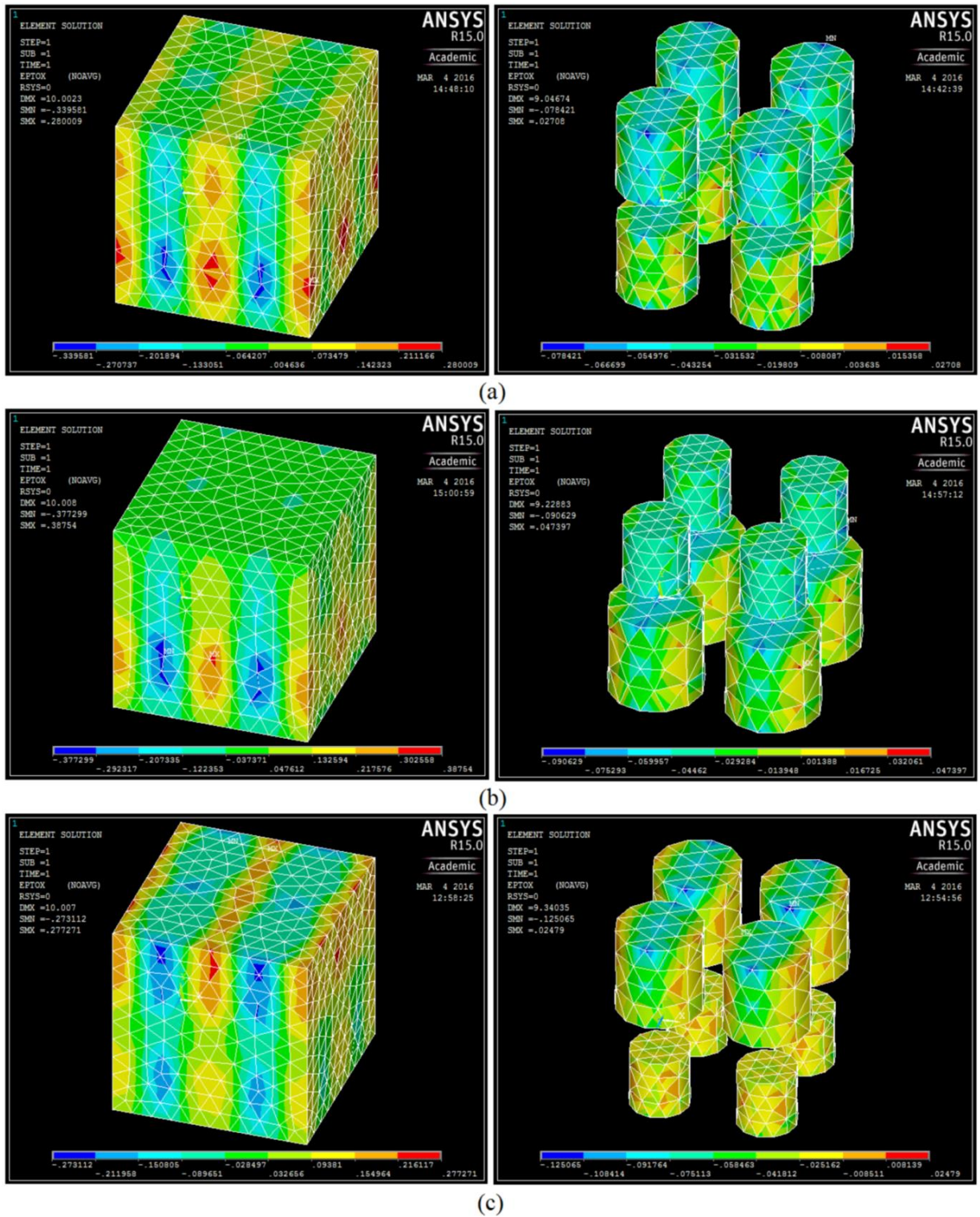


Figure 6.4: Counter of strain in RVE with weight ratio of banana and jute fiber as (a) 1:1, (b) 1:3, and (c) 3:1 at 30 wt.% of fiber loading

6.1.1.3 Boundary Conditions for Evaluation of Effective Thermal Conductivity

From the constituent material properties, one-dimensional steady state heat transfer simulations are performed by using FEA to predict the effective thermal conductivity of the hybrid composites. The prescribed boundary conditions with the direction of heat flow for the conduction problem is shown in Figure 6.5. The temperature at the nodes along the surface EFGH is kept at T_2 ($=30^\circ\text{C}$), and the corresponding surface ABCD is kept at T_1 ($=120^\circ\text{C}$) in order to maintain the temperature difference of 90°C . The other surfaces parallel to the direction of the heat flow are assumed to be adiabatic. The thermal conductivity of the hybrid composite is calculated by using equation (6.3).

$$k = \frac{q}{\Delta T / \Delta a} \quad (6.3)$$

$$q = \frac{Q}{A}$$

Where, ΔT is the temperature difference across the thickness (Δa) of the composite, Q is the heat rate along the direction obtained from simulation in W, q is the heat flux in the direction in W/m^2 , A is the cross-sectional area across the flux in m^2 and k is the effective thermal conductivity of the hybrid composite. Figure 6.6 shows the temperature distribution of square RVE with different weight ratio of banana and jute fiber at 30 wt.% of fiber loading.

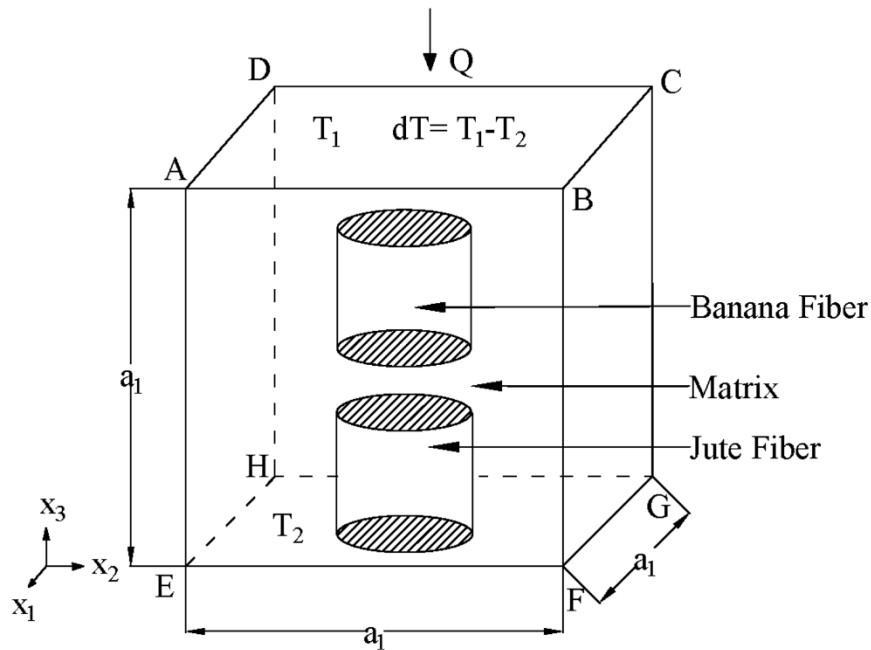


Figure 6.5: The heat flow direction and boundary conditions for the square RVE

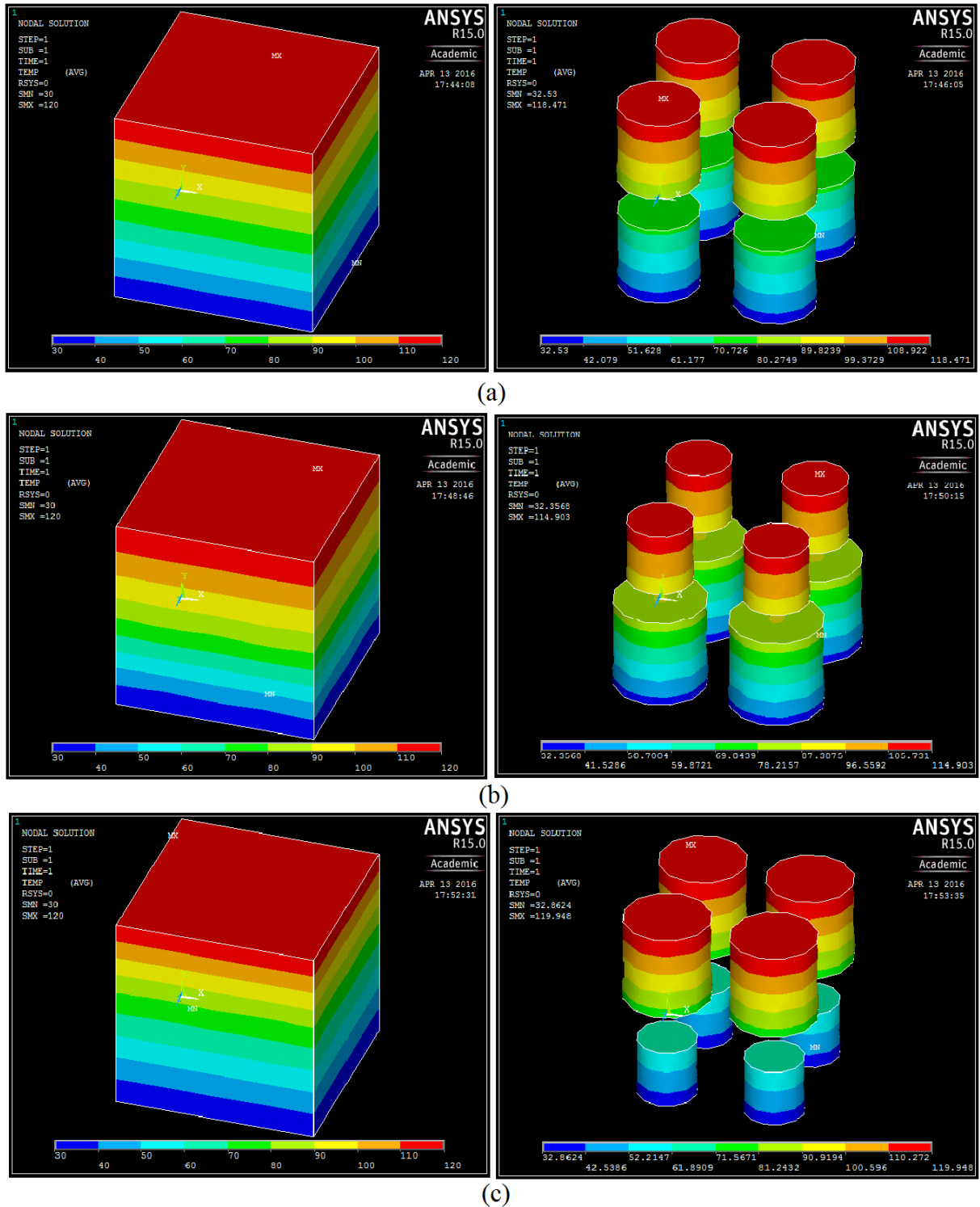


Figure 6.6: Temperature distribution in RVE with weight ratio of banana and jute fiber as (a) 1:1, (b) 1:3, and (c) 3:1 at 30 wt.% of fiber loading

6.1.2 Elastic Properties of Short Fiber Reinforced Hybrid Composites

6.1.2.1 Effective Elastic Modulus of Composites

The effective elastic modulus of natural fiber reinforced hybrid composites depend on many parameters such as type of reinforcement, type of matrix, fiber length, fiber orientation, fiber strength and modulus, aspect ratio and the interfacial bonding between fiber and matrix [101]. The influence of fiber loading and weight ratio on effective elastic modulus of the epoxy and polyester based banana-jute composites are shown in Figures 6.7 and 6.8 respectively. It is clearly visible that with the increase in fiber loading, the elastic modulus of the composites also increases. The increasing trend is practically same for both the epoxy and polyester based composites. Similar observations have also been observed in case of randomly oriented short banana and sisal hybrid composites by Idicula et al. [42]. The polymer specimens exhibit brittle in nature and the banana and jute fibers are flexible in nature and hence reduce the disintegration of matrix i.e. reduces the brittle fracture of the polymer matrix and therefore elastic modulus increases with fiber loading. For epoxy based composites, the maximum elastic modulus is found to be 4.017 GPa, 4.195 GPa, and 3.864 GPa at 40 wt.% of fiber loading with weight ratio of banana and jute fiber as 1:1, 1:3, and 3:1, respectively. The percentage increment in elastic modulus of the composites with weight ratio of banana and jute fiber as 1:1, 1:3 and 3:1 is found to be 27.92%, 33.59%, and 23.05% respectively, over the neat epoxy.

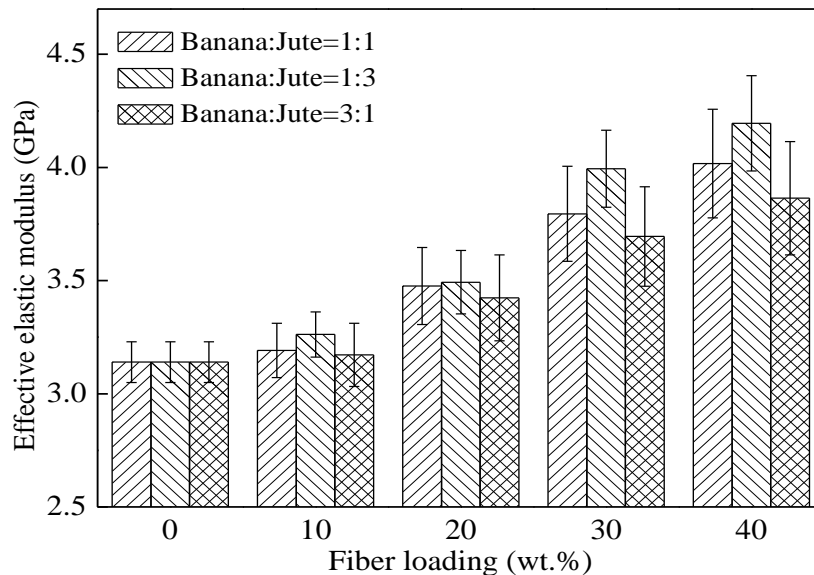


Figure 6.7: Effect of fiber loading and weight ratio on effective elastic modulus of epoxy based hybrid composites

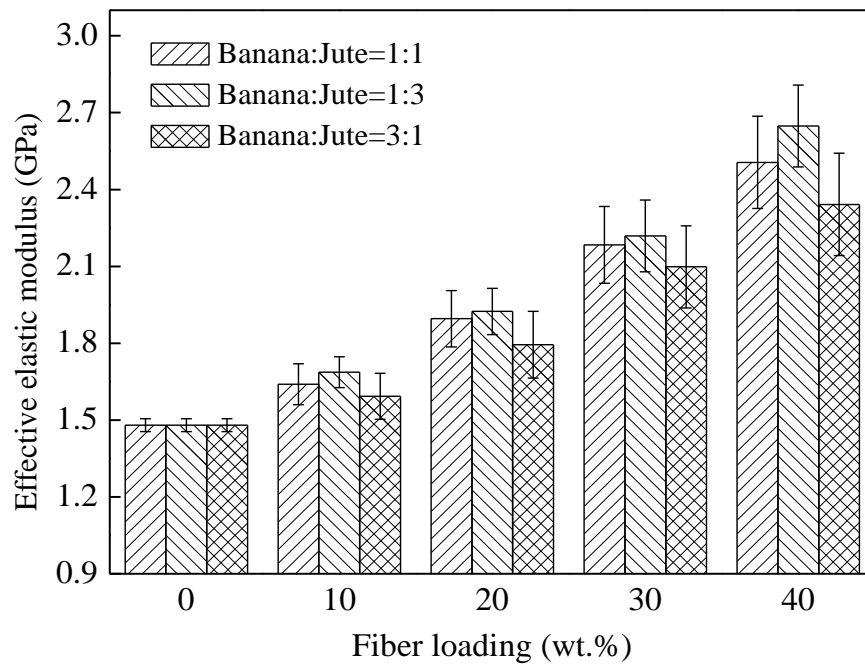


Figure 6.8: Effect of fiber loading and weight ratio on effective elastic modulus of polyester based hybrid composites

Similarly, for polyester based composites, the maximum elastic modulus of the composite is found to be 2.506 GPa, 2.648 GPa, and 2.342 GPa at 40 wt.% of fiber loading with weight ratio of banana and jute fiber as 1:1, 1:3, and 3:1, respectively. The percentage increment in elastic modulus of the composites with weight ratio of banana and jute fiber as 1:1, 1:3 and 3:1 is found to be 69.32%, 78.91%, and 58.24%, respectively, over the neat polyester. The maximum effective elastic modulus is obtained for the hybrid composite with weight ratio of banana and jute fiber as 1:3 at 40 wt.% of fiber loading. Figures 6.9 to 6.11 shows the comparison of experimental results with the analytical and numerical results of epoxy based hybrid composites, whereas the corresponding results for polyester based hybrid composites are shown in Figures 6.12 to 6.14. Similar trend of increase in elastic modulus with the increase in fiber loading is observed for all the analytical and numerical methods. It can also be observed that the analytical and numerical predictions are generally close to the experimental results. The experimental elastic modulus values are more close to the geometric mean model as compared to the other analytical methods. It is also observed that there a marginal difference between the finite element results and experimental values. The finite element results are in good agreement with the Lewis and Nielsen, Halpin–Tsai and geometric mean results as compared to the rule of hybrid mixture. It is observed from all the figures that the rule of hybrid mixture shows the upper bound for the analytical models and

the experimental results. The reason may be due to the fact that the rule of hybrid mixture model assumes that the fibers are oriented and fully strained along their length.

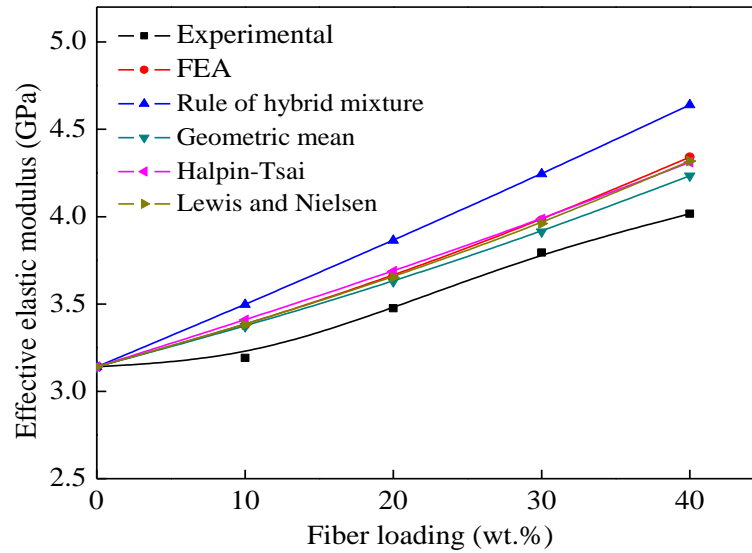


Figure 6.9: Comparison of effective elastic modulus values of epoxy based composites with the weight ratio of banana and jute fiber as 1:1

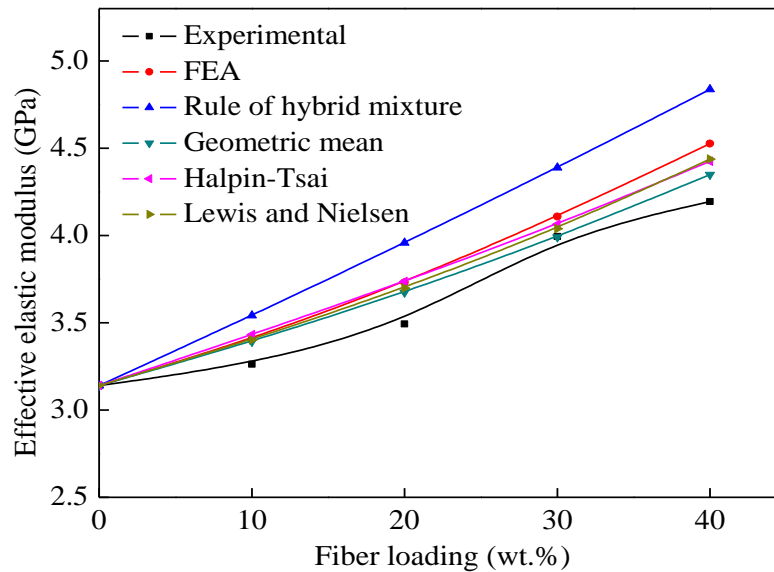


Figure 6.10: Comparison of effective elastic modulus values of epoxy based composites with the weight ratio of banana and jute fiber as 1:3

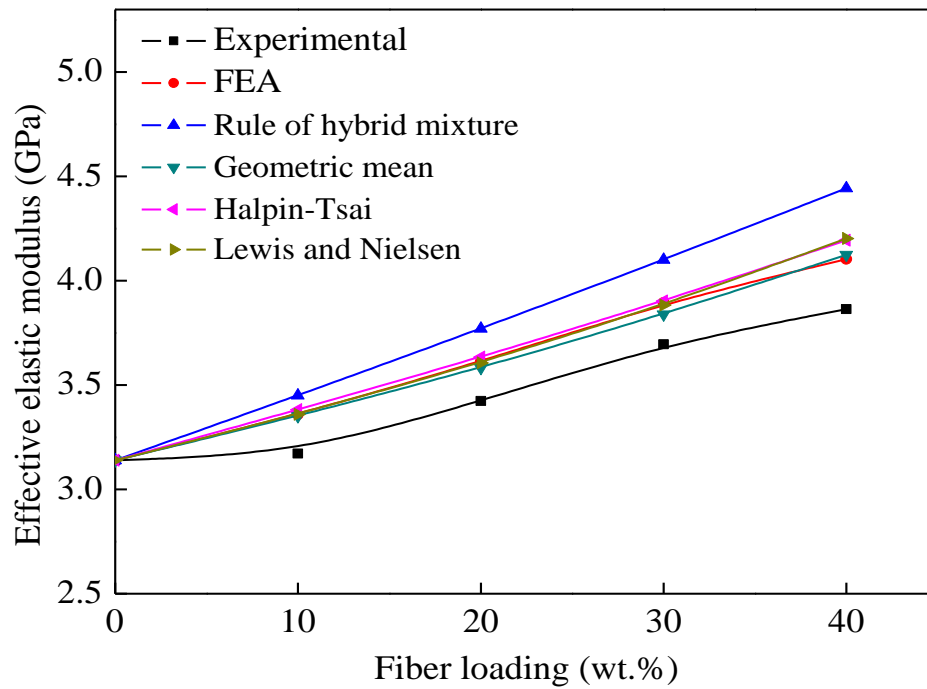


Figure 6.11: Comparison of effective elastic modulus values of epoxy based composites with the weight ratio of banana and jute fiber as 3:1

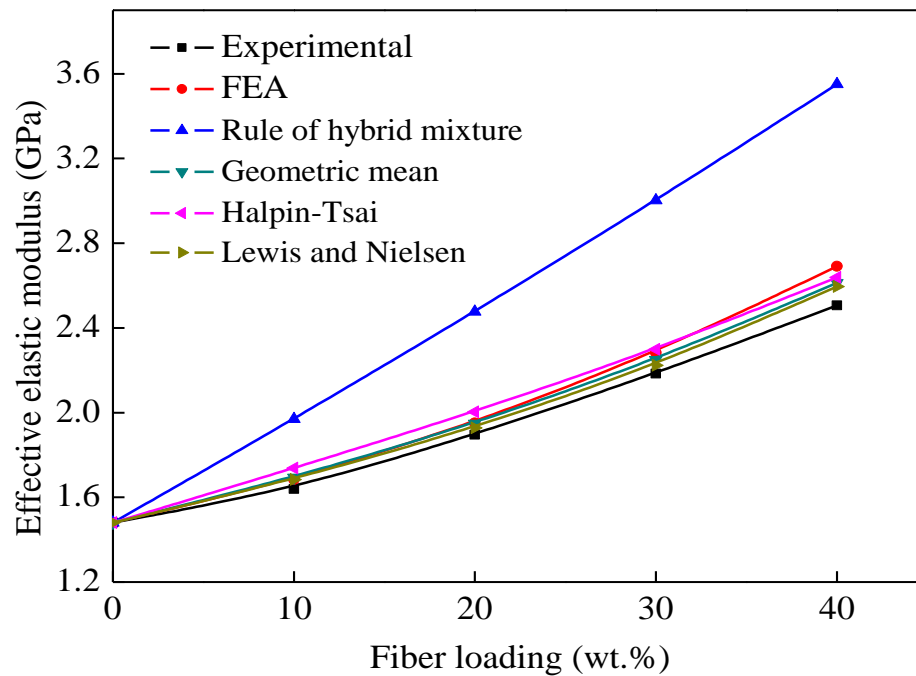


Figure 6.12: Comparison of effective elastic modulus values of polyester based composites with the weight ratio of banana and jute fiber as 1:1

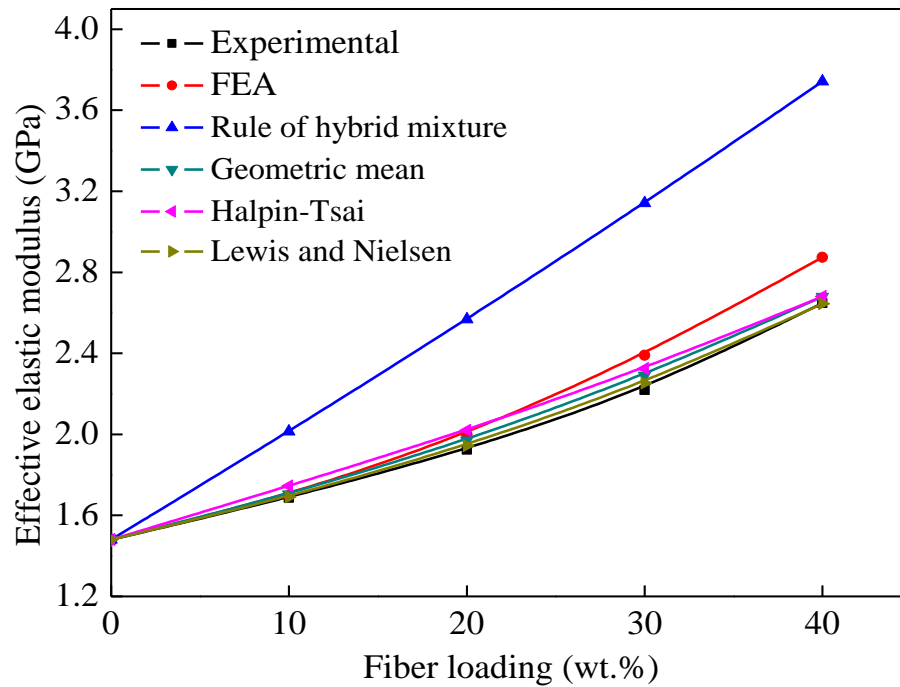


Figure 6.13: Comparison of effective elastic modulus values of polyester based composites with the weight ratio of banana and jute fiber as 1:3

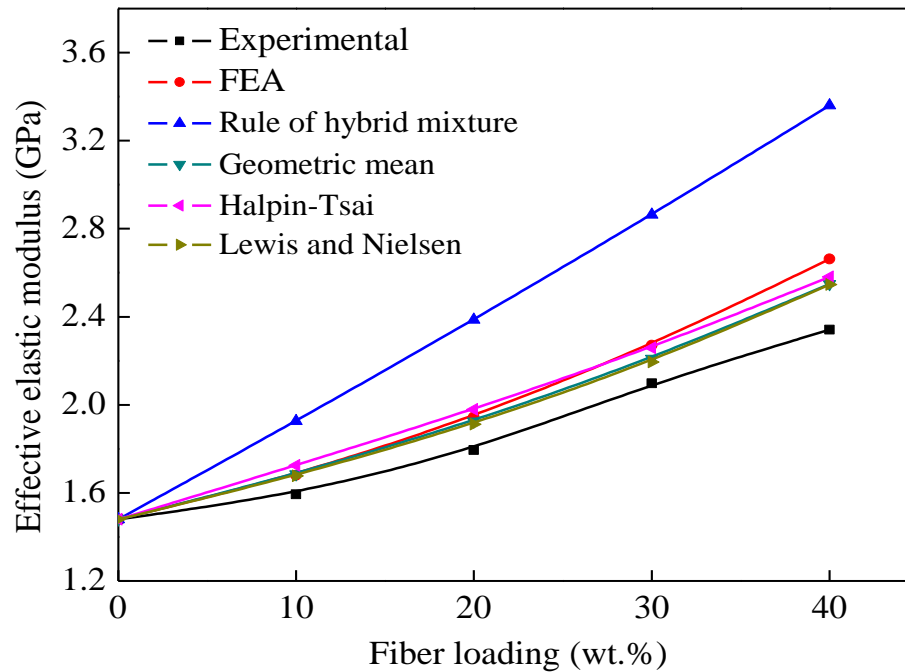


Figure 6.14: Comparison of effective elastic modulus values of polyester based composites with the weight ratio of banana and jute fiber as 3:1

The other analytical and finite element model assumes that there is a perfect interaction between the reinforcement and the matrix. The agreement of the experimental results with these models may be due to the existence of significant bonding between the natural fibers and the polymer matrix, i.e., polar-polar interaction. By comparing the FEA results and the Lewis and Nielsen model, the maximum relative error of 1.98% and 2.46% is observed for epoxy and polyester based composites, respectively. The maximum relative error for Halpin–Tsai model is found to be 2.26% and 6.71% for epoxy and polyester based composites, respectively. Similarly, the maximum relative error for the geometric mean model is found to be 3.95% and 6.81% for epoxy and polyester based composites, respectively.

6.1.2.2 Shear Modulus of Composites

The effect of fiber loading on the shear modulus of short banana-jute fiber reinforced epoxy based hybrid composites are shown in Figures 6.15 to 6.17. Whereas, the comparison results for polyester based composites are shown in Figures 6.18 to 6.20. It is observed from the figures that with the increase in fiber loading, shear modulus of the composites increases for both the epoxy and polyester based composites. The shear modulus values predicted by the FEA are in good agreement with those by the analytical models. At low fiber loading, the finite element result is very close to the analytical methods. With increasing fiber loading the finite element results are deviates from the analytical results. This can be explained by the growing influence of the fibers on the behaviour of the composite. At low fiber loading, the fibers are almost rigid and the composite shear modulus is mainly controlled by the stiffness of the matrix, whereas at high fiber loading, the deformation within the fibers starts to have an effect [210]. Compared to all the analytical models, rule of hybrid mixture and Halpin–Tsai model presents the lower bound of the shear modulus, whereas these models show a clear difference with the FEA results. By comparing the FEA results and the rule of hybrid mixture model, the maximum relative error are found to be 14.22% and 35.44% for epoxy and polyester hybrid composites, respectively, whereas the maximum relative error for Halpin–Tsai model are found to be 14.21% and 29.28% for epoxy and polyester hybrid composites, respectively. The FEA results are close to the predicted values obtained using the Lewis and Nielsen model and within the maximum relative error of 4.36% and 16.68% for epoxy and polyester based hybrid composites, respectively. From these observations, it is suggested that the Lewis and Nielsen model is more suitable to predict shear modulus of natural fiber reinforced hybrid composites than the other analytical predictions.

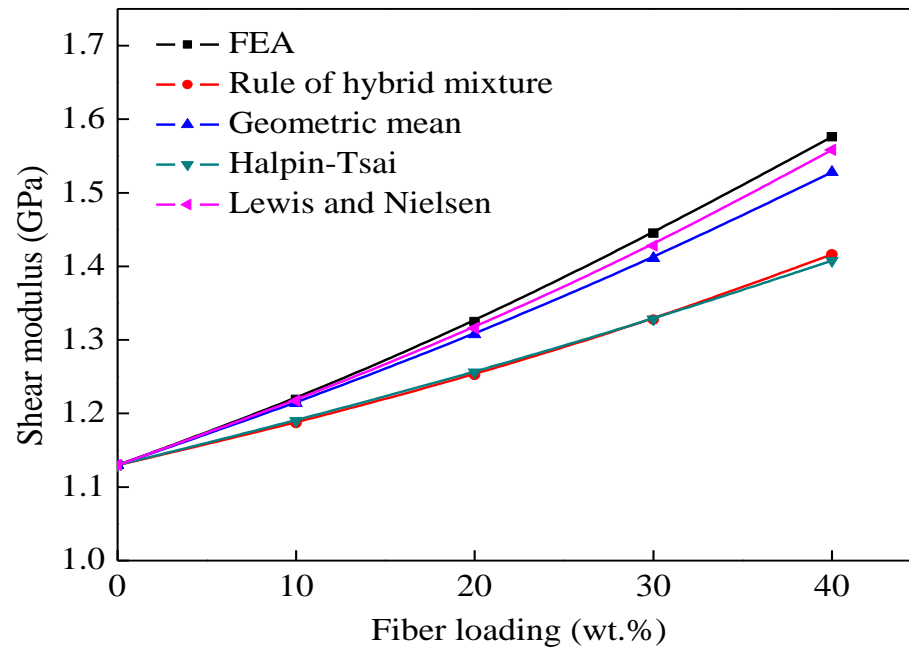


Figure 6.15: Comparison of shear modulus values of epoxy based composites with the weight ratio of banana and jute fiber as 1:1

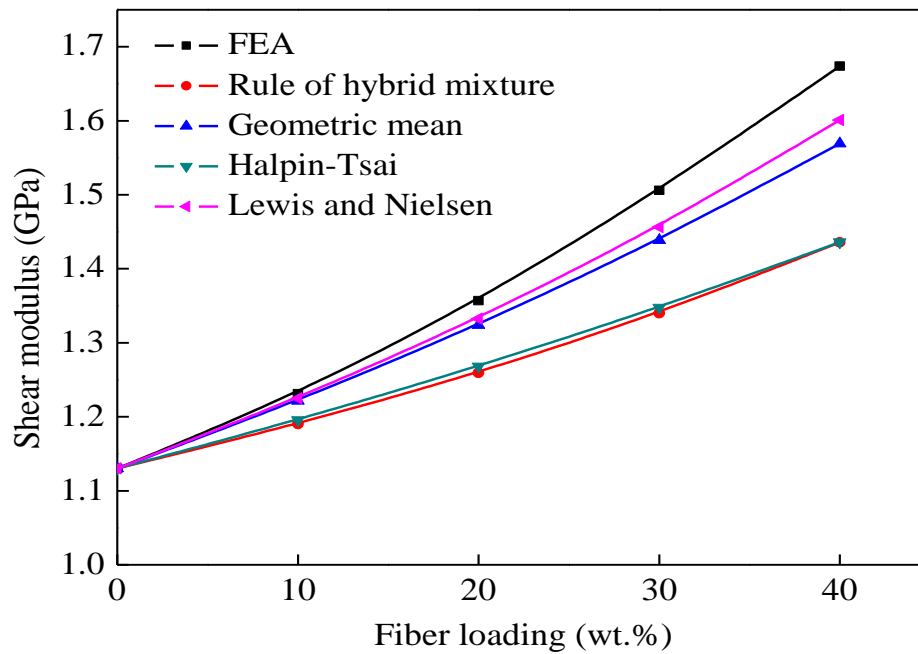


Figure 6.16: Comparison of shear modulus values of epoxy based composites with the weight ratio of banana and jute fiber as 1:3

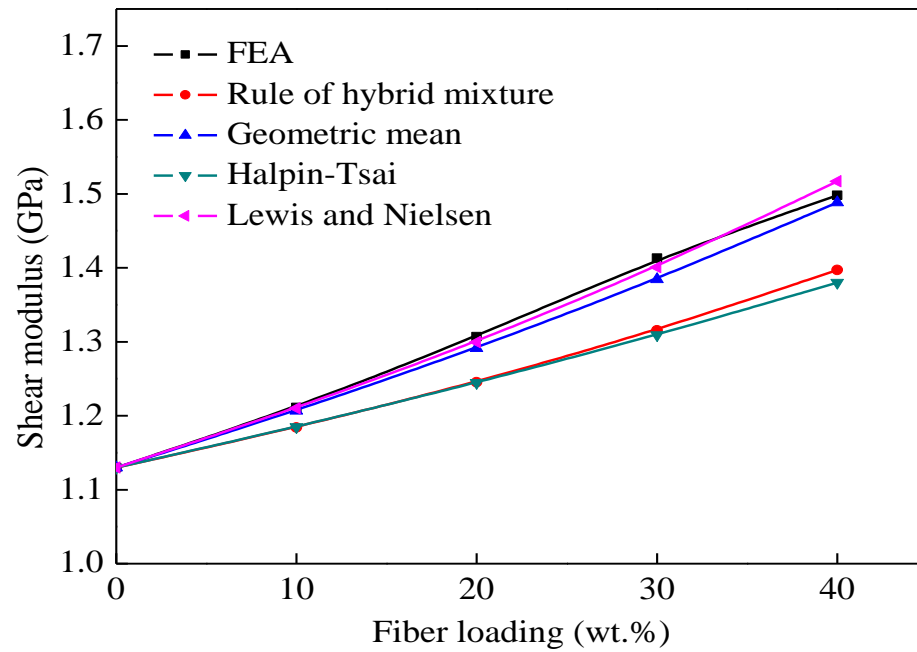


Figure 6.17: Comparison of shear modulus values of epoxy based composites with the weight ratio of banana and jute fiber as 3:1

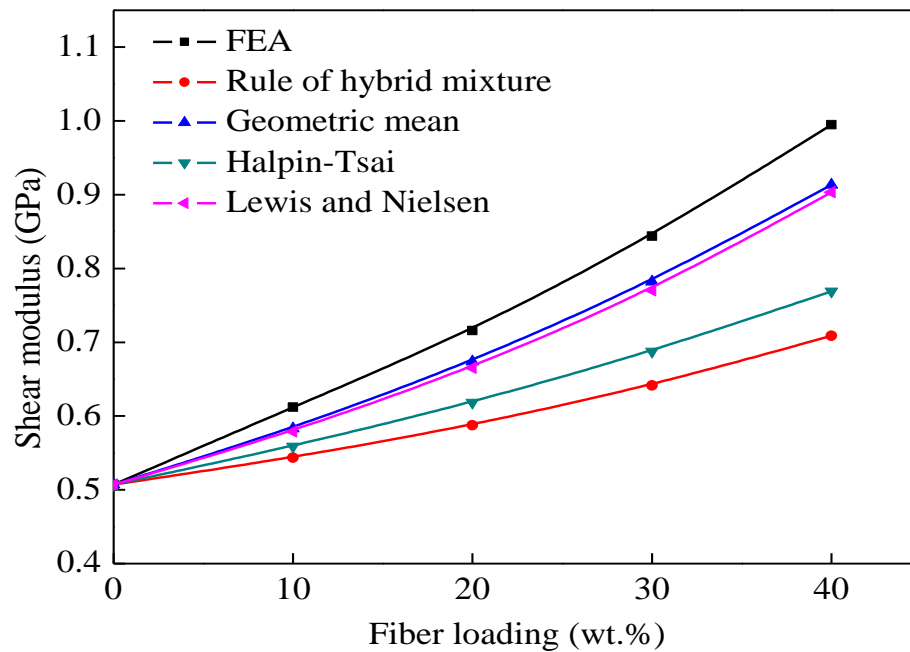


Figure 6.18: Comparison of shear modulus values of polyester based composites with the weight ratio of banana and jute fiber as 1:1

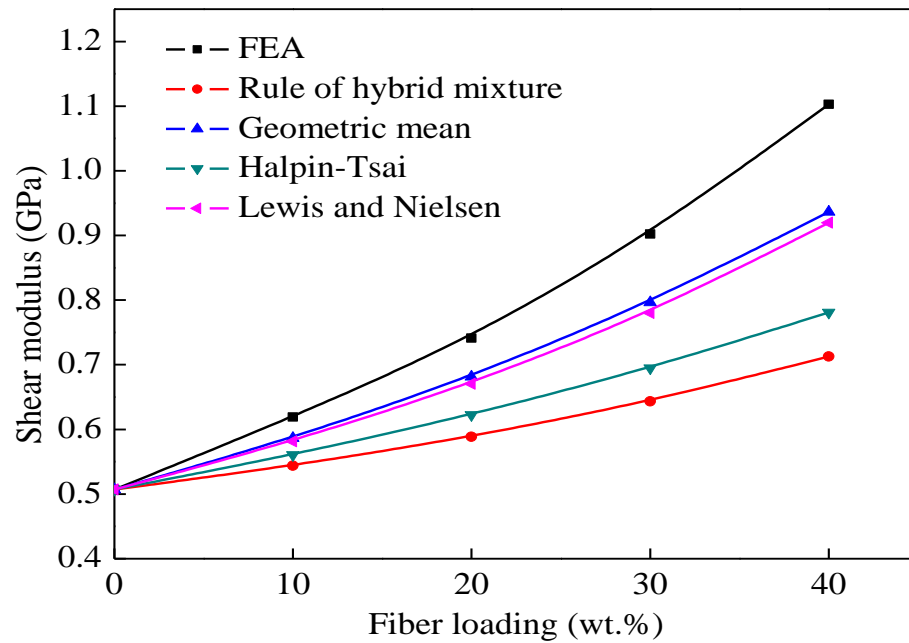


Figure 6.19: Comparison of shear modulus values of polyester based composites with the weight ratio of banana and jute fiber as 1:3

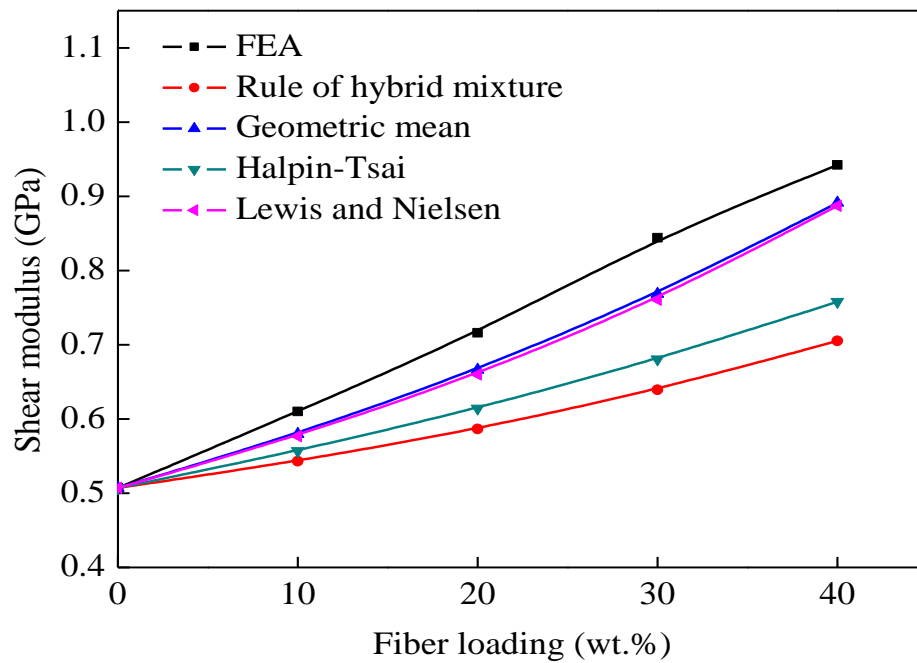


Figure 6.20: Comparison of shear modulus values of polyester based composites with the weight ratio of banana and jute fiber as 3:1

6.1.3 Thermal Conductivity of Short Fiber Reinforced Hybrid Composites

The effective thermal conductivity of epoxy and polyester based composites reinforced with short banana and jute fibers are evaluated theoretically, numerically and experimentally. In addition, the interpretation and comparison of thermal conductivity obtained from different methods for hybrid composites with different fiber loading and weight ratio are also presented.

6.1.3.1 Effect of Temperature on Thermal Conductivity of Composites

The effective thermal conductivity of short banana-jute fiber reinforced epoxy based hybrid composites as a function of temperature is shown in Figure 6.21, whereas polyester based composites is shown in Figure 6.22. It is observed from the figures that the thermal conductivity of all the composites increases with the increase in temperature due to the evaporation of moisture in the fibers [162]. The results show that the thermal conductivity of the epoxy based composites are higher than that of the polyester based composites due to the higher thermal conductivity of epoxy resin.

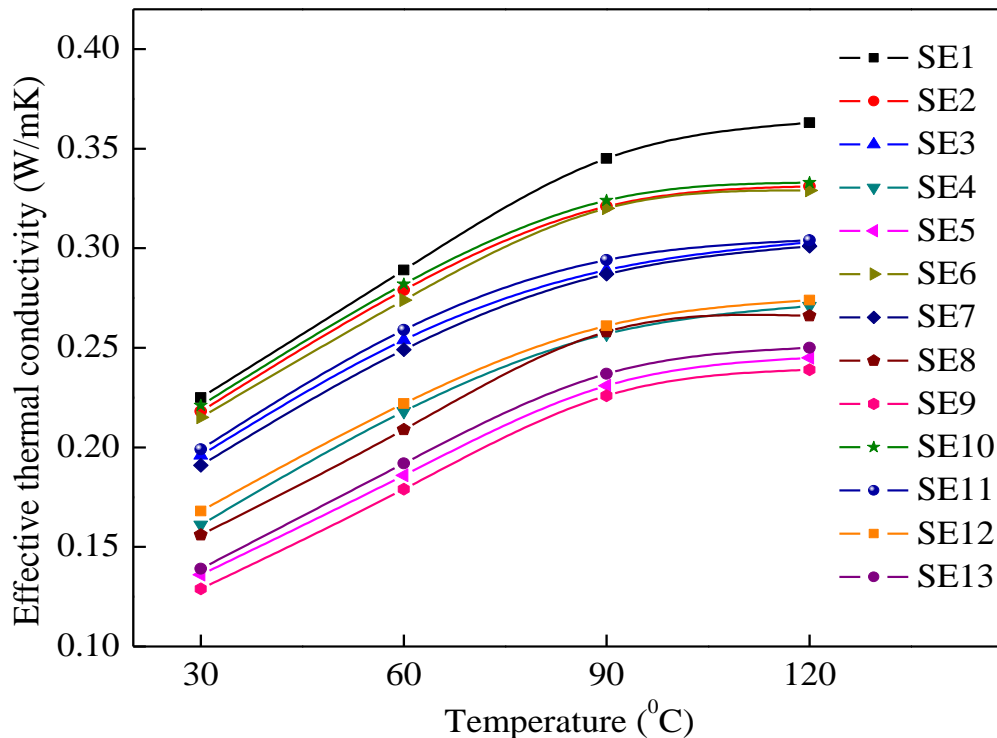


Figure 6.21: Effect of temperature on effective thermal conductivity of epoxy based hybrid composites

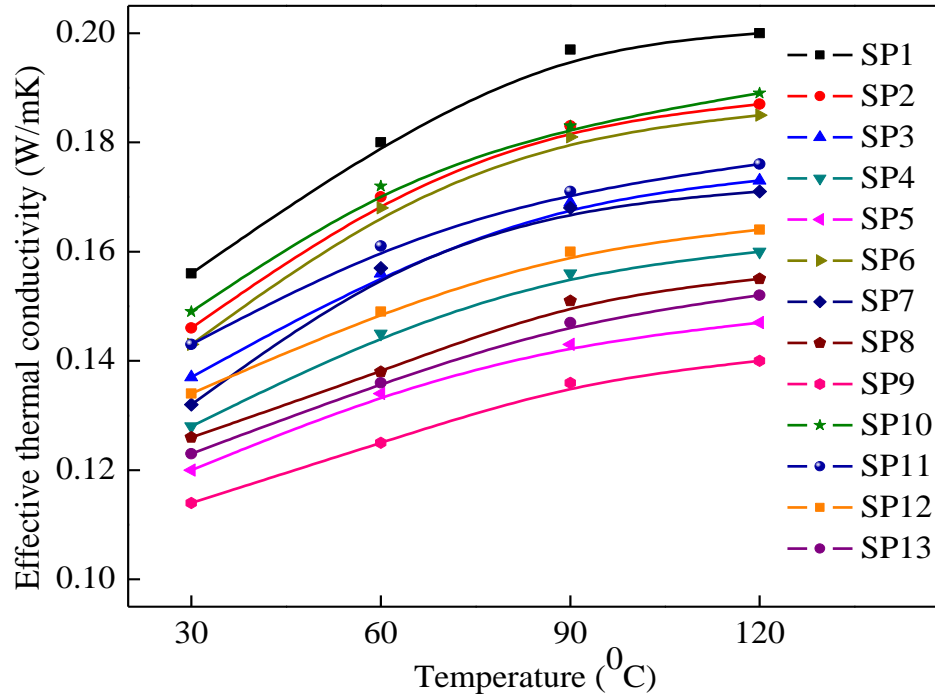


Figure 6.22: Effect of temperature on effective thermal conductivity of polyester based hybrid composites

6.1.3.2 Effective Thermal Conductivity of Composites

Determination of effective thermal conductivity by using proposed theoretical model:

In this study, a micromechanical model has been developed to study the effective thermal conductivity of the short fiber reinforced hybrid composites. Effective thermal conductivity values of the hybrid composites have also been estimated theoretically by using the correlation given in equation (3.47) derived on the basis of the one-dimensional heat conduction model proposed in this work. The details of model development have already been described in Chapter 3. The proposed correlation for the present analysis is written as follows:

$$k_{\text{eff}} = \left[\left(\frac{1}{2k_m} - \frac{1}{k_m \left(\frac{\pi}{4\Phi_{fb}} \right)^{\frac{1}{3}}} + \frac{\left(\frac{16\pi}{\Phi_{fb}} \right)^{\frac{1}{3}}}{k_m \left(\frac{2\pi}{\Phi_{fb}} \right)^{\frac{2}{3}} + \pi(k_{fb} - k_m)} \right) + \left(\frac{1}{2k_m} - \frac{1}{k_m \left(\frac{\pi}{4\Phi_{fj}} \right)^{\frac{1}{3}}} + \frac{\left(\frac{16\pi}{\Phi_{fj}} \right)^{\frac{1}{3}}}{k_m \left(\frac{2\pi}{\Phi_{fj}} \right)^{\frac{2}{3}} + \pi(k_{fj} - k_m)} \right) \right]^{-1} \quad (6.4)$$

Where, k_{fb} , k_{fj} and k_m are the respective heat conductivities of the banana fiber, jute fiber and matrix material, Φ_{fb} , Φ_{fj} and Φ_m are the respective volume fraction of the banana fiber, jute fiber and matrix material. The effective thermal conductivity of epoxy based composites reinforced with short banana and jute fibers with fiber loading ranging from 0 to 40 wt.% is shown in Figure 6.23, whereas for polyester based composites is shown in Figure 6.24. It is observed from the figures that the effective thermal conductivity of composites decrease with the increase in fiber loading. This behaviour of the effective thermal conductivity of the fiber reinforced polymer hybrid composites seems to be justified because the low thermal conductivity of fibers than the polymer matrix. Therefore, the effective thermal conductivity of hybrid composites is less as compared to the thermal conductivity of neat polymer matrix. The reduction in thermal conductivity is also due to the addition of more air-filled lumen fibers which create resistance to heat flow, as the composite filled with air acted as scattering points for phonons [294].

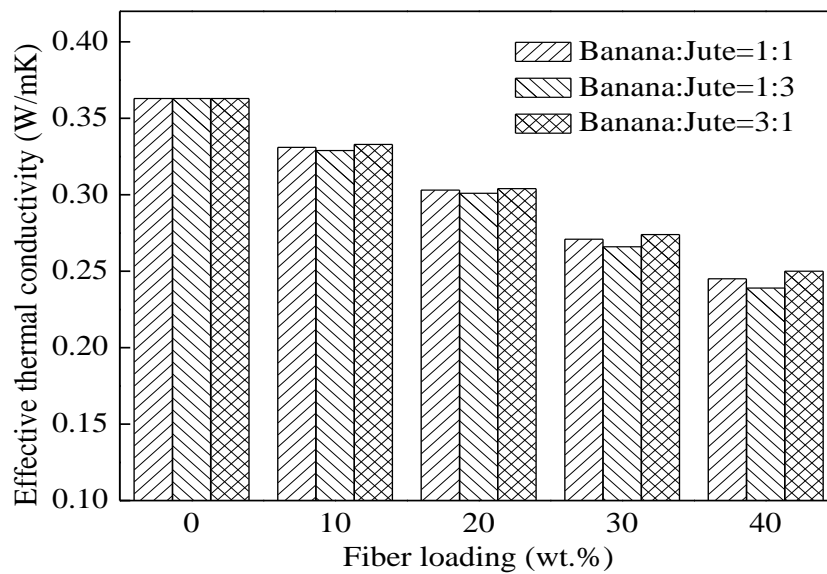


Figure 6.23: Effect of fiber loading and weight ratio on effective thermal conductivity of epoxy based hybrid composites

For epoxy based composites with 40 wt.% of fiber loading and weight ratio of banana and jute fiber as 1:1, 1:3, and 3:1 exhibits effective thermal conductivity values of 0.245 W/m-K, 0.239 W/m-K and 0.250 W/m-K, respectively. The thermal conductivity of the composites with weight ratio of banana and jute fiber as 1:1, 1:3 and 3:1 is decreased by 32.50%, 34.15% and 31.12%, respectively at the maximum fiber content over the neat epoxy. Similarly, in polyester based composites at 40 wt.% of fiber loading, the hybrid composites

show the effective thermal conductivity values of 0.147 W/m-K, 0.140 W/m-K and 0.152 W/m-K, with weight ratio of banana and jute fiber as 1:1, 1:3, and 3:1, respectively. The thermal conductivity values are found to be decreased by 26.5%, 30%, and 24% with the weight ratio of banana and jute fiber as 1:1, 1:3 and 3:1, respectively as compared to the neat polyester. It is observed from the figures that the hybrid composites with weight ratio of banana and jute fiber as 1:3 shows minimum thermal conductivity followed by composites with weight ratio of 1:1 and 3:1.

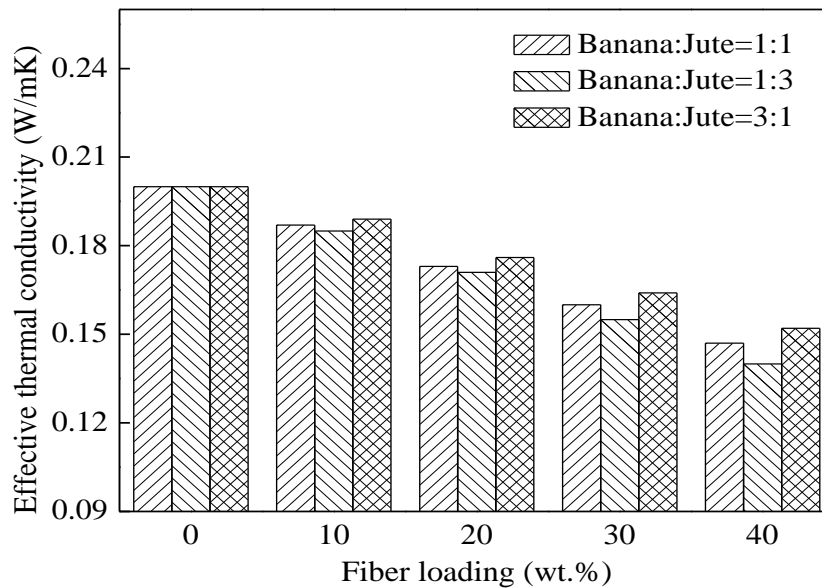


Figure 6.24: Effect of fiber loading and weight ratio on effective thermal conductivity of polyester based hybrid composites

The comparison of experimental results with the results obtained using analytical, numerical and proposed theoretical model are shown in Figures 6.25 to 6.27. The corresponding results for polyester based composites are shown in Figure 6.28 to 6.30. It is observed from the figures that the results obtained from the experimental and proposed model are in good agreement with the rule of hybrid mixture model as compared to other analytical methods. The experimentally measured values are less than the values obtained from proposed micromechanical model and finite element results for each sample. It is because, some actual factors are not considered while developing the micromechanical model, such as void content and thermal resistance between fiber and matrix material. The volume fraction of voids present in the hybrid composite material is a very important factor which affects its effective thermal conductivity. In experimental work, hybrid fibers arrangement is not a regular periodic array as assumed but very much randomly distributed in

the matrix. With increasing the fiber loading, this randomness causes some fibers to be in contact with other fibers and hence causes a higher thermal resistance and a lower thermal conductivity for the hybrid composite.

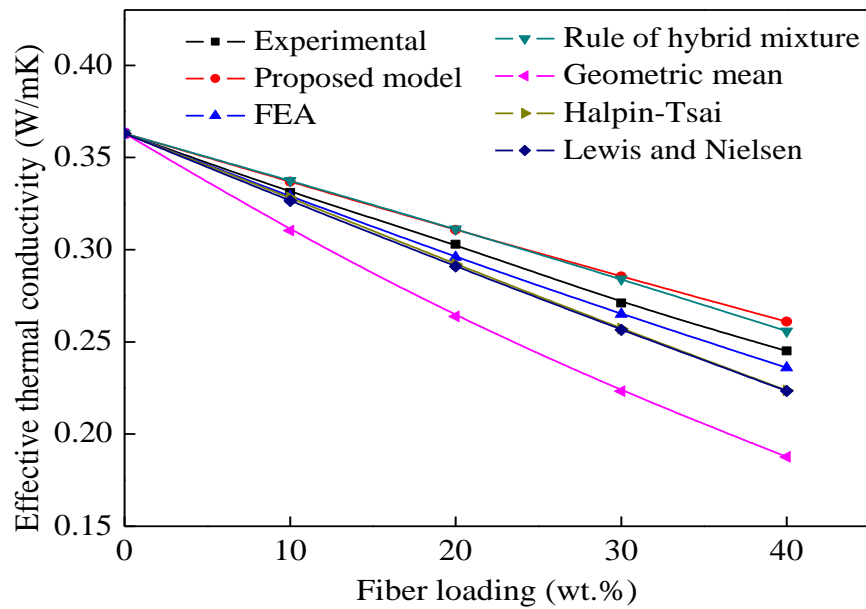


Figure 6.25: Comparison of effective thermal conductivity values of epoxy based composites with the weight ratio of banana and jute fiber as 1:1

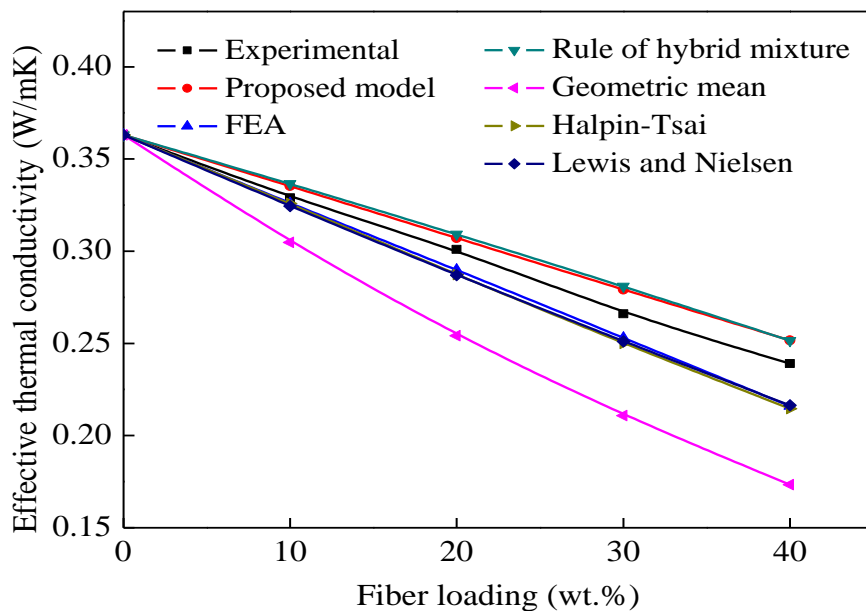


Figure 6.26: Comparison of effective thermal conductivity values of epoxy based composites with the weight ratio of banana and jute fiber as 1:3

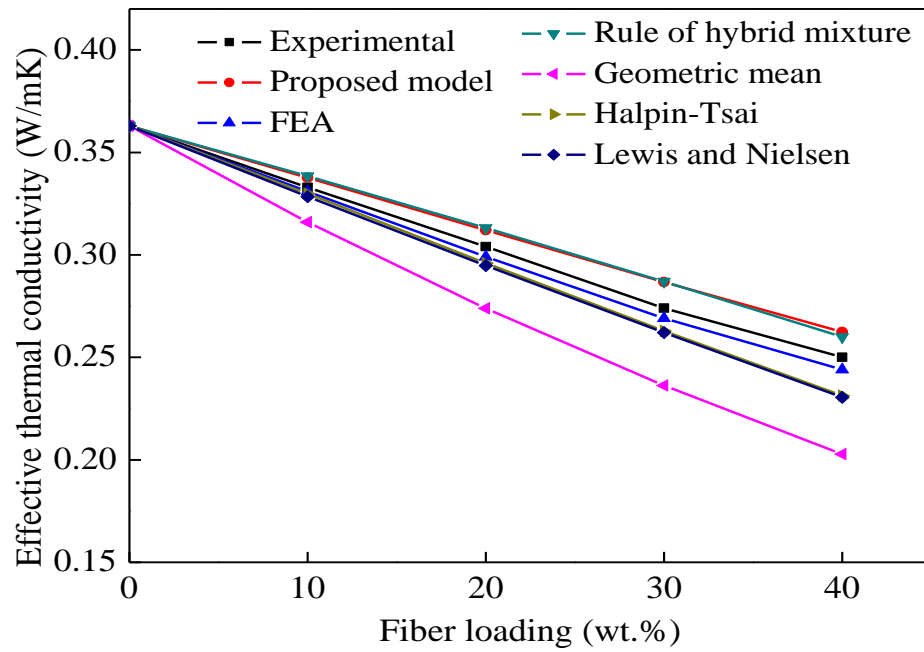


Figure 6.27: Comparison of effective thermal conductivity values of epoxy based composites with the weight ratio of banana and jute fiber as 3:1

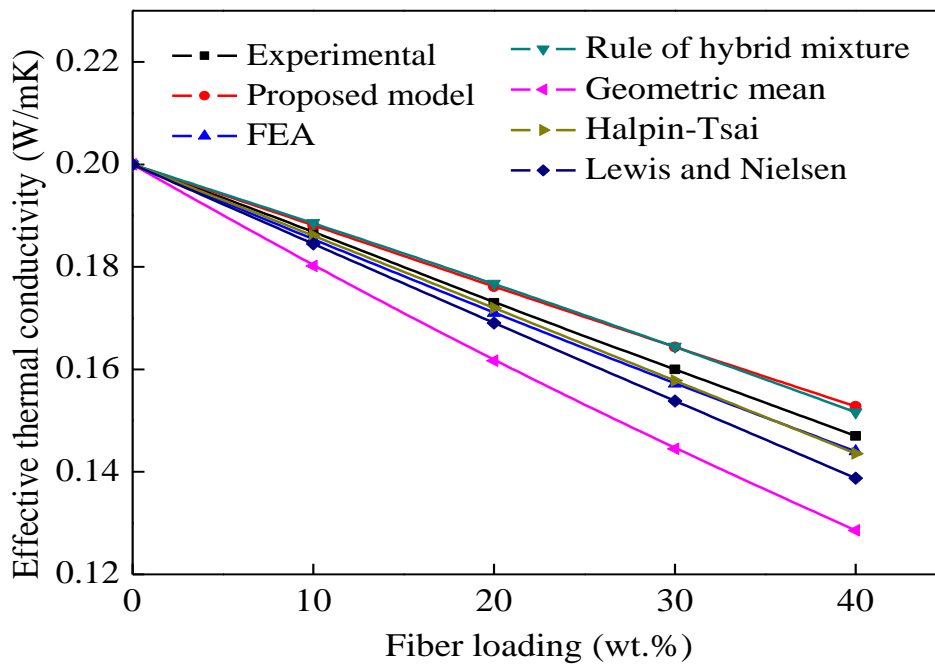


Figure 6.28: Comparison of effective thermal conductivity values of polyester based composites with the weight ratio of banana and jute fiber as 1:1

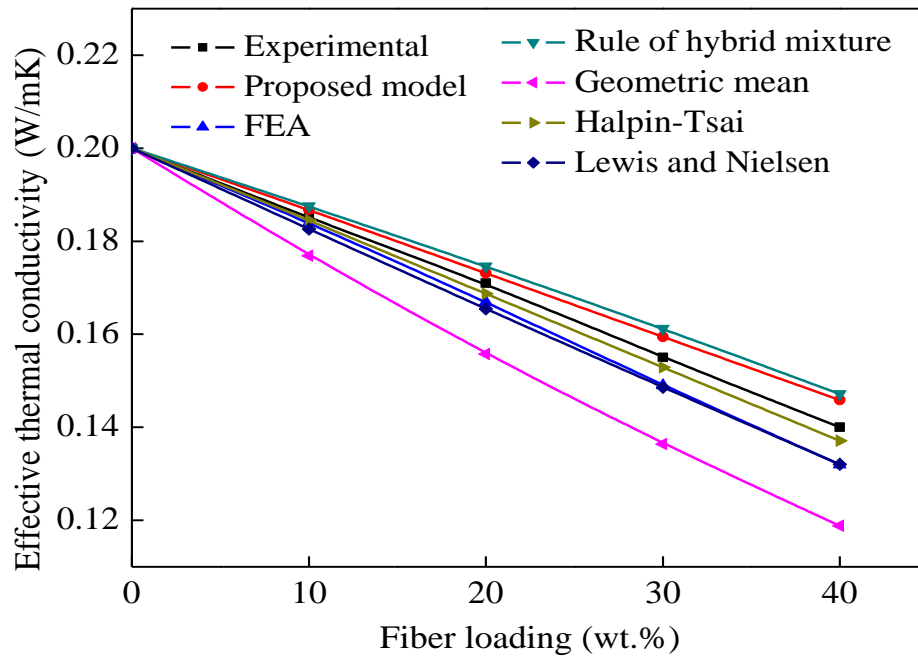


Figure 6.29: Comparison of effective thermal conductivity values of polyester based composites with the weight ratio of banana and jute fiber as 1:3

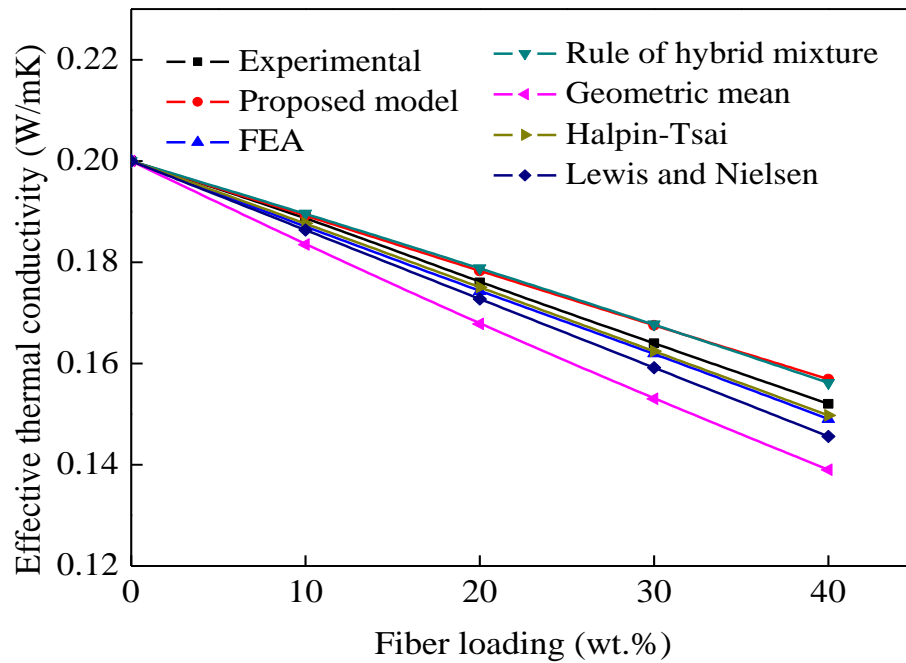


Figure 6.30: Comparison of effective thermal conductivity values of polyester based composites with the weight ratio of banana and jute fiber as 3:1

Tables 6.1 and 6.2 presents the percentage errors associated with the effective thermal conductivity values of epoxy and polyester based composites obtained from different models/correlations with respect to the corresponding experimental results. It can be observed from the results that there is a good agreement between the experimental results and the analytical methods except geometric mean model. From the Table 6.1, it is also clear that the percentage error for the proposed model and FEA results with the experimental values of the epoxy based composites are 0-6.2% and 0-11%, respectively, whereas the polyester based composites are 0-3.9% and 0-6.1%, respectively as shown in Table 6.2. The reason for this marginal deviation is because of the assumptions taken while deriving the correlation.

Table 6.1: Percentage errors associated with the effective thermal conductivity values of epoxy based composites obtained from different models

Composite	Experimental value (W/m-K)	Percentage errors					
		Proposed model	FEA	Rule of hybrid mixture	Geometric mean	Halpin -Tsai	Lewis and Nielsen
SE1	0.363	0	0	0	0	0	0
SE2	0.331	1.751	0.607	1.933	6.672	0.663	1.403
SE3	0.303	3.153	1.689	3.274	14.082	1.803	3.483
SE4	0.271	5.045	2.264	4.588	21.411	2.809	5.622
SE5	0.245	6.13	3.813	4.207	30.636	5.476	9.685
SE6	0.329	1.908	0.920	2.254	7.973	0.598	1.419
SE7	0.301	1.986	3.793	2.665	18.414	3.001	4.877
SE8	0.266	4.693	5.138	5.336	26.193	2.858	5.953
SE9	0.239	5.007	10.648	4.985	37.829	5.829	10.460
SE10	0.333	1.362	0.604	1.613	5.385	0.726	1.385
SE11	0.304	2.564	1.672	2.916	11.017	1.631	3.135
SE12	0.274	4.463	1.858	4.547	15.955	2.007	4.521
SE13	0.25	4.689	2.459	3.828	23.314	4.705	8.480

Table 6.2: Percentage errors associated with the effective thermal conductivity values of polyester based composites obtained from different models

Composite	Experimental value (W/m-K)	Percentage errors					
		Proposed model	FEA	Rule of hybrid mixture	Geometric mean	Halpin -Tsai	Lewis and Nielsen
SP1	0.2	0	0	0	0	0	0
SP2	0.187	0.602	0.887	0.834	3.797	0.888	1.368
SP3	0.173	1.788	1.169	2.109	7.014	1.226	2.335
SP4	0.160	2.658	1.774	2.718	10.747	2.114	4.009
SP5	0.147	3.803	2.083	3.080	14.346	3.102	5.948
SP6	0.185	0.953	0.543	1.354	4.585	0.726	1.309
SP7	0.171	1.219	2.395	2.061	9.818	2.018	3.360
SP8	0.155	2.789	4.026	3.840	13.649	2.045	4.296
SP9	0.140	4.014	6.060	4.867	17.821	2.676	6.016
SP10	0.189	0.110	1.069	0.320	3.007	1.042	1.419
SP11	0.176	1.281	0.975	1.593	4.875	1.021	1.905
SP12	0.164	2.089	1.234	2.227	7.190	1.521	3.046
SP13	0.152	3.102	2.013	2.658	9.338	2.075	4.384

6.2 Physical, Mechanical and Thermal Behaviour of Short Fiber Reinforced Composites

This part of the chapter presents the measured values of physical, mechanical and thermal properties of the epoxy and polyester based short fiber reinforced hybrid composites. The relative effects of fiber loading and different weight ratio of fiber on composite properties have also been discussed.

6.2.1 Physical Properties

6.2.1.1 Density and Void Content

The theoretical density and measured densities along with the corresponding void content of the short banana-jute reinforced epoxy and polyester based composites are presented in Tables 6.3 and 6.4, respectively. It can be seen that the void content in the epoxy and polyester based composites increases with the increase in fiber loading. Natural fibers generally contain large amounts of the hydroxyl group, which makes them polar and hydrophilic in nature. However, most plastics are hydrophobic in nature. This polar nature also results in high moisture sorption in natural fiber based composites, leading to fiber swelling and voids in the fiber-matrix interface [295]. From the Tables 6.3 and 6.4, it is found that pure epoxy and polyester resins has the minimum void content as compared to the respective fiber reinforced composites. It is observed that with the addition of 40 wt.% fiber loading in epoxy resin, the void content increases to 5.935%, 5.592% and 6.199% for composites with weight ratio of banana and jute fiber as 1:1, 1:3, and 3:1, respectively. Similarly, for polyester based composites, the void content increases to 6.945%, 6.755% and 7.047% for composites with weight ratio of banana and jute fiber as 1:1, 1:3, and 3:1, respectively. Void content in polymer composites is mainly attributed to the several processing effects such as residual solvents, volatiles arising during curing of the resin, entrapped air bubbles within the matrix and moisture absorption during the material processing [130]. As the fiber loading increases, the processing may be difficult due to the fiber agglomeration leading to void formation inside the composite. Shrinkage during curing of the matrix and the rate of cooling also play an important role in void formation. A higher void content in the hybrid composites shows that matrix has not thoroughly surrounded the reinforcement and resulting in weaker interfacial strength which in turn reduces the stiffness, strength and resistance to environmental degradation of hybrid composites [296].

Table 6.3: Theoretical and measured densities of the epoxy based composites

Weight ratio of banana and jute fiber	Composite	Theoretical density (g/cm ³)	Measured density (g/cm ³)	Void content (%)
	SE1	1.150	1.146	0.348
1:1	SE2	1.169	1.149	1.711
	SE3	1.189	1.152	3.112
	SE4	1.209	1.155	4.467
	SE5	1.230	1.157	5.935
1:3	SE6	1.170	1.155	1.282
	SE7	1.191	1.159	2.687
	SE8	1.212	1.163	4.043
	SE9	1.234	1.165	5.592
3:1	SE10	1.168	1.147	1.797
	SE11	1.187	1.148	3.285
	SE12	1.206	1.149	4.726
	SE13	1.226	1.150	6.199

Table 6.4: Theoretical and measured densities of the polyester based composites

Weight ratio of banana and jute fiber	Composite	Theoretical density (g/cm ³)	Measured density (g/cm ³)	Void content (%)
	SP1	1.100	1.095	0.454
1:1	SP2	1.122	1.105	1.515
	SP3	1.145	1.111	3.144
	SP4	1.170	1.112	5.042
	SP5	1.195	1.110	6.945
1:3	SP6	1.123	1.107	1.424
	SP7	1.147	1.114	2.877
	SP8	1.172	1.117	4.692
	SP9	1.199	1.118	6.755
3:1	SP10	1.121	1.102	1.695
	SP11	1.144	1.107	3.41
	SP12	1.167	1.108	5.141
	SP13	1.192	1.105	7.047

6.2.1.2 Water Absorption

Figures 6.31 and 6.32 shows the variation of water absorption of short fiber reinforced epoxy and polyester based composites with the immersion time. It is observed from the figures that the water absorption percentage of hybrid composites increases with increase in the fiber loading. The reason may be due to the hydrophilic nature of natural fibers. It has been reported that the water uptake in natural lignocellulosic fibers greatly depends on their physical, chemical, and morphology structures [297]. As the fiber loading increases the cellulose fibers have a lumen, which allows absorption of more water via the capillary effect [298]. It is also observed from the figure that the water absorption rate increases with the immersion time, reaching a certain value at a saturation point where no more water is absorbed. The maximum water absorption content of 0.48% for neat epoxy and 0.59% for neat polyester is observed. However, the composites with 40 wt.% of fiber loading shows the maximum water absorption content of 12.14%, 11.51% and 12.61% with corresponding weight ratio of banana and jute fiber as 1:1, 1:3, and 3:1, respectively.

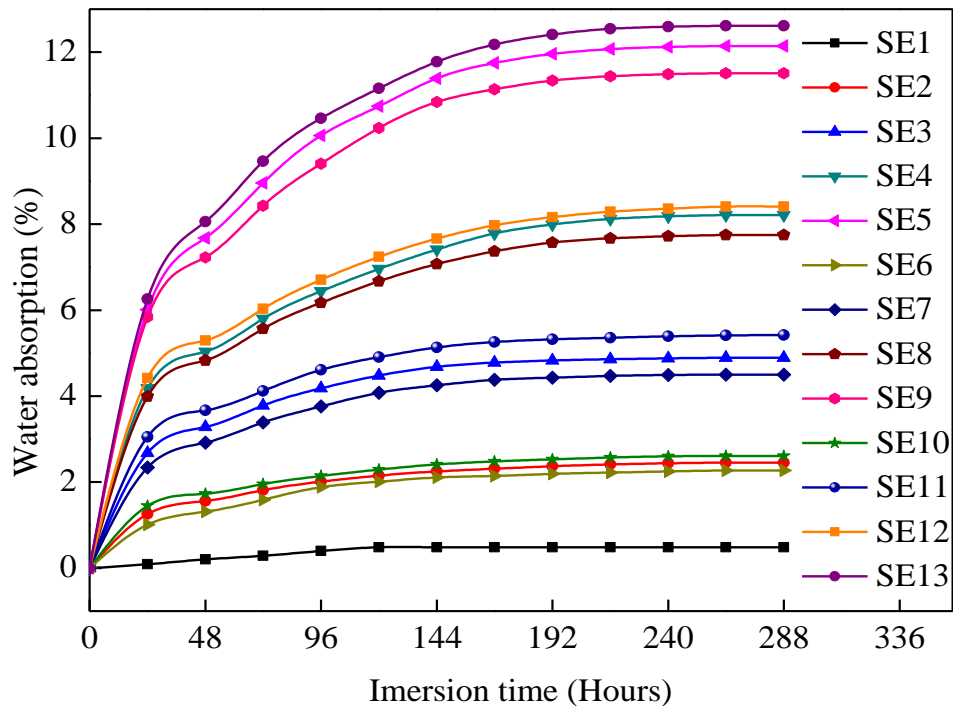


Figure 6.31: Variation of water absorption of short fiber reinforced epoxy composites with immersion time

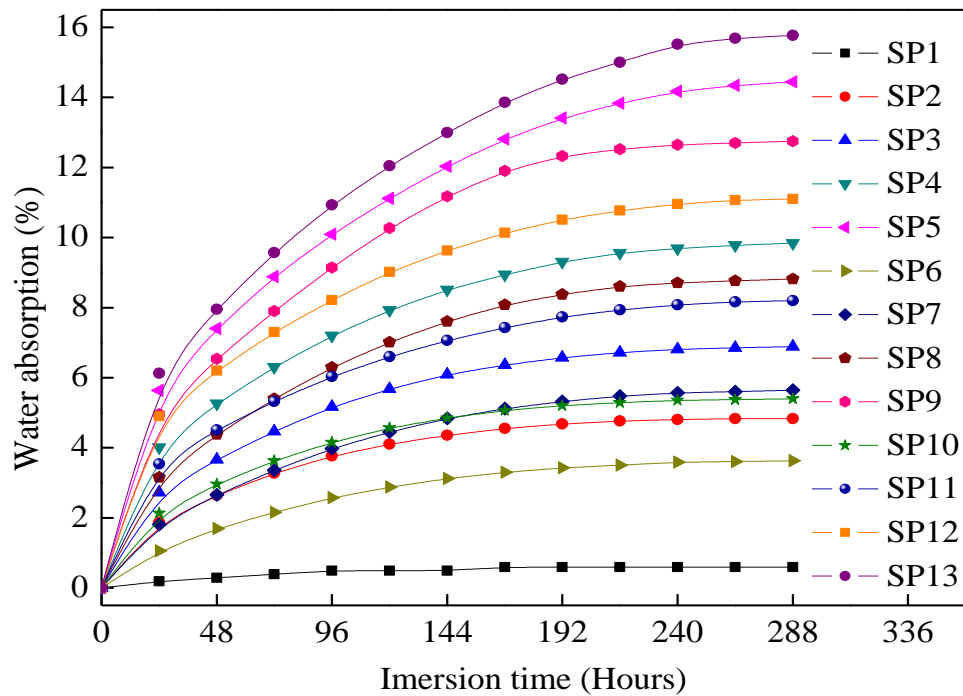


Figure 6.32: Variation of water absorption of short fiber reinforced polyester composites with immersion time

Similarly, for polyester based composites at 40 wt.% of fiber loading, the maximum water absorption content is found to be 14.44%, 12.75% and 15.76% with corresponding weight ratio of banana and jute fiber as 1:1, 1:3, and 3:1, respectively. For the composites at 40 wt.% fiber loading and the weight ratio of banana and jute fiber as 3:1 shows more water absorption as compared to the other two types. The result of water absorption however is in good agreement with the previous work reported by Dhakal et al. [299] on hemp fiber reinforced unsaturated polyester composites.

6.2.1.3 Transport Coefficients in Water Absorption

The values of the parameters n and k resulting from the fitting are presented in Table 6.5 for all the composite samples. The water absorption in banana-jute fiber reinforced composites approaches towards the Fickian diffusion case, as the values of n are very similar for all the composite samples and they are very close to the value of 0.5. This confirms that the Fickian diffusion can be used to adequately describe water absorption in the hybrid composites. The maximum water uptake (M_m), diffusion coefficient (D), sorption coefficient (S) and permeability coefficient (P) values of the short fiber reinforced epoxy and polyester based hybrid composites are given in Tables 6.6 and 6.7.

Table 6.5: The dependence of moisture sorption constant n and k for all formulations

Short fiber reinforced epoxy composites			Short fiber reinforced polyester composites		
Composite	n	k (g/g min ²)	Composite	n	k (g/g min ²)
SE1	0.914	5.206	SP1	1.082	6.200
SE2	0.323	1.887	SP2	0.465	2.701
SE3	0.311	1.801	SP3	0.448	2.617
SE4	0.325	1.906	SP4	0.421	2.471
SE5	0.353	2.049	SP5	0.426	2.517
SE6	0.414	2.398	SP6	0.588	3.423
SE7	0.334	1.938	SP7	0.543	3.172
SE8	0.324	1.898	SP8	0.491	2.872
SE9	0.344	1.998	SP9	0.459	2.685
SE10	0.283	1.66	SP10	0.454	2.638
SE11	0.291	1.692	SP11	0.389	2.295
SE12	0.311	1.826	SP12	0.38	2.24
SE13	0.348	2.021	SP13	0.426	2.521

Table 6.6: Values of maximum water uptake, diffusion coefficient, sorption coefficient, and permeability coefficient for short fiber reinforced epoxy composites

	Maximum water uptake (%)	Diffusion coefficient (mm ² /sec) × 10 ⁻⁶	Sorption coefficient (g/g)	Permeability coefficient (mm ² /sec) × 10 ⁻⁷
SE1	0.4866	3.6811	0.0049	0.1791
SE2	2.445	4.5358	0.0244	1.109
SE3	4.8734	4.9092	0.0487	2.3924
SE4	8.2085	5.5551	0.082	4.5599
SE5	12.1228	6.2421	0.1212	7.5672
SE6	2.2556	4.2128	0.0225	0.9502
SE7	4.496	4.6764	0.0449	2.1025
SE8	7.7498	5.2051	0.0774	4.0338
SE9	11.4962	5.7474	0.1149	6.6074
SE10	2.6001	4.9935	0.026	1.2983
SE11	5.4075	5.7355	0.054	3.1015
SE12	8.4063	6.4698	0.084	5.4387
SE13	12.5952	7.4835	0.1259	9.4256

The diffusion coefficient of the hybrid composites describes the ability of water molecules to diffuse through the matrix material. It can be seen that the diffusion coefficient values appear to increase with the fiber loading. These results are consistent with the previous findings on natural fiber reinforced polymer composites [140], [300]. For epoxy based composites at 40 wt.% fiber loading, the diffusion coefficient significantly increases by 69.57%, 56.13% and 103.29% with corresponding weight ratio of banana and jute fiber as 1:1, 1:3, and 3:1 as compared to neat epoxy. Similarly, for polyester based composites at same fiber loading, the diffusion coefficient increases by 82.58%, 61.84% and 126.72% with weight ratio of banana and jute fiber as 1:1, 1:3, and 3:1, respectively as compared to neat polyester. The increase is more pronounced for the composite specimens with weight ratio of banana and jute fiber as 3:1. The values of sorption coefficient and permeability coefficient of the hybrid composites with different fiber loading and weight ratio are presented in the same Tables 6.6 and 6.7. It is evident that these values are increases with the increase in fiber loading and follows the same trend as that of diffusion coefficient.

Table 6.7: Values of maximum water uptake, diffusion coefficient, sorption coefficient, and permeability coefficient for short fiber reinforced polyester composites

	Maximum water uptake (%)	Diffusion coefficient ($\text{mm}^2/\text{sec}) \times 10^{-6}$	Sorption coefficient (g/g)	Permeability coefficient ($\text{mm}^2/\text{sec}) \times 10^{-7}$
SP1	0.5953	4.1177	0.0059	0.2451
SP2	4.8287	5.6173	0.0482	2.7124
SP3	6.8911	6.1434	0.0689	4.2335
SP4	9.8378	6.8570	0.0983	6.7458
SP5	14.4402	7.5181	0.1444	10.8564
SP6	3.6282	5.0339	0.0362	1.8264
SP7	5.6416	5.5813	0.0564	3.1488
SP8	8.8152	6.2765	0.0881	5.5329
SP9	12.7553	6.6644	0.1275	8.5008
SP10	5.3959	6.0194	0.0539	3.2481
SP11	8.2013	6.9888	0.0820	5.7318
SP12	11.1049	7.8675	0.1110	8.7368
SP13	15.7681	9.3360	0.1576	14.7213

6.2.2 Mechanical Properties

6.2.2.1 Tensile Properties

The experimental results of tensile strength of the short banana-jute fiber reinforced epoxy and polyester based composites with different fiber loading and weight ratio are shown in Figures 6.33 and 6.34, respectively. Results revealed that with the addition of fibers up to 30 wt.%, a gradual increase in tensile strength is observed in both type of polymer composites. This may be due to the proper adhesion between the fiber and the matrix and the reinforcement imparted by the fibers which allow stress transfer from the matrix to the fibers. However, further increase in fiber loading, i.e., up to 40 wt.%, there is a decrease in the tensile strength [87]. The reason may be due to the fact that the matrix content is highly reduced by the accumulation of excess fibers in the hybrid composites. Moreover, the possibility of fiber entanglements and agglomeration results in the hybrid composite that leads to decrease in stress transfer between the matrix and the fiber [30]. It is observed from the Figure 6.33 that the tensile strength of neat epoxy resin is 32.28 MPa. The tensile strength of the epoxy based hybrid composites with weight ratio of banana and jute fiber as 1:1, 1:3, and 3:1 is 60.38 MPa, 65.84 MPa, and 56.76 MPa, respectively at 30 wt.% of fiber loading.

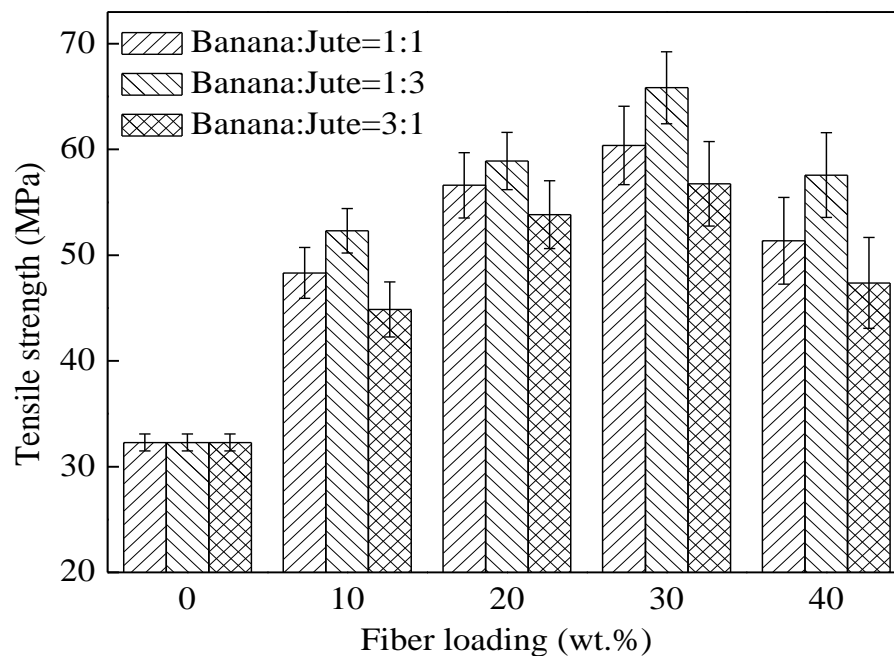


Figure 6.33: Effect of fiber loading and weight ratio on tensile strength of epoxy based hybrid composites

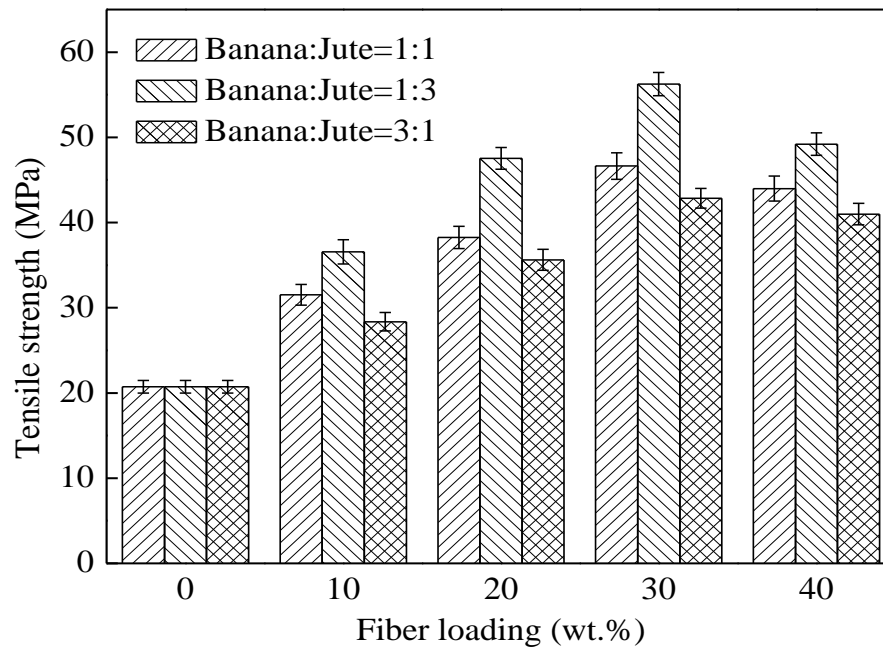


Figure 6.34: Effect of fiber loading and weight ratio on tensile strength of polyester based hybrid composites

Similarly, the tensile strength of neat polyester is 20.7 MPa which is increased to 46.6 MPa, 56.2 MPa, and 42.8 MPa with the addition of banana and jute fibers of 30 wt.% with weight ratio as 1:1, 1:3, and 3:1, respectively. Hybrid composites with weight ratio of banana and jute fiber as 1:3 show higher tensile strength irrespective of fiber loading and matrix types. The surface area of the fiber in a unit area of the composite is higher in a jute fiber than that of a banana fiber because the diameter of jute fiber is less than that of banana fiber. Hence, stress-transfer in the unit area as well as physical interaction is higher in the case of weight ratio as 1:3 of banana-jute fiber based composites [180], [282].

6.2.2.2 Flexural Properties

The effect of fiber loading on the flexural strength of short banana-jute fiber reinforced epoxy and polyester based composites are shown in Figures 6.35 and 6.36, respectively. Similarly, the effect of fiber loading on the flexural modulus of epoxy and polyester based composites are shown in Figures 6.37 and 6.38. It is observed that the flexural properties of all hybrid composites considered in the present study increases with the increase in fiber loading up to 30 wt.%. However, further increase in fiber loading the properties decreases. The decrease in flexural properties at higher weight percentages of fiber may be due to weak interfacial bonding, fiber agglomeration, increased fiber-to-fiber interactions and also dispersion problem [72], [139]. According to Mohanty et al. [119], the optimum fiber loading

varies with the fiber aspect ratio, nature of fiber and matrix, fiber–matrix adhesion, etc. For epoxy based composites at 30 wt.% of fiber loading, the increase in flexural strength of 112%, 146% and 101% is observed with weight ratio of banana and jute fiber as 1:1, 1:3, and 3:1 respectively as compare to the neat epoxy. Similarly, for polyester based composites, the increase in flexural strength of 83%, 98% and 67% is observed as the fiber content in polyester increased from 0 to 30 wt.% fiber loading with weight ratio of banana and jute fiber as 1:1, 1:3, and 3:1, respectively. The flexural modulus of the neat epoxy resin is found to be 3.32 GPa and is increased by 110%, 120% and 87% for epoxy based composites at 30 wt.% of fiber loading with weight ratio of banana and jute fiber as 1:1, 1:3, and 3:1, respectively. Similarly, the flexural modulus of the neat polyester matrix is found to be 1.61 GPa and is increased by 78%, 91%, and 70% for polyester based composites at 30 wt.% of fiber loading with weight ratio of banana and jute fiber as 1:1, 1:3, and 3:1, respectively. The high strength jute fiber layers are able to bear the applied tensile and compressive stresses subjected on the hybrid composites. This leads to an increase in the flexural properties of the hybrid composites with weight ratio of banana and jute fiber as 1:3. However, the flexural properties of the composites also influenced by various other parameters such as degree of crystallinity, the porosity content, and the size of lumen Bledzki and Gassan [301].

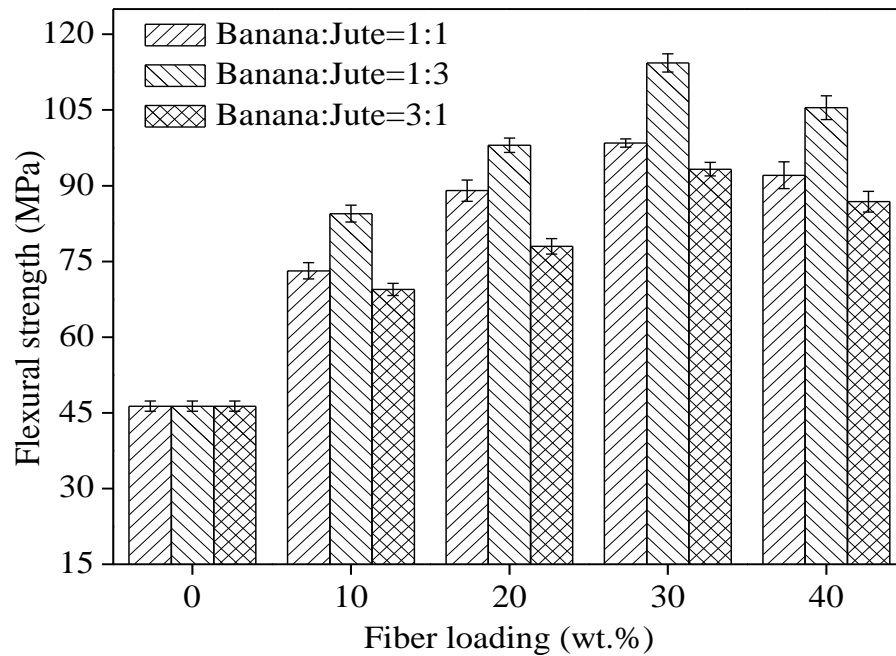


Figure 6.35: Effect of fiber loading and weight ratio on flexural strength of epoxy based hybrid composites

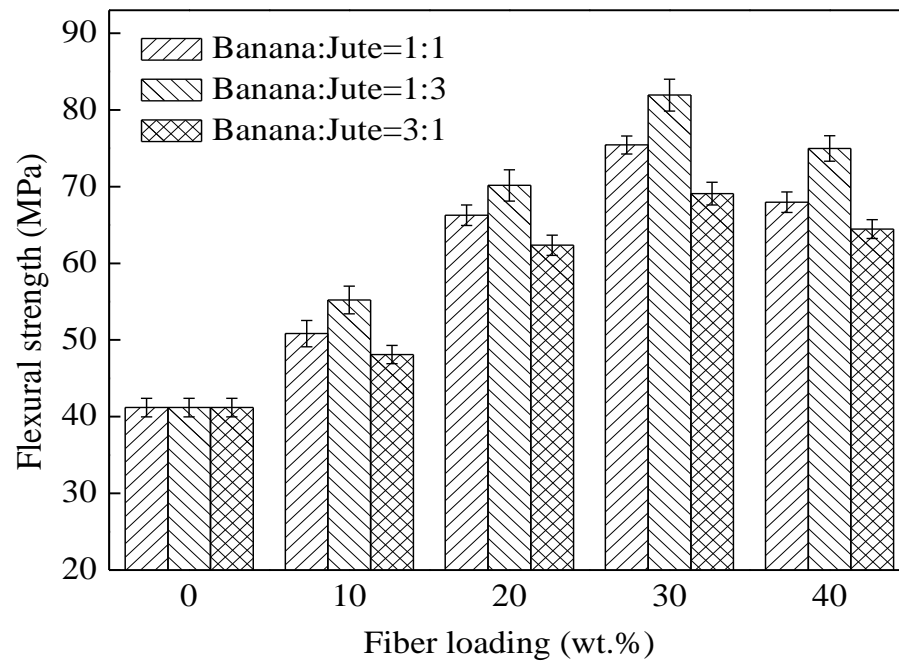


Figure 6.36: Effect of fiber loading and weight ratio on flexural strength of polyester based hybrid composites

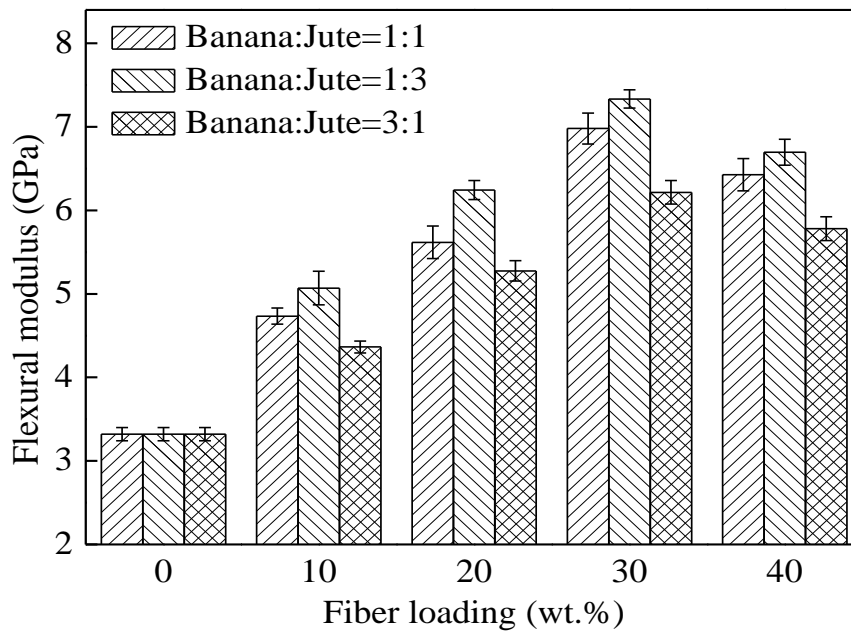


Figure 6.37: Effect of fiber loading and weight ratio on flexural modulus of epoxy based hybrid composites

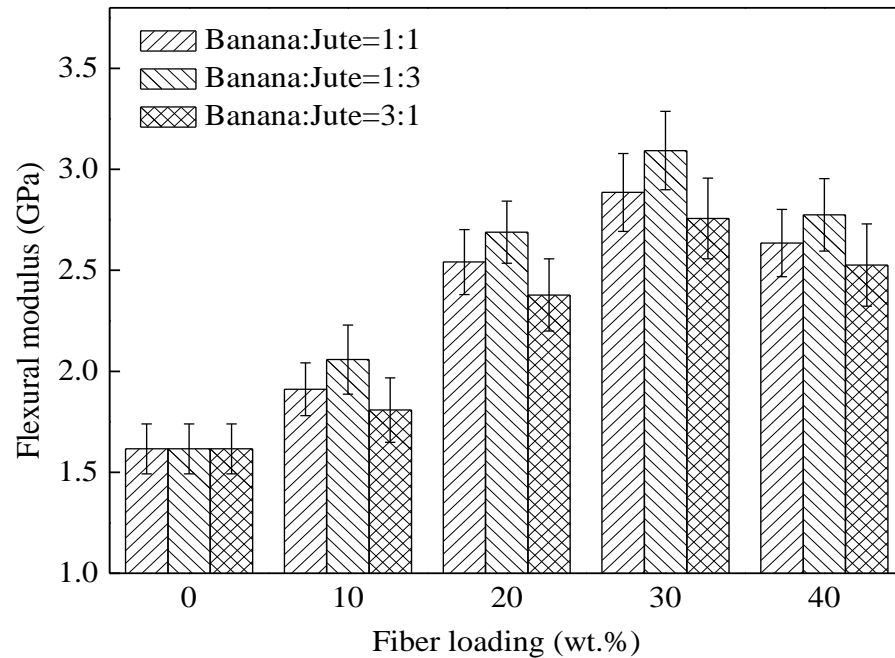


Figure 6.38: Effect of fiber loading and weight ratio on flexural modulus of polyester based hybrid composites

6.2.2.3 Impact Energy

The effect of fiber loading and weight ratio on the impact energy of the short fiber reinforced epoxy and polyester based composites are shown in Figures 6.39 and 6.40, respectively. It is evident from the figures that the impact energy increases with the increase in fiber loading, and the maximum impact energy value is observed at the fiber loading of 40 wt.%. The high impact energy of the hybrid composites attributed to the extra energy dissipation mechanism. At lower fiber loading, short banana and jute fibers are embedded in the resin and, hence, fibers pull out and fiber breakage occurs on the application of a sudden load. At higher fiber loading, the contact area between the reinforcement and matrix will increase. If there is good impregnation of fibers in the resin, then the impact resistance increases [302]. For epoxy based composites at 40 wt.% of fiber loading, the impact energy of the composite with weight ratio of banana and jute fiber as 1:1, 1:3, and 3:1 is found to be 202%, 181%, and 209% higher than that of neat epoxy. Similarly, for polyester based composites, as the fiber content in polyester increased from 0 to 40 wt.%, the energy absorbed by the hybrid composite is found to be 202%, 181%, and 209% higher than that of pure polyester resin for hybrid composites with the weight ratio of banana and jute fiber as 1:1, 1:3, and 3:1, respectively.

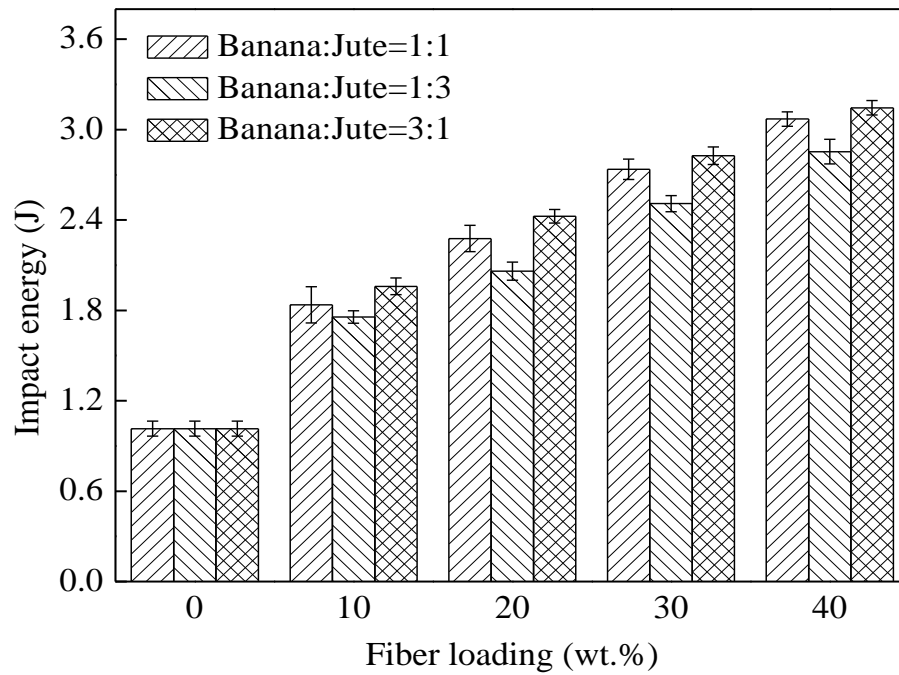


Figure 6.39: Effect of fiber loading and weight ratio on impact energy of epoxy based hybrid composites

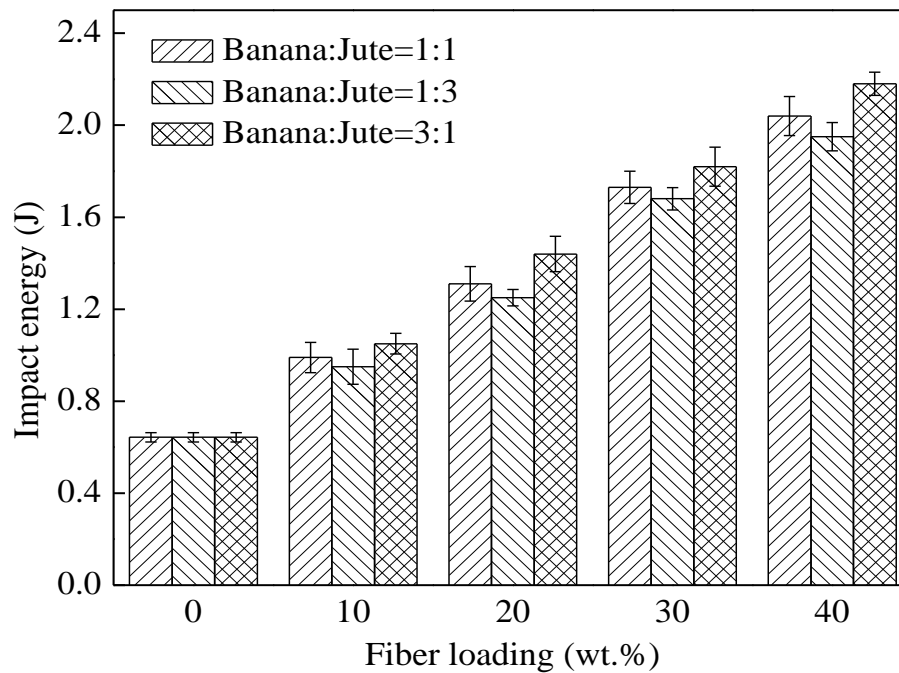


Figure 6.40: Effect of fiber loading and weight ratio on impact energy of polyester based hybrid composites

It is observed that the impact energy of the composites with weight ratio of banana and jute fiber as 3:1 is more compared to that of the composites with weight ratio of 1:1 and 1:3. Generally, the natural fibers having a high microfibrillar angle shows a higher composite fracture-toughness than those with a small microfibrillar angle [301]. The microfibrillar angle of banana fiber is 11° which is more than the jute fiber microfibrillar angle i.e. 8° . Therefore, the increase in impact energy of the composites with more percentage of banana fiber is obtained may be due to the above reason. Idicula et al. [282] also reported a similar trend of increase in impact strength of short banana and sisal fiber reinforced hybrid composites. In their study, it is observed that composites with sisal fibers (microfibrillar angle 20°) show good impact properties than the banana fibers (microfibrillar angle 11°).

6.2.3 Thermal Properties

6.2.3.1 Specific Heat and Thermal Diffusivity

The variation of specific heat and the thermal diffusivity of epoxy and polyester based hybrid composites as a function of fiber loading and weight ratio are presented in Table 6.8. It is observed that the specific heat capacity of the hybrid composite materials decreased gradually with the increase in fiber loading in both the epoxy and polyester based composites. The specific heat capacities of the neat epoxy and polyester resins are found to be 3.02 kJ/kg-K and 2.68 kJ/kg-K, respectively. The epoxy based composite at 40 wt.% of fiber loading with weight ratio of banana and jute fiber as 1:3 shows 26.15% lesser specific heat capacity value than that of neat epoxy. Similarly, for polyester based composites, at same fiber loading and weight ratio, the specific heat capacity shows 25% lesser than that of neat polyester matrix. It is observed from the figure that the thermal diffusivity of the hybrid composites decreases with the increase in fiber loading. The low thermal diffusivity of the composites indicates that the composites require a longer heating and cooling period, which is favorable in thermal insulation applications. The thermal diffusivity of the neat epoxy and polyester resins are found to be $1.049 \times 10^{-7} \text{ m}^2/\text{s}$ and $6.815 \times 10^{-8} \text{ m}^2/\text{s}$, respectively. For epoxy based composites, the lowest thermal diffusivity of $0.914 \times 10^{-7} \text{ m}^2/\text{s}$ is observed for composite with weight ratio of banana and jute fiber as 1:3 and it is 12.86% lesser than that of neat epoxy matrix. Similarly, for polyester based composites, the lowest thermal diffusivity of $5.934 \times 10^{-8} \text{ m}^2/\text{s}$ is observed for composite with weight ratio of banana and jute fiber as 1:3 and it is 12.92% lesser than that of neat polyester matrix. A similar trend of decrease in thermal diffusivity is observed for vakka natural fiber reinforced polyester composites by past researchers [148], [154].

Table 6.8: Specific heat and thermal diffusivity of the short fiber reinforced hybrid composites

Short fiber reinforced epoxy composites			Short fiber reinforced polyester composites		
Composite	Specific heat (kJ/kg-K)	Thermal diffusivity (m ² /s) ×10 ⁻⁷	Composite	Specific heat (kJ/kg-K)	Thermal diffusivity (m ² /s) ×10 ⁻⁸
SE1	3.02	1.049	SP1	2.68	6.815
SE2	2.78	1.036	SP2	2.56	6.610
SE3	2.61	1.007	SP3	2.39	6.515
SE4	2.43	0.965	SP4	2.24	6.423
SE5	2.25	0.941	SP5	2.04	6.491
SE6	2.85	0.999	SP6	2.62	6.378
SE7	2.72	0.954	SP7	2.46	6.239
SE8	2.50	0.914	SP8	2.32	5.981
SE9	2.29	0.895	SP9	2.11	5.934
SE10	2.73	1.063	SP10	2.54	6.752
SE11	2.56	1.034	SP11	2.37	6.708
SE12	2.42	0.985	SP12	2.23	6.637
SE13	2.23	0.974	SP13	2.01	6.843

6.2.3.2 Thermal Degradation Analysis

The influence of processing temperature on natural fiber reinforced composite materials is very important because there is always thermal stress during the manufacturing of composites. TGA is a useful technique that based on the measurement of weight loss related to temperature for the quantitative determination of the degradation behavior and the decomposition of the composite. The weight loss in natural fibers occurs due to the decomposition of cellulose, hemicellulose and lignin constituents during heating. Higher decomposition temperatures give greater thermal stability [303]. The thermal degradation of banana-jute hybrid composites at 40 wt.% fiber loading with different weight ratio is observed. The thermogravimetric curves of epoxy and polyester based composites are presented in Figures 6.41 and 6.42, respectively. The graphs exhibit three-stage thermal degradation; an initial thermal degradation is below 100°C, which is corresponding to the moisture evaporation of the natural fibers.

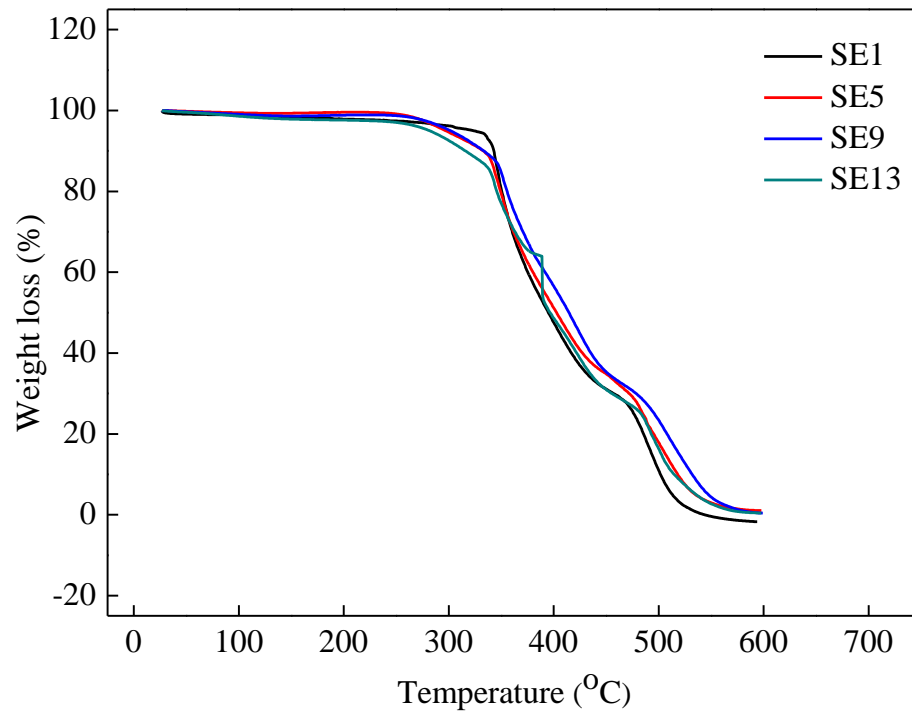


Figure 6.41: Effect of weight ratio on thermal degradation of epoxy based hybrid composites

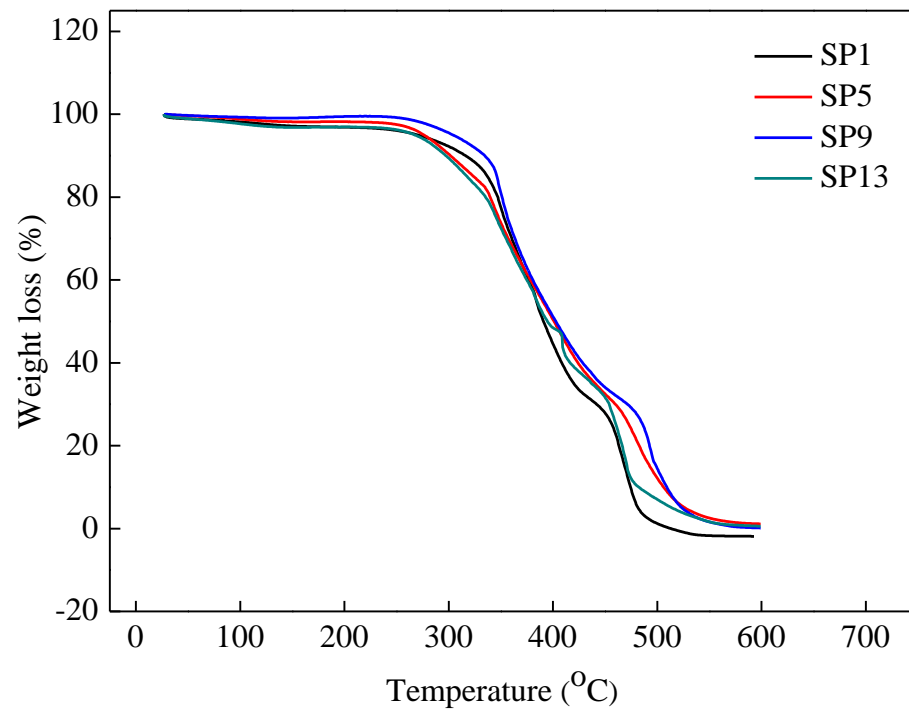


Figure 6.42: Effect of weight ratio on thermal degradation of polyester based hybrid composites

The second thermal degradation is observed at 270°C to 350°C, which is due to the degradation of hemicellulose and part of cellulose. The maximum peak of the third thermal degradation phase is approximately at 480°C to 570°C, which represents the decomposition of the lignin. The thermal degradation characteristics of natural fiber reinforced composites are influenced by the contributions of the individual thermal degradation properties of both the fibers and matrix [304]. At lower temperature, the short banana-jute fiber reinforced composites shows the weaker thermal stability as compared to the neat polymer. It indicates that the moisture content in the hybrid composites increases with the addition of more natural fibers into the polymer composites. The incompatibility between the hydrophilic fibers and the hydrophobic thermosetting resin results the poor interfacial bonding. The reduction in thermal stability of the hybrid composites with the increase in fiber content became obvious due to the less stable fibers and dehydration process. Lee and Wang [305] also observed that the addition of natural fibers causes reduction in the thermal stability of the composites due to the influence of the less stable fibers.

Table 6.9: Thermal degradation of the short fiber reinforced hybrid composites

Epoxy based composites			Polyester based composites		
Composite	Second degradation temperature (°C)	Final degradation temperature (°C)	Composite	Second degradation temperature (°C)	Final degradation temperature (°C)
SE1	345	504	SP1	321	486
SE5	284	557	SP5	286	522
SE9	295	565	SP9	292	534
SE13	272	532	SP13	278	510

It is observed that the thermal degradation of all the composite specimens has taken place within the scheduled temperature range of 30°C-600°C for both the epoxy and polyester based composites. The decomposition of neat epoxy started at a temperature of 345°C and 98.8% decomposition occurred at 504°C. Similarly, the decomposition of neat polyester started at a temperature of 321°C and 98% decomposition occurred at 486°C. The composites with weight ratio of banana and jute fiber as 1:3 show better thermal stability at highest temperature as compared to others. Incorporation of jute fiber has resulted in considerable increase in the thermal stability of hybrid composites which is possibly due to higher thermal stability of jute fiber than banana fiber.

Chapter Summary

This chapter has provided:

- The results of the micromechanical analysis and experiments conducted to evaluate the elastic properties and thermal conductivity of the short banana-jute fiber reinforced hybrid composites under study
- The validation of proposed model for effective thermal conductivity of short fiber reinforced hybrid composites developed in Chapter 3 of this thesis through results obtained by micromechanical analysis and experimental results
- The results of the physical, mechanical and thermal behaviour of short banana-jute fiber reinforced hybrid composites.
- The effect of fiber loading and weight ratio on the physical, mechanical and thermal behaviour of short banana-jute fiber reinforced hybrid composites.

The next chapter presents the summary of the findings of the research work, specific conclusions drawn from the experimental, analytical and numerical efforts, recommended applications and directions for future research.

Chapter 7

Conclusions and Scope for Future Work

7.1 Conclusions

The present analytical, experimental and numerical investigation of epoxy and polyester based composites reinforced with banana and jute fiber has led to the following conclusions:

1. Fabrication of unidirectional and short banana-jute fiber reinforced epoxy and polyester based composites with different fiber loading and weight ratio has been done successfully.
2. The micromechanical analysis of hybrid composites based on three-dimensional RVE with a square and hexagonal packing geometry is successfully implemented by using finite element code ANSYS to calculate the elastic properties and thermal conductivity. For unidirectional fiber reinforced hybrid composites, the longitudinal and transverse elastic modulus values are found always higher than that of neat polymer. The maximum longitudinal elastic modulus of epoxy and polyester based composites at 40 wt.% fiber loading with weight ratio of banana and jute fiber as 1:3 are found to be 4.295 GPa and 3.372 GPa, respectively. Similarly, the maximum transverse elastic modulus of epoxy and polyester based composites at 30 wt.% fiber loading with weight ratio of banana and jute fiber as 1:3 are found to be 3.685 GPa and 2.128 GPa, respectively. For short fiber reinforced hybrid composites, the effective elastic modulus of epoxy increases from 3.14 GPa to 4.195 GPa and that of polyester increases from 1.48 GPa to 2.648 GPa with the reinforcement of 40 wt.% fiber loading with the weight ratio of banana and jute fiber as 1:3.
3. Two theoretical models based on the law of minimal thermal resistance and equal law of specific equivalent thermal conductivity to estimate the transverse thermal conductivity of unidirectional fiber reinforced hybrid composites and effective thermal conductivity of short fiber reinforced hybrid composites are proposed. It is concluded that the proposed correlations are in good agreement with the analytical and numerical methods. The proposed models can very well be used to estimate the

thermal conductivity for unidirectional and short fiber reinforced polymer hybrid composites.

4. It is encouraging to see that the incorporation of banana and jute fibers results in significant improvement in the thermal insulation capability of both the epoxy and polyester matrices. For unidirectional fiber based composites, with the incorporation of 10 wt.% banana and 30 wt.% jute fiber, the longitudinal thermal conductivity of neat epoxy reduced by 32.23% and reaches to 0.246 W/m-K and that of neat polyester reduced by 28.50% and reaches to 0.143 W/m-K. Whereas, with similar fiber loading, the transverse thermal conductivity of neat epoxy and polyester reaches to 0.202 W/m-K and 0.122 W/m-K, respectively. For short fiber based composites, with the incorporation of 10 wt.% banana and 30 wt.% jute, the effective thermal conductivity of epoxy reduces from 0.363 W/m-K to 0.239 W/m-K and that of polyester reduces from 0.20 W/m-K to 0.14 W/m-K.
5. The density, void content and water absorption coefficients of the unidirectional and short fiber based hybrid composites are greatly affected by the type of fiber material, fiber loading, weight ratio and type of matrix materials. With increase in fiber loading, density, void content and water absorption coefficients increases invariably for both the epoxy and polyester based composites. The epoxy based hybrid composites shows relatively low amount of voids and water absorption as compared to the polyester based hybrid composites.
6. The mechanical properties of the hybrid composites are improved by adding the banana and jute fiber reinforcements in polymer matrix. For unidirectional fiber based composites, with addition of 7.5 wt.% banana and 22.5 wt.% jute fiber as reinforcement, the longitudinal tensile strength of epoxy increases from 32.28 MPa to 84.48 MPa and that of polyester increases from 20.72 MPa to 66.89 MPa. Whereas for 5 wt.% of banana and 15 wt.% of jute fiber, the transverse tensile strength of epoxy and polyester increases to 43.65 MPa and 35.06 MPa, respectively. The maximum longitudinal flexural modulus and strength of epoxy and polyester based composites are observed for 7.5 wt.% of banana and 22.5 wt.% of jute fiber. Whereas, the maximum transverse flexural modulus and strength of epoxy and polyester based composites are observed for 2.5 wt.% of banana and 7.5 wt.% of jute fiber. The ILSS of epoxy increases from 6.92 MPa to 20.53 MPa and that of polyester increases from

- 4.05 MPa to 16.16 MPa with reinforcement of 7.5 wt.% of banana and 22.5 wt.% of jute fiber. The impact energy of epoxy increases from 1.01 J to 3.77 J and that of polyester increases from 0.64 J to 2.55 J with the incorporation of 30 wt.% banana and 10 wt.% jute fiber. With the reinforcement of 10 wt.% of banana and 30 wt.% of jute, the micro-hardness of epoxy increases from 25.10 Hv to 43.57 Hv and that of polyester increases from 16.88 Hv to 37.78 Hv.
7. For short fiber based composites, with the addition of 7.5 wt.% banana and 22.5 wt.% jute as reinforcement, tensile strength of epoxy increased by 103% and reaches 65.84 MPa, flexural strength of epoxy increased by 146% and reaches to 114.31 MPa and its flexural modulus increased by 120% and reaches to 7.33 GPa. Whereas, in polyester based hybrid composites with similar fiber loading, the tensile strength of polyester increased by 171% and reaches to 56.25 MPa, flexural strength of polyester increased by 98.9% and reaches to 81.93 MPa and its flexural modulus increased by 91.39% and reaches to 3.09 GPa. Maximum impact energy of 3.14 J and 2.18 J is observed for the epoxy and polyester based composites at 40 wt.% of fiber loading with the weight ratio of banana and jute fiber as 3:1.
 8. The specific heat and thermal diffusivity of the unidirectional and short fiber based composites are decreased gradually with the increase in the fiber loading in both the epoxy and polyester based composites. The effect of fiber loading has a great influence on these results. However, the influence of weight ratio of the fibers on these properties is found negligible.
 9. The study reveals that the performance of hybrid composites with the weight ratio of banana and jute fiber as 1:3 shows better than the weight ratio of 1:1 and 3:1. The longitudinal properties of the hybrid composites show better than that of the transverse and short fiber reinforced hybrid composites.

7.2 Recommendation for Potential Application

Natural fiber reinforced composite materials show excellent performance, starting from their applications in manufacturing and aerospace industries to house-hold appliances. It is mainly due to their low density, light weight, economical, biodegradability, high strength to weight ratio and renewability. The banana-jute fiber reinforced polymer hybrid composites fabricated and experimented under this investigation are expected to have adequate potential

for a wide variety of applications. The hybrid composites can be used in automotive industries for preparing interior panels, armrests, headliners, package trays, seat backs, consoles and dashboards to improve energy efficiency. The present study reveals that these hybrid composites exhibited better thermal insulation performance. Therefore, the use of these composites may also be recommended for building materials such as panels, door shutters, door frames, roofing sheets, partition, windows and insulation boards to possess excellent thermal and sound insulation.

7.3 Scope for Future Work

The present research work leaves a wide scope for future investigators to explore many other aspects of natural fiber reinforced polymer hybrid composites. Some recommendations for future research includes:

- Development of theoretical models for fiber reinforced hybrid composites of different shapes taking into account the fiber-matrix interface resistance.
- The present study has been carried out using simple hand lay-up technique to fabricate the composites. However, the research work can be extended further by considering other manufacturing process for composite fabrication and the effect of manufacturing techniques on the performance of hybrid composites can similarly be analyzed.
- Besides many advantages of natural fibers, the main disadvantages of natural fibers in composites are the relative high moisture absorption due to their hydrophilic nature and the poor interfacial bonding between fiber and matrix. The study can be extended further by considering the chemical treatments in modifying the fiber surface properties to improve the bonding between fiber and matrix materials and the study can be analyzed similarly.
- Cost analysis of these hybrid composites to assess their economic viability in industrial applications.

Bibliography

- [1] S. Ghosh, *Micromechanical Analysis and Multi-scale Modeling Using the Voronoi Cell Finite Element Method*. Florida: CRC Press, 2011.
- [2] D. Das and B. Pourdeyhimi, *Composite Nonwoven Materials: Structure, Properties and Applications*. Cambridge: Woodhead Publishing, 2014.
- [3] V. K. Thakur, *Green Composites from Natural Resources*. Florida: CRC Press, 2014.
- [4] D. Gay, *Composite Materials: Design and Applications*. Florida: CRC Press, 2002.
- [5] A. Lbnyaich, “Modification of the Properties Biobased Thermoset Resin using Cellulose Nano-Whiskers (CNW) as an Additive,” Luleå University Technology, Luleå, 2010.
- [6] E. Bozkurt, E. Kaya, and M. Tanoğlu, “Mechanical and thermal behavior of non-crimp glass fiber reinforced layered clay/epoxy nanocomposites,” *Compos. Sci. Technol.*, vol. 67, no. 15, pp. 3394–3403, 2007.
- [7] M. W. Nielsen, J. W. Schmidt, J. H. Hogh, J. P. Waldbjorn, J. H. Hattel, T. L. Andersen, and C. M. Markussen, “Life cycle strain monitoring in glass fibre reinforced polymer laminates using embedded fibre Bragg grating sensors from manufacturing to failure,” *J. Compos. Mater.*, vol. 48, no. 3, pp. 365–381, Feb. 2014.
- [8] M. Schwartz, *Smart Materials*. Florida: CRC Press, 2009.
- [9] G. Arpitha, M. Sanjay, and B. Yogesha, “State-of-Art on Hybridization of Natural Fiber Reinforced Polymer Composites,” *Colloid Surf. Sci.*, vol. 2, no. 2, pp. 59–65, 2017.
- [10] N. Chand and M. Fahim, *Tribology of Natural Fiber Polymer Composites*. Florida: CRC Press, 2008.
- [11] N. Venkateshwaran and A. Elayaperumal, “Banana fiber reinforced polymer composites - A review,” *J. Reinf. Plast. Compos.*, vol. 29, no. 15, pp. 2387–2396, Aug. 2010.
- [12] T. Munikenche Gowda, A. C. B. Naidu, and R. Chhaya, “Some mechanical properties of untreated jute fabric-reinforced polyester composites,” *Compos. Part A Appl. Sci. Manuf.*, vol. 30, no. 3, pp. 277–284, 1999.

- [13] D. Gon, K. Das, P. Paul, S. Maity, D. Gon, K. Das, P. Paul, and S. Maity, "Jute composites as wood substitute," *Int. J. Text. Sci.*, vol. 1, no. 6, pp. 84–93, 2012.
- [14] J. Summerscales, N. P. J. Dissanayake, A. S. Virk, and W. Hall, "A review of bast fibres and their composites. Part 1 – Fibres as reinforcements," *Compos. Part A Appl. Sci. Manuf.*, vol. 41, no. 10, pp. 1329–1335, 2010.
- [15] C. Alves, P. M. C. Ferrão, A. J. Silva, L. G. Reis, M. Freitas, L. B. Rodrigues, and D. E. Alves, "Ecodesign of automotive components making use of natural jute fiber composites," *J. Clean. Prod.*, vol. 18, no. 4, pp. 313–327, 2010.
- [16] D. H. Mueller and A. Krobjilowski, "New discovery in the properties of composites reinforced with natural fibers," *J. Ind. Text.*, vol. 33, no. 2, pp. 111–130, Oct. 2003.
- [17] S. V. Joshi, L. T. Drzal, A. K. Mohanty, and S. Arora, "Are natural fiber composites environmentally superior to glass fiber reinforced composites?," *Compos. Part A Appl. Sci. Manuf.*, vol. 35, no. 3, pp. 371–376, 2004.
- [18] A. K. Bledzki, A. A. Mamun, and O. Faruk, "Abaca fibre reinforced PP composites and comparison with jute and flax fibre PP composites," *Express Polym. Lett.*, vol. 1, no. 11, pp. 755–762, 2007.
- [19] S. Mukhopadhyay, R. Figueiro, Y. Arpac, and Ü. Şentürk, "Banana fibers—variability and fracture behaviour," *J. Eng. Fiber. Fabr.*, vol. 3, no. 2, pp. 39–45, 2008.
- [20] E. U. Akubueze, C. S. Ezeanyanaso, S. Muniru, G. Affo, and C. C. Igwe, "Extraction & Production of Agro – Sack from Banana (*Musa Sapientum*) & Plantain (*Musa Paradisiaca* l) Fibres for Packaging Agricultural Produce," *Int. J. Agric. Crop Sci.*, vol. 9, no. 1, pp. 9–14, 2015.
- [21] N. A. A. Nik Yusuf, E. S. Rosly, M. Mohamed, M. B. Abu Bakar, M. Yusoff, M. A. Sulaiman, and M. I. Ahmad, "Waste Banana Peel and its Potentialization in Agricultural Applications: Morphology Overview," *Mater. Sci. Forum*, vol. 840, pp. 394–398, Jan. 2016.
- [22] J. L. Kardos, "Critical issues in achieving desirable mechanical properties for short fiber composites," *Pure Appl. Chem.*, vol. 57, no. 11, pp. 1651–1657, Jan. 1985.
- [23] J. K. Kim and J. H. Song, "Rheological properties and fiber orientations of short fiber-reinforced plastics," *J. Rheol. (N. Y. N. Y.)*, vol. 41, no. 5, pp. 1061–1085, 1997.
- [24] A. M. Papadopoulos, "State of the art in thermal insulation materials and aims for

- future developments,” *Energy Build.*, vol. 37, no. 1, pp. 77–86, 2005.
- [25] H. T. Hahn and S. W. Tsai, “Nonlinear elastic behavior of unidirectional composite laminae,” *J. Compos. Mater.*, vol. 7, no. 1, pp. 102–118, Jan. 1973.
- [26] J. Aboudi, “Micromechanical analysis of composites by the method of cells,” *Appl. Mech. Rev.*, vol. 42, no. 7, p. 193, 1989.
- [27] C. T. Sun and R. S. Vaidya, “Prediction of composite properties from a representative volume element,” *Compos. Sci. Technol.*, vol. 56, no. 2, pp. 171–179, Jan. 1996.
- [28] D. N. Saheb and J. P. Jog, “Natural fiber polymer composites: A review,” *Adv. Polym. Technol.*, vol. 18, no. 4, pp. 351–363, Jan. 1999.
- [29] R. Kozłowski and M. Władysław-Przybylak, “Flammability and fire resistance of composites reinforced by natural fibers,” *Polym. Adv. Technol.*, vol. 19, no. 6, pp. 446–453, Jun. 2008.
- [30] K. L. Pickering, M. G. A. Efendy, and T. M. Le, “A review of recent developments in natural fibre composites and their mechanical performance,” *Compos. Part A Appl. Sci. Manuf.*, vol. 83, pp. 98–112, 2016.
- [31] O. Faruk, A. K. Bledzki, H. P. Fink, and M. Sain, “Biocomposites reinforced with natural fibers: 2000–2010,” *Prog. Polym. Sci.*, vol. 37, no. 11, pp. 1552–1596, 2012.
- [32] S. K. Ramamoorthy, M. Skrifvars, and A. Persson, “A review of natural fibers used in biocomposites: Plant, animal and regenerated cellulose fibers,” *Polym. Rev.*, vol. 55, no. 1, pp. 107–162, Jan. 2015.
- [33] L. Y. Mwaikambo, “Review of the history, properties and application of plant fibres,” *African J. Sci. Technol.*, vol. 7, no. 2, pp. 120–133, 2006.
- [34] M. J. John and R. D. Anandjiwala, “Recent developments in chemical modification and characterization of natural fiber-reinforced composites,” *Polym. Compos.*, vol. 29, no. 2, pp. 187–207, Feb. 2008.
- [35] T. Sathishkumar, P. Navaneethakrishnan, S. Shankar, R. Rajasekar, and N. Rajini, “Characterization of natural fiber and composites - A review,” *J. Reinf. Plast. Compos.*, vol. 32, no. 19, pp. 1457–1476, Oct. 2013.
- [36] A. K. Mohanty, M. Misra, and G. Hinrichsen, “Biofibres, biodegradable polymers and biocomposites: An overview,” *Macromol. Mater. Eng.*, vol. 276–277, no. 1, pp. 1–24, Mar. 2000.

- [37] S. Taj, M. Munawar, and S. Khan, “natural fiber reinforced polymer composites,” *Proc. Pakistan Acad. Sci.*, vol. 44, no. 2, pp. 129–144, 2007.
- [38] M. Z. Rong, M. Q. Zhang, Y. Liu, G. C. Yang, and H. M. Zeng, “The effect of fiber treatment on the mechanical properties of unidirectional sisal-reinforced epoxy composites,” *Compos. Sci. Technol.*, vol. 61, no. 10, pp. 1437–1447, 2001.
- [39] J. G. Cook, *Hand Book of Textile Fibers*. Abington: Woodhead Publishing, 1984.
- [40] M. M. Kabir, H. Wang, T. Aravinthan, F. Cardona, and K.-T. Lau, “Effects of Natural Fibre Surface on Composite Properties: A Review,” in *1st International Postgraduate Conference on Engineering, Designing and Developing the Built Environment for Sustainable Wellbeing*, 2011.
- [41] M. Xanthos, *Functional Fillers for Plastics*. Weinheim: Wiley-VCH, 2010.
- [42] M. Idicula, K. Joseph, and S. Thomas, “Mechanical performance of short banana/sisal hybrid fiber reinforced polyester composites,” *J. Reinf. Plast. Compos.*, vol. 29, no. 1, pp. 12–29, Jan. 2010.
- [43] J. Gassan, A. Chate, and A. K. Bledzki, “Calculation of elastic properties of natural fibers,” *J. Mater. Sci.*, vol. 36, no. 15, pp. 3715–3720, 2001.
- [44] R. Karnani, M. Krishnan, and R. Narayan, “Biofiber-reinforced polypropylene composites,” *Polym. Eng. Sci.*, vol. 37, no. 2, pp. 476–483, Feb. 1997.
- [45] A. Vazquez, V. A. Dominguez, and J. M. Kenny, “Bagasse fiber-polypropylene based composites,” *J. Thermoplast. Compos. Mater.*, vol. 12, no. 6, pp. 477–497, Nov. 1999.
- [46] C. N. Zarate, M. I. Aranguren, and M. M. Reboredo, “Resol-vegetable fibers composites,” *J. Appl. Polym. Sci.*, vol. 77, no. 8, pp. 1832–1840, Aug. 2000.
- [47] M. M. Thwe and K. Liao, “Environmental effects on bamboo-glass/polypropylene hybrid composites,” *J. Mater. Sci.*, vol. 38, no. 2, pp. 363–376, 2003.
- [48] A. V. Rajulu, S. A. Baksh, G. R. Reddy, and K. N. Chary, “Chemical resistance and tensile properties of short bamboo fiber reinforced epoxy composites,” *J. Reinf. Plast. Compos.*, vol. 17, no. 17, pp. 1507–1511, 1998.
- [49] A. P. Deshpande, M. Bhaskar Rao, and C. Lakshmana Rao, “Extraction of bamboo fibers and their use as reinforcement in polymeric composites,” *J. Appl. Polym. Sci.*, vol. 76, no. 1, pp. 83–92, Apr. 2000.

- [50] L. A. Pothan, J. George, and S. Thomas, "Effect of fiber surface treatments on the fiber–matrix interaction in banana fiber reinforced polyester composites," *Compos. Interfaces*, vol. 9, no. 4, pp. 335–353, Jan. 2002.
- [51] S. Joseph, M. S. Sreekala, Z. Oommen, P. Koshy, and S. Thomas, "A comparison of the mechanical properties of phenol formaldehyde composites reinforced with banana fibres and glass fibres," *Compos. Sci. Technol.*, vol. 62, no. 14, pp. 1857–1868, 2002.
- [52] S. J. Son, Y. M. Lee, and S. S. Im, "Transcrystalline morphology and mechanical properties in polypropylene composites containing cellulose treated with sodium hydroxide and cellulase," *J. Mater. Sci.*, vol. 35, no. 22, pp. 5767–5778, 2000.
- [53] S. Dong, S. Sapiaha, and H. P. Schreiber, "Rheological properties of corona modified cellulose/polyethylene composites," *Polym. Eng. Sci.*, vol. 32, no. 22, pp. 1734–1739, 1992.
- [54] I. M. Low, P. Schmidt, and J. Lane, "Synthesis and properties of cellulose-fibre/epoxy laminates," *J. Mater. Sci. Lett.*, vol. 14, no. 3, pp. 170–172, 1995.
- [55] C. A. S. Hill and H. P. S. Abdul Khalil, "Effect of fiber treatments on mechanical properties of coir or oil palm fiber reinforced polyester composites," *J. Appl. Polym. Sci.*, vol. 78, no. 9, pp. 1685–1697, Nov. 2000.
- [56] L. Y. Mwaikambo and E. T. Bisanda, "The performance of cotton–kapok fabric–polyester composites," *Polym. Test.*, vol. 18, no. 3, pp. 181–198, 1999.
- [57] K. Van de Velde and P. Kiekens, "Development of a flax/polypropylene composite with optimal mechanical characteristics by fiber and matrix modification," *J. Thermoplast. Compos. Mater.*, vol. 15, no. 4, pp. 281–300, Jul. 2002.
- [58] A. Stamboulis, C. Baillie, and E. Schulz, "Interfacial characterisation of flax fibre-thermoplastic polymer composites by the pull-out test," *Die Angew. Makromol. Chemie*, vol. 272, no. 1, pp. 117–120, Dec. 1999.
- [59] D. G. Hepworth, J. F. V. Vincent, G. Jeronimidis, and D. M. Bruce, "The penetration of epoxy resin into plant fibre cell walls increases the stiffness of plant fibre composites," *Compos. Part A Appl. Sci. Manuf.*, vol. 31, no. 6, pp. 599–601, 2000.
- [60] M. Hughes, G. Sèbe, J. Hague, C. Hill, M. Spear, and L. Mott, "An investigation into the effects of micro-compressive defects on interphase behaviour in hemp-epoxy composites using half-fringe photoelasticity," *Compos. Interfaces*, vol. 7, no. 1, pp.

- 13–29, Jan. 2000.
- [61] M. Hughes, C. A. S. Hill, and J. R. B. Hague, “The fracture toughness of bast fibre reinforced polyester composites Part 1 Evaluation and analysis,” *J. Mater. Sci.*, vol. 37, no. 21, pp. 4669–4676, 2002.
- [62] W. Thielemans, E. Can, S. S. Morye, and R. P. Wool, “Novel applications of lignin in composite materials,” *J. Appl. Polym. Sci.*, vol. 83, no. 2, pp. 323–331, Jan. 2002.
- [63] A. K. Rana, A. Mandal, and S. Bandyopadhyay, “Short jute fiber reinforced polypropylene composites: effect of compatibiliser, impact modifier and fiber loading,” *Compos. Sci. Technol.*, vol. 63, no. 6, pp. 801–806, 2003.
- [64] S. S. Tripathy, L. Di Landro, D. Fontanelli, A. Marchetti, and G. Levita, “Mechanical properties of jute fibers and interface strength with an epoxy resin,” *J. Appl. Polym. Sci.*, vol. 75, no. 13, pp. 1585–1596, Mar. 2000.
- [65] A. C. de Albuquerque, K. Joseph, L. Hecker de Carvalho, and J. R. M. D’Almeida, “Effect of wettability and ageing conditions on the physical and mechanical properties of uniaxially oriented jute-roving-reinforced polyester composites,” *Compos. Sci. Technol.*, vol. 60, no. 6, pp. 833–844, 2000.
- [66] D. Ray, B. K. Sarkar, and N. R. Bose, “Impact fatigue behaviour of vinylester resin matrix composites reinforced with alkali treated jute fibres,” *Compos. Part A Appl. Sci. Manuf.*, vol. 33, no. 2, pp. 233–241, 2002.
- [67] J. Zimmerman and N. Losure, “Mechanical properties of kenaf bast fiber reinforced epoxy matrix composite panels,” *J. Adv. Mater.*, vol. 30, no. 2, pp. 32–38, 1998.
- [68] N. Dansiri, N. Yanumet, J. W. Ellis, and H. Ishida, “Resin transfer molding of natural fiber reinforced polybenzoxazine composites,” *Polym. Compos.*, vol. 23, no. 3, pp. 352–360, Jun. 2002.
- [69] M. S. Sreekala, M. G. Kumaran, and S. Thomas, “Water sorption in oil palm fiber reinforced phenol formaldehyde composites,” *Compos. Part A Appl. Sci. Manuf.*, vol. 33, no. 6, pp. 763–777, 2002.
- [70] R. Agrawal, N. S. Saxena, M. S. Sreekala, and S. Thomas, “Effect of treatment on the thermal conductivity and thermal diffusivity of oil-palm-fiber-reinforced phenolformaldehyde composites,” *J. Polym. Sci. Part B Polym. Phys.*, vol. 38, no. 7, pp. 916–921, Apr. 2000.

- [71] J. George, S. Thomas, and S. S. Bhagawan, "Effect of strain rate and temperature on the tensile failure of pineapple fiber reinforced polyethylene composites," *J. Thermoplast. Compos. Mater.*, vol. 12, no. 6, pp. 443–464, Nov. 1999.
- [72] L. U. Devi, S. S. Bhagawan, and S. Thomas, "Mechanical properties of pineapple leaf fiber-reinforced polyester composites," *J. Appl. Polym. Sci.*, vol. 64, no. 9, pp. 1739–1748, May 1997.
- [73] R. Mangal, N. S. Saxena, M. S. Sreekala, S. Thomas, and K. Singh, "Thermal properties of pineapple leaf fiber reinforced composites," *Mater. Sci. Eng. A*, vol. 339, no. 1, pp. 281–285, 2003.
- [74] L. G. Angelini, A. Lazzeri, G. Levita, D. Fontanelli, and C. Bozzi, "Ramie (*Boehmeria nivea* (L.) Gaud.) and Spanish Broom (*Spartium junceum* L.) fibres for composite materials: agronomical aspects, morphology and mechanical properties," *Ind. Crops Prod.*, vol. 11, no. 2, pp. 145–161, 2000.
- [75] M. A. Lopez-Manchado, J. Biagiotti, and J. M. Kenny, "Comparative study of the effects of different fibers on the processing and properties of polypropylene matrix composites," *J. Thermoplast. Compos. Mater.*, vol. 15, no. 4, pp. 337–353, Jul. 2002.
- [76] P. V. Joseph, K. Joseph, and S. Thomas, "Effect of processing variables on the mechanical properties of sisal-fiber-reinforced polypropylene composites," *Compos. Sci. Technol.*, vol. 59, no. 11, pp. 1625–1640, 1999.
- [77] K. Oksman, L. Wallström, L. A. Berglund, and R. D. T. Filho, "Morphology and mechanical properties of unidirectional sisal- epoxy composites," *J. Appl. Polym. Sci.*, vol. 84, no. 13, pp. 2358–2365, Jun. 2002.
- [78] V. J. Fernandes, A. S. Araujo, V. M. Fonseca, N. S. Fernandes, and D. R. Silva, "Thermogravimetric evaluation of polyester/sisal flame retarded composite," *Thermochim. Acta*, vol. 392, pp. 71–77, 2002.
- [79] S. C. Jana and A. Prieto, "On the development of natural fiber composites of high-temperature thermoplastic polymers," *J. Appl. Polym. Sci.*, vol. 86, no. 9, pp. 2159–2167, Nov. 2002.
- [80] K. Oksman, H. Lindberg, and A. Holmgren, "The nature and location of SEBS-MA compatibilizer in polyethylene-wood flour composites," *J. Appl. Polym. Sci.*, vol. 69, no. 1, pp. 201–209, Jul. 1998.

- [81] N. E. Marcovich, M. I. Aranguren, and M. M. Reboredo, "Modified woodflour as thermoset fillers Part I. Effect of the chemical modification and percentage of filler on the mechanical properties," *Polymer (Guildf)*., vol. 42, no. 2, pp. 815–825, 2001.
- [82] R. Kahraman, S. Abbasi, and B. Abu-Sharkh, "Influence of Epolene G-3003 as a coupling agent on the mechanical behavior of palm fiber-polypropylene composites," *Int. J. Polym. Mater.*, vol. 54, no. 6, pp. 483–503, Apr. 2005.
- [83] U. C. Jindal, "Development and testing of bamboo-fibres reinforced plastic composites," *J. Compos. Mater.*, vol. 20, no. 1, pp. 19–29, Jan. 1986.
- [84] J. Rout, M. Misra, A. K. Mohanty, S. K. Nayak, and S. S. Tripathy, "SEM observations of the fractured surfaces of coir composites," *J. Reinf. Plast. Compos.*, vol. 22, no. 12, pp. 1083–1100, Jan. 2003.
- [85] V. Mishra and S. Biswas, "Physical and mechanical properties of bi-directional jute fiber epoxy composites," *Procedia Eng.*, vol. 51, pp. 561–566, 2013.
- [86] S. L. Bai, R. K. Y. Li, L. C. M. Wu, H. M. Zeng, and Y. W. Mai, "Tensile failure mechanisms of sisal fibers in composites," *J. Mater. Sci. Lett.*, vol. 17, no. 21, pp. 1805–1807, 1998.
- [87] L. A. Pothan, S. Thomas, and N. R. Neelakantan, "Short banana fiber reinforced polyester composites: Mechanical, failure and aging characteristics," *J. Reinf. Plast. Compos.*, vol. 16, no. 8, pp. 744–765, 1997.
- [88] M. Shibata, K. I. Takachiyo, K. Ozawa, R. Yosomiya, and H. Takeishi, "Biodegradable polyester composites reinforced with short abaca fiber," *J. Appl. Polym. Sci.*, vol. 85, no. 1, pp. 129–138, Jul. 2002.
- [89] A. Haneefa, P. Bindu, I. Aravind, and S. Thomas, "Studies on tensile and flexural properties of short banana/glass hybrid fiber reinforced polystyrene composites," *J. Compos. Mater.*, vol. 42, no. 15, pp. 1471–1489, Aug. 2008.
- [90] R. Gujjala, S. Ojha, S. Acharya, and S. Pal, "Mechanical properties of woven jute-glass hybrid-reinforced epoxy composite," *J. Compos. Mater.*, vol. 48, no. 28, pp. 3445–3455, Dec. 2014.
- [91] M. Ashok Kumar, G. Ramachandra Reddy, Y. Siva Bharathi, S. Venkata Naidu, and V. Naga Prasad Naidu, "Frictional coefficient, hardness, impact strength, and chemical resistance of reinforced sisal-glass fiber epoxy hybrid composites," *J. Compos. Mater.*,

- vol. 44, no. 26, pp. 3195–3202, Dec. 2010.
- [92] H. P. S. A. Khalil, S. Hanida, C. W. Kang, and N. A. N. Fuaad, “Agro-hybrid composite: The effects on mechanical and physical properties of oil palm fiber (EFB)/glass hybrid reinforced polyester composites,” *J. Reinf. Plast. Compos.*, vol. 26, no. 2, pp. 203–218, Jan. 2007.
- [93] L. U. Devi, S. S. Bhagawan, and S. Thomas, “Dynamic mechanical analysis of pineapple leaf/glass hybrid fiber reinforced polyester composites,” *Polym. Compos.*, vol. 31, no. 6, pp. 956–965, 2009.
- [94] M. M. Davoodi, S. M. Sapuan, D. Ahmad, A. Ali, A. Khalina, and M. Jonoobi, “Mechanical properties of hybrid kenaf/glass reinforced epoxy composite for passenger car bumper beam,” *Mater. Des.*, vol. 31, no. 10, pp. 4927–4932, 2010.
- [95] S. M. Sapuan, H. Y. Lok, M. R. Ishak, and S. Misri, “Mechanical properties of hybrid glass/sugar palm fibre reinforced unsaturated polyester composites,” *Chinese J. Polym. Sci.*, vol. 31, no. 10, pp. 1394–1403, Oct. 2013.
- [96] V. K. Bhagat, S. Biswas, and J. Dehury, “Physical, mechanical, and water absorption behavior of coir/glass fiber reinforced epoxy based hybrid composites,” *Polym. Compos.*, vol. 35, no. 5, pp. 925–930, May 2014.
- [97] M. Karina, H. Onggo, A. A. H. D. Abdullah, and A. Syampurwadi, “Effect of oil palm empty fruit bunch fiber on the physical and mechanical properties of fiber glass reinforced polyester resin,” *J. Biol. Sci.*, vol. 8, no. 1, pp. 101–106, Jan. 2008.
- [98] M. Ramesh, T. S. A. Atreya, U. S. Aswin, H. Eashwar, and C. Deepa, “Processing and mechanical property evaluation of banana fiber reinforced polymer composites,” *Procedia Eng.*, vol. 97, pp. 563–572, 2014.
- [99] W. H. Zhu, B. C. Tobias, and R. S. P. Coutts, “Banana fibre strands reinforced polyester composites,” *J. Mater. Sci. Lett.*, vol. 14, no. 7, pp. 508–510, 1995.
- [100] A. V. Ratna Prasad and K. Mohana Rao, “Mechanical properties of natural fibre reinforced polyester composites: Jowar, sisal and bamboo,” *Mater. Des.*, vol. 32, no. 8, pp. 4658–4663, 2011.
- [101] R. M. N. Arib, S. M. Sapuan, M. M. H. M. Ahmad, M. T. Paridah, and H. M. D. K. Zaman, “Mechanical properties of pineapple leaf fibre reinforced polypropylene composites,” *Mater. Des.*, vol. 27, no. 5, pp. 391–396, 2006.

- [102] H. Hargitai, “Reinforcing of Polypropylene with Hydrophil Fibers,” Budapest University of Technology and Economics, Hungary, 2004.
- [103] V. P. Kommula, K. O. Reddy, M. Shukla, T. Marwala, and A. V. Rajulu, “Physico-chemical, tensile, and thermal characterization of napier grass (Native African) fiber strands,” *Int. J. Polym. Anal. Charact.*, vol. 18, no. 4, pp. 303–314, May 2013.
- [104] M. Haameem J.A., M. S. Abdul Majid, M. Afendi, H. F. A. Marzuki, I. Fahmi, and A. G. Gibson, “Mechanical properties of Napier grass fibre/polyester composites,” *Compos. Struct.*, vol. 136, pp. 1–10, 2016.
- [105] P. Noorunnisa Khanam, M. Mohan Reddy, K. Raghu, K. John, and S. Venkata Naidu, “Tensile, flexural and compressive properties of sisal/silk hybrid composites,” *J. Reinf. Plast. Compos.*, vol. 26, no. 10, pp. 1065–1070, Jul. 2007.
- [106] P. A. Sreekumar, K. Joseph, G. Unnikrishnan, and S. Thomas, “A comparative study on mechanical properties of sisal-leaf fibre-reinforced polyester composites prepared by resin transfer and compression moulding techniques,” *Compos. Sci. Technol.*, vol. 67, no. 3, pp. 453–461, 2007.
- [107] C. Udaya Kiran, G. Ramachandra Reddy, B. M. Dabade, and S. Rajesham, “Tensile properties of sun hemp, banana and sisal fiber reinforced polyester composites,” *J. Reinf. Plast. Compos.*, vol. 26, no. 10, pp. 1043–1050, Jul. 2007.
- [108] V. K. Thakur and A. S. Singha, “Mechanical and water absorption properties of natural fibers/polymer biocomposites,” *Polym. Plast. Technol. Eng.*, vol. 49, no. 7, pp. 694–700, Jun. 2010.
- [109] A. Athijayamani, M. Thiruchitrambalam, V. Manikandan, and B. Pazhanivel, “Mechanical properties of natural fibers reinforced polyester hybrid composite,” *Int. J. Plast. Technol.*, vol. 14, no. 1, pp. 104–116, Jun. 2010.
- [110] K. S. Kumar, I. Siva, N. Rajini, P. Jeyaraj, and J. W. Jappes, “Tensile, impact, and vibration properties of coconut sheath/sisal hybrid composites: Effect of stacking sequence,” *J. Reinf. Plast. Compos.*, vol. 33, no. 19, pp. 1802–1812, Oct. 2014.
- [111] D. G. Hepworth, R. N. Hobson, D. M. Bruce, and J. W. Farrent, “The use of unretted hemp fibre in composite manufacture,” *Compos. Part A Appl. Sci. Manuf.*, vol. 31, no. 11, pp. 1279–1283, Nov. 2000.
- [112] V. Alvarez, A. Vazquez, and C. Bernal, “Effect of microstructure on the tensile and

- fracture properties of sisal fiber/starch-based composites,” *J. Compos. Mater.*, vol. 40, no. 1, pp. 21–35, Jun. 2005.
- [113] M. J. John and R. D. Anandjiwala, “Chemical modification of flax reinforced polypropylene composites,” *Compos. Part A Appl. Sci. Manuf.*, vol. 40, no. 4, pp. 442–448, 2009.
- [114] R. Sana, K. Foued, B. M. Yossier, J. Mounir, M. Slah, and D. Bernard, “Flexural properties of typha natural fiber-reinforced polyester composites,” *Fibers Polym.*, vol. 16, no. 11, pp. 2451–2457, Nov. 2015.
- [115] I. Van de Weyenberg, T. Chi Truong, B. Vangrimde, and I. Verpoest, “Improving the properties of UD flax fibre reinforced composites by applying an alkaline fibre treatment,” *Compos. Part A Appl. Sci. Manuf.*, vol. 37, no. 9, pp. 1368–1376, 2006.
- [116] S. Shibata, Y. Cao, and I. Fukumoto, “Flexural modulus of the unidirectional and random composites made from biodegradable resin and bamboo and kenaf fibres,” *Compos. Part A Appl. Sci. Manuf.*, vol. 39, no. 4, pp. 640–646, 2008.
- [117] L. Osorio, E. Trujillo, A. W. Van Vuure, and I. Verpoest, “Morphological aspects and mechanical properties of single bamboo fibers and flexural characterization of bamboo/ epoxy composites,” *J. Reinf. Plast. Compos.*, vol. 30, no. 5, pp. 396–408, Mar. 2011.
- [118] T. Yu, Y. Li, and J. Ren, “Preparation and properties of short natural fiber reinforced poly(lactic acid) composites,” *Trans. Nonferrous Met. Soc. China*, vol. 19, pp. s651–s655, Dec. 2009.
- [119] A. K. Mohanty, M. A. Khan, and G. Hinrichsen, “Influence of chemical surface modification on the properties of biodegradable jute fabrics—polyester amide composites,” *Compos. Part A Appl. Sci. Manuf.*, vol. 31, no. 2, pp. 143–150, 2000.
- [120] Y. Shindo, R. Wang, and K. Horiguchi, “Analytical and experimental studies of short-beam interlaminar shear strength of G-10CR glass-cloth/epoxy laminates at cryogenic temperatures,” *J. Eng. Mater. Technol.*, vol. 123, no. 1, pp. 112–118, 2001.
- [121] J. R. Cox, “Single-Lap Shear Testing to Investigate Pan-Based Carbon Nanofiber and Vapor Grown Carbon Nanofiber Sheet Reinforcement of Laminated Graphite/Epoxy Composite Interlaminar Shear Strength,” Tennessee Technological University, Tennessee, 2007.

- [122] R. Pai, M. S. Kamath, and R. M. V. G. K. Rao, "Acid resistance of glass fibre composites with different layup sequencing part II: Degradation studies," *J. Reinf. Plast. Compos.*, vol. 16, no. 11, pp. 1013–1019, 1997.
- [123] S. H. Hamdan, A. Z. Abidin, and Z. Ahmad, "Tensile and interlaminar shear strength of unidirectional kenaf fibre reinforced polymer with overlapping joint," in *InCIEC 2013*, Singapore: Springer Singapore, 2014, pp. 689–700.
- [124] D. Romanzini, A. Lavoratti, H. L. Ornaghi, S. C. Amico, and A. J. Zattera, "Influence of fiber content on the mechanical and dynamic mechanical properties of glass/ramie polymer composites," *Mater. Des.*, vol. 47, pp. 9–15, 2013.
- [125] K. V. Arun, S. Basavarajappa, and B. S. Sherigara, "Damage characterisation of glass/textile fabric polymer hybrid composites in sea water environment," *Mater. Des.*, vol. 31, no. 2, pp. 930–939, 2010.
- [126] G. Venkata Reddy, T. Shobha Rani, K. Chowdoji Rao, and S. Venkata Naidu, "Flexural, compressive, and interlaminar shear strength properties of kapok/glass composites," *J. Reinf. Plast. Compos.*, vol. 28, no. 14, pp. 1665–1677, Jul. 2009.
- [127] Y. Zhang, Y. Li, H. Ma, and T. Yu, "Tensile and interfacial properties of unidirectional flax/glass fiber reinforced hybrid composites," *Compos. Sci. Technol.*, vol. 88, pp. 172–177, 2013.
- [128] D. S. Bhowmick M, "Mechanical properties of unidirectional jute-polyester composite," *J. Text. Sci. Eng.*, vol. 5, no. 4, pp. 1–6, 2015.
- [129] S. Thomas and L. A. Pothan, *Natural Fibre Reinforced Polymer Composites: From Macro to Nanoscale*. Paris: Archives Contemporaines Ltd, 2008.
- [130] B. Öztürk, "Hybrid effect in the mechanical properties of jute/rockwool hybrid fibres reinforced phenol formaldehyde composites," *Fibers Polym.*, vol. 11, no. 3, pp. 464–473, Jun. 2010.
- [131] H. N. Dhakal, Z. Y. Zhang, M. O. W. Richardson, and O. A. Z. Errajhi, "The low velocity impact response of non-woven hemp fibre reinforced unsaturated polyester composites," *Compos. Struct.*, vol. 81, no. 4, pp. 559–567, 2007.
- [132] K. Mysamy and I. Rajendran, "Influence of alkali treatment and fibre length on mechanical properties of short Agave fibre reinforced epoxy composites," *Mater. Des.*, vol. 32, no. 8, pp. 4629–4640, 2011.

- [133] F. Rezaei, R. Yunus, N. A. Ibrahim, and E. S. Mahdi, "Effect of fiber loading and fiber length on mechanical and thermal properties of short carbon fiber reinforced polypropylene composite," *Malaysian J. Anal. Sci.*, vol. 11, no. 1, pp. 181–188, 2007.
- [134] C. V. Srinivasa and K. N. Bharath, "Impact and hardness properties of areca fiber-epoxy reinforced composites," *J. Mater. Environ. Sci.*, vol. 2, no. 4, pp. 351–356, 2011.
- [135] G. Venkata Reddy, S. Venkata Naidu, and T. Shobha Rani, "Kapok/glass polyester hybrid composites: Tensile and hardness properties," *J. Reinf. Plast. Compos.*, vol. 27, no. 16–17, pp. 1775–1787, Nov. 2008.
- [136] I. O. Oladele, "Effect of bagasse fibre reinforcement on the mechanical properties of polyester composites," *J. Assoc. Prof. Eng. Trinidad Tobago*, vol. 42, no. 1, pp. 12–15, 2014.
- [137] J. R. Aseer, K. Sankaranarayanan, P. Jayabalan, R. Natarajan, and K. Priya Dasan, "Mechanical and water absorption properties of municipal solid waste and banana fiber-reinforced urea formaldehyde composites," *Environ. Prog. Sustain. Energy*, vol. 34, no. 1, pp. 211–221, Jan. 2015.
- [138] H. Jena, A. K. Pradhan, and M. K. Pandit, "Studies on water absorption behaviour of bamboo-epoxy composite filled with cenosphere," *J. Reinf. Plast. Compos.*, vol. 33, no. 11, pp. 1059–1068, Jun. 2014.
- [139] C. Deo and S. K. Acharya, "Effect of moisture absorption on mechanical properties of chopped natural fiber reinforced epoxy composite," *J. Reinf. Plast. Compos.*, vol. 29, no. 16, pp. 2513–2521, Aug. 2010.
- [140] H. Alamri and I. M. Low, "Mechanical properties and water absorption behaviour of recycled cellulose fibre reinforced epoxy composites," *Polym. Test.*, vol. 31, no. 5, pp. 620–628, 2012.
- [141] M. Tajvidi, S. K. Najafi, and N. Moteei, "Long-term water uptake behavior of natural fiber/polypropylene composites," *J. Appl. Polym. Sci.*, vol. 99, no. 5, pp. 2199–2203, Mar. 2006.
- [142] P. A. Sreekumar, S. P. Thomas, J. Marc Saiter, K. Joseph, G. Unnikrishnan, and S. Thomas, "Effect of fiber surface modification on the mechanical and water absorption characteristics of sisal/polyester composites fabricated by resin transfer molding," *Compos. Part A Appl. Sci. Manuf.*, vol. 40, no. 11, pp. 1777–1784, 2009.

- [143] S. Panthapulakkal and M. Sain, “Studies on the Water Absorption Properties of Short Hemp–Glass Fiber Hybrid Polypropylene Composites,” *J. Compos. Mater.*, vol. 41, no. 15, pp. 1871–1883, Aug. 2007.
- [144] H. Takagi, A. N. Nakagaito, and K. Liu, “Heat transfer analyses of natural fibre composites,” in *High Performance and Optimum Design of Structures and Materials*, W. P. De Wilde, S. Hernández, and C. A. Brebbia, Eds. WIT Transactions on The Built Environment, 2014, pp. 237–243.
- [145] J. D. D. Melo, G. S. Marinho, and R. M. Mendonça, “Thermal and mechanical properties analyses of sisal fiber composites,” in *18th International Congress of Mechanical Engineering*, 2005.
- [146] H. Takagi, S. Kako, K. Kusano, and A. Ousaka, “Thermal conductivity of PLA-bamboo fiber composites,” *Adv. Compos. Mater.*, vol. 16, no. 4, pp. 377–384, Jan. 2007.
- [147] K. Ramanaiah, A. V. Ratna Prasad, and K. H. Chandra Reddy, “Mechanical properties and thermal conductivity of typha angustifolia natural fiber–reinforced polyester composites,” *Int. J. Polym. Anal. Charact.*, vol. 16, no. 7, pp. 496–503, Oct. 2011.
- [148] K. Ramanaiah, A. V. Ratna Prasad, and K. Hema Chandra Reddy, “Thermal and mechanical properties of waste grass broom fiber-reinforced polyester composites,” *Mater. Des.*, vol. 40, pp. 103–108, 2012.
- [149] S. W. Kim, S. H. Lee, J. S. Kang, and K. H. Kang, “Thermal conductivity of thermoplastics reinforced with natural fibers,” *Int. J. Thermophys.*, vol. 27, no. 6, pp. 1873–1881, Nov. 2006.
- [150] S. Luo and A. N. Netravali, “Mechanical and thermal properties of environment-friendly green composites made from pineapple leaf fibers and poly(hydroxybutyrate-co-valerate) resin,” *Polym. Compos.*, vol. 20, no. 3, pp. 367–378, Jun. 1999.
- [151] R. Chollakup, R. Tantatherdtam, S. Ujjin, and K. Ssiroth, “Pineapple leaf fiber reinforced thermoplastic composites: Effects of fiber length and fiber content on their characteristics,” *J. Appl. Polym. Sci.*, vol. 119, no. 4, pp. 1952–1960, Feb. 2011.
- [152] M. Kuranska and A. Prociak, “Porous polyurethane composites with natural fibres,” *Compos. Sci. Technol.*, vol. 72, no. 2, pp. 299–304, 2012.

- [153] L. Yusriah, S. M. Sapuan, E. S. Zainudin, M. Mariatti, and M. Jawaaid, “Thermophysical, thermal degradation, and flexural properties of betel nut husk fiber reinforced vinyl ester composites,” *Polym. Compos.*, vol. 37, no. 7, pp. 2008–2017, Jul. 2016.
- [154] K. Ramanaiah, A. R. Prasad, and K. H. C. Reddy, “Thermophysical and fire properties of vakka natural fiber reinforced polyester composites,” *J. Reinf. Plast. Compos.*, vol. 32, no. 15, pp. 1092–1098, Aug. 2013.
- [155] A. Majumdar, S. Mukhopadhyay, and R. Yadav, “Thermal properties of knitted fabrics made from cotton and regenerated bamboo cellulosic fibres,” *Int. J. Therm. Sci.*, vol. 49, no. 10, pp. 2042–2048, 2010.
- [156] S. Kawabata and R. S. Rengasamy, “Thermal conductivity of unidirectional fibre composites made from yarns and computation of thermal conductivity of yarns,” *Indian J. Fibre Text. Res.*, vol. 27, no. 3, pp. 217–223, 2002.
- [157] R. S. Rengasamy, S. Yoshida, and S. Kawabata, “Measurement of thermal conductivity of cotton fibre,” in *22nd Textile Research Symposium.*, 1993.
- [158] I. S. Aji, E. S. Zainudin, A. Khalina, S. M. Sapuan, and M. D. Khairul, “Thermal property determination of hybridized kenaf/PALF reinforced HDPE composite by thermogravimetric analysis,” *J. Therm. Anal. Calorim.*, vol. 109, no. 2, pp. 893–900, Aug. 2012.
- [159] M. Chikhi, B. Agoudjil, A. Boudenne, and A. Gherabli, “Experimental investigation of new biocomposite with low cost for thermal insulation,” *Energy Build.*, vol. 66, pp. 267–273, 2013.
- [160] X. Li, L. G. Tabil, I. N. Oguocha, and S. Panigrahi, “Thermal diffusivity, thermal conductivity, and specific heat of flax fiber–HDPE biocomposites at processing temperatures,” *Compos. Sci. Technol.*, vol. 68, no. 7, pp. 1753–1758, 2008.
- [161] G. Kalaprasad, P. Pradeep, G. Mathew, C. Pavithran, and S. Thomas, “Thermal conductivity and thermal diffusivity analyses of low-density polyethylene composites reinforced with sisal, glass and intimately mixed sisal/glass fibres,” *Compos. Sci. Technol.*, vol. 60, no. 16, pp. 2967–2977, 2000.
- [162] M. Mounika, K. Ramaniah, and A. V. R. Prasad, “Thermal conductivity characterization of bamboo fiber reinforced polyester composite,” *J. Mater. Environ. Sci.*, vol. 3, no. 6, pp. 1109–1116, 2012.

- [163] D. U. Shah, M. C. D. Bock, H. Mulligan, and M. H. Ramage, “Thermal conductivity of engineered bamboo composites,” *J. Mater. Sci.*, vol. 51, no. 6, pp. 2991–3002, Mar. 2016.
- [164] Z. N. Azwa and B. F. Yousif, “Thermal degradation study of kenaf fibre/epoxy composites using thermo gravimetric analysis,” in *In Proceedings of the 3rd Malaysian Postgraduate Conference*, 2013, pp. 256–264.
- [165] L. B. Manfredi, E. S. Rodríguez, M. Wladyka-Przybylak, and A. Vázquez, “Thermal degradation and fire resistance of unsaturated polyester, modified acrylic resins and their composites with natural fibres,” *Polym. Degrad. Stab.*, vol. 91, no. 2, pp. 255–261, 2006.
- [166] A. Trigui, M. Karkri, L. Pena, C. Boudaya, Y. Candau, S. Bouffi, and F. Vilaseca, “Thermal and mechanical properties of maize fibres-high density polyethylene biocomposites,” *J. Compos. Mater.*, vol. 47, no. 11, pp. 1387–1397, May 2013.
- [167] R. D. Sweeting and X. L. Liu, “Measurement of thermal conductivity for fibre-reinforced composites,” *Compos. Part A Appl. Sci. Manuf.*, vol. 35, no. 7, pp. 933–938, 2004.
- [168] R. Agarwal, N. Saxena, and K. Sharma, “Thermal conduction and diffusion through glass-banana fiber polyester composites,” *Indian J. Pure Appl. Phys.*, vol. 41, no. 6, pp. 448–452, 2003.
- [169] A. V. Ratna Prasad, K. M. Rao, and G. Nagasrinivasulu, “Mechanical properties of banana empty fruit bunch fibre reinforced polyester composites,” *Indian J. fibre Text. Res.*, vol. 34, no. 2, pp. 162–167, 2009.
- [170] N. Venkateshwaran, A. ElayaPerumal, and M. S. Jagatheeshwaran, “Effect of fiber length and fiber content on mechanical properties of banana fiber/epoxy composite,” *J. Reinf. Plast. Compos.*, vol. 30, no. 19, pp. 1621–1627, Oct. 2011.
- [171] M. Sumaila, I. Amber, and M. Bawa, “Effect of fiber length on the physical and mechanical properties of random oriented, nonwoven short banana (*musa balbisiana*) fibre/epoxy composite,” *Asian J. Nat. Appl. Sci.*, vol. 2, pp. 39–49, 2013.
- [172] P. A. Sreekumar, P. Albert, G. Unnikrishnan, K. Joseph, and S. Thomas, “Mechanical and water sorption studies of ecofriendly banana fiber-reinforced polyester composites fabricated by RTM,” *J. Appl. Polym. Sci.*, vol. 109, no. 3, pp. 1547–1555, Aug. 2008.

- [173] N. Venkateshwaran, A. ElayaPerumal, A. Alavudeen, and M. Thiruchitrambalam, "Mechanical and water absorption behaviour of banana/sisal reinforced hybrid composites," *Mater. Des.*, vol. 32, no. 7, pp. 4017–4021, 2011.
- [174] L. Herrera-Estrada, S. Pillay, and U. Vaidya, "Banana fiber composites for automotive and transportation applications," in *In: 8th annual SPE automotive composites conference and exhibition*, 2008.
- [175] M. Jawaid, H. P. S. Abdul Khalil, and A. Abu Bakar, "Woven hybrid composites: Tensile and flexural properties of oil palm-woven jute fibres based epoxy composites," *Mater. Sci. Eng. A*, vol. 528, no. 15, pp. 5190–5195, 2011.
- [176] S. K. Samal, S. Mohanty, and S. K. Nayak, "Banana/glass fiber-reinforced polypropylene hybrid composites: fabrication and performance evaluation," *Polym. Plast. Technol. Eng.*, vol. 48, no. 4, pp. 397–414, Apr. 2009.
- [177] L. A. Pothan, P. Potschke, R. Habler, and S. Thomas, "The static and dynamic mechanical properties of banana and glass fiber woven fabric-reinforced polyester composite," *J. Compos. Mater.*, vol. 39, no. 11, pp. 1007–1025, Jun. 2005.
- [178] V. P. Arthanarieswaran, A. Kumaravel, and M. Kathirselvam, "Evaluation of mechanical properties of banana and sisal fiber reinforced epoxy composites: Influence of glass fiber hybridization," *Mater. Des.*, vol. 64, pp. 194–202, 2014.
- [179] M. Ramesh, K. Palanikumar, and K. H. Reddy, "Mechanical property evaluation of sisal–jute–glass fiber reinforced polyester composites," *Compos. Part B Eng.*, vol. 48, pp. 1–9, 2013.
- [180] S. K. Saw, K. Akhtar, N. Yadav, and A. K. Singh, "Hybrid composites made from jute/coir fibers: water absorption, thickness swelling, density, morphology, and mechanical properties," *J. Nat. Fibers*, vol. 11, no. 1, pp. 39–53, Jan. 2014.
- [181] K. S. Ahmed and S. Vijayarangan, "Tensile, flexural and interlaminar shear properties of woven jute and jute-glass fabric reinforced polyester composites," *J. Mater. Process. Technol.*, vol. 207, no. 1, pp. 330–335, 2008.
- [182] S. M. Sapuan, A. Leenie, M. Harimi, and Y. K. Beng, "Mechanical properties of woven banana fibre reinforced epoxy composites," *Mater. Des.*, vol. 27, no. 8, pp. 689–693, 2006.
- [183] A. Satapathy, A. K. Alok Kumar Jha, S. Mantry, S. K. Singh, and A. Patnaik,

- “Processing and characterization of jute-epoxy composites reinforced with SiC derived from rice husk,” *J. Reinf. Plast. Compos.*, vol. 29, no. 18, pp. 2869–2878, Sep. 2010.
- [184] M. Mariatti, M. Jannah, A. Abu Bakar, and H. P. S. A. Khalil, “Properties of banana and pandanus woven fabric reinforced unsaturated polyester composites,” *J. Compos. Mater.*, vol. 42, no. 9, pp. 931–941, May 2008.
- [185] V. S. Srinivasan, S. Rajendra Boopathy, D. Sangeetha, and B. Vijaya Ramnath, “Evaluation of mechanical and thermal properties of banana–flax based natural fibre composite,” *Mater. Des.*, vol. 60, pp. 620–627, 2014.
- [186] D. Shanmugam and M. Thiruchitrabalam, “Static and dynamic mechanical properties of alkali treated unidirectional continuous Palmyra Palm Leaf Stalk Fiber/jute fiber reinforced hybrid polyester composites,” *Mater. Des.*, vol. 50, pp. 533–542, 2013.
- [187] T. Sathishkumar, P. Navaneethakrishnan, S. Shankar, and J. Kumar, “Mechanical properties of randomly oriented snake grass fiber with banana and coir fiber-reinforced hybrid composites,” *J. Compos. Mater.*, vol. 47, no. 18, pp. 2181–2191, Aug. 2013.
- [188] B. Vijaya Ramnath, R. Sharavanan, M. Chandrasekaran, C. Elanchezhian, R. Sathyanarayanan, R. Niranjana Raja, and S. Junaid Kokan, “Experimental determination of mechanical properties of banana jute hybrid composite,” *Fibers Polym.*, vol. 16, no. 1, pp. 164–172, Jan. 2015.
- [189] M. Idicula, A. Boudenne, L. Umadevi, L. Ibos, Y. Candau, and S. Thomas, “Thermophysical properties of natural fibre reinforced polyester composites,” *Compos. Sci. Technol.*, vol. 66, no. 15, pp. 2719–2725, 2006.
- [190] M. Boopalan, M. Niranjanaa, and M. J. Umapathy, “Study on the mechanical properties and thermal properties of jute and banana fiber reinforced epoxy hybrid composites,” *Compos. Part B Eng.*, vol. 51, pp. 54–57, 2013.
- [191] E. S. Zainudin, S. M. Sapuan, K. Abdan, and M. T. M. Mohamad, “Thermal degradation of banana pseudo-stem filled unplasticized polyvinyl chloride (UPVC) composites,” *Mater. Des.*, vol. 30, no. 3, pp. 557–562, 2009.
- [192] M. Jawaid, H. A. Khalil, A. A. Bakar, A. Hassan, and R. Dungani, “Effect of jute fibre loading on the mechanical and thermal properties of oil palm-epoxy composites,” *J. Compos. Mater.*, vol. 47, no. 13, pp. 1633–1641, Jun. 2013.

- [193] P. Sathish, R. Kesavan, B. V. Ramnath, and C. Vishal, “Effect of fiber orientation and stacking sequence on mechanical and thermal characteristics of banana-kenaf hybrid epoxy composite,” *Silicon*, pp. 1–9, Aug. 2015.
- [194] S. Pujari, A. Ramakrishna, and K. T. Balaram Padal, “Investigations on thermal conductivities of jute and banana fiber reinforced epoxy composites,” *J. Inst. Eng. Ser. D*, pp. 1–5, Jan. 2016.
- [195] L. K. Sreepathi, K. S. Ahmed, and S. Vijayarangan, “Measurement of Thermal Conductivity of Jute Fiber Reinforced Polyester Composites,” in *Proceedings of the National Conference on Advances in Mechanical Engineering*, 2010.
- [196] H. Ahmad, M. Islam, and M. Uddin, “Thermal and mechanical properties of epoxy-jute fiber composite,” *J. Chem. Eng.*, vol. 27, no. 2, pp. 77–82, Jan. 2014.
- [197] Z. Hashin and B. W. Rosen, “The elastic moduli of fiber-reinforced materials,” *J. Appl. Mech.*, vol. 31, no. 2, pp. 223–232, 1964.
- [198] Z. Hashin, “Analysis of properties of fiber composites with anisotropic constituents,” *J. Appl. Mech.*, vol. 46, no. 3, pp. 543–550, 1979.
- [199] Z. Hashin, “Analysis of composite materials—A survey,” *J. Appl. Mech.*, vol. 50, no. 3, p. 481, 1983.
- [200] P. Valavala and G. Odegard, “Modeling techniques for determination of mechanical properties of polymer nanocomposites,” *Rev. Adv. Mater. Sci.*, vol. 9, pp. 34–44, 2005.
- [201] J. C. Halpin, “Stiffness and expansion estimates for oriented short fiber composites,” *J. Compos. Mater.*, vol. 3, no. 4, pp. 732–734, 1969.
- [202] X. A. Zhong and J. Padovan, “Influence of geometrical features of unidirectional fibrous lamina on its transverse responses,” in *Proceedings of the 15th ASCE Engineering Mechanics Conference*, 2002.
- [203] I. M. Daniel and O. Ishai, *Engineering mechanics of composite materials*. Oxford University Press, 1994.
- [204] T. B. Lewis and L. E. Nielsen, “Dynamic mechanical properties of particulate-filled composites,” *J. Appl. Polym. Sci.*, vol. 14, no. 6, pp. 1449–1471, Jun. 1970.
- [205] D. Kumlutas and I. H. Tavman, “A numerical and experimental study on thermal conductivity of particle filled polymer composites,” *J. Thermoplast. Compos. Mater.*, vol. 19, no. 4, pp. 441–455, Jul. 2006.

- [206] J. P. Gardener, "Micromechanical modeling of composite materials in finite element analysis using an embedded cell approach," MIT, 1994.
- [207] W. Sun, F. Lin, and X. Hu, "Computer-aided design and modeling of composite unit cells," *Compos. Sci. Technol.*, vol. 61, no. 2, pp. 289–299, 2001.
- [208] C. L. Tucker III and E. Liang, "Stiffness predictions for unidirectional short-fiber composites: Review and evaluation," *Compos. Sci. Technol.*, vol. 59, no. 5, pp. 655–671, 1999.
- [209] D. F. Adams and D. A. Crane, "Finite element micromechanical analysis of a unidirectional composite including longitudinal shear loading," *Comput. Struct.*, vol. 18, no. 6, pp. 1153–1165, Jan. 1984.
- [210] M. R. Nedele and M. R. Wisnom, "Finite element micromechanical modelling of a unidirectional composite subjected to axial shear loading," *Composites*, vol. 25, no. 4, pp. 263–272, Apr. 1994.
- [211] A. Patnaik, P. Kumar, S. Biswas, and M. Kumar, "Investigations on micro-mechanical and thermal characteristics of glass fiber reinforced epoxy based binary composite structure using finite element method," *Comput. Mater. Sci.*, vol. 62, pp. 142–151, 2012.
- [212] P. E. J. Babu, S. Savithri, U. T. S. Pillai, and B. C. Pai, "Micromechanical modeling of hybrid composites," *Polymer (Guildf.)*, vol. 46, no. 18, pp. 7478–7484, Aug. 2005.
- [213] S. Li, "General unit cells for micromechanical analyses of unidirectional composites," *Compos. Part A Appl. Sci. Manuf.*, vol. 32, no. 6, pp. 815–826, 2001.
- [214] S. Li, "On the unit cell for micromechanical analysis of fibre-reinforced composites," *Proc. R. Soc. A Math. Phys. Eng. Sci.*, vol. 455, no. 1983, pp. 815–838, Mar. 1999.
- [215] Y. M. Shabana and N. Noda, "Numerical evaluation of the thermomechanical effective properties of a functionally graded material using the homogenization method," *Int. J. Solids Struct.*, vol. 45, no. 11, pp. 3494–3506, 2008.
- [216] S. Banerjee and B. V. Sankar, "Mechanical properties of hybrid composites using finite element method based micromechanics," *Compos. Part B Eng.*, vol. 58, pp. 318–327, 2014.
- [217] A. G. Facca, M. T. Kortschot, and N. Yan, "Predicting the elastic modulus of natural fibre reinforced thermoplastics," *Compos. Part A Appl. Sci. Manuf.*, vol. 37, no. 10,

- pp. 1660–1671, 2006.
- [218] O. Bacarreza, D. Abe, M. H. Aliabadi, and N. K. Ragavan, “Micromechanical modeling of advanced composites,” *J. Multiscale Model.*, vol. 40, no. 2, p. 1250005, 2012.
- [219] J. Mirbagheri, M. Tajvidi, J. C. Hermanson, and I. Ghasemi, “Tensile properties of wood flour/kenaf fiber polypropylene hybrid composites,” *J. Appl. Polym. Sci.*, vol. 105, no. 5, pp. 3054–3059, Sep. 2007.
- [220] B. Pal and M. Riyazuddin Haseebuddin, “Analytical estimation of elastic properties of polypropylene fiber matrix composite by finite element analysis,” *Adv. Mater. Phys. Chem.*, vol. 2, no. 1, pp. 23–30, 2012.
- [221] H. J. Ott, “Thermal conductivity of composite materials,” *Plast. Rubber Process. Appl.*, vol. 1, no. 1, pp. 9–24, 1981.
- [222] C. H. Chen and Y. C. Wang, “Effective thermal conductivity of misoriented short-fiber reinforced thermoplastics,” *Mech. Mater.*, vol. 23, no. 3, pp. 217–228, Jul. 1996.
- [223] R. C. Progelhof, J. L. Throne, and R. R. Ruetsch, “Methods for predicting the thermal conductivity of composite systems: A review,” *Polym. Eng. Sci.*, vol. 16, no. 9, pp. 615–625, Sep. 1976.
- [224] G. S. Springer and S. W. Tsai, “Thermal Conductivities of Unidirectional Materials,” *J. Compos. Mater.*, vol. 1, no. 2, pp. 166–173, Jan. 1967.
- [225] W. Gogo and P. Furmanski, “Some investigations of effective thermal conductivity of unidirectional fiber-reinforced composites,” *J. Compos. Mater.*, vol. 14, no. 1, pp. 167–176, Jan. 1980.
- [226] L. S. Han and A. A. Cosner, “Effective thermal conductivities of fibrous composites,” *J. Heat Transfer*, vol. 103, no. 2, pp. 387–392, 1981.
- [227] M. R. Islam and A. Pramila, “Thermal conductivity of fiber reinforced composites by the FEM,” *J. Compos. Mater.*, vol. 33, no. 18, pp. 1699–1715, Sep. 1999.
- [228] X. Xiao and A. Long, “A solution for transverse thermal conductivity of composites with quadratic or hexagonal unidirectional fibres,” *Sci. Eng. Compos. Mater.*, vol. 21, no. 1, pp. 99–109, Jan. 2014.
- [229] M. Zou, B. Yu, and D. Zhang, “An analytical solution for transverse thermal conductivities of unidirectional fibre composites with thermal barrier,” *J. Phys. D.*

- Appl. Phys.*, vol. 35, no. 15, pp. 1867–1874, Aug. 2002.
- [230] B. Ascioğlu, S. Adanur, L. Gumusel, and H. Bas, “Modeling of transverse direction thermal conductivity in micro-nano fiber-reinforced composites,” *Text. Res. J.*, vol. 79, no. 12, pp. 1059–1066, Aug. 2009.
- [231] F. A. Al-Sulaiman, Y. N. Al-Nassar, and E. M. A. Mokheimer, “Prediction of the thermal conductivity of the constituents of fiber-reinforced composite laminates: Voids effect,” *J. Compos. Mater.*, vol. 40, no. 9, pp. 797–814, Jul. 2005.
- [232] S. M. Grove, “A model of transverse thermal conductivity in unidirectional fibre-reinforced composites,” *Compos. Sci. Technol.*, vol. 38, no. 3, pp. 199–209, Jan. 1990.
- [233] S.-Y. Lu, “The effective thermal conductivities of composites with 2-D arrays of circular and square cylinders,” *J. Compos. Mater.*, vol. 29, no. 4, pp. 483–506, Mar. 1995.
- [234] J. Z. Liang and F. H. Li, “Heat transfer in polymer composites filled with inorganic hollow micro-spheres: A theoretical model,” *Polym. Test.*, vol. 26, no. 8, pp. 1025–1030, 2007.
- [235] J. Z. Liang and F. H. Li, “Simulation of heat transfer in hollow-glass-bead-filled polypropylene composites by finite element method,” *Polym. Test.*, vol. 26, no. 3, pp. 419–424, 2007.
- [236] S. Sihn and A. K. Roy, “Micromechanical analysis for transverse thermal conductivity of composites,” *J. Compos. Mater.*, vol. 45, no. 11, pp. 1245–1255, Jun. 2011.
- [237] K. Liu, H. Takagi, and Z. Yang, “Evaluation of transverse thermal conductivity of Manila hemp fiber in solid region using theoretical method and finite element method,” *Mater. Des.*, vol. 32, no. 8, pp. 4586–4589, 2011.
- [238] K. Ramani and A. Vaidyanathan, “Finite element analysis of effective thermal conductivity of filled polymeric composites,” *J. Compos. Mater.*, vol. 29, no. 13, pp. 1725–1740, Sep. 1995.
- [239] C. Cao, A. Yu, and Q. H. Qin, “Evaluation of effective thermal conductivity of fiber-reinforced composites,” *Int. J. Archit. Eng. Constr.*, vol. 1, no. 1, pp. 14–29, 2012.
- [240] A. Agrawal and A. Satapathy, “Mathematical model for evaluating effective thermal conductivity of polymer composites with hybrid fillers,” *Int. J. Therm. Sci.*, vol. 89, pp. 203–209, 2015.

- [241] M. Haddadi, B. Agoudjil, N. Benmansour, A. Boudenne, and B. Garnier, “Experimental and modeling study of effective thermal conductivity of polymer filled with date palm fibers,” *Polym. Compos.*, Jul. 2015.
- [242] T. Behzad and M. Sain, “Measurement and prediction of thermal conductivity for hemp fiber reinforced composites,” *Polym. Eng. Sci.*, vol. 47, no. 7, pp. 977–983, Jul. 2007.
- [243] Y. K. Sahu, J. Banjare, A. Agrawal, and A. Satapathy, “Establishment of an analytical model to predict effective thermal conductivity of fiber reinforced polymer composites,” *Int. J. Plast. Technol.*, vol. 18, no. 3, pp. 368–373, Dec. 2014.
- [244] S. Y. Fu and Y. W. Mai, “Thermal conductivity of misaligned short-fiber-reinforced polymer composites,” *J. Appl. Polym. Sci.*, vol. 88, no. 6, pp. 1497–1505, May 2003.
- [245] J. Z. Liang and G. S. Liu, “A new heat transfer model of inorganic particulate-filled polymer composites,” *J. Mater. Sci.*, vol. 44, no. 17, pp. 4715–4720, Sep. 2009.
- [246] R. E. Skochdopole, “The thermal conductivity of foamed plastics,” *Chem. Eng. Prog.*, vol. 57, pp. 55–59, 1961.
- [247] B. Mortaigne, S. Bourbigot, M. Le Bras, G. Cordellier, A. Baudry, and J. Dufay, “Fire behaviour related to the thermal degradation of unsaturated polyesters,” *Polym. Degrad. Stab.*, vol. 64, no. 3, pp. 443–448, 1999.
- [248] S. V. Szokolay, *Introduction to Architectural Science: The Basis of Sustainable Design*. Burlington: Architectural Press, 2008.
- [249] B. D. Agarwal and L. J. Broutman, *Analysis and Performance of Fiber Composites*. New York: John Wiley & Sons, 1990.
- [250] A. Espert, F. Vilaplana, and S. Karlsson, “Comparison of water absorption in natural cellulosic fibres from wood and one-year crops in polypropylene composites and its influence on their mechanical properties,” *Compos. Part A Appl. Sci. Manuf.*, vol. 35, no. 11, pp. 1267–1276, 2004.
- [251] M. M. Thwe and K. Liao, “Effects of environmental aging on the mechanical properties of bamboo–glass fiber reinforced polymer matrix hybrid composites,” *Compos. Part A Appl. Sci. Manuf.*, vol. 33, no. 1, pp. 43–52, 2002.
- [252] A. C. Loos, G. S. Springer, B. A. Sanders, and R. W. Tung, “Moisture absorption of polyester-E glass composites,” *J. Compos. Mater.*, vol. 14, no. 2, pp. 142–154, Jan.

- 1980.
- [253] J. Crank, *The Mathematics of Diffusion*. Oxford: Oxford University Press, 1979.
- [254] R. Gopalan, R. M. V. G. K. Rao, M. V. V. Murthy, and B. Dattaguru, “Diffusion studies on advanced fibre hybrid composites,” *J. Reinf. Plast. Compos.*, vol. 5, no. 1, pp. 51–61, Jan. 1986.
- [255] S. B. Harogopad and T. M. Aminabhavi, “Diffusion and sorption of organic liquids through polymer membranes. II. Neoprene, SBR, EPDM, NBR, and natural rubber versus n-alkanes,” *J. Appl. Polym. Sci.*, vol. 42, no. 8, pp. 2329–2336, Apr. 1991.
- [256] E. H. Ratcliffe, “Estimation of effective thermal conductivity of two-phase media,” *J. Appl. Chem.*, vol. 18, pp. 25–31, 1968.
- [257] D. Hull and T. W. Clyne, *An introduction to Composite Materials*. Cambridge: Cambridge university press, 1996.
- [258] E. J. Barbero, *Finite Element Analysis of Composite Materials*. Boca Raton: CRC Press, 2008.
- [259] Z. Xia, C. Zhou, Q. Yong, and X. Wang, “On selection of repeated unit cell model and application of unified periodic boundary conditions in micro-mechanical analysis of composites,” *Int. J. Solids Struct.*, vol. 43, no. 2, pp. 266–278, 2006.
- [260] Z. Xia, Y. Zhang, and F. Ellyin, “A unified periodical boundary conditions for representative volume elements of composites and applications,” *Int. J. Solids Struct.*, vol. 40, no. 8, pp. 1907–1921, 2003.
- [261] P. Suquet, “Elements of homogenization theory for inelastic solid mechanics,” in *Homogenization Techniques in Composite Media*, E. Sanchez-Palencia and A. Zaoui, Eds. Berlin: Springer-Verlag, 1987, pp. 194–278.
- [262] K. K. Chawla, *Composite Materials: Science and Engineering*. New York: Springer-Verlag, 1987.
- [263] R. Reixach, F. X. Espinach, E. Franco-Marquès, F. Ramirez de Cartagena, N. Pellicer, J. Tresserras, and P. Mutjé, “Modeling of the tensile moduli of mechanical, thermomechanical, and chemi-thermomechanical pulps from orange tree pruning,” *Polym. Compos.*, vol. 34, no. 11, pp. 1840–1846, Nov. 2013.
- [264] H. Ku, H. Wang, N. Pattarachaiyakoop, and M. Trada, “A review on the tensile properties of natural fiber reinforced polymer composites,” *Compos. Part B Eng.*, vol.

- 42, no. 4, pp. 856–873, 2011.
- [265] S. A. Paul, K. Joseph, G. Mathew, L. A. Pothan, and S. Thomas, “Preparation of polypropylene fiber/banana fiber composites by novel commingling method,” *Polym. Compos.*, vol. 31, no. 5, pp. 816–824, 2009.
- [266] B. Madsen and H. Lilholt, “Physical and mechanical properties of unidirectional plant fibre composites—an evaluation of the influence of porosity,” *Compos. Sci. Technol.*, vol. 63, no. 9, pp. 1265–1272, 2003.
- [267] S. Kari, “Micromechanical modeling and numerical homogenization of fiber and particle reinforced composites,” Otto-von-Guericke-University of Magdeburg, Germany, 2006.
- [268] K. S. Ahmed and S. Vijayarangan, “Elastic property evaluation of jute-glass fibre hybrid composite using experimental and CLT approach,” *Indian J. Eng. Mater. Sci.*, vol. 13, no. 5, pp. 435–442, 2006.
- [269] M. Jawaid, H. P. S. A. Khalil, A. Hassan, and E. Abdallah, “Bi-layer hybrid biocomposites: Chemical resistant and physical properties,” *BioResources*, vol. 7, no. 2, pp. 2344–2355, Apr. 2012.
- [270] M. Jawaid, H. P. S. Abdul Khalil, P. Noorunnisa Khanam, and A. Abu Bakar, “Hybrid composites made from oil Palm empty fruit bunches/jute fibres: water absorption, thickness swelling and density behaviours,” *J. Polym. Environ.*, vol. 19, no. 1, pp. 106–109, Mar. 2011.
- [271] R. Masoodi and K. M. Pillai, “A study on moisture absorption and swelling in bio-based jute-epoxy composites,” *J. Reinf. Plast. Compos.*, vol. 31, no. 5, pp. 285–294, Mar. 2012.
- [272] H. P. S. A. Khalil, M. Jawaid, and A. A. Bakar, “Woven hybrid composites: water absorption and thickness swelling behaviours,” *BioResources*, vol. 6, no. 2, pp. 1043–1052, 2011.
- [273] M. M. Hassan, M. H. Wagner, H. U. Zaman, and M. A. Khan, “Physico-mechanical performance of hybrid betel nut (*Areca catechu*) short fiber/seaweed polypropylene composite,” *J. Nat. Fibers*, vol. 7, no. 3, pp. 165–177, Aug. 2010.
- [274] T. Sathishkumar, P. Navaneethakrishnan, S. Shankar, and R. Rajasekar, “Mechanical properties and water absorption of snake grass longitudinal fiber reinforced isophthalic

- polyester composites,” *J. Reinf. Plast. Compos.*, vol. 32, no. 16, pp. 1211–1223, Aug. 2013.
- [275] J. Zhou and J. P. Lucas, “The effects of a water environment on anomalous absorption behavior in graphite/epoxy composites,” *Compos. Sci. Technol.*, vol. 53, no. 1, pp. 57–64, Jan. 1995.
- [276] H. Rashed, M. Islam, and F. Rizvi, “Effects of process parameters on tensile strength of jute fiber reinforced thermoplastic composites,” *J. Nav. Archit. Mar. Eng.*, vol. 3, no. 1, pp. 1–6, Jun. 2008.
- [277] M. Jacob, S. Thomas, and K. T. Varughese, “Mechanical properties of sisal/oil palm hybrid fiber reinforced natural rubber composites,” *Compos. Sci. Technol.*, vol. 64, no. 7, pp. 955–965, 2004.
- [278] R. P. Kumar, M. L. G. Amma, and S. Thomas, “Short sisal fiber reinforced styrene-butadiene rubber composites,” *J. Appl. Polym. Sci.*, vol. 58, no. 3, pp. 597–612, Oct. 1995.
- [279] K. Joseph, S. Thomas, C. Pavithran, and M. Brahmakumar, “Tensile properties of short sisal fiber-reinforced polyethylene composites,” *J. Appl. Polym. Sci.*, vol. 47, no. 10, pp. 1731–1739, Mar. 1993.
- [280] M. S. Sreekala, J. George, M. G. Kumaran, and S. Thomas, “The mechanical performance of hybrid phenol-formaldehyde-based composites reinforced with glass and oil palm fibres,” *Compos. Sci. Technol.*, vol. 62, no. 3, pp. 339–353, 2002.
- [281] M. Z. M. Yusoff, M. S. Salit, N. Ismail, and R. Wirawan, “Mechanical properties of short random oil palm fibre reinforced epoxy composites,” *Sains Malaysiana*, vol. 39, pp. 87–92, 2010.
- [282] M. Idicula, N. R. Neelakantan, Z. Oommen, K. Joseph, and S. Thomas, “A study of the mechanical properties of randomly oriented short banana and sisal hybrid fiber reinforced polyester composites,” *J. Appl. Polym. Sci.*, vol. 96, no. 5, pp. 1699–1709, Jun. 2005.
- [283] M. Jawaid, O. Y. Alothman, M. T. Paridah, and H. P. S. A. Khalil, “Effect of oil palm and jute fiber treatment on mechanical performance of epoxy hybrid composites,” *Int. J. Polym. Anal. Charact.*, vol. 19, no. 1, pp. 62–69, Jan. 2014.
- [284] A. I. Selmy, A. R. Elsesi, N. A. Azab, and M. A. Abd El-baky, “Interlaminar shear

- behavior of unidirectional glass fiber (U)/random glass fiber (R)/epoxy hybrid and non-hybrid composite laminates,” *Compos. Part B Eng.*, vol. 43, no. 4, pp. 1714–1719, 2012.
- [285] N. A. St John and J. R. Brown, “Flexural and interlaminar shear properties of glass-reinforced phenolic composites,” *Compos. Part A Appl. Sci. Manuf.*, vol. 29, no. 8, pp. 939–946, 1998.
- [286] R. Velmurugan and V. Manikandan, “Mechanical properties of palmyra/glass fiber hybrid composites,” *Compos. Part A Appl. Sci. Manuf.*, vol. 38, no. 10, pp. 2216–2226, 2007.
- [287] P. Wambua, J. Ivens, and I. Verpoest, “Natural fibres: can they replace glass in fibre reinforced plastics?,” *Compos. Sci. Technol.*, vol. 63, no. 9, pp. 1259–1264, 2003.
- [288] A. Kumar and S. Singh, “Analysis of mechanical properties and cost of glass/jute fiber-reinforced hybrid polyester composites,” *Proc. Inst. Mech. Eng. Part L J. Mater. Des. Appl.*, vol. 229, no. 3, pp. 202–208, Jun. 2015.
- [289] S. K. Saw and C. Datta, “Thermomechanical properties of jute/bagasse hybrid fibre reinforced epoxy thermoset composites,” *BioResources*, vol. 4, no. 4, pp. 1455–1475, 2009.
- [290] C. Pavithran, P. S. Mukherjee, and M. Brahmakumar, “Coir-glass intermingled fibre hybrid composites,” *J. Reinf. Plast. Compos.*, vol. 10, no. 1, pp. 91–101, Jan. 1991.
- [291] N. Chand and B. Das Jhod, “Mechanical, electrical, and thermal properties of maleic anhydride modified rice husk filled PVC composites,” *BioResources*, vol. 3, no. 4, pp. 1228–1243, 2008.
- [292] R. Kaundal, A. Patnaik, and A. Satapathy, “Solid particle erosion of short glass fiber reinforced polyester composite,” *Am. J. Mater. Sci.*, vol. 2, pp. 22–27, 2012.
- [293] N. C. Paul, D. H. Richards, and D. Thompson, “An aliphatic amine cured rubber modified epoxide adhesive: 1. Preparation and preliminary evaluation using a room temperature cure,” *Polymer (Guildf.)*, vol. 18, no. 9, pp. 945–950, Sep. 1977.
- [294] S. Tangjuank and S. Kumfu, “Particle boards from papyrus fibers as thermal insulation,” *J. Appl. Sci.*, vol. 11, no. 14, pp. 2640–2645, Dec. 2011.
- [295] H. M. Akil, M. F. Omar, A. A. M. Mazuki, S. Safiee, Z. A. M. Ishak, and A. Abu Bakar, “Kenaf fiber reinforced composites: A review,” *Mater. Des.*, vol. 32, no. 8, pp.

4107–4121, 2011.

- [296] F. Y. C. Boey, “Reducing the void content and its variability in polymeric fibre reinforced composite test specimens using a vacuum injection moulding process,” *Polym. Test.*, vol. 9, no. 6, pp. 363–377, Jan. 1990.
- [297] M. Jacob, K. T. Varughese, and S. Thomas, “Water sorption studies of hybrid biofiber-reinforced natural rubber biocomposites,” *Biomacromolecules*, vol. 6, no. 6, pp. 2969–2979, Nov. 2005.
- [298] H. J. Kim and D. W. Seo, “Effect of water absorption fatigue on mechanical properties of sisal textile-reinforced composites,” *Int. J. Fatigue*, vol. 28, no. 10, pp. 1307–1314, 2006.
- [299] H. N. Dhakal, Z. Y. Zhang, and M. O. W. Richardson, “Effect of water absorption on the mechanical properties of hemp fibre reinforced unsaturated polyester composites,” *Compos. Sci. Technol.*, vol. 67, no. 7, pp. 1674–1683, 2007.
- [300] W. Wang, M. Sain, and P. A. Cooper, “Study of moisture absorption in natural fiber plastic composites,” *Compos. Sci. Technol.*, vol. 66, no. 3, pp. 379–386, 2006.
- [301] A. K. Bledzki and J. Gassan, “Composites reinforced with cellulose based fibres,” *Prog. Polym. Sci.*, vol. 24, no. 2, pp. 221–274, 1999.
- [302] D. Åkesson, M. Skrifvars, J. Seppälä, and M. Turunen, “Thermoset lactic acid-based resin as a matrix for flax fibers,” *J. Appl. Polym. Sci.*, vol. 119, no. 5, pp. 3004–3009, 2011.
- [303] M. M. Kabir, M. M. Islam, and H. Wang, “Mechanical and thermal properties of jute fibre reinforced composites,” *J. Multifunct. Compos.*, vol. 1, no. 1, pp. 71–77, 2013.
- [304] D. Ray, B. K. Sarkar, R. K. Basak, and A. K. Rana, “Thermal behavior of vinyl ester resin matrix composites reinforced with alkali-treated jute fibers,” *J. Appl. Polym. Sci.*, vol. 94, no. 1, pp. 123–129, 2004.
- [305] S. H. Lee and S. Wang, “Biodegradable polymers/bamboo fiber biocomposite with bio-based coupling agent,” *Compos. Part A Appl. Sci. Manuf.*, vol. 37, no. 1, pp. 80–91, 2006.

Dissemination

International Journals

1. Siva Bhaskara Rao Devireddy and Sandhyarani Biswas, Effect of Fiber Geometry and Representative Volume Element on Elastic and Thermal Properties of Unidirectional Fiber-Reinforced Composites, *Journal of Composites*, 2014, 1-12.
2. Siva Bhaskara Rao Devireddy and Sandhyarani Biswas, Physical and Mechanical Behavior of Unidirectional Banana/Jute Fiber Reinforced Epoxy Based Hybrid Composites, *Polymer Composites*, 2015, DOI 10.1002/pc.23706.
3. Siva Bhaskara Rao Devireddy and Sandhyarani Biswas, Physical and Thermal Properties of Unidirectional Banana–Jute Hybrid Fiber-Reinforced Epoxy Composites, *Journal of Reinforced Plastics and Composites*, 2016, Vol. 35(15) 1157–1172.
4. Siva Bhaskara Rao Devireddy and Sandhyarani Biswas, Thermophysical properties of short banana-jute fiber reinforced epoxy based hybrid composites, *Journal of Materials: Design and Applications*, 2016, DOI: 10.1177/1464420716656883.
5. Siva Bhaskara Rao Devireddy and Sandhyarani Biswas, Effect of Fiber Parameters on Mechanical Behavior of Short Banana-Jute Hybrid Fiber Reinforced Epoxy Composites, *Journal of Composite Materials* (Under Revision).

National and International Conferences

1. Siva Bhaskara Rao Devireddy and Sandhyarani Biswas, “Numerical Prediction of Thermal Conductivity of Banana Fiber Reinforced Polymer Composites”, 4th National Conference on Processing and Characterization of Materials (NCPCM 2014), December 5–6, 2014, NIT Rourkela.
2. Siva Bhaskara Rao Devireddy and Sandhyarani Biswas, “Prediction of Elastic Properties of Banana Fiber Reinforced Polymer Composites by Micromechanical Approach”, 4th National Conference on Processing and Characterization of Materials (NCPCM 2014), December 5–6, 2014, NIT Rourkela.
3. Siva Bhaskara Rao Devireddy and Sandhyarani Biswas, “Thermal Conductivity of Hybrid Natural Fiber Reinforced Polymer Composites by Theoretical and Finite

- Element Method”, National Seminar on Polymer Nanocomposites for Engineering Applications, March 14, 2015, NIT Rourkela.
4. Siva Bhaskara Rao Devireddy and Sandhyarani Biswas, “Processing and Mechanical Characterization of Short Banana-Jute Hybrid Fiber Reinforced Polyester Composites”, 4th International Conference on Polymer Processing and Characterization, December 9–11, 2016, Mahatma Gandhi University, Kottayam.

Brief Bio-Data of the Author

The author, Siva Bhaskara Rao Devireddy, born on 06-06-1988 graduated in Mechanical Engineering from St. Ann's College of Engineering and Technology, Chirala, India in the year 2009. He did his postgraduate study in Mechanical Engineering with specialization in Computer Integrated Manufacturing from K L University, Guntur, in the year 2011. Before joining for the Ph.D. programme at the National Institute of Technology, Rourkela, he had served as a faculty in the Department of Mechanical Engineering at Mekapati Rajamohan Reddy Institute of Technology & Science, Udayagiri.

The author is engaged in active research in the area of composite materials since August 2012 at National Institute of Technology, Rourkela under the Institute Research Fellowship scheme. He has 5 research papers to his credit which have been published in various international journals. He has also presented 10 research papers in the area of polymer composites at various national and international conferences.
